5-2011

# Effects of inlet conditions on diffuser outlet performance

Zaccary A. Poots
*University of Nevada, Las Vegas*

# EFFECTS OF INLET CONDITIONS ON DIFFUSER OUTLET PERFORMANCE

by

Zaccary A. Poots

Bachelor of Science in Mechanical Engineering
University of Nevada, Las Vegas
2009

A thesis document submitted in partial fulfillment
of the requirements for the

**Master of Science in Mechanical Engineering**
**Department of Mechanical Engineering**
**Howard R. Hughes College of Engineering**

**Graduate College**
**University of Nevada, Las Vegas**
**May 2011**

UNLV
UNIVERSITY OF NEVADA LAS VEGAS

THE GRADUATE COLLEGE

We recommend the dissertation prepared under our supervision by

**Zaccary A. Poots**

entitled

**Effects of Inlet Conditions on Diffuser Outlet Performance**

be accepted in partial fulfillment of the requirements for the degree of

**Master of Science in Mechanical Engineering**

Douglas Reynolds, Ph. D., Committee Chair

Brian Landsberger, Ph. D., Committee Member

Samir Moujaes, Ph. D., Committee Member

Sandra Catlin, Ph. D., Graduate Faculty Representative

Ronald Smith, Ph. D., Vice President for Research and Graduate Studies
and Dean of the Graduate College

**May 2011**

ABSTRACT

**Effects of Inlet Conditions on Diffuser Outlet Performance**

by

Zaccary A. Poots

Dr. Douglas Reynolds, Examination Committee Chair
Professor of Mechanical Engineering
University of Nevada, Las Vegas

Building air distribution terminal system designers and system installers require accurate quantitative information on the performance of the installed system to achieve optimum efficiency and levels of human comfort. This requires field installation adjustment values from published ideal pressure loss, air distribution and sound generation installation performance. This study documents the air output performance of different installation configurations of six types of ceiling diffusers and compares the results to performance when installed according to ANSI/ASHRAE Standard 70-2006. A diffuser inlet supply plenum was designed for optimum flow and used to acquire a baseline set of data covering the six types of diffusers at different inlet neck sizes and inlet airflow rates. Full scale laboratory testing of typical field installation variations was completed for the same conditions with variations in damper installation, duct approach angle, duct type, duct vertical height above the diffuser and duct branch to main supply duct installation. A set of simple algorithms were developed that can be used to easily predict how an inlet configuration would affect the performance of a wide variety of installation conditions.

ACKNOWLEDGEMENTS

First and foremost, I would like to thank my primary advising professor, Dr. Brian J. Landsberger, for the wisdom he bestowed upon me, the constant explanations that seemed to make things much more approachable and his desire to help me succeed. Without his constant guidance, his knowledge and his friendship, I would have never managed to get this far. I wish you nothing but the best in your future endeavors.

I would also like to thank Dr. Douglas D. Reynolds and the rest of my thesis committee members for their contributions and guidance in my research. Thank you to the entire staff of the mechanical engineering department at UNLV and to the folks at the Las Vegas Valley Water District, with whom I interned, for their time and patience. To my fellow peers, without whom I would not have enjoyed my time at UNLV as much as I did, thank you for making my college experience something I will never forget.

Finally, I would like to extend my deepest gratitude to my family and friends for their love and support. If not for them, my pursuit to further my education may have ended sooner rather than later. Most of all, I would like to thank my parents, Lisa and Gregg Poots, for everything they have done for me throughout my life and college career. I could never thank you enough for helping make me the man I am today.

TABLE OF CONTENTS

ABSTRACT ..... iii

ACKNOWLEDGEMENTS ..... iv

LIST OF FIGURES ..... vii

LIST OF TABLES ..... x

CHAPTER 1 INTRODUCTION ..... 1

CHAPTER 2 DIFFUSER SUPPLY PLENUM OPTIMIZATION ..... 5
2.1 Background ..... 5
2.2 Objective ..... 6
2.3 Methodology ..... 7
2.4 Results ..... 16
2.5 Analysis ..... 20

CHAPTER 3 BASELINE DIFFUSER CHARACTERIZATION ..... 24
3.1 Background ..... 24
3.2 Objective ..... 25
3.3 Methodology ..... 25
3.4 Results ..... 35
3.5 Analysis ..... 43

CHAPTER 4 FIELD CONDITION AIR OUTLET PERFORMANCE ..... 52
4.1 Background ..... 52
4.2 Objective ..... 53
4.3 Methodology ..... 54
4.4 Results ..... 60
4.5 Analysis ..... 66

CHAPTER 5 CLOSE COUPLING AIR OUTLET PERFORMANCE ..... 88
5.1 Background ..... 89
5.2 Objective ..... 89
5.3 Methodology ..... 89
5.4 Results ..... 96
5.5 Analysis ..... 103

CHAPTER 6 CONCLUSIONS AND RECOMMENDATIONS ..... 115
6.1 Diffuser Supply Plenum Design ..... 115
6.2 Standard 70 Characterization ..... 116
6.3 Field Installations ..... 117
6.4 Close Coupling ..... 118
6.5 Recommendations for Designers and Installers ..... 119

APPENDIX A TEST FACILITY ..... 120

APPENDIX B FIELD INSTALLATION TEST RESULTS DIFFUSER DISCHARGE AIRFLOW ZONE PLOTS ..... 136

APPENDIX C CLOSE COUPLING TEST RESULTS DIFFUSER DISCHARGE AIRFLOW ZONE PLOTS ..... 159

BIBLIOGRAPHY ..... 171

VITA ..... 173

LIST OF FIGURES


Figure 1. Picture of the test plenum. ..... 10
Figure 2. Pictures of the different types (left) and the different sizes (right) of the flow equalization disks. ..... 11
Figure 3. Diffuser inlet configuration. ..... 12
Figure 4. Diffuser inlet variation testing configuration. ..... 13
Figure 5. Actual test configuration using TSI Ventilation Meter. ..... 13
Figure 6. Signal to noise ratio results of the noise experiment. ..... 15
Figure 7. Main effects plots for the optimization test. ..... 17
Figure 8. Interaction plots for the optimization test. ..... 20
Figure 9. Duct height added from diffuser inlet to inlet cone. ..... 22
Figure 10. Standard 70 vertical ducted method. ..... 27
Figure 11. Boom microphone configuration. ..... 28
Figure 12. Array of draft meters. ..... 30
Figure 13. Standard 70 Zone Plot. ..... 34
Figure 14. Velocity profile of 12 inch square diffuser at 1200 fpm. ..... 35
Figure 15. Velocity profile of 8 inch square diffuser at 1200 fpm. ..... 36
Figure 16. Noise criterion level for 12 inch square diffuser at 1200 fpm. ..... 37
Figure 17. Plenum total pressure for 12 inch square diffuser at 1200 fpm. ..... 37
Figure 18. Standard 70 zone plot for all square diffusers. ..... 43
Figure 19. Standard 70 zone plot for plaque diffusers. ..... 45
Figure 20. Standard 70 zone plot for perforated round diffusers. ..... 46
Figure 21. Standard 70 zone plot for perforated round/modular core diffusers. ..... 47
Figure 22. Standard 70 zone plot for round diffusers. ..... 48
Figure 23. Standard 70 zone plot for louvered diffusers. ..... 49
Figure 24. Cross flow scan pattern for the forward side of a diffuser. ..... 50
Figure 25. Cross flow scan of 8” perforated round diffuser using vertical ducted method. ..... 51
Figure 26. Experimental setup for field installation condition laboratory testing. ..... 56
Figure 27. Standard 70 throw data at 1200 fpm for 12” square diffuser. ..... 60
Figure 28. Standard 70 zone plot for 12” square diffuser, where (x1,y1) symbolizes start of zone 3 (yellow dot) and (pink dot) gives the x2 value when y2 is 0.2. ..... 62
Figure 29. Field installation run #3 forward throw at 1200 fpm. ..... 63
Figure 30. Field installation run #3 backward throw at 1200 fpm. ..... 64
Figure 31. Zone plot of field install run #3 forward throw 1200 fpm. ..... 64
Figure 32. Zone plot of field install run #3 backward throw 1200 fpm. ..... 65
Figure 33. Main effects plot for field installations forward throw. ..... 67
Figure 34. Interaction plots for field installations forward throw. ..... 68
Figure 35. Experimental setup for close coupling laboratory testing. ..... 91
Figure 36. Top view of close coupling scan pattern. ..... 93
Figure 37. Example close coupling configuration. ..... 95
Figure 38. Standard 70 throw data at 1200 fpm for 12” square diffuser. ..... 97
Figure 39. Close coupling forward throw data at 1150 fpm (in main duct) for Run #3. 97
Figure 40. Close coupling backward throw data at 1150 fpm (in main duct)

for Run #3. 98
Figure 41. Run #3 forward throw zone plot data. 99
Figure 42. Run #3 backward throw zone plot data. 100
Figure 43. Zone plot for forward throw of Run #1 without ceiling. 101
Figure 44. Styrofoam ceiling for Run #1 redo. 102
Figure 45. Zone plot for forward throw of Run #1 with ceiling. 102
Figure 46. Comparison between change in sound [dB] and main duct velocity. 110
Figure 47. Side view of the UNLV throw room [15]. 123
Figure 48. Labview main interface for monitoring system conditions. 124
Figure 49. Interface for monitoring throw room surface temperatures. 125
Figure 50. Throw room LabView motion controller interface. 125
Figure 51. Throw velocity sensor path setup interface. 126
Figure 52. Calibrated nozzle chamber versus Ebtron unit. 130
Figure 53. VAV unit calibration. 131
Figure 54. Plenum pressure test. 133
Figure 55. Published NC contour curves. 134
Figure 56. Sound capture interface using the boom microphone. 135
Figure 57. Forward throw for Run #1. 137
Figure 58. Backward throw for Run #1. 138
Figure 59. Forward throw for Run #2. 138
Figure 60. Backward throw for Run #2. 139
Figure 61. Right side throw for Run #2. 139
Figure 62. Forward throw for Run #3. 140
Figure 63. Backward throw for Run #3. 140
Figure 64. Forward throw for Run #4. 141
Figure 65. Backward throw for Run #4. 141
Figure 66. Right side throw for Run #4. 142
Figure 67. Forward throw for Run #5. 142
Figure 68. Backward throw for Run #5. 143
Figure 69. Left side throw for Run #5. 143
Figure 70. Forward throw for Run #6. 144
Figure 71. Backward throw for Run #6. 144
Figure 72. Forward throw for Run #7. 145
Figure 73. Backward throw for Run #7. 145
Figure 74. Forward throw for Run #8. 146
Figure 75. Backward throw for Run #8. 146
Figure 76. Forward throw for Run #9. 147
Figure 77. Backward throw for Run #9. 147
Figure 78. Right side throw for Run #9. 148
Figure 79. Forward throw for Run #10. 148
Figure 80. Backward throw for Run #10. 149
Figure 81. Forward throw for Run #11. 149
Figure 82. Backward throw for Run #11. 150
Figure 83. Forward throw for Run #12. 150
Figure 84. Backward throw for Run #12. 151
Figure 85. Forward throw for Run #13. 151

Figure 86. Backward throw for Run #13. ..... 152
Figure 87. Forward throw for Run #14. ..... 152
Figure 88. Backward throw for Run #14. ..... 153
Figure 89. Right side throw for Run #14. ..... 153
Figure 90. Forward throw for Run #15. ..... 154
Figure 91. Backward throw for Run #15. ..... 154
Figure 92. Forward throw for Run #16. ..... 155
Figure 93. Backward throw for Run #16. ..... 155
Figure 94. Forward throw for Run #17. ..... 156
Figure 95. Backward throw for Run #17. ..... 156
Figure 96. Right side throw of Run #17. ..... 157
Figure 97. Left side flow for Run #17. ..... 157
Figure 98. Forward throw for Run #18. ..... 158
Figure 99. Backward throw for Run #18. ..... 158
Figure 100. Forward throw for Run #1 with no ceiling. ..... 160
Figure 101. Backward throw for Run #1 with no ceiling. ..... 161
Figure 102. Forward throw for Run #1 with ceiling. ..... 161
Figure 103. Backward throw for Run #1 with ceiling. ..... 162
Figure 104. Forward throw for Run #2. ..... 162
Figure 105. Backward throw for Run #2. ..... 163
Figure 106. Forward throw for Run #3. ..... 163
Figure 107. Backward throw for Run #3. ..... 164
Figure 108. Forward throw for Run #4. ..... 164
Figure 109. Backward throw for Run #4. ..... 165
Figure 110. Forward throw for Run #5. ..... 165
Figure 111. Backward throw for Run #5. ..... 166
Figure 112. Forward throw for Run #6. ..... 166
Figure 113. Backward throw for Run #6. ..... 167
Figure 114. Forward throw for Run #7. ..... 167
Figure 115. Backward throw for Run #7. ..... 168
Figure 116. Forward throw for Run #8. ..... 168
Figure 117. Backward throw for Run #8. ..... 169
Figure 118. Forward throw for Run #9. ..... 169
Figure 119. Backward throw for Run #9. ..... 170

LIST OF TABLES


Table 1. Test Parameter and Noise Condition List for Test Array. ..... 10
Table 2. Test Array with One 4-Level Parameter, Four 3-Level Parameters And One Noise Parameter at 2 Levels. ..... 16
Table 3. Analysis of variation for standard deviation for the optimization test. ..... 19
Table 4. Verification testing results. ..... 21
Table 5. Effect of added height variations for 12-inch diffuser inlet. ..... 22
Table 6. 1/1 and 1/3 octave band center frequencies. ..... 29
Table 7. Vertical draft meter sensor locations. ..... 31
Table 8. Test parameters and noise conditions with corresponding states. ..... 32
Table 9. Test array for Standard 70 testing with output measures. ..... 33
Table 10. Final results for square diffuser at corresponding velocities. ..... 38
Table 11. Final results for plaque diffuser at corresponding velocities. ..... 38
Table 12. Final results for perforated round diffuser at corresponding velocities. ..... 39
Table 13. Final results for perforated square/modular core diffuser at corresponding velocities. ..... 40
Table 14. Final results for round diffuser at corresponding velocities. ..... 41
Table 15. Final results for louvered diffuser at corresponding velocities. ..... 42
Table 16. Plaque total pressure and sound comparisons of manufacturer data and Standard 70 data from this experiment. ..... 44
Table 17. Modular core total pressure and sound comparisons of manufacturer and Standard 70 data. ..... 47
Table 18. Test parameters and noise conditions with different states. ..... 58
Table 19. Test array for field condition variations testing. ..... 59
Table 20. Output array at high state noise condition for the field installation experiment. ..... 59
Table 21. Diffuser output throw ratios, noise criteria level changes and total pressure ratios for field installations compared to Standard 70 data. ..... 66
Table 22. Predicted values and corresponding errors for forward throw. ..... 72
Table 23. Verification testing configurations. ..... 73
Table 24. Results of verification testing configurations for forward throw. ..... 73
Table 25. Predicted and corresponding values for backward throw. ..... 77
Table 26. Predicted and corresponding error values for pressure. ..... 81
Table 27. Verification testing configurations. ..... 81
Table 28. Results of verification testing for pressure. ..... 82
Table 29. Predicted values and corresponding errors for sound level. ..... 85
Table 30. Verification testing configurations. ..... 86
Table 31. Results of verification testing for sound level. ..... 86
Table 32. Summary of standard deviations for field-testing analysis. ..... 87
Table 33. Test parameters and noise conditions with different states. ..... 94
Table 34. Test array for close coupling experiment. ..... 95
Table 35. Output array for the close coupling experiment. ..... 96
Table 36. Diffuser output throw ratios and noise criteria level changes for close coupling compared to Standard 70 data. ..... 100
Table 37. Predicted values and corresponding error for forward throw. ..... 105

Table 38. Predicted values and corresponding errors for backward throw..... 107
Table 39. Predicted values and corresponding errors for total pressure ratio..... 109
Table 40. Adjusted NC levels that account for damper and not main duct velocity. ... 112
Table 41. Predicted values in dB and corresponding errors for sound (NC) level. ..... 114
Table 42. Throw room instrumentation used along with NI LabView..... 127
Table 43. Testing equipment used in part with throw room. ..... 128
Table 44. Systems used in part with the throw room..... 129
Table 45. Inlet conditions for field testing runs. ..... 137
Table 46. Inlet conditions for close coupling runs..... 160

# CHAPTER 1

# INTRODUCTION

It is widely known that under typical field conditions ceiling diffusers and other air outlets are typically installed with inlet conditions significantly different from those specified in Standard 70 resulting in performance differences from manufacturer published performance data. Diffusers often have a flexible duct or a direct elbow duct connection. The air duct running to the diffuser may have a hard radius or an angled entrance into the device, and many have an air-balancing device at or near the diffuser inlet. These inlet conditions can dramatically change the performance of outlets compared to data obtained following Standard 70.

The primary information sources for VAV duct design are ASHRAE's HVAC Applications Handbook [1], California Energy Commission's (CEC) Advanced Variable Air Volume Design Guide [2], and the ASHRAE Handbook of Fundamentals. [3] Information available covering the performance of the air distribution system section from the VAV box to the diffuser includes duct design issues, performance issues, and installation problems. A recent article in HVAC&R Research by Landsberger covers energy and acoustic performance effects of installation variations. [4] Since the mid 1950's, detailed measurements of acceptable mean diffuser velocity speeds and air temperatures in occupied spaces have been available to designers for ventilation spaces. [5]

Dynamics of air movement can have an effect on the air distribution system performance. Supply air traveling within ductwork develops considerable momentum. When the supply-air duct empties its air into the air-conditioned space, this momentum is utilized to help mix the supply air with the room air. How air is delivered and removed from a space is known as room air distribution. [6] This helps to ensure homogeneous or isothermal temperature and

air movement throughout the occupied zone of the conditioned space. This is accomplished by understanding the manipulation of an outlet's throw, drop and spread characteristics. Throw of air is the horizontal and vertical distance a supply-air jet travels before reaching a specified air velocity value after leaving the outlet. The drop of air is the vertical distance the jet travels at its lower edge before reaching the end throw value. The spread of air indicates the divergence of the air-stream after leaving the outlet. This knowledge leads into the description of the flow as it propagates away from the diffuser into the four zones of expansion. [7] These zones of expansion play a major roll in the analysis of the supplemental data recorded during this project.

Installation variations that can result in significant performance variation from ASHRAE Standard 70 installation predominantly concern the length and type of the duct branch, how duct turns are accomplished and how the duct approaches the diffuser. Without sufficient length to develop a uniform flow profile, the flow in duct branches too close to the VAV terminal or in a previous branch being non-uniform, an increase in pressure loss is often the result. If elbows and junctions, such as those made to avoid obstructions in the path of the duct work, are not constructed with minimal friction effects, pressure loss and aerodynamically generated noise will increase. [1] Round flexible ducts can serve as transmitters of breakout sound and also be effective attenuators of upstream sound sources. [1]

The duct approach to the diffuser is also very important, since detrimental effects of improper duct approach cannot be corrected by the diffuser itself. Accepted guidance states that the velocity of the air stream should be as uniform as possible over the entire outlet connection to the duct and must be perpendicular to the outlet face. However, few outlets are installed in this manner. [1,3] Flexible duct connections at the inlet of the diffuser can

increase pressure drop and non-uniform air distribution from the diffuser outlet. [1] An elbow, transition or damper too close to the diffuser inlet, can result in highly directional airflow, increased sound level and increased pressure drop across the outlet of standard diffusers. [1]

Each diffuser manufacturer has published sound levels, for a given diffuser and flow rate, under ideal conditions, per ASHRAE Standard 70. However, duct connections encountered in the field result in significantly different and usually higher sound levels for the same airflow rate. One can assume a 5 point increase in NC for typical field installations compared to published data. [8] For example, an offset of the flexible duct connection between the diffuser and the supply duct can increase the sound power level as much as 12 to 15 dB. [1] A recent laboratory investigation found that a ninety degree elbow from a horizontal duct run to the diffuser, with minimal vertical run, on average increases diffuser sound levels by 6 dB, while a hard turn in the duct run, even several feet from the diffuser, added 4 dB to the sound level. [4] Also, diffusers with a perforated face have been seen to have a higher sound distortion with poor inlet conditions than diffusers with large open cones.

The magnitude of the sound and performance effects associated with installation variations will also depend on variations out of the control of the installer such as variable flow rates. Diffusers are designed to optimally distribute the air at some particular load condition and air volume, but in a typical VAV type installation, air volume rate will vary. Consequently, diffuser throw, room airflow velocity and sound levels can be significantly different from that specified design point. [1]

This research, funded by ASHRAE, Inc. under project 1335-RP, identified quantitative data on the performance differences between ASHRAE Standard 70 baseline data and typical field installations for ceiling diffusers. This data can provide the HVAC

design engineer the information necessary to predict diffuser performance in a wide variety of field installations. The engineer can use the data from this project to adjust installations to achieve the best performance possible in a given situation. The results can lead directly to improved system designs with likely benefits to energy efficiency, occupant comfort and worker productivity.

This report is organized into four chapters covering the step-by-step process taken to determine the quantitative differences between Standard 70 data and typical field installations that take into account different inlet conditions. Chapter 2 covers the design of a diffuser supply air inlet plenum that substantially exceeds Standard 70 requirements and gives a method for efficient supply plenum design for any throw room. Chapter 3 covers Standard 70 testing using the optimized plenum, where the baseline data for the output measures (throw, sound and pressure data) were recorded and analyzed for each type of ceiling diffuser. In Chapter 4, the baseline data was compared to data from field condition testing for a number of different diffuser inlet combinations. Predictive algorithms for each output measure based on diffuser inlet conditions were developed. Chapter 5 covers a comparison of the baseline Standard 70 output measures against data from a close coupling setup. Finally, conclusions are made and recommendations given to better improve further testing and real world installations.

# CHAPTER 2

# DIFFUSER SUPPLY PLENUM OPTIMIZATION

An outlet diffuser airflow supply plenum design was experimentally optimized to minimize spatial variation in airflow velocity at the inlet of the test diffuser. Standard 70 specifies a maximum variation of 10 percent. Variation achieved was a standard deviation of 2.6 percent, which gives a maximum variation of 5.2 percent for over ninety-seven percent of the inlet area. To achieve minimal variation in airflow velocity, four test parameters were varied. There were three for the flow equalization device and one for plenum air supply inlet configuration. To minimize airflow velocity variation across a wide spectrum of user conditions, testing was completed across two user selectable conditions, inlet diameter and volume flow rate. Main effect and interaction results were analyzed using analysis of variation. This design gives specific build guidance towards achieving the best plenum performance.

## 2.1 Background

ANSI/ASHRAE Standard 70-2006 is the accepted method of testing the performance of air outlets. [9] The standard defines laboratory methods of testing air outlets used to terminate ducted and non-ducted systems for distribution and return of building air. For air outlet testing, the standard describes two methods of testing, ducted and plenum. The ducted method can be considered an ideal installation with a long, vertical rigid duct leading to the diffuser. The plenum method is a laboratory simulation of an ideal installation, with the diffuser inlet connected to a large plenum with ideally stagnant air. The plenum method is often the method of choice because it allows for quick change-out

of diffusers with different inlet shapes and sizes, and a smaller requirement for vertical space above the ceiling in the test facility.

The standard specifies that construction of the plenum should provide uniform and unidirectional air velocities such that the velocity profile at the entrance plane of the test device must be within 10 percent at any location. The standard also notes that since practical considerations will limit the shape and volume of the plenum, equalization devices may be required to accomplish the flow uniformity but does not specify the equalization device construction or placement in the plenum. Also, the designer is left to decide the volume, shape and supply air inlet configuration of the plenum. Thus, the design of the plenum and accompanying flow equalization device has become an art based on knowledge of the physics of airflow and experience in test device design.

## 2.2 Objective

The objective of this experiment was to design and build a plenum that could be used to characterize diffuser performance, as well as, develop guidance for other designs with similar flow objectives. The goal for that objective was that the performance of the plenum should not only meet Standard 70 specifications but come as close as possible to ideal. The main quality measure was the level of uniformity of airflow at the entrance of the test diffusers. A secondary objective was to develop and perfect the test methods for measuring diffuser throw and sound generation for the laboratory and the design of experimental methods used to test for parameter and noise variation effects. These testing and experimental design methods were to be used for all the following tests performed in this project. [10]

## 2.3 Methodology

The one output measure was the airflow velocity across the plane of the diffuser inlet. The quality characteristic derived from this measure was the variation in airflow velocity across the plane. To meet the experiment objectives economically, a Taguchi designed fractional factorial experiment was developed using the four test parameters most likely to be used for similar use plenums and that would be most likely to affect the output. Other parameters were held constant during the experiment. To cover the standard range of test airflow rates and diffuser inlet diameters, testing was performed near the two extremes of airflows reported in published performance data for two different inlet diameters.

### 2.3.1 Experimental Design

The ideal energy transformation is for air to flow into the plenum and exit at the inlet to the diffuser with a uniform vertical velocity and zero horizontal velocity. Thus, any variations from ideal would be variations in either direction or airspeed across the plane of the diffuser inlet. The variations of interest would be large enough and across enough of the inlet plane to cause some variation in diffuser performance from ideal conditions. Considering a circular diffuser inlet, a variation in flow velocity that would likely result in a significant variation in diffuser output velocity would cover an angle of at least 90 degrees. This assumes that less extensive variations would tend to diffuse into the flow and not be detectable in the output flow. Therefore, an angular frequency of two cycles for a rotation around the inlet or $1/\pi$ (one cycle per 180 degrees) was used. That required four samples around the inlet plane. These measurements were taken equally spaced, approximately 1.5 inches inside of the circumference. Across the radius, a variation in

flow velocity that would likely result in a significant variation in diffuser output velocity, would be a difference in velocity between the center and any velocity near the edge. Therefore, a maximum spatial frequency of 1 (one cycle per diameter) was used requiring a long any diameter line that traced the circumference of the inlet diameter and had a center point along with two points, each near opposite ends of the circumference. Thus, in total, five measurements were made in the inlet plane for each test run. From these measurements a standard deviation for each run condition was determined.

In product optimization, noise conditions are conditions that are not controlled by the designer but are set by the product user or result from external factors not controlled by either the designer or user. The noise conditions considered that could affect the output were the diffuser inlet size and the volume airflow rate. Tests were conducted with the volume airflow rate at a low and high level that corresponds to the typical low and high levels reported in the diffuser performance specifications. Thus, for an 8-inch diameter inlet, low flow was 200 cfm, high was 800 cfm, and for a 12-inch diameter inlet, low was 400 cfm, high was 1200 cfm.

Test conditions are parameters that the designer can adjust to obtain optimum performance. For the plenum, three parameters determined the design of the flow equalization device in the plenum between the top inlet to the plenum and the inlet to the diffuser. The flow equalization device tested was a circular perforated plate. The flow equalization device parameters were the distance from the plenum inlet, the size of the flow equalization disk, and the percentage of open area (due to perforation dimension and quantity) of the disk. A forth parameter was the ratio of flow from the top to the flow from two inlets on the sides of the plenum. A list of the test parameters and noise

conditions is shown in Table 1. A picture of the plenum exterior showing the inlet configuration is shown in Figure 1. The plenum has dimensions of 72 inches long by 41 inches high by 45 inches wide. The top inlet duct has a 12-inch diameter, the two side inlet ducts are 10-inches in diameter. An 18-inch outlet transition piece is placed between all ducts and the plenum wall. The different types of flow equalization disks and their sizes are shown in Figure 2.

Obviously, there are many more parameters in the plenum design that could affect the inlet velocity variation. Among them are plenum size (three dimensions), diameter of plenum flow inlet ducts, number of plenum flow inlet ducts, design of the inlet cone attached to the diffuser inlet, and length of straight duct between the diffuser inlet and the inlet cone. Based on logical argument, a designer can generally assume that increases in any of those parameters would not result in significant degradation of the results presented here, and could result in some improvement. In this experiment a small plenum with relatively small diameter plenum inlet ducts, one to three plenum inlet ducts, and minimum straight duct between the diffuser inlet and the inlet cone were used, thus providing an economical value for these parameters while still designing to exceeding Standard 70 requirements.

Table 1. Test Parameter and Noise Condition List for Test Array.

| Parameter | Low State | Mid State | High State |
|---|---|---|---|
| 1. Inlet air configuration | All from center inlet | Center and side inlets open | Center inlet partially closed |
| 2. Distance of flow equalization to center inlet | 4 inches | 8 inches | 12 inches |
| 3. Size of flow equalization disk | 8 inches diameter | 12 inches diameter | 18 inches diameter |
| 4. Open area of flow equalization disk | 50 percent | 40 percent | 13 percent |
| Noise Condition | Low State | | High State |
| 1. Diffuser inlet diameter | 8 inches | | 12 inches |
| 2. Volume flow rate | Low | | High |

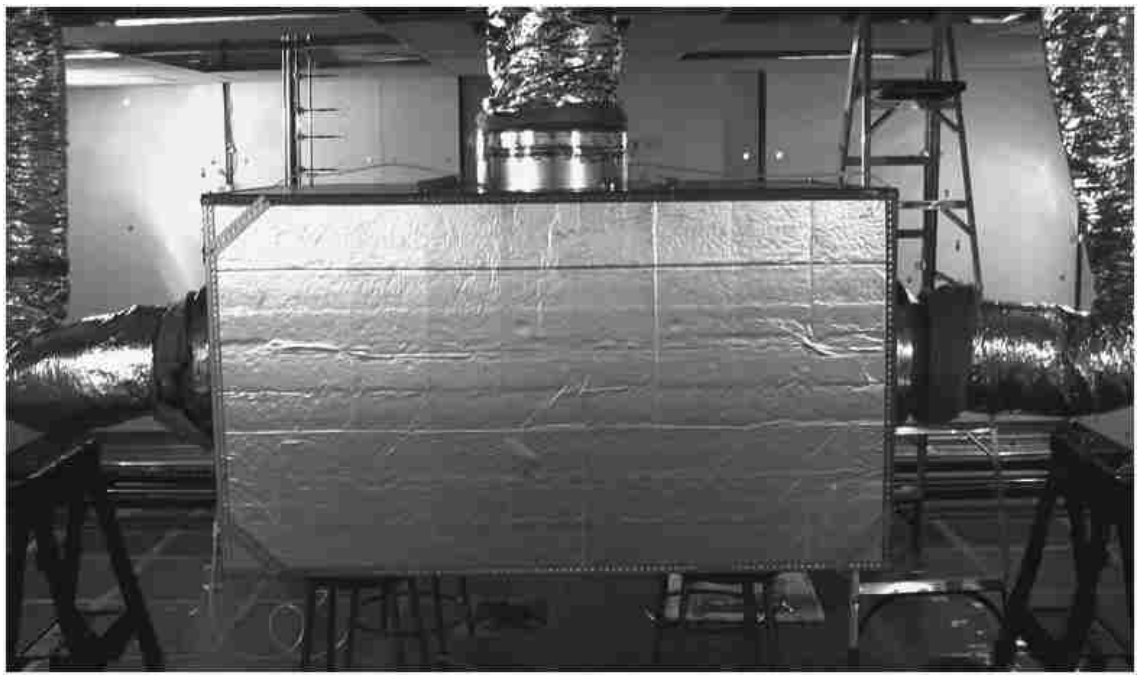

Figure 1. Picture of the test plenum.

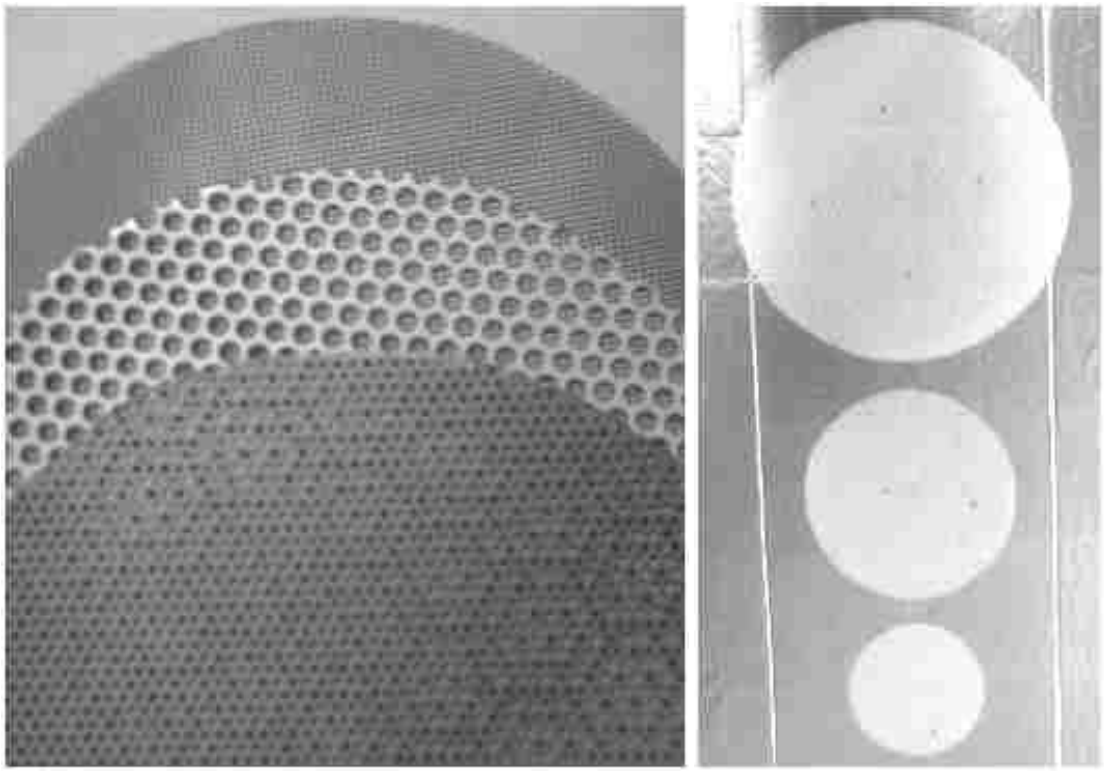

Figure 2. Pictures of the different types (left) and the different sizes (right) of the flow equalization disks.

The diffuser inlet condition used for the experiment was a round inlet formed by the back of a standard perforated diffuser with a short inlet cone attached to the diffuser as shown in Figure 3. The inlet cone is expected to create a smooth transition of the airflow from zero velocity to the velocity of the diffuser inlet. The core outer diameters were 14 inches for the 8-inch inlet, 16 inches for the 10-inch inlet, and 18 inches for the 12-inch inlet.

Figure 3. Diffuser inlet configuration.

2.3.2 Laboratory Instrumentation

All tests for this project were run under steady-state isothermal conditions. Plenum volume airflow was set using a variable frequency drive fan motor and measured with an Ebtron precision airflow/temperature meter in the supply duct with an installed airflow accuracy of ±3 percent of reading and a repeatability of ±0.25 percent of reading. Since the output of concern is airspeed variation, the absolute value of the volume airflow (a noise condition) is not critical so long as it is close to the noise condition. In these tests, volume airflow within 5 percent of the noise condition level was considered acceptable. Each of the five measurements, shown in Figure 4, for a test run were an average of measurements taken every two seconds over at least one minute. Points one through four were taken approximately 1.5 inches from the edge of the diffuser inlet walls. Airspeed measurements were taken using a TSI VelociCalc Plus Multi-parameter Ventilation Meter with a published accuracy of ±3 percent of reading, examples given in Figure 5.

Measurements taken for this experiment are used for comparison and not for absolute values. The replication variation (from one test to another) of the instrument is anticipated to be less than 1.3 percent.

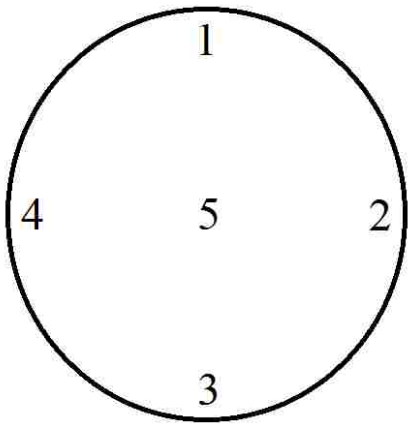


Figure 4. Diffuser inlet variation testing configuration.

Figure 5. Actual test configuration using TSI Ventilation Meter.

### 2.3.3 Noise Experiment

Prior to performing the optimization experiment, a 'noise experiment' was performed, where the plenum test parameters are set at a nominal level and the noise factors are varied from high to low to determine the effect of noise levels on the output variation. The noise factors for this test were diffuser inlet size and volume flow rate. The nominal design configuration had all four test parameters set at a mid-state. For the noise test, a full factorial test was performed where all four combinations of diffuser inlet size and volume flow rate were tested. Airspeed data was taken at the five measurement points previously described. The five individual airspeed measurements were normalized to the average of the five measurements. A signal-to-noise ratio (S/N) was calculated for each test run using the formula,

$$S/N = -10\log_{10} s^2 ,$$

where $s$ is the sample standard deviation in non-dimensional form of a fraction of mean airspeed.

Signal-to-noise is a standard parameter used for determining the level of output variation due to parameters in the test matrix, in this case the two noise conditions. The higher the signal-to-noise ratio, the smaller the output variation due to noise. The results are shown in Figure 6. From the results it was determined that variation increases significantly with size of inlet and slightly with increased airflow. The goal of the parameter experiment is to determine the parameter levels that achieve the lowest airflow velocity variation under all the noise conditions. Figure 6 shows that certain levels of the

noise conditions result in greater average variation in the noise experiment and would be expected to cause similar effects in the parameter design experiment. As a result, to create a robust design where output is less sensitive to noise effects, parameter optimization testing should include those levels of the noise conditions. Therefore, the noise condition for the optimization testing was high and low airflow with all test runs at the largest diffuser inlet diameter.

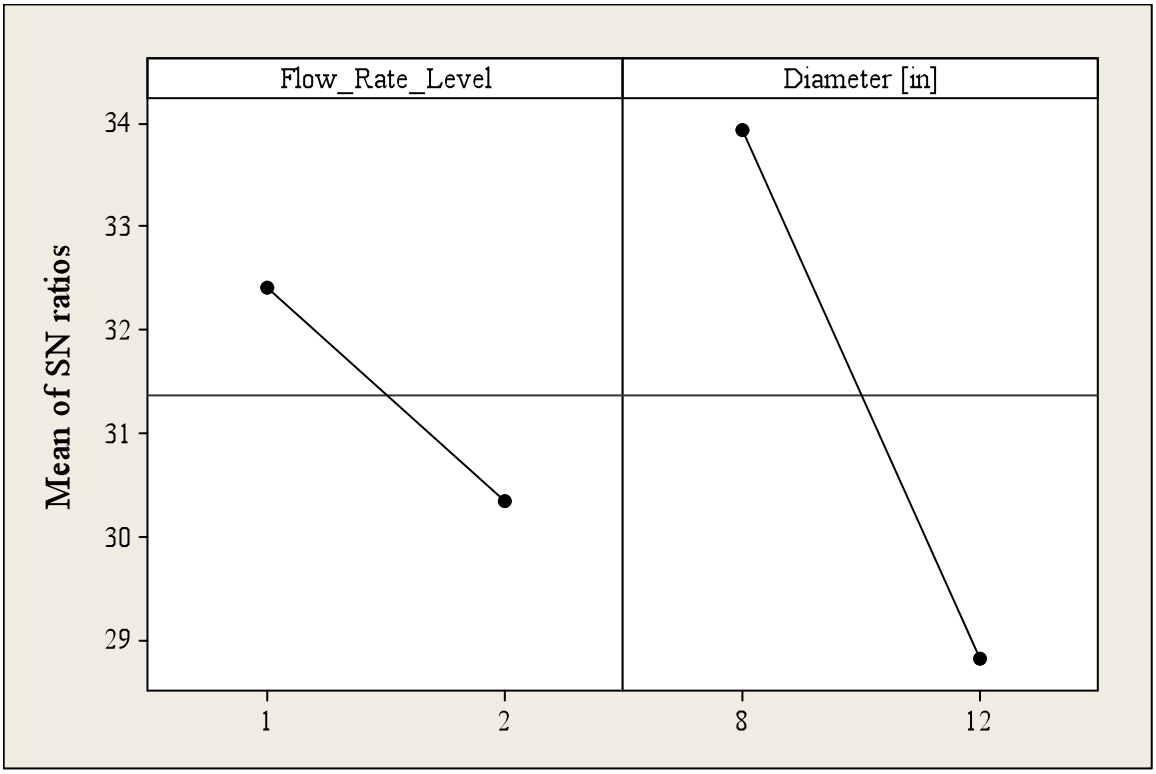


Figure 6. Signal to noise ratio results of the noise experiment.

2.3.4 Optimization Experiment

A Taguchi Orthogonal Array was used to test the system for all the parameter variations and the noise condition of the two airflow rates. The L9 array, shown in Table 2, was chosen for this experiment. The array required nine tests and has the ability to

evaluate the main effects of four parameters at three levels. The array is balanced by choosing parameter levels such that any condition of any parameter is tested with an equal number of high and low conditions of the other parameters. This testing method reduces interaction effects in the average output and exposes all parameters to the different levels of the other parameters.

Table 2. Test Array with One 4-Level Parameter, Four 3-Level Parameters And One Noise Parameter at 2 Levels.

| | Parameters | | | | Noise Condition Level | |
|---|---|---|---|---|---|---|
| Test No. | Inlet Configuration | Flow Equalizer Distance [in] | Flow Restriction | Flow Equalizer Diameter [in] | Low Flow 400cfm | High Flow 1200cfm |
| 1 | 1 | 4 | 1 | 8 | | |
| 2 | 1 | 8 | 2 | 12 | | |
| 3 | 1 | 12 | 3 | 18 | | |
| 4 | 2 | 4 | 2 | 18 | | |
| 5 | 2 | 8 | 3 | 8 | | |
| 6 | 2 | 12 | 1 | 12 | | |
| 7 | 3 | 4 | 3 | 12 | | |
| 8 | 3 | 8 | 1 | 18 | | |
| 9 | 3 | 12 | 2 | 8 | | |

Similar to the noise experiment, the five airspeed measurements were normalized to the average of the five measurements for each noise condition and a signal-to-noise ratio (S/N) was calculated for each run from the ten normalized airspeed measurements.

## 2.4 Results

The information used to analyze the optimization experiment included the main effects on airspeed variation from each of the four parameters, the interaction between

parameters in airspeed variation and the statistical significance of the main effects of each parameter.

2.4.1 Optimization Experiment

Plots of the main effects for the optimization experiment are shown in Figure 7. The plots show the signal-to-noise ratio at the three different levels of each parameter.

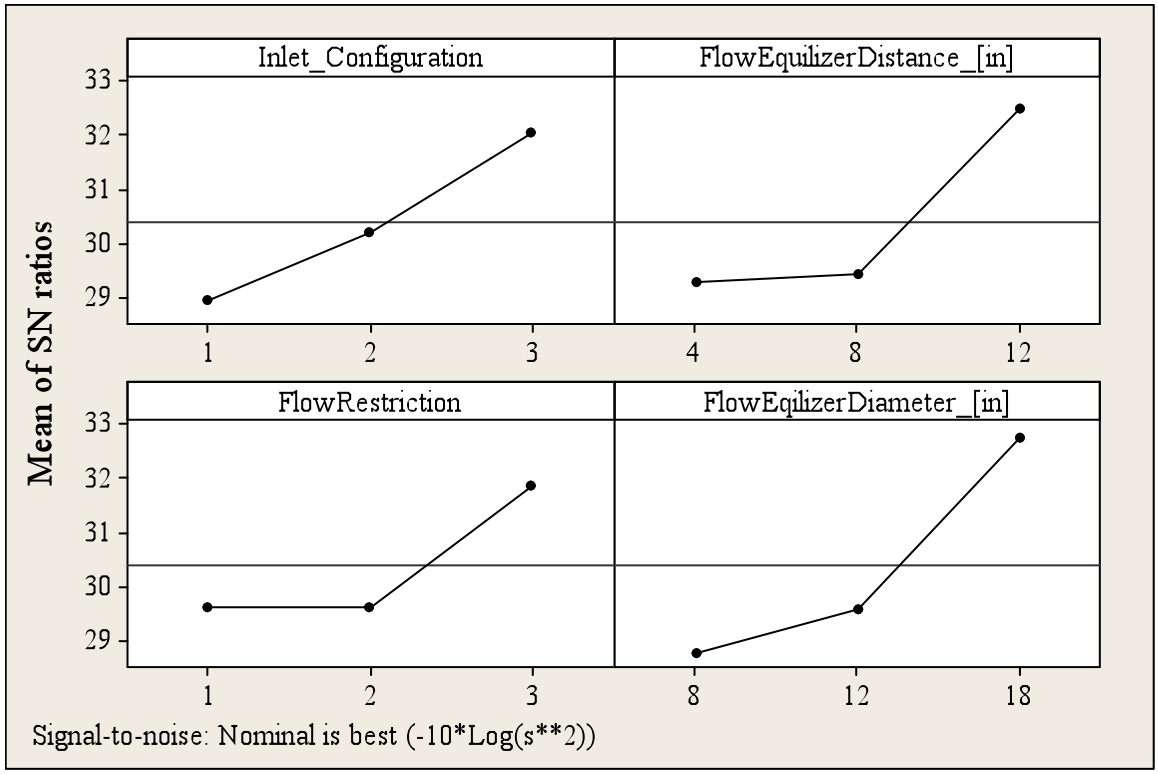


Figure 7. Main effects plots for the optimization test.

These results show that inlet flow condition 3 (flow primarily from the side inlets), flow equalizer position 3 (18 inches from the top plenum inlet), flow equalizer disk size 3 (18 inch diameter disk), and flow equalizer open area 3 (most restrictive) produced the highest signal-to-noise ratio, which should equate to the configuration with the lowest flow velocity variation which is the signal in this case. In other words, this configuration

is predicted to have the least variation in output across the inlet area and at the two test airflow rates.

The significance of the main effects were calculated using an analysis of variatiance. The results are shown in Table 3 (Note that only two to three digits are significant). The adjusted sum of the squares (Adj SS) shows how much of the total variation was due to the corresponding factor. For example, inlet configuration had an adjusted sum of the squares of 0.000740, the total sequential sum of the squares (Seq SS) was 0.00282, thus the fraction of the variation due to inlet configuration was 0.00074/0.00282 or roughly 0.26 or 26 percent. The F-statistic shows the ratio of variation due to that factor and the variation due to noise when taking into account degrees of freedom. The higher the more significant. The P-value shows the significance of the factor variation in terms of the probability that this variation could be due to random sampling. Normally, a confidence level of 95 percent, or P-value of less than 0.05 or 5 percent is needed to consider results significant. For inlet configuration, the P-value shows a 0.7 percent chance that the variation was due to random sampling (a 99 percent confidence level). The summary of this analysis shows that the variation measured for inlet configuration, flow equalization distance and flow equalization diameter were significant and the variation measured for flow restriction was marginally significant. This gives valuable information on the levels of confidence that should be given to the results.

Table 3. Analysis of variation of standard deviations for the optimization test.

| Source | DF | Adj SS | Adj MS | F | P |
|---|---|---|---|---|---|
| Inlet Configuration | 2 | 0.0007396 | 0.0003698 | 9.24 | 0.007 |
| Flow Equalizer Dist_[in] | 2 | 0.0006198 | 0.0003099 | 7.74 | 0.011 |
| Flow Restriction | 2 | 0.0003064 | 0.0001532 | 3.83 | 0.063 |
| Flow Equalizer Diameter_[in] | 2 | 0.0008012 | 0.0004006 | 10.01 | 0.005 |
| Error | 9 | 0.0003602 | 0.0000400 | | |
| Total | 17 | 0.00028237 | | | |

Before going with these levels, the interaction plots were checked to determine if there were any strong interactions that would indicate any inaccuracy in a choice based solely on the main effects. The interaction plots are shown in Figure 8. These plots show a strong interaction between some parameters. Generally speaking, in an interaction plot, parallel lines show no interaction, non-parallel but matched increasing or decreasing lines show moderate interaction, and non-parallel and non-matched increasing or decreasing lines show strong interaction. For example, for interaction between inlet configuration and flow equalization distance, the top left plot, we see a non-parallel and non-similar increasing or decreasing lines showing a strong interaction between inlet configuration and flow equalizer distance. At flow equalization distance of 4, inlet configuration 1 has the highest standard deviation, but at an flow equalization distance of 12, inlet configuration 1 has the lowest. This and many of the other interactions could be anticipated on physical grounds since the flow equalization device was primarily inline with the main plenum inlet and thus would be expected to have its greatest effect on inlet configuration 1 and only a small effect on inlet configuration 3.

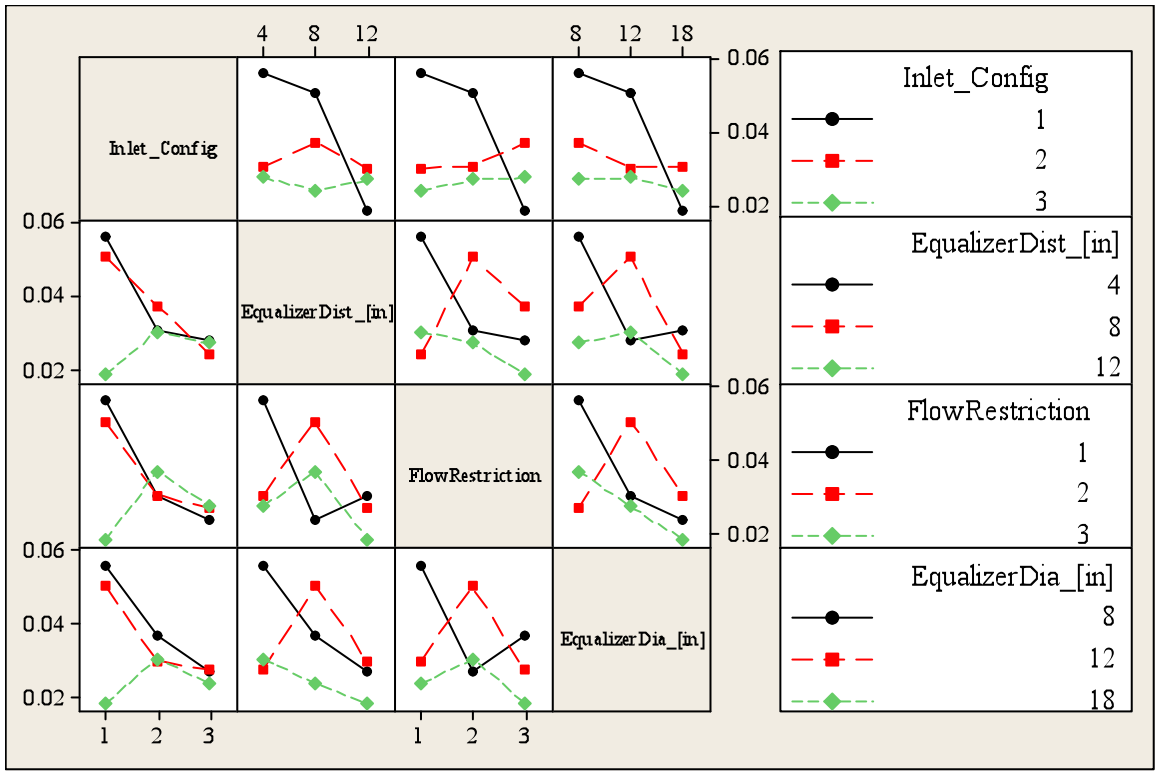


Figure 8. Interaction plots for the optimization test.

## 2.5 Analysis

For the optimum configuration predicted as inlet configuration 3, flow equalization distance 12, flow restriction level 3, and flow equalization disk size 18, the model predicted a standard deviation of 0.31 percent. Note however that the interaction plots showed that although the lowest average standard deviation for the levels of inlet configuration was level 3, the lowest single value of standard deviation occurred with inlet configuration 1, when the other parameters were at the level predicted to be the optimum. Because of the high interaction levels, verification testing was done for inlet configuration at all three levels, while the other three parameters were held at the predicted optimum levels. The predicted and measured results are shown in Table 4. These verification tests show that although all actual measured standard deviations were

well within Standard 70 guidelines, they were higher than predicted by the model. Also, instead of plenum inlet configuration 3, configuration 2 had the lowest standard deviation. These inaccuracies in the model can be attributed to the interaction between parameters. The experimentally verified optimum configuration, test number 2 in Table 4, had a standard deviation of 0.8158 percent. This means that any value must be off by slightly over six standard deviations to reach the limit of ±5 (6*0.8158 = 4.8948) percent variation. This happens less than one time per million.

Table 4. Verification testing results.

| Test Number | Test Parameter Configuration | | | | Total s |
|---|---|---|---|---|---|
| | Inlet configuration | Flow equalization distance [in] | Flow restriction | Flow equalization diameter [in] | Standard Deviation [%] |
| 1 | 1 | 12 | 3 | 18 | 1.3763 |
| 2 | 2 | 12 | 3 | 18 | 0.8158 |
| 3 (predicted optimum) | 3 | 12 | 3 | 18 | 2.6261 |

Through plenum optimization testing, it was determined that by having the inlet cone directly on the diffuser inlet gave the least among of variance in flow at the diffuser inlet.

2.5.1 Performance Variation Effects Due to Inlet Duct Length

It was later determined that for a perforated diffuser with an 8-inch inlet that had 0-inches of added height from cone to diffuser inlet lead to significantly decreased distance in throw from the diffuser when compared to testing using the vertical duct method of Standard 70. Further investigation showed that a section of 7-10 inches of straight duct added to the 8-inch diffuser inlet, as shown in Figure 9, resulted in diffuser output identical to using the ducted method. Table 5 shows that, experimentally, the addition of

the straight duct onto the 12-inch inlet resulted in slightly higher standard deviation of flow velocity across the inlet of the diffuser.

Figure 9. Duct height added from diffuser inlet to inlet cone.

Table 5. Effect of added height variations for 12-inch diffuser inlet.

| | Added height between Cone and Diffuser Inlet | | | |
|---|---|---|---|---|
| Location | 15 [in] | 10 [in] | 4 [in] | 0 [in] |
| E [1] | 1.00616 | 0.992602 | 0.99046 | 1.008282 |
| S [2] | 0.982781 | 0.978368 | 0.976613 | 1.00112 |
| W [3] | 0.977307 | 0.979422 | 0.9947 | 1.006629 |
| N [4] | 0.984915 | 1.002091 | 0.997462 | 0.997264 |
| MID [5] | 1.048838 | 1.047517 | 1.040764 | 0.986704 |
| STDEV | 0.02942 | 0.028321 | 0.024157 | 0.008632 |
| STDEV CIR | 0.012659 | 0.011344 | 0.009257 | 0.005069 |

### 2.5.2 Performance Variation Effects Due to Inlet Cone Design

One improvement to flow equalization might be to have a cone with a smooth rate of increase in cross-sectional area such as an exponential horn. This report used a linear cone, with a constant rate of cross-section area increase. That cone was very inexpensive to obtain, yet may have caused flow variation at the diffuser inlet. Figure 3 shows the linear cone as it would be installed directly on the diffuser inlet.

# CHAPTER 3

# BASELINE DIFFUSER CHARACTERIZATION

Ideal diffuser performance data was collected experimentally for six typical ceiling diffuser types using primarily an airflow supply plenum in accordance with ASHRAE Standard 70. Testing covered two diffuser parameters, diffuser type and inlet diameter, and one system parameter, diffuser inlet neck velocity. From the experimental data, diffuser throw, sound power, and pressure differential across the diffuser was determined for each test condition. These results were used as a baseline for comparison against results from typical field installation conditions.

## 3.1 Background

ANSI/ASHRAE Standard 70-2006 is the accepted method of testing the performance of air outlets. [9] The standard defines laboratory methods of testing air outlets used to terminate ducted and non-ducted systems for distribution and return of building air. For air outlet testing, the standard describes two methods of testing, ducted and plenum. The plenum method was the primary method used in these experiments because it allows for quick change-out of diffusers with different inlet sizes and shapes, and in some cases a smaller requirement for vertical space above the ceiling in the test facility. Details of the plenum design and qualification were given previously in Chapter 2. For one case (12-inch inlet, round diffuser) the ducted method was used because the diffuser size was too large for the plenum outlet. As a crosscheck of the two methods, a few diffusers were tested using both plenum and ducted methods.

## 3.2 Objective

The objective was to obtain diffuser throw, sound power, and backpressure performance data when operating at what is considered ideal installation conditions. The data was collected at three different flow rates on eighteen different diffusers (six different types of ceiling diffusers, each at three different inlet neck sizes). This data was the basis of comparison against real world field installation conditions that are examined in Chapters 4 and 5.

## 3.3 Methodology

Output measures and derived output measures included:

1. Room 1/3 octave band sound power level and resulting room NC.
2. Pressure difference between the inside of plenum and inside test room.
3. Diffuser throw distance from center of diffuser.

Sound power level in the test room was measured at 1/3 octave bands from 25 to 10,000 Hz. From a subset of those levels, the octave band sound power levels from 125 to 4,000 Hz is calculated, which are then used to determine the room Noise Criteria (NC) level based on ANSI/ASA 12.2 as recommended by ASHRAE. [9] The total pressure in the plenum is measured according to ANSI/ASHRAE Standard 70-2006 as the difference between the pressure in an air line with four pressure taps spaced around the perimeter of the inside of the plenum and the pressure in the throw room. The static pressure in both the plenum and the throw room are assumed to be the same as the total pressure in each space. In the few cases where a vertical duct was used for the diffuser inlet instead of the

plenum, the static pressure was measured at three duct diameters from the diffuser inlet. Total pressure in the duct was determined by summing the static pressure and the velocity pressure, which was based on inlet size. Draft air velocity is measured with a horizontal scan from the diffuser using a vertical array of draft sensors. The measurement thus covered a vertical plane. That plane was normally perpendicular to the edge of the diffuser, but in a few cases, the maximum throw direction was found to be non-perpendicular to the diffuser edge. The maximum throw direction was identified from results of a scan in the vertical plane parallel to the diffuser edge and six feet downstream. From diffuser throw scans in the maximum throw direction, the maximum velocity at each distance from the diffuser is the maximum velocity measured in the vertical plane from which the 150, 100, and 50 fpm throw distances are determined.

### 3.3.1 Laboratory Instrumentation

A National Instruments LabView virtual instrument was used to monitor and record airflow, supply air temperature, room temperature, supply static pressure, draft meter array position and draft meter readings. Sound level measurements were made with all systems off except for the air supply, boom microphone and the monitoring and recording computer. Sound measurements were taken with the air supply on and off to record the diffuser generated sound due to airflow and a background or ambient noise level without airflow.

### 3.3.2 Experimental Setup

As described in the previous chapter, the plenum was designed so that the flow entering the diffuser inlet would be symmetrical with a maximum of 10 percent variation at any point measured around the inlet as per Standard 70. The diffuser was installed

flush with the suspended ceiling, and ten feet from the nearest wall. There were no obstructions breaking the plane of the ceiling.

To crosscheck the plenum method used for Standard 70 testing, for several cases, a replicate test was conducted using the vertical ducted method described in the ANSI/ASHRAE Standard 70-2006. This method called for a minimum vertical inlet duct length of six diameters and a pressure ring measurement at three diameters from the diffuser inlet. In this setup, shown in Figure 10, the vertical duct should be sufficiently long for the flow to stabilize with a uniform velocity cross-section before entering the diffuser. The results showed that the results from the plenum testing were nearly identical to results from the vertical duct method.

All tests for this project were run under steady-state conditions. Volume airflow corresponding to the required inlet velocity was set and allowed to stabilize. Testing was performed under isothermal conditions.

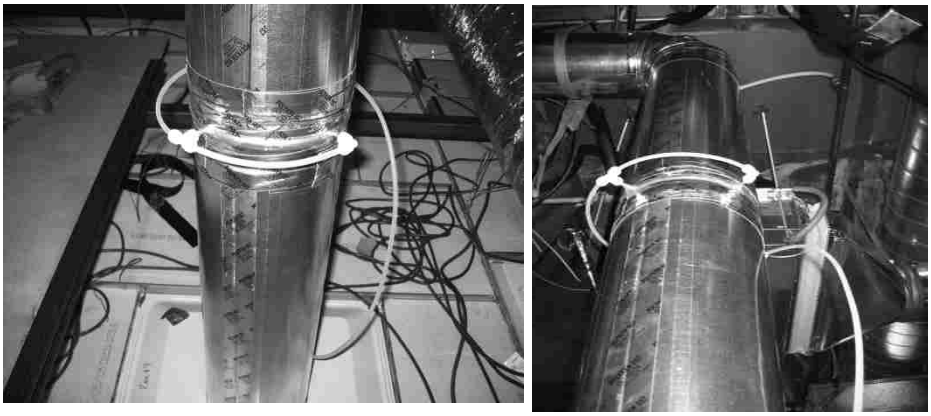

Figure 10. Standard 70 vertical ducted method.

The ideal energy transformation is for air to flow into the diffuser inlet and exit at the diffuser discharge with no pressure loss other than velocity pressure, no sound generation

and the intended discharge velocity profile. Actual ideal installation measurements show variations from ideal output due to flow restrictions in the diffuser, turbulence induced in the flow due to diffuser structure and anomalies in discharge throw due to the geometry of the diffuser design.

Sound measurements were made using a rotating boom microphone placed in a location that was determined to be in the reverberant field, meaning the reverberant field was dominant. Physically, it was as far from the diffuser as possible, near a corner while maintaining a distance of five feet from either wall as shown in Figure 11.

Figure 11. Boom microphone configuration.

The sound signal was captured by the analysis computer and converted to 1/3 octave band sound levels. In post-processing, the 1/3 octave band levels were transformed to 1/1 octave band levels and corrected for a room background sound level. Then, for each octave band a room reverberation correction and a standard room correction of minus 10 dB, to convert from sound power to sound pressure, were applied to the noise criteria curves to obtain the noise criteria level (NC) for the sound generated by the discharge. [3] The room reverberation correction was an average of corrections derived from both the time it takes for the sound pressure level in a room to decrease 60 dB and the measured

sound level in the room with a calibrated source. It was recommended by ASHRAE, in Standard 70, that the 1/1 octave band levels of most significance were: 125, 250, 500, 1000, 2000 and 4000 Hz center frequencies. [9] The 1/3 octave band frequencies that make up the 125 Hz 1/1 octave band frequency are 100, 125 and 160 Hz. A simple equation was used to take the sound pressure level averages from each 1/3 octave band frequencies and average them into the 1/1 octave band center frequency sound pressure level, Lp, of 125 Hz, measured in decibels. Table 6 shows the other 1/1 center frequencies and the corresponding 1/3 octave band frequencies suggested in Standard 70.

$$Lp(1/1,125\ Hz) = 10\log_{10}(10^{Lp(1/3,100\ Hz)/10} + 10^{Lp(1/3,125\ Hz)/10} + 10^{Lp(1/3,160\ Hz)/10})$$

Table 6. 1/1 and 1/3 octave band center frequencies.

| 1/1 Octave Bands | 1/3 Octave Bands |
|---|---|
| 125 Hz | 100,125,160 Hz |
| 250 Hz | 200,250,315 Hz |
| 500 Hz | 400,500,630 Hz |
| 1000 Hz | 800,1000,1250 Hz |
| 2000 Hz | 1600,2000,2500 Hz |
| 4000 Hz | 3150,4000,5000 Hz |

The noise criterion curves produced by Beranek specify maximum sound levels permitted in each octave band for a specific NC curve. [11] Algorithms based off the NC curve levels for each center frequency determined the overall NC level for each test.

A vertical array of draft meters, as shown in Figure 12, was used to record diffuser throw velocities at varying distances from the diffuser. The height of each sensor is listed in Table 7 where TV17 is the top sensor. The draft sensor vertical array was scanned in

the direction of maximum flow velocity on the diffuser side that had the longest run distance from the center of the diffuser. This gave the greatest amount of useful data that could be used for comparison with the future field installations.

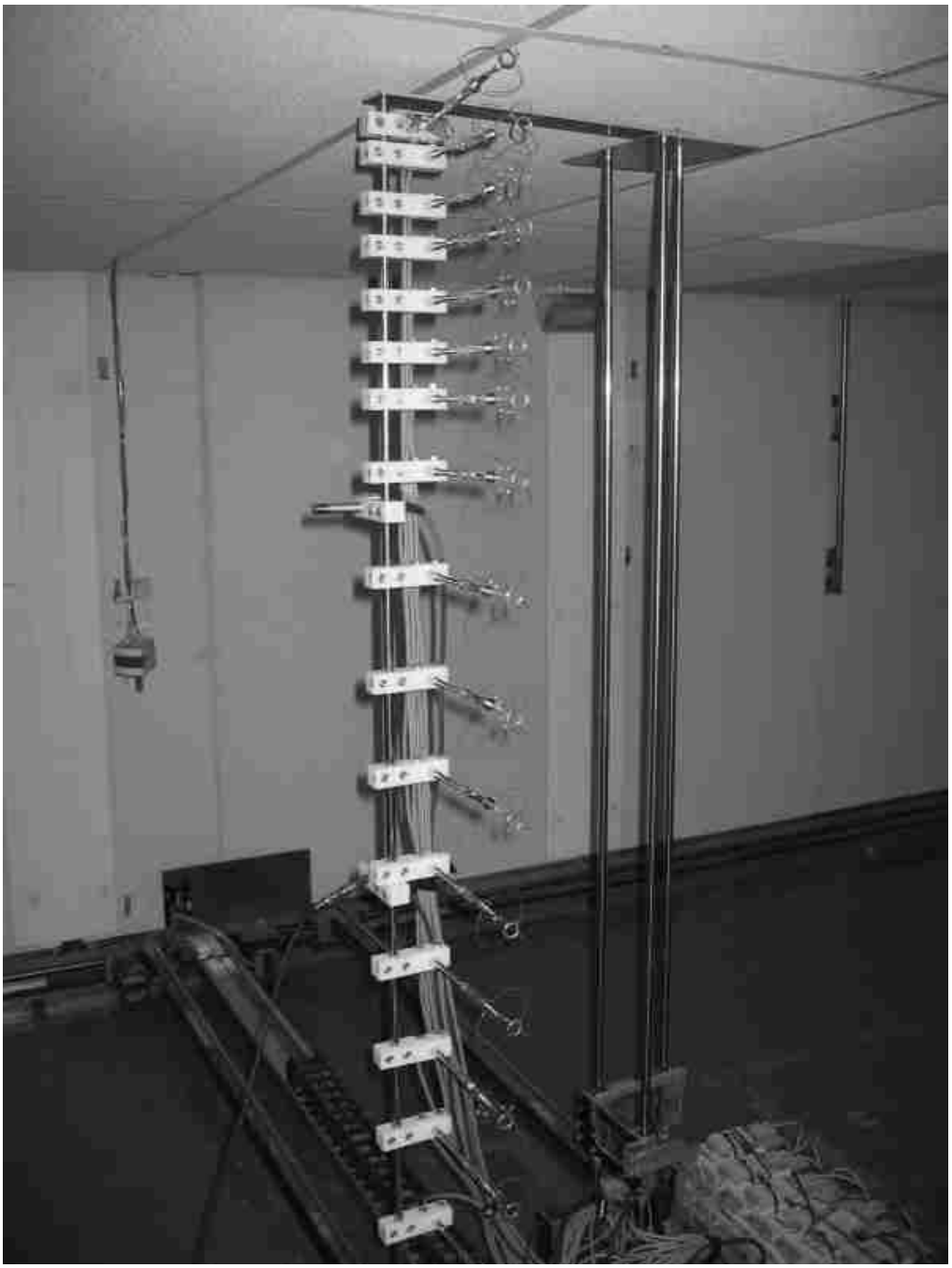

Figure 12. Array of draft meters.

Table 7. Vertical draft meter sensor locations.

| Sensor # | Height from Floor [in] | Height from Ceiling [in] |
|---|---|---|
| TV17 | 107.25 | 0.75 |
| TV16 | 104.75 | 3.25 |
| TV15 | 102.5 | 5.5 |
| TV14 | 100 | 8 |
| TV13 | 97.75 | 10.25 |
| TV12 | 95.5 | 12.5 |
| TV11 | 93 | 15 |
| TV10 | 90 | 18 |
| TV9 | 85 | 23 |
| TV8 | 78.75 | 29.25 |
| TV7 | 73.75 | 34.25 |
| TV6 | 67.75 | 40.25 |
| TV5 | 56 | 52 |
| TV4 | 44 | 64 |
| TV3 | 31 | 77 |
| TV2 | 25 | 83 |
| TV1 | 16 | 92 |

Inlet duct velocity was the noise condition for the Standard 70 testing. Inlet duct airflow velocities used were 1200, 800, and 500 fpm. These velocities cover a large span of typical diffuser flow conditions, including what is typically seen in actual installations. For the test array, this parameter was considered a noise condition because it is not controlled by the installation. Under modern systems, where a VAV unit of some type is used, a typical diffuser will be required to perform under large variations in airflow.

Two design parameters were used in the performance characterization experiment. They were diffuser type and diffuser inlet diameter. The design parameters and noise condition with corresponding levels are shown in Table 8.

Table 8. Test parameters and noise conditions with corresponding states.

| Parameter | State 1 | State 2 | State 3 | State 4 | State 5 | State 6 |
|---|---|---|---|---|---|---|
| 1.Diffuser Type | Square | Plaque | Perforated Round Neck | Modular Core Perforated | Round | Louvered |
| 2.Inlet Diameter | 8 inches | 10 inches | 12 inches | | | |
| Noise Condition | Low State | Medium State | High State | | | |
| 1.Diffuser inlet velocity | 500 fpm | 800 fpm | 1200 fpm | | | |

A full factorial array was used to set up the experiment. The experimental outputs were used to extract the main effects of the test parameters and the variation of those main effects due to the noise conditions. The test array has 18 runs, one parameter at six levels and one parameter at three levels. There were three sets of output measures, one for each noise condition. The array is shown in Table 9. Note that for diffusers with a square inlet (modular core and louvered), a round to square adaptor was used.

From the diffuser velocity profile data, the data was normalized so that diffusers of the same type with different inlet sizes, at differing velocities, could be compared side-by-side. To do this, the zone plot method of the diffuser velocity data was used. This method is described in Appendix C of ANSI/ASHRAE Standard 70-2006 and is described by the zones of expansion from an air outlet. Using this method, the non-dimensional diffuser discharge velocity is plotted corresponding to the non-dimensional measurement distance. The non-dimensional discharge velocity is the ratio of discharge velocity to inlet duct air velocity, $V_x/V_k$. The non-dimensional measurement distance is the measurement distance divided by the square root of the diffuser neck area, $X/(A_k)^{1/2}$.

The results are plotted on a log-log plot and a linear regression curve is drawn to pass through the data points. For any diffusers characterized by this regression curve, all data points should fall within ±20 percent of the line as shown in Figure 13. [9]

Table 9. Test array for Standard 70 testing with output measures.

| Run # | Diffuser Type | Inlet Size [in] | Throw Data at corresponding velocity [ft] | | | Sound Data [dB] | Total Pressure Data [in- $H_2O$] |
|---|---|---|---|---|---|---|---|
| | | | 150fpm | 100fpm | 50fpm | | |
| 1 | Square | 8 | | | | | |
| 2 | Square | 10 | | | | | |
| 3 | Square | 12 | | | | | |
| 4 | Plaque | 8 | | | | | |
| 5 | Plaque | 10 | | | | | |
| 6 | Plaque | 12 | | | | | |
| 7 | Perf Rnd | 8 | | | | | |
| 8 | Perf Rnd | 10 | | | | | |
| 9 | Perf Rnd | 12 | | | | | |
| 10 | Mod Core | 8 | | | | | |
| 11 | Mod Core | 10 | | | | | |
| 12 | Mod Core | 12 | | | | | |
| 13 | Round | 8 | | | | | |
| 14 | Round | 10 | | | | | |
| 15 | Round | 12 | | | | | |
| 16 | Louvered | 8 | | | | | |
| 17 | Louvered | 10 | | | | | |
| 18 | Louvered | 12 | | | | | |

The log-log plot in Figure 13 shows a zone linear regression line and the corresponding ±20 percent error lines. This line has been split into three zones labeled 2, 3 and 4. These are standard zones that have a slope based on typical discharge flow velocity phenomena. Zone 1 (not shown in Figure 13) is known as the short zone and was rarely seen during analysis of the experimental data. Zone 2 is called the transition zone

and can extend eight to ten diameters from the air outlet. Zone 3 is the zone of fully established turbulent flow and is usually the region that reaches the occupied zone making its importance the greatest. Zone 4 is the terminal zone meaning the residual velocity decays into large-scale turbulence at a rapid rate. [12] The regression equation for zone 1 is $y = a*x^{(0)} + b$, zone 2 is $y = a*x^{(-1/2)} + b$, zone 3 is $y = a*x^{(-1)} + b$ and zone 4 is $y = a*x^{(-2)} + b$. After taking the log of both sides of each equation, notice that the exponent of x is actually the slope of the regression line in each zone, the value a is the y value at x = 1 and b is ideally zero. The value of *x* refers to the y-axis value, $V_x/V_k$, and the value of *y* refers to the x-axis value, $X/(A_k)^{1/2}$.

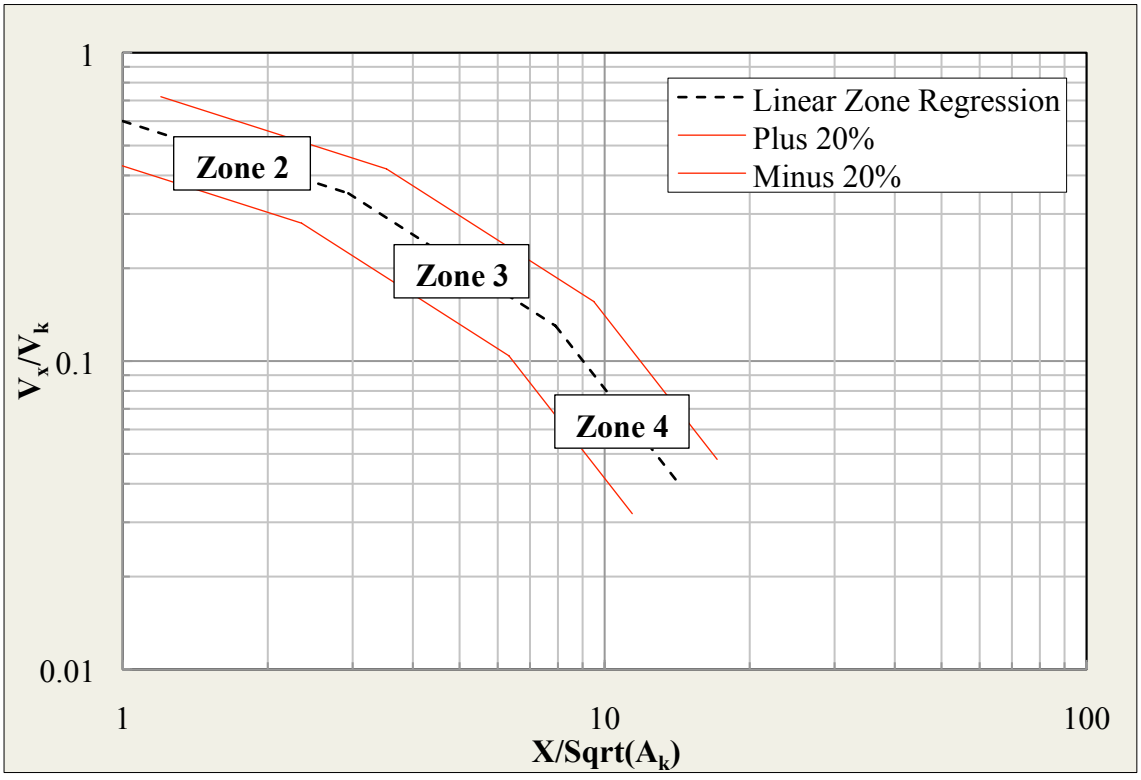


Figure 13. Standard 70 Zone Plot.

## 3.4 Results

Data from the square diffusers are presented as an example of the testing and analysis performed on all the diffusers. For all test runs, draft meter measurements were used to plot the diffuser discharge velocity versus distance from the diffuser at various heights below the ceiling. Figure 14 and Figure 15 show the results for a 12-inch square diffuser and an 8-inch square diffuser both at 1200 fpm inlet flow velocity. The plot line labeled TV17-v is the top draft sensor closest to the ceiling at 0.75 inches from the ceiling, while TV16-v is 3.25 inches from the ceiling, as stated in Table 7. The sensors show that the flow leaving the diffuser outlet is primarily confined to the space near the ceiling. The flow spreads out and mixes with air in the room resulting in the velocity slowly dropping off over a distance of about seven to nine feet. This is a typical ceiling diffuser velocity profile. From this data comes the throw data distance from the diffuser center for the velocity points of 150, 100, and 50 fpm.

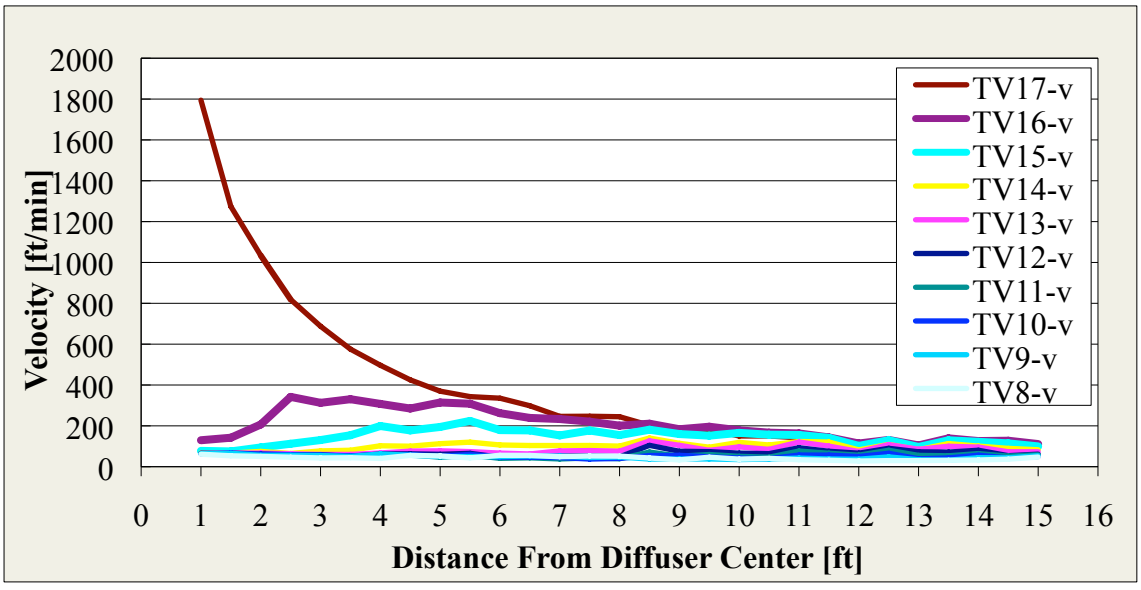


Figure 14. Velocity profile of 12 inch square diffuser at 1200 fpm.

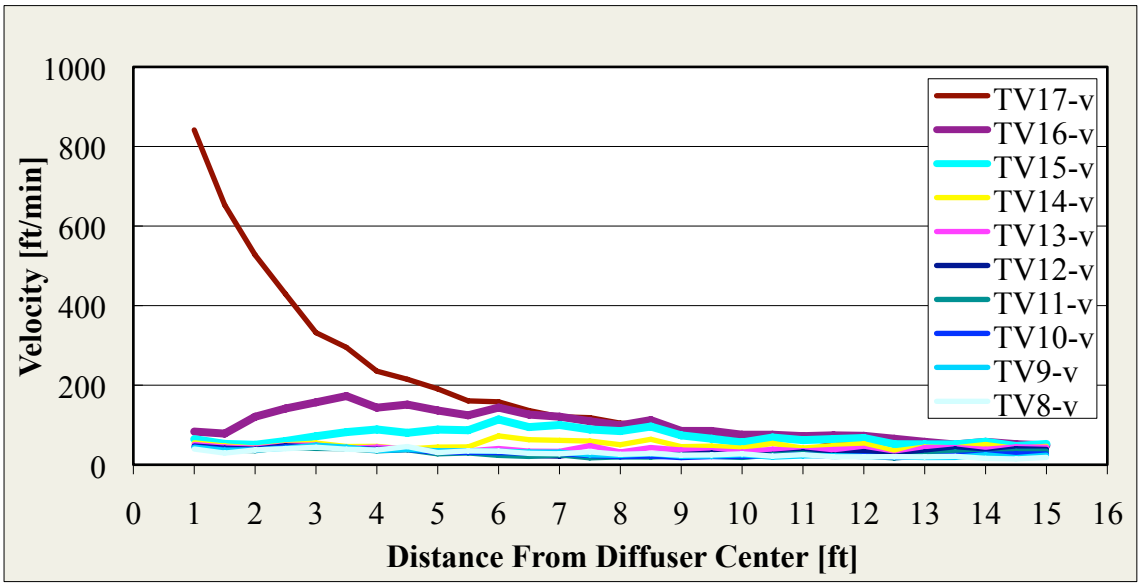


Figure 15. Velocity profile of 8 inch square diffuser at 1200 fpm.

Figure 16 shows the calculated room noise criterion (NC) level for a 12-inch square diffuser at 1200 fpm for forty samples. In all cases, there were a minimum twenty samples taken over a two minute time period for each diffuser at each of the three noise conditions (flow rates). Samples were excluded from the average if there was evidence of a temporary background noise above the background noise level. The plenum total pressure was recorded every four seconds during the draft meter flow testing as shown in Figure 17 and averaged for each test run. Table 10 through Table 15 show the final Standard 70 results for every diffuser type and inlet size tested for diffuser throw distance data at 150/100/50 feet per minute, total pressure data inside the plenum in inches of water, and the room noise criterion (NC) level in decibels.

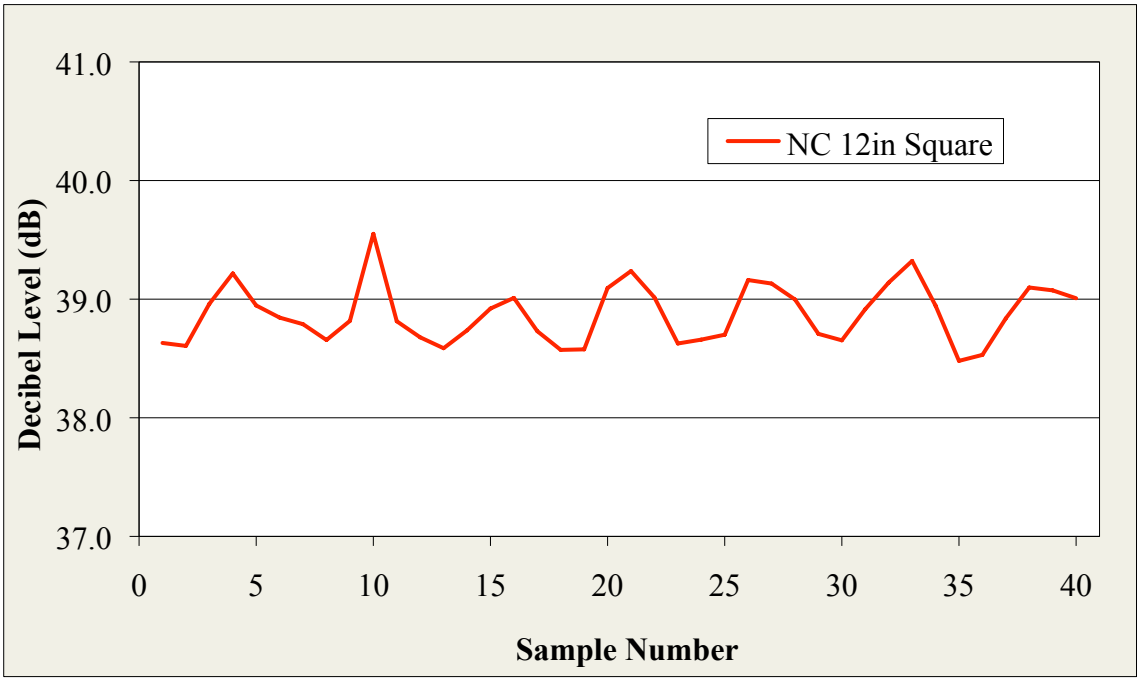


Figure 16. Noise criterion level for 12 inch square diffuser at 1200 fpm.

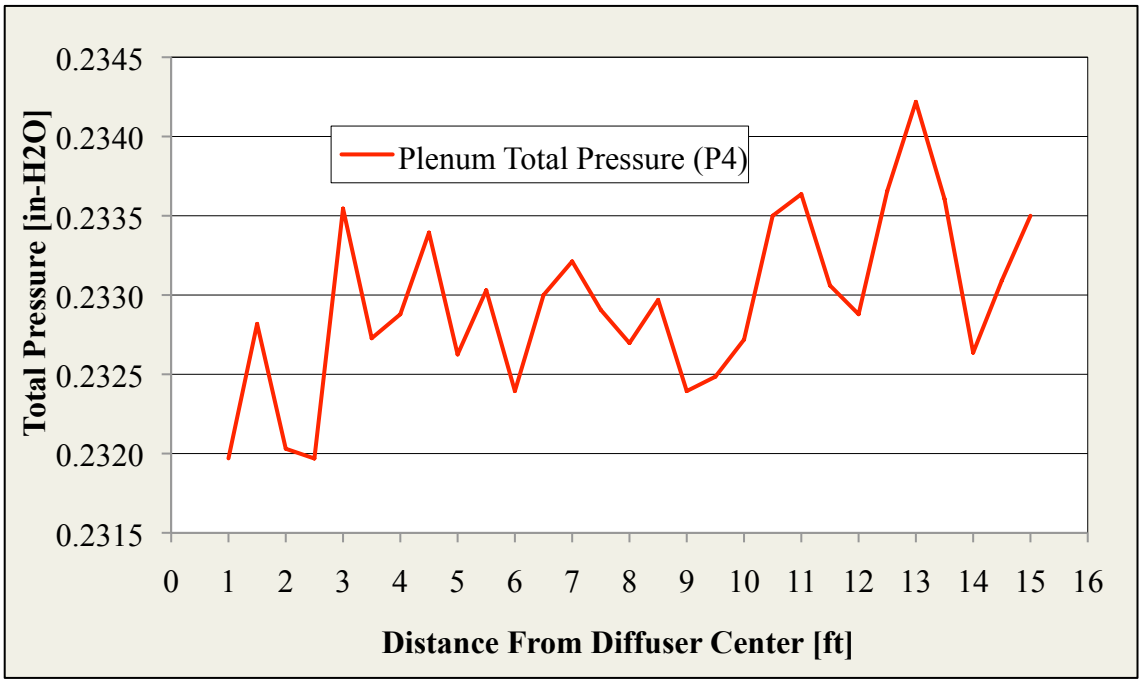


Figure 17. Plenum total pressure for 12 inch square diffuser at 1200 fpm.

Table 10. Final results for square diffuser at corresponding velocities.

| Manf. | Neck Size [in] | Neck Velocity | | | | | | | | | |
|---|---|---|---|---|---|---|---|---|---|---|---|
| | $A_K$ [$ft^2$] | [fpm] | 500 | | | 800 | | | 1200 | | |
| A | 8<br>0.3491 | Flow [cfm] | 175 | | | 280 | | | 420 | | |
| | | Total Pressure [in-wt] | 0.0322 | | | 0.0652 | | | 0.1301 | | |
| | | Throw [ft] | 3 | 4 | 9 | 5 | 6 | 10 | 6 | 8 | 13 |
| | | NC [dB] | - | | | <21 | | | 33 | | |
| | 10<br>0.5454 | Flow [cfm] | 273 | | | 436 | | | 654 | | |
| | | Total Pressure [in-wt] | 0.035 | | | 0.081 | | | 0.175 | | |
| | | Throw [ft] | 0 | 0 | 0 | 0 | 0 | 0 | 0 | 0 | 0 |
| | | NC [dB] | <21 | | | 24.5 | | | 36 | | |
| | 12<br>0.7854 | Flow [cfm] | 393 | | | 630 | | | 940 | | |
| | | Total Pressure [in-wt] | 0.044 | | | 0.0968 | | | 0.2330 | | |
| | | Throw [ft] | 0 | 0 | 0 | 7 | 10 | 15+ | 10 | 13 | 15+ |
| | | NC [dB] | <21 | | | 28 | | | 38.5 | | |
| C | 10<br>0.5454 | Flow [cfm] | 273 | | | 436 | | | 654 | | |
| | | Total Pressure [in-wt] | - | | | 0.08 | | | 0.169 | | |
| | | NC [dB] | <21 | | | 22 | | | 36 | | |

Table 11. Final results for plaque diffuser at corresponding velocities.

| Manf. | Neck Size [in] | Neck Velocity | | | | | | | | | |
|---|---|---|---|---|---|---|---|---|---|---|---|
| | $A_K$ [$ft^2$] | [fpm] | 500 | | | 800 | | | 1200 | | |
| C | 8<br>0.3491 | Flow [cfm] | 175 | | | 279 | | | 419 | | |
| | | Total Pressure [in-wt] | 0.03664 | | | 0.077101 | | | 0.155035 | | |
| | | Throw [ft] | 3 | 4 | 8 | 4 | 6 | 12 | 6 | 8 | 15 |
| | | NC [dB] | - | | | <21 | | | 28 | | |
| | 10<br>0.5454 | Flow [cfm] | 273 | | | 436 | | | 654 | | |
| | | Total Pressure [in-wt] | 0.048 | | | 0.102 | | | 0.213 | | |
| | | NC [dB] | - | | | <21 | | | 32.5 | | |
| | 12<br>0.7854 | Flow [cfm] | 393 | | | 628 | | | 942 | | |
| | | Total Pressure [in-wt] | 0.05829 | | | 0.137448 | | | 0.325853 | | |
| | | Throw [ft] | 5 | 8 | 12 | 8 | 11 | 14 | 12 | 15 | 15+ |
| | | NC [dB] | <21 | | | 23.5 | | | 36 | | |
| A | 10<br>0.5454 | Flow [cfm] | 273 | | | 436 | | | 654 | | |
| | | Total Pressure [in-wt] | - | | | 0.122 | | | 0.269 | | |
| | | NC [dB] | <21 | | | 27 | | | 39.5 | | |

Table 12. Final results for perforated round diffuser at corresponding velocities.

| Manf. | Neck Size [in] | Neck Velocity | | | | | | | | |
|---|---|---|---|---|---|---|---|---|---|---|
| | $A_K$ [$ft^2$] | [fpm] | 500 | | | 800 | | | 1200 | | |
| B | 8<br>0.3491 | Flow [cfm] | 175 | | | 279 | | | 419 | | |
| | | Total Pressure [in-wt] | 0.04049 | | | 0.085043 | | | 0.171406 | | |
| | | Throw [ft] | 1 | 1 | 1 | 1 | 1 | 2 | 1 | 1 | 2 |
| | | NC [dB] | <21 | | | 23.5 | | | 37 | | |
| | 10<br>0.5454 | Flow [cfm] | 273 | | | 436 | | | 654 | | |
| | | Total Pressure [in-wt] | 0.051 | | | 0.115 | | | 0.247868 | | |
| | | Throw [ft] | - | - | - | - | - | - | 6 | 9 | 14 |
| | | NC [dB] | <21 | | | 32 | | | 46.5 | | |
| | 12<br>0.7854 | Flow [cfm] | 393 | | | 628 | | | 942 | | |
| | | Total Pressure [in-wt] | 0.05477 | | | 0.128645 | | | 0.308087 | | |
| | | Throw [ft] | 4 | 5 | 12 | 6 | 8 | 15 | 9 | 13 | 15+ |
| | | NC [dB] | <21 | | | 36 | | | 52 | | |
| C | 10<br>0.5454 | Flow [cfm] | 273 | | | 436 | | | 654 | | |
| | | Total Pressure [in-wt] | 0.04677 | | | 0.102477 | | | 0.232094 | | |
| | | Throw [ft] | 1 | 1 | 3 | 2 | 3 | 4 | 3 | 4 | 6 |
| | | NC [dB] | <21 | | | 32.5 | | | 46.5 | | |

Table 13. Final results for perf square/modular core diffuser at corresponding velocities.

| Manf. | Neck Size [in] | Neck Velocity | | | | | | | | |
|---|---|---|---|---|---|---|---|---|---|---|
| | $A_K$ [$ft^2$] | [fpm] | 500 | | | 800 | | | 1200 | | |
| D | 8x8 0.3491 | Flow [cfm] | 175 | | | 279 | | | 419 | | |
| | | Total Pressure [in-wt] | 0.05327 | | | 0.107491 | | | 0.202241 | | |
| | | Throw [ft] | 3 | 4 | 7 | 4 | 6 | 10 | 5 | 7 | 12 |
| | | NC [dB] | <21 | | | 30 | | | 42 | | |
| | 10x10 0.5454 | Flow [cfm] | 273 | | | 436 | | | 654 | | |
| | | Total Pressure [in-wt] | 0.04428 | | | 0.097157 | | | 0.217667 | | |
| | | NC [dB] | <21 | | | 30.5 | | | 44.5 | | |
| | 12x12 0.7854 | Flow [cfm] | 393 | | | 628 | | | 942 | | |
| | | Total Pressure [in-wt] | 0.04617 | | | 0.110369 | | | 0.268157 | | |
| | | Throw [ft] | 4 | 5 | 10 | 6 | 9 | 15 | 10 | 14 | 15+ |
| | | NC [dB] | <21 | | | 33 | | | 49 | | |
| B | 8x8 0.3491 | Flow [cfm] | 175 | | | 279 | | | 419 | | |
| | | Total Pressure [in-wt] | 0.03309 | | | 0.066259 | | | 0.132328 | | |
| | | Throw [ft] | 1 | 1 | 4 | 2 | 3 | 6 | 3 | 5 | 8 |
| | | NC [dB] | - | | | <21 | | | 33 | | |
| | 10x10 0.5454 | Flow [cfm] | 273 | | | 436 | | | 654 | | |
| | | Total Pressure [in-wt] | - | | | - | | | 0.187947 | | |
| | | Throw [ft] | - | - | - | - | - | - | 6 | 9 | 15 |
| | | NC [dB] | - | | | - | | | 42.5 | | |

Table 14. Final results for round diffuser at corresponding velocities.

| Manf. | Neck Size [in] | Neck Velocity | | | | | | | | |
|---|---|---|---|---|---|---|---|---|---|---|
| | $A_K$ [$ft^2$] | [fpm] | 500 | | | 800 | | | 1200 | | |
| C | 8<br>0.3491 | Flow [cfm] | 175 | | | 279 | | | 419 | | |
| | | Total Pressure [in-wt] | 0.0432 | | | 0.086761 | | | 0.167 | | |
| | | Throw [ft] | 3 | 4 | 7 | 4 | 6 | 11 | 6 | 9 | 14 |
| | | NC [dB] | - | | | <21 | | | 25.5 | | |
| | 10<br>0.5454 | Flow [cfm] | 273 | | | 436 | | | 654 | | |
| | | Total Pressure [in-wt] | - | | | - | | | 0.154607 | | |
| | | Throw [ft] | - | - | - | - | - | - | 8 | 12 | 15+ |
| | | NC [dB] | - | | | <21 | | | 29 | | |
| | 12<br>0.7854 | Flow [cfm] | 393 | | | 628 | | | 942 | | |
| | | Total Pressure [in-wt] | 0.03391 | | | 0.074948 | | | 0.170686 | | |
| | | Throw [ft] | 3 | 5 | 7 | 5 | 8 | 11 | 9 | 12 | 15+ |
| | | NC [dB] | <21 | | | 25 | | | 38.5 | | |
| B | 10<br>0.5454 | Flow [cfm] | 273 | | | 436 | | | 654 | | |
| | | Total Pressure [in-wt] | 0.03871 | | | 0.082677 | | | 0.185251 | | |
| | | Throw [ft] | 3 | 5 | 7 | 4 | 6 | 10 | 6 | 10 | 15+ |
| | | NC [dB] | <21 | | | 24.5 | | | 36.5 | | |

Table 15. Final results for louvered diffuser at corresponding velocities.

| Manf. | Neck Size [in] | Neck Velocity | | | | | | | | |
|---|---|---|---|---|---|---|---|---|---|---|
| | $A_K$ [$ft^2$] | [fpm] | 500 | | | 800 | | | 1200 | | |
| D | 9x9 0.3491 | Flow [cfm] | 175 | | | 279 | | | 419 | | |
| | | Total Pressure [in-wt] | 0.03793 | | | 0.075525 | | | 0.146374 | | |
| | | Throw [ft] | 5 | 7 | 12 | 7 | 10 | 15+ | 10 | 14 | 15+ |
| | | NC [dB] | - | | | <21 | | | 29.5 | | |
| | 12x12 0.5454 | Flow [cfm] | 273 | | | 436 | | | 654 | | |
| | | Total Pressure [in-wt] | 0.03094 | | | 0.064216 | | | 0.13822 | | |
| | | Throw [ft] | 5 | 8 | 14 | 8 | 10 | 15+ | 10 | 15 | 15+ |
| | | NC [dB] | - | | | <21 | | | 34 | | |
| | 15x15 0.7854 | Flow [cfm] | 393 | | | 628 | | | 942 | | |
| | | Total Pressure [in-wt] | 0.02845 | | | 0.062111 | | | 0.142311 | | |
| | | Throw [ft] | 6 | 8 | 15 | 8 | 12 | 15+ | 11 | 15 | 15+ |
| | | NC [dB] | - | | | <21 | | | 34 | | |
| A | 9x9 0.3491 | Flow [cfm] | 169 | | | 279 | | | 394 | | |
| | | Total Pressure [in-wt] | 0.054089 | | | - | | | 0.21424 | | |
| | | Throw [ft] | 5 | 8 | 14 | - | - | - | 10 | 15 | 15+ |
| | | NC [dB] | <21 | | | - | | | 38.5 | | |
| | 15x15 0.7854 | Flow [cfm] | 393 | | | 628 | | | 942 | | |
| | | NC [dB] | <21 | | | 23.5 | | | 38 | | |

Note that all diffuser manufacturers' products may not have the same performance and the above data may or may not coincide with Standard 70 data published by all manufacturers.

Figure 18 shows a typical example zone plot of throw data for a type of diffuser, in this case, all the square diffusers tested. The data includes runs with different neck sizes and manufacturers at several different duct air velocities. What can be seen from the plot data is that the non-dimensional data for the different diffusers nearly overlap one another. This shows the value of the zone plot for using data taken at a few neck sizes and duct air velocities. This data can be used to predict diffuser performance at different neck sizes and velocities without having to test at every neck size and flow velocity.

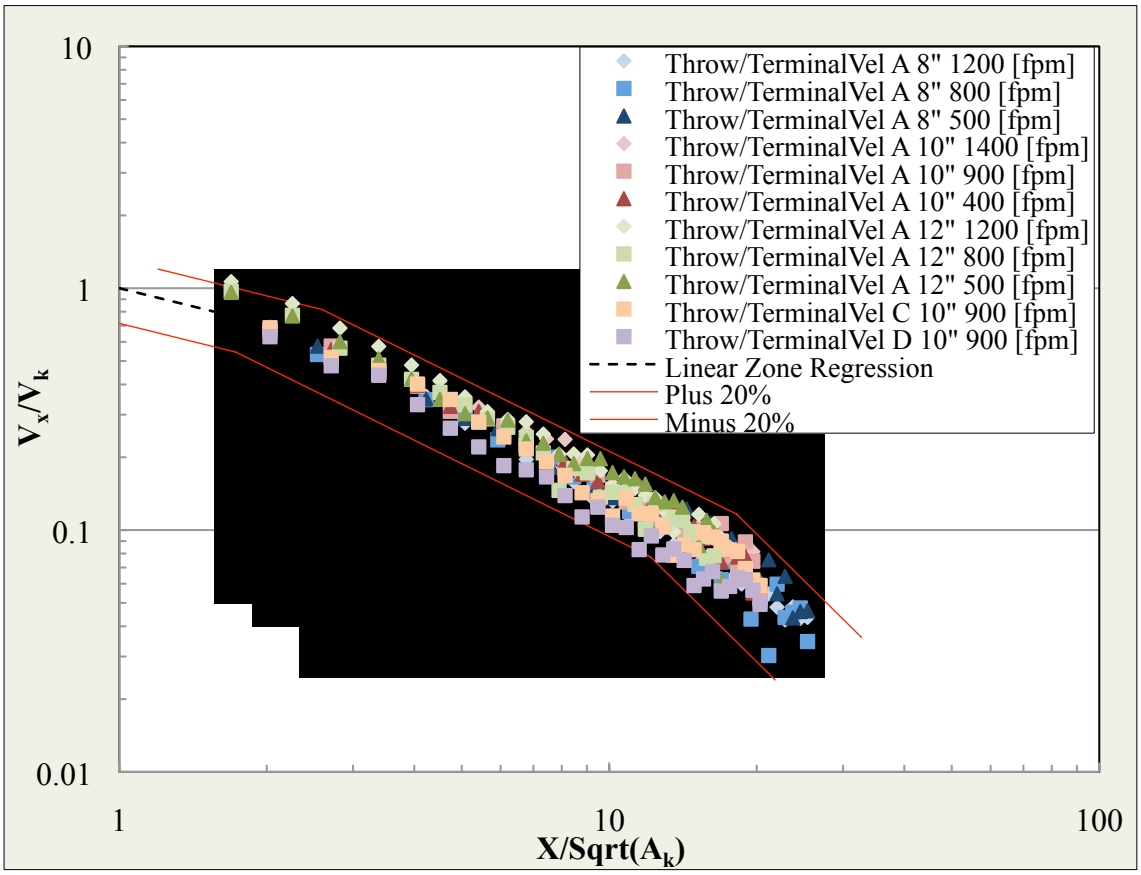


Figure 18. Standard 70 zone plot for all square diffusers.

## 3.5 Analysis

This section covers the analysis of each type of diffuser examined for Standard 70 data. Noise criterion data was not attainable at levels below 21.5 dB due to the background noise level in the throw room. Therefore, at the low duct air velocity condition for most diffusers, there is no value.

### 3.5.1 Square Diffuser

As shown in the zone plot in Figure 18, it is apparent that for all manufacturer diffusers and all inlet sizes, the throw data fits within the ±20 percent margins specified by Standard 70. Sound data is nearly identical based on inlet size and manufacturer.

There are some minor differences in the total pressure for differing diffuser manufacturers. This lead to the conclusion that the differences in manufacturer design of the square diffuser resulted in small enough effects in the performance of the diffuser output that the same performance zone plot could be used to predict diffuser performance (see Table 10).

3.5.2 Plaque Diffuser

The throw data for the plaque diffusers is much like that of the square diffusers. Despite the difference in manufacturer designs, the projections of flow from the output of the diffusers are again closely comparable within the ±20 percent margins. This does not hold true for the noise data. The difference in diffuser design has resulted in changes in NC levels greater than 3 dB between manufacturers, leading to differences in total pressure (see Table 11).

Table 16. Plaque diffuser total pressure and sound comparisons of Standard 70 test results from manufacturer published data and UNLV throw room data.

| | | Manufacturer Data | | UNLV Data | |
|---|---|---|---|---|---|
| | | Sound [dB] | Pressure [in-$H_2O$] | Sound [dB] | Pressure [in-$H_2O$] |
| A , 10 “ | 800 fpm | 26 | 0.101 | 27 | 0.122 |
| | 1200 fpm | 37 | 0.229 | 39.5 | 0.269 |
| C , 10 “ | 800 fpm | 22 | 0.115 | <21.5 | 0.103 |
| | 1200 fpm | 36 | 0.259 | 32.5 | 0.216 |

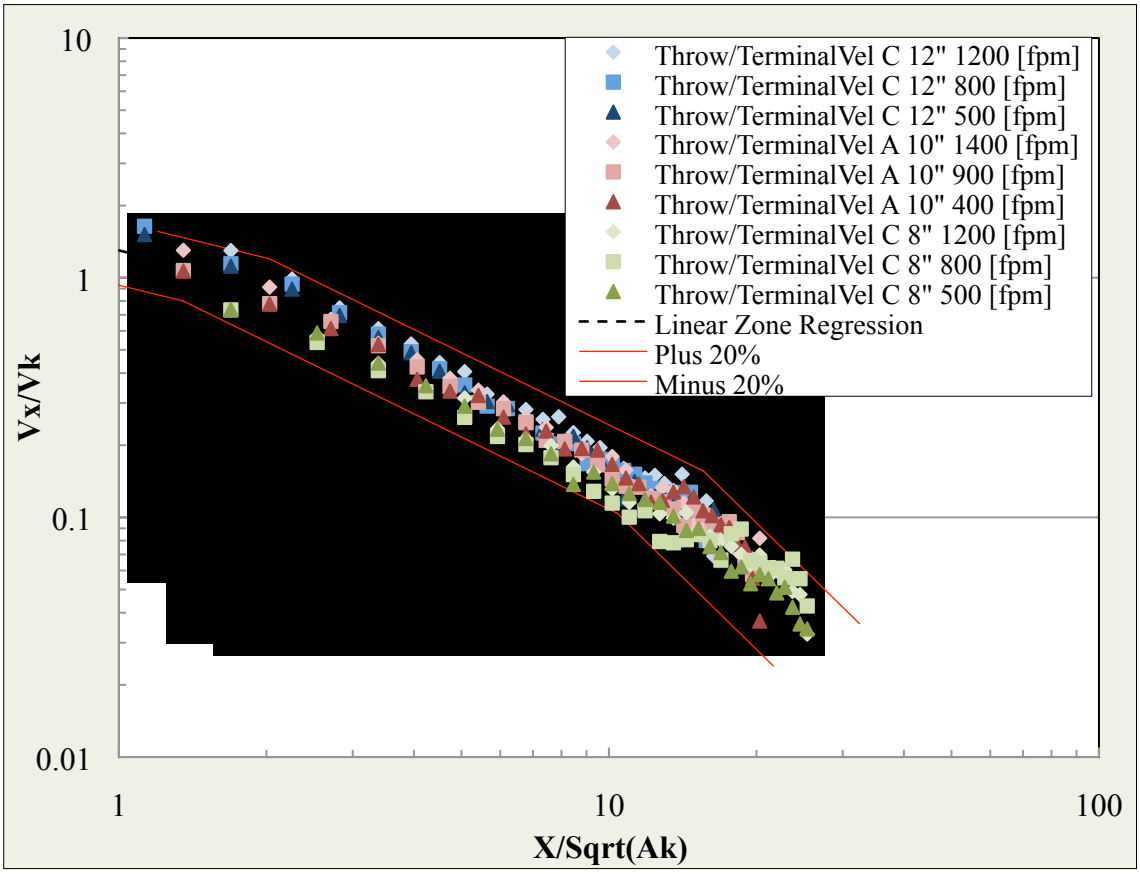


Figure 19. Standard 70 zone plot for plaque diffusers.

### 3.5.3 Perforated Round Diffuser

The maximum throw direction for the round inlet, perforated face diffusers were not always perpendicular to the diffuser edge. A cross flow scan was used to find the peak throw direction for data collection. Figure 20 shows the data for two different manufacturers at various inlet sizes and duct air flow velocities. It is clear that the differences in the two manufacturer's designs result in unique zone plots. Much like the square diffuser, the sound and pressure data for the perforated round diffuser were almost identical for corresponding inlet sizes and manufacturers (see Table 12).

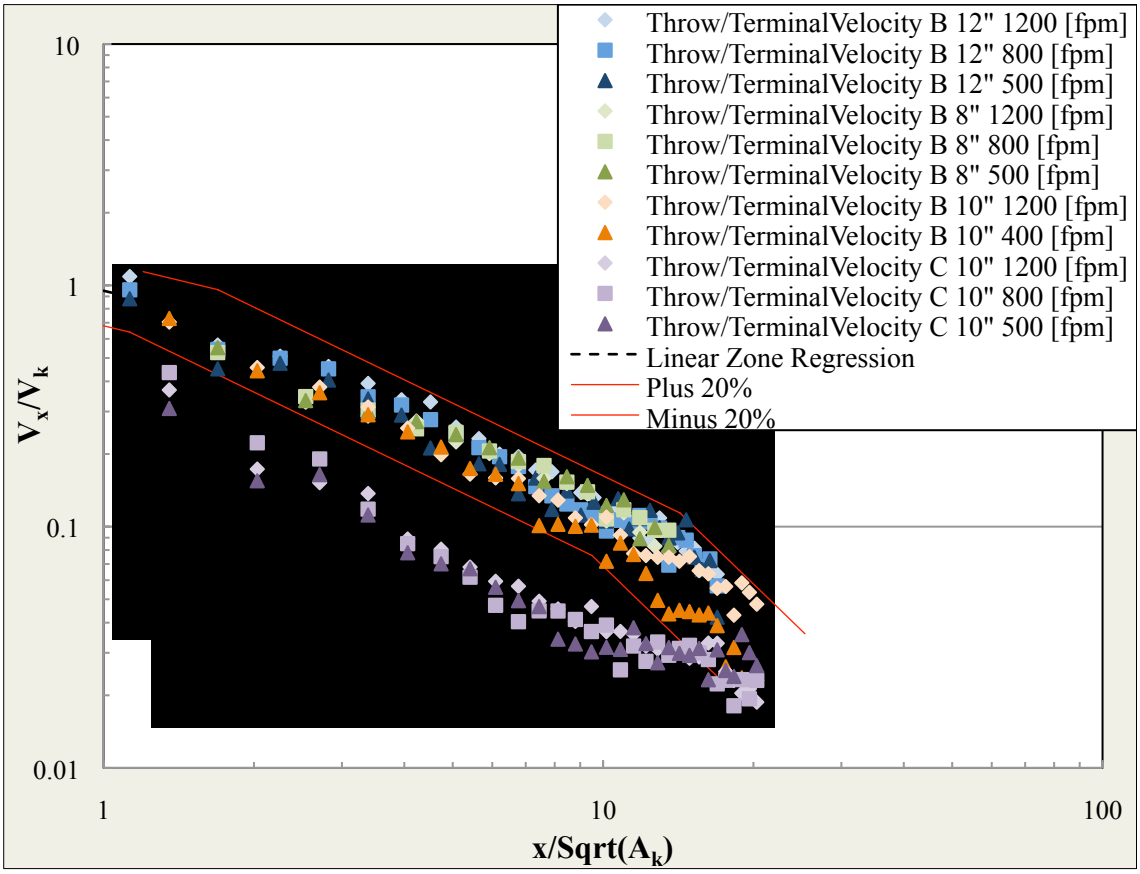


Figure 20. Standard 70 zone plot for perforated round diffusers.

### 3.5.4 Modular Core/Perforated Square Diffuser

The data for manufacturer D used a perforated square diffuser that has a set of directional veins fixed inside the diffuser inlet, giving the diffuser the name modular core. The data for manufacturer B used a normal perforated square diffuser with an open inlet. The perforated square, modular core, diffusers from manufacturer D performed nearly identical based on inlet size. Regular perforated square diffusers were used from manufacturer B, each inlet size for the differing perforated square types does not fall within the ±20 percent margins for the modular core diffuser of manufacturer D. As noted earlier, performance data developed in this investigation did not always match

manufacturer published data. In this case, the NC levels are approximately 6 dB above that of the manufacturer's published data for the modular core 8x8" inlet size, and the total pressure was approximately twice the published data (see Table 13).

Table 17. Modular core total pressure and sound comparisons of Standard 70 test results from manufacturer published data and UNLV throw room data.

| | | Manufacturer Data | | UNLV Data | |
|---|---|---|---|---|---|
| | | Sound [dB] | Pressure | Sound [dB] | Pressure |
| D , 8x8 " | 500 fpm | -- | 0.02 | -- | 0.0533 |
| | 800 fpm | 24 | 0.05 | 30 | 0.108 |
| | 1200 fpm | 36 | 0.11 | 42 | 0.202 |

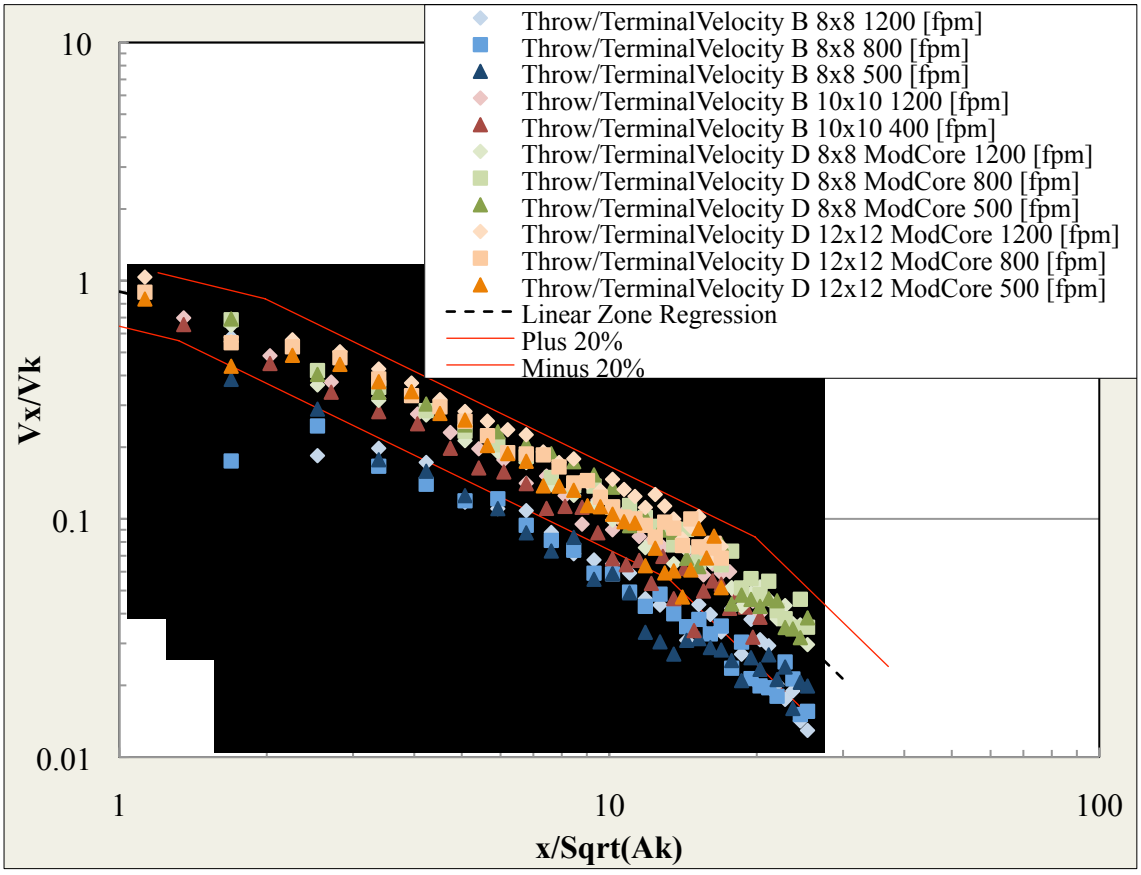


Figure 21. Standard 70 zone plot for perforated round/modular core diffusers.

3.5.5 Round Diffuser

The round diffusers behave much like the square diffusers. All throw data fits within the ±20 percent margins of the zone plot regression lines. Note also that the NC levels for some manufacturers were much less than what was previously published, in some cases, 10 dB or more. Other manufacturers follow very closely to published data (see Table 14).

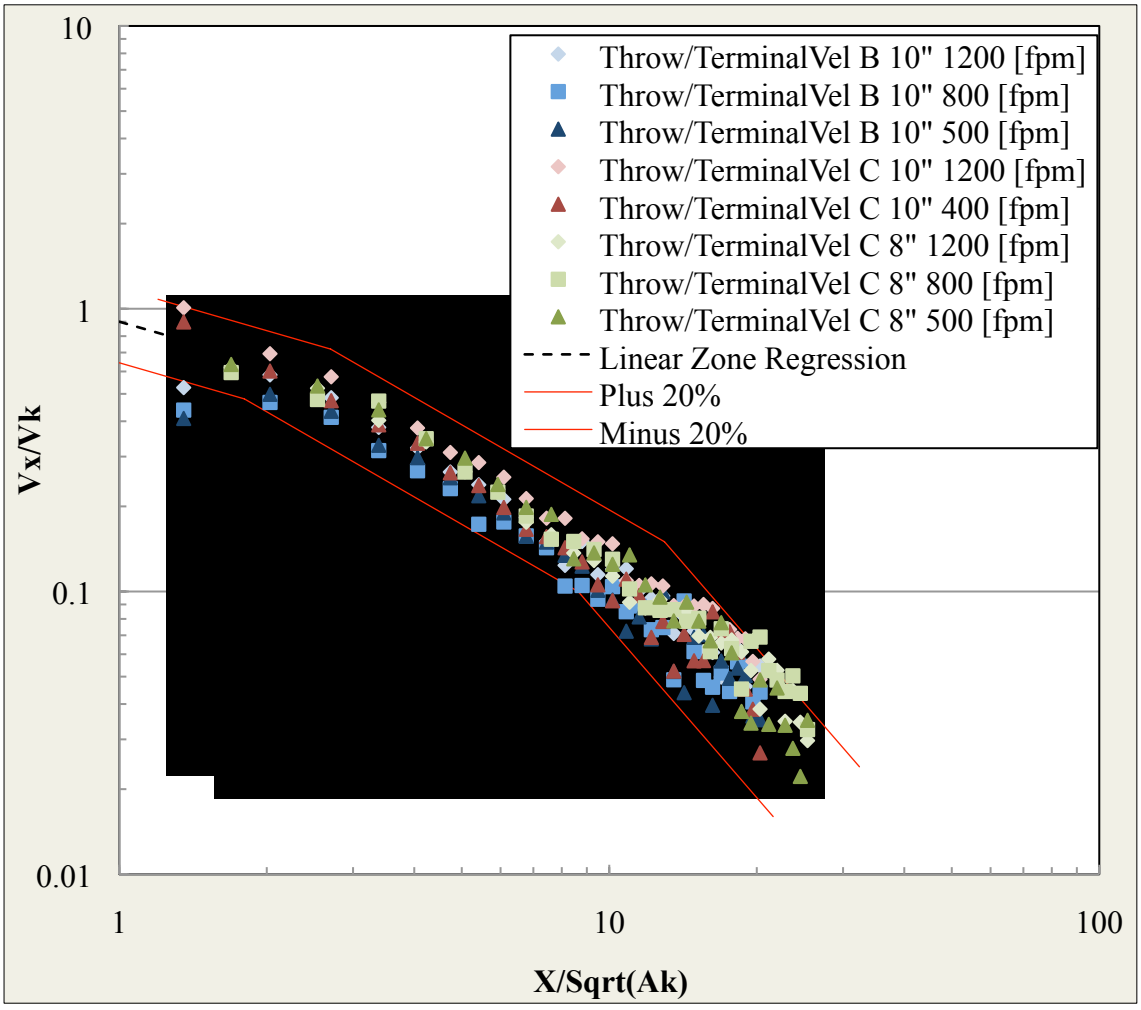


Figure 22. Standard 70 zone plot for round diffusers.

### 3.5.6 Louvered Diffuser

Again, just like the square diffuser, the louvered diffuser performs almost identical for each inlet size and brand. All throw data fits within the ±20 percent margins of the zone plot linear regression lines (see Table 15).

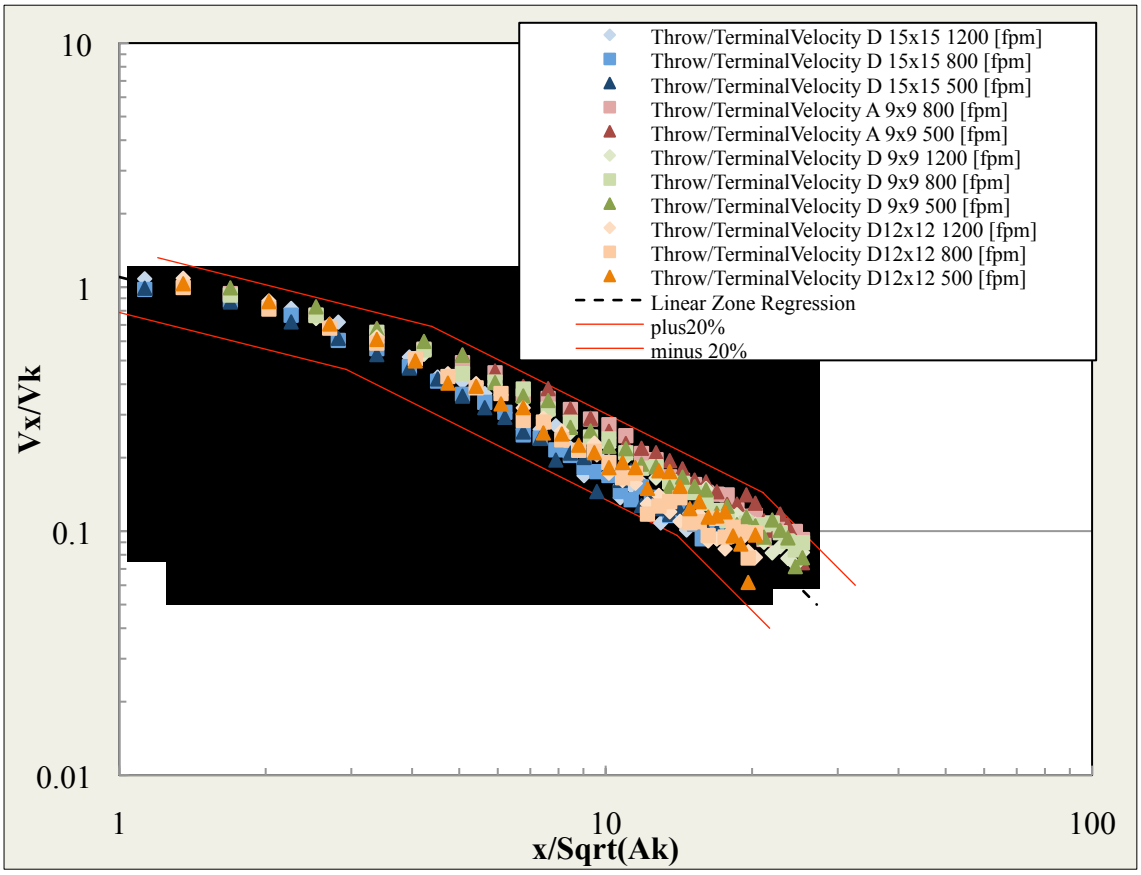


Figure 23. Standard 70 zone plot for louvered diffusers.

### 3.5.7 Performance Variation Effects Due to Non-Perpendicular Flow

It was later determined that diffuser throw could be skewed, in a non-perpendicular direction form the diffuser face despite the equalized flow entering the diffuser inlet. Cross flow scans, parallel to the diffuser face, showed exactly where the maximum throw

from the diffuser occurred. A similar scan was then performed on the opposite side. If necessary, cross-flow scans of all four sides were performed to get a total picture of the diffuser discharge flow. A top view of a typical cross flow scan pattern for the forward side of a diffuser is shown in Figure 24. Once the direction for the maximum throw was determined, a linear scan was completed in that direction. Note that based on the direction of maximum throw, the linear scan could traverse in directions non-perpendicular to the diffuser side.

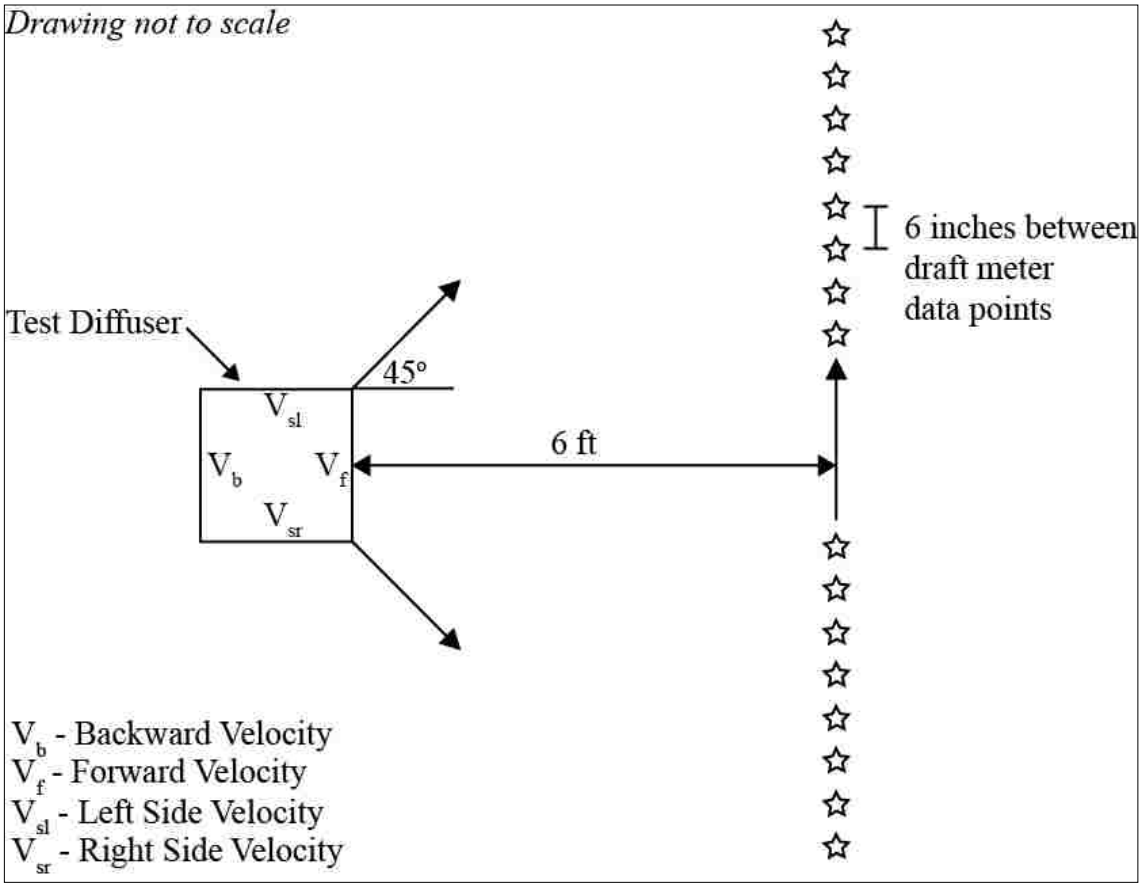


Figure 24. Cross flow scan pattern for the forward side of a diffuser.

One case was found during verification testing of the 8” perforated round diffuser using the vertical ducted method from Standard 70 where a cross flow scan was performed to pinpoint the direction of the peak throw velocity. Figure 25 shows that the peak throw velocity occurs six inches to the right of the diffuser center at a distance of six feet. The linear scan of the diffuser throw was adjusted to the proper angle to capture the maximum throw.

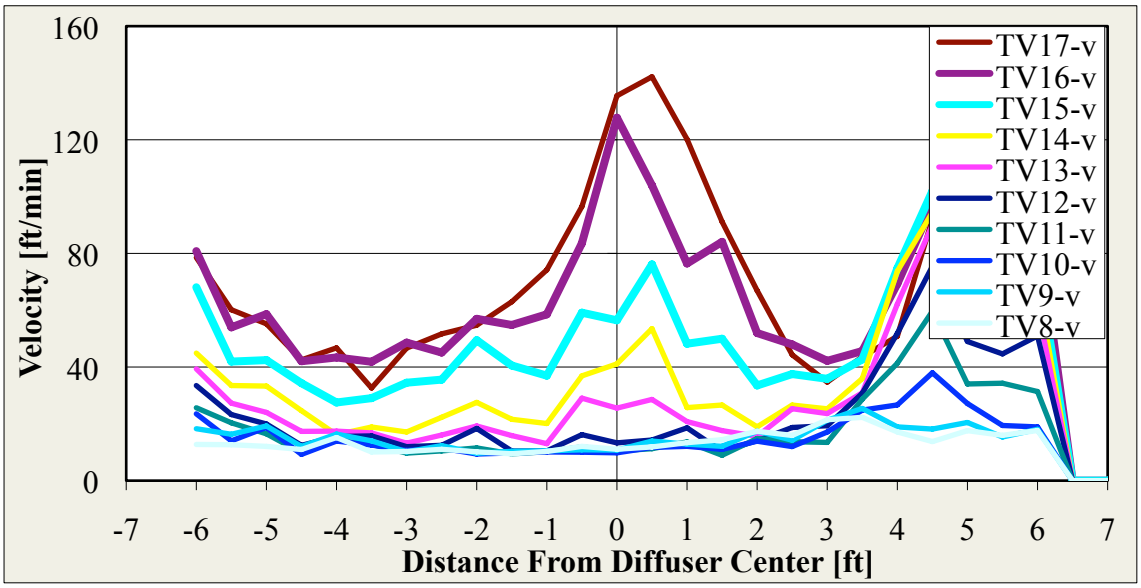


Figure 25. Cross flow scan of 8” perforated round diffuser using vertical ducted method.

# CHAPTER 4

# FIELD CONDITION AIR OUTLET PERFORMANCE

Laboratory full scale testing of diffuser performance, when installed with the typical variation of field installation practices was conducted and compared to the results of Standard 70 characterization. The installation variations included type of duct going to the diffuser, approach direction of the duct, vertical duct height going into the diffuser intake, and use of a damper in the intake. The airflow total pressure loss, discharge symmetry and noise generation were all affected by the variations in installation. Invariably, the standard 70 characterizations had the lowest pressure loss, least discharge asymmetry and lowest noise generation, although some field installation approached Standard 70 levels. The increases in these output measures were quantified by comparison to the output levels measured in a Standard 70 installation. Installers and engineers, to predict the actual performance of a variety of field installations, can use this quantitative information.

## 4.1 Background

Manufacturers of ceiling diffusers publish values of throw, pressure (static and total) and noise criteria levels (NC) based on testing conducted according to Standard 70 the accepted method of testing the performance of air outlets. [9] However, under typical field conditions, diffusers and outlets are seldom installed with the same conditions as measured under ASHRAE Standard 70. Installation variations that can result in significant performance variation from ASHRAE Standard 70 installation include the

length and type of the duct branch, how duct turns are accomplished and how the duct approaches the diffuser.

The duct approach to the diffuser is particularly important, since detrimental effects of improper duct approach cannot be totally corrected by the diffuser itself. Accepted guidance states that the velocity of the air stream should be as uniform as possible over the entire outlet connection to the duct and must be perpendicular to the outlet face. However, few outlet installations achieve this goal. [3,4]

Manufacturers publish sound levels versus flow rate for a given diffuser installed as called for in ASHRAE Standard 70. However, duct connections encountered in the field result in significantly different and usually higher sound levels for the same airflow rate. [1] Also, diffusers with a perforated face have been found to have a higher sound distortion with poor inlet conditions than diffusers with large open cones.

The magnitude of the sound and performance effects associated with installation variations will also depend on variations out of the control of the installer such as variable flow rates. Diffusers are designed to optimally distribute the air across a limited range of load condition and air volume, but in a typical VAV type installation, air volume rate can have large variation. Consequently, the throw, room airflow velocity and sound levels can be significantly different from the specified design point. [1]

## 4.2 Objective

The objective of this testing was to develop guidelines that will relate manufactures' air outlet cataloged data that have been obtained using ASHRAE Standard 70 to field installed application conditions. Data was collected for diffusers obtained under a

collection of real world inlet conditions and compared to base performance data obtained from testing using ASHRAE Standard 70. From that comparison, correction factors for diffuser throw, pressure and sound data were developed.

## 4.3 Methodology

Output measures and derived output measures included:

1. Sound Power Level and Resulting Room NC.
2. Ratio of total pressure in field installation to total pressure in a Standard 70 test.
3. Diffuser throw distance ratio of throw in field installation to throw in a Standard 70 test for at least two diffuser sides.

Sound power level is the level in decibels of the sound power at third octave bands from 16 to 10,000 Hz. From a subset of those levels, the room Noise Criteria (NC) levels were calculated based on ANSI/ASA 12.2 as recommended by ASHRAE. [9] The same process used during the Standard 70 baseline testing was repeated for the field-testing sound capture with the rotating boom microphone setup in Figure 11. The throw ratio is the ratio of the installed throw distance of the specific configuration tested divided by the throw distance from the standard 70 configuration. Pressure loss is the difference of the total pressure upstream of the diffuser minus the total pressure in the throw room. The total pressure in the upstream duct is the summation of the static and dynamic pressures while the total pressure in the throw room is assumed to be the static pressure in the throw room. The velocity profile is the two-dimensional profile of the diffuser discharge velocity in a vertical plane that is parallel to the horizontal duct feeding the diffuser. A

profile in the vertical plane perpendicular to the horizontal duct may also be obtained. The flow factor change is related to the pressure required to achieve a given airflow rate through a duct or diffuser. In this case, the parameters related to the elbow in the duct, the damper and diffuser combined system all affect the airflow resistance.

### 4.3.1 Laboratory Instrumentation

All tests for this project were run under steady-state conditions similar to the Standard 70 tests. Volume airflow corresponding to the required inlet velocity was set and allowed to stabilize. The throw room measurement instrument configuration was the same as in the Standard 70 testing. Also, the same LabView virtual instrument was used to monitor and record airflow, supply air temperature, room temperature, supply static pressure, draft meter array position and draft meter readings. Sound level measurements were made with all systems off except for the air supply, boom microphone and the monitoring and recording computer. Sound measurements were taken with the air supply on and off to record the diffuser generated sound with airflow and a background noise level without airflow.

### 4.3.2 Experimental Design

The ideal energy transformation is for air to flow into the diffuser inlet and exit at the diffuser discharge with no pressure loss, other than velocity pressure, no sound generation and a discharge velocity pattern as intended by the diffuser design. Thus, any variations from ideal would be variations in pressure measured in the duct upstream of the diffuser inlet, increases in sound level measured in the discharge room and unintended asymmetry in diffuser throw measured in the discharge room. Comparisons with Standard 70 measurements show variations from ideal due to flow restrictions in the

diffuser, turbulence induced in the flow due to diffuser structure and anomalies in discharge throw due to the geometry of the diffuser design. In this experiment, the Standard 70 results are used as a standard while the test results are compared to that standard. The experimental setup is diagrammed in Figure 26.

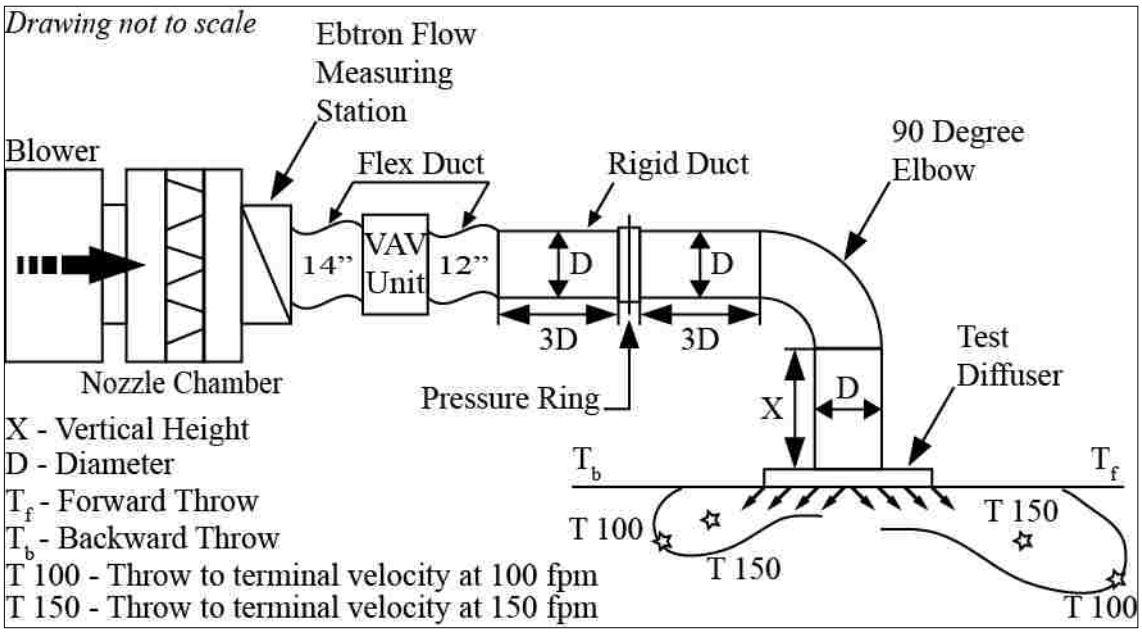


Figure 26. Experimental setup for field installation condition laboratory testing.

Experimental output measures were obtained using the same or comparable methods used for standard 70 testing and thus can be compared to Standard 70 measurements. Static pressure was measured three duct diameters upstream of the elbow that connects to the vertical duct section leading into the diffuser. Velocity pressure was calculated from measurement of the total airflow and knowledge of the duct cross-sectional area. Total pressure was calculated by adding the velocity pressure to the static pressure.

Diffuser discharge velocities at incremental distances from the diffuser were measured using the array of draft meters used in the Standard 70 measurements. The array of draft meters was scanned in the direction of the greatest discharge. Because the field installation, in many cases, resulted in non-uniform changes to the discharge velocity when compared to Standard 70 testing results, care was taken to determine the location and direction of the highest discharge throw for all sides of the diffuser. This was accomplished with a cross-flow scan at a set distance from the diffuser side from which the discharge flow directional characteristics could be determined. Refer to section 3.5.7 in Chapter 3 for details pertaining to cross-flow scans.

For this experiment, inlet duct velocity was the noise condition. Noise conditions, in product optimization, are conditions that are not controlled by the designer but are set by the product user or result from external factors not controlled by either the designer or the user. Diffuser inlet duct airflow velocities used were 1200, 800, and 500 fpm. These velocities cover a large span of typical diffuser flow conditions including what is typically seen in actual installations. This parameter was considered a noise parameter, since it is not controlled by the installation. Under modern systems, where a VAV unit of some type is used, a typical diffuser installation will be required to perform under large variations in airflow.

Six parameters were used in the performance characterization experiment. They were diffuser type, diffuser inlet diameter, vertical duct height directly above the diffuser inlet, the type of duct, damper configuration in the diffuser inlet, and the angle of approach to the diffuser side of the horizontal duct run. The parameter and noise configurations with levels are shown in Table 18.

Table 18. Test parameters and noise conditions with different states.

| Parameter | State 1 | State 2 | State 3 | State 4 | State 5 | State 6 |
|---|---|---|---|---|---|---|
| 1. Diffuser Type | Square | Plaque | Perforated Round Neck | Modular Core Perforated | Round | Louvered |
| 2.Inlet Diameter | 8 inches | 10 inches | 12 inches | | | |
| 3. Vertical Duct Height | 0 duct diameters | 1.5 duct diameters | 3 duct diameters | | | |
| 4. Type of Duct | All rigid | Rigid elbow, flex duct | All flex | | | |
| 5. Damper | No damper | Damper parallel to duct | Damper perpendicular to duct | | | |
| 6. Approach Angle | 0 degrees | 23 degrees | 45 degrees | | | |
| Noise Condition | Low State | Medium State | High State | | | |
| 1. Diffuser inlet velocity | 500 fpm | 800 fpm | 1200 fpm | | | |

The most economical (least number of test runs) Taguchi fractional factorial mixed array was used to set up the experiment that could be used to extract the main effects of the test parameters and the variation of those main effects due to the noise conditions. A modified L18 array, called an L18 mixed array was used. [10] The test array has 18 runs, one parameter at six levels and five parameters at three levels. The total degrees of freedom (DOF) needed for the main effects are 15 and this array has 17 DOF. This was determined for the main effects by taking the total number of levels in each parameter, subtracting one from each for the mean, and adding them together. The DOF for the test array is merely the number of runs minus one for mean to determine variability. The array is shown in Table 19.

Table 19. Test array for field condition variations testing.

| Run Order | Run # | Diffuser Type | Inlet | Duct Height | Type Duct | Damper | Damper Type | Approach Angle |
|---|---|---|---|---|---|---|---|---|
| 2 | 1 | Square | 8 | 0 | Rigid | None | RndSliding | 0 |
| 5 | 2 | Square | 10 | 1.5 | Mix | Perpendicular | RndSliding | 23 |
| 16 | 3 | Square | 12 | 3 | Flex | Parallel | RndSliding | 45 |
| 12 | 4 | Plaque | 8 | 0 | Mix | Perpendicular | RndSliding | 45 |
| 8 | 5 | Plaque | 10 | 1.5 | Flex | Parallel | RndSliding | 0 |
| 1 | 6 | Plaque | 12 | 3 | Rigid | None | RndSliding | 23 |
| 14 | 7 | Perf Rnd | 8 | 1.5 | Rigid | Parallel | RndSliding | 23 |
| 6 | 8 | Perf Rnd | 10 | 3 | Mix | None | RndSliding | 45 |
| 15 | 9 | Perf Rnd | 12 | 0 | Flex | Perpendicular | RndSliding | 0 |
| 3 | 10 | Mod Core | 8 | 3 | Flex | Perpendicular | SqOpBld | 23 |
| 17 | 11 | Mod Core | 10 | 0 | Rigid | Parallel | SqOpBld | 45 |
| 11 | 12 | Mod Core | 12 | 1.5 | Mix | None | SqOpBld | 0 |
| 13 | 13 | Round | 8 | 1.5 | Flex | None | RndSliding | 45 |
| 18 | 14 | Round | 10 | 3 | Rigid | Perpendicular | RndSliding | 0 |
| 9 | 15 | Round | 12 | 0 | Mix | Parallel | RndSliding | 23 |
| 4 | 16 | Louvered | 8 | 3 | Mix | Parallel | SqOpBld | 0 |
| 7 | 17 | Louvered | 10 | 0 | Flex | None | SqOpBld | 23 |
| 10 | 18 | Louvered | 12 | 1.5 | Rigid | Perpendicular | SqOpBld | 45 |

There were three sets of output measures, one for each noise condition. The output array for the noise condition, 1200 fpm, is shown in Table 20.

Table 20. Output array at high state noise condition for the field installation experiment.

| Run # | Forward Throw Asymmetry, $T_f$ 1200 fpm | Backward Throw Asymmetry, $T_b$ 1200 fpm | Change in NC [dB] 1200 fpm | Total Pressure Ratio 1200 fpm |
|---|---|---|---|---|
| 1 | | | | |
| 2 | | | | |
| … | | | | |
| 17 | | | | |
| 18 | | | | |

All duct leading to the diffuser was round, either rigid or flex. For diffusers with a square inlet (modular core and louvered), a round to square adaptor was used. Damper types used where the round sliding and the square opposed blade dampers. Approach angle is measured from perpendicular to the diffuser side.

## 4.4 Results

Each diffuser output measure is a comparison of the real-world installation configurations against the corresponding data from the base Standard 70 tests. The Standard 70 data used for comparison was the data from the same diffuser type of the same manufacturer at the same flow rate used in the field installation. The asymmetry was determined by comparing the throw distance in zone 3 of the zone plots from the real-world configurations and the Standard 70 tests. Figure 27 shows the velocity profile of a 12-inch square diffuser at 1200 fpm, which is used to develop the zone plot in Figure 28.

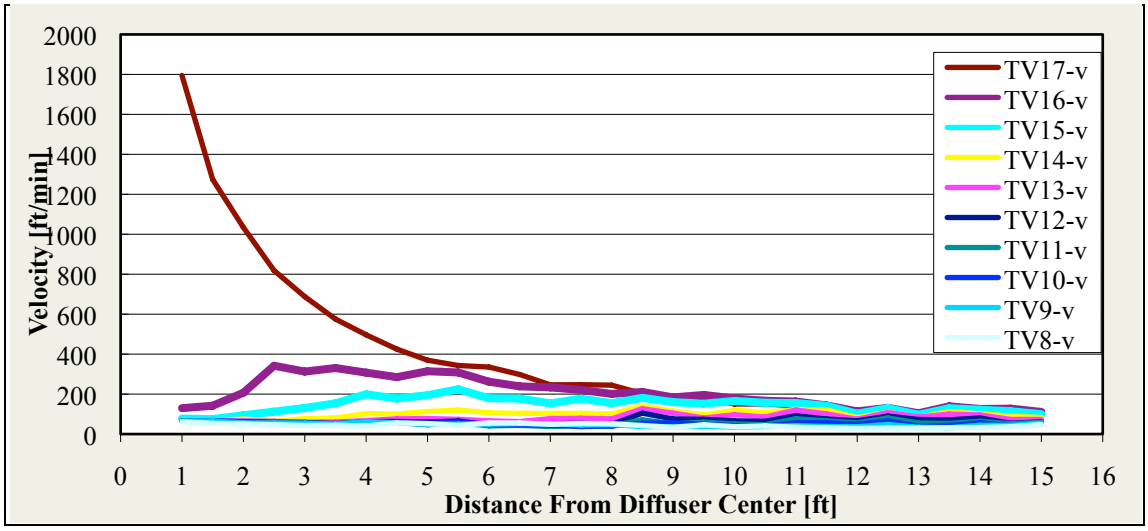


Figure 27. Standard 70 throw data at 1200 fpm for 12” square diffuser.

To determine the zone throw distance at each recorded data point, a ratio was determined between the maximum throw velocity at each data point versus the calculated neck velocity based on the air flow rate and diffuser neck size, or $V_x/V_k$. This ratio is used as the y-axis of the zone plot in Figure 28. Then a ratio that accounts for throw distance from the center of the diffuser versus the neck area was calculated. The square root of the neck area was taken to linearize the data points into proper zone profiling, giving $X/(A_k)^{1/2}$. This ratio was the x-axis of the zone plot in Figure 28 resulting in a log-log plot deemed a diffuser zone plot. This shows how the discharge air is reacting as it propagates away from the center of the diffuser. All values are put into units of feet before becoming non-dimensional ratios.

Referring to Figure 13 for zone plot slope information and the description in Chapter 3, the following analysis described using the zone plot in Figure 28 was performed to compare Standard 70 throw data to the field installation configuration throw data. This determined the asymmetry of the field-testing installations.

The zone plots for the field-testing results and the Standard 70 test results were used to determine the effects on throw due to the field installation. Using the starting x1 and y1 values for the zone three slope (yellow dot), at a constant y2 value of 0.2 for the throw velocity over the inlet velocity, which was held constant for each comparison, a value for x2 (pink dot), throw distance over square root of the inlet area, was calculated. The equation for slope, ([y2-y1]/[x2-x1]), is used to find the x2 value where the y2 value is 0.2. This method was used to obtain a ratio between this x2 value (Standard 70 test) and the corresponding x2 value for the field installation test. The ratio is the ratio-of-throw distance for the two conditions. The y-axis value was held constant at 0.2 because for

every test configuration this point was in zone three and so that the comparison of each configuration could then be related on the same scale for predicting the output. The x2 value was calculated for each standard 70 and field installation in the same manner. From those values, throw ratios of each field installation noise condition to standard 70, (x2/x2std70) of the calculated x2 values, were made to show how much throw was affected by the installation parameters.

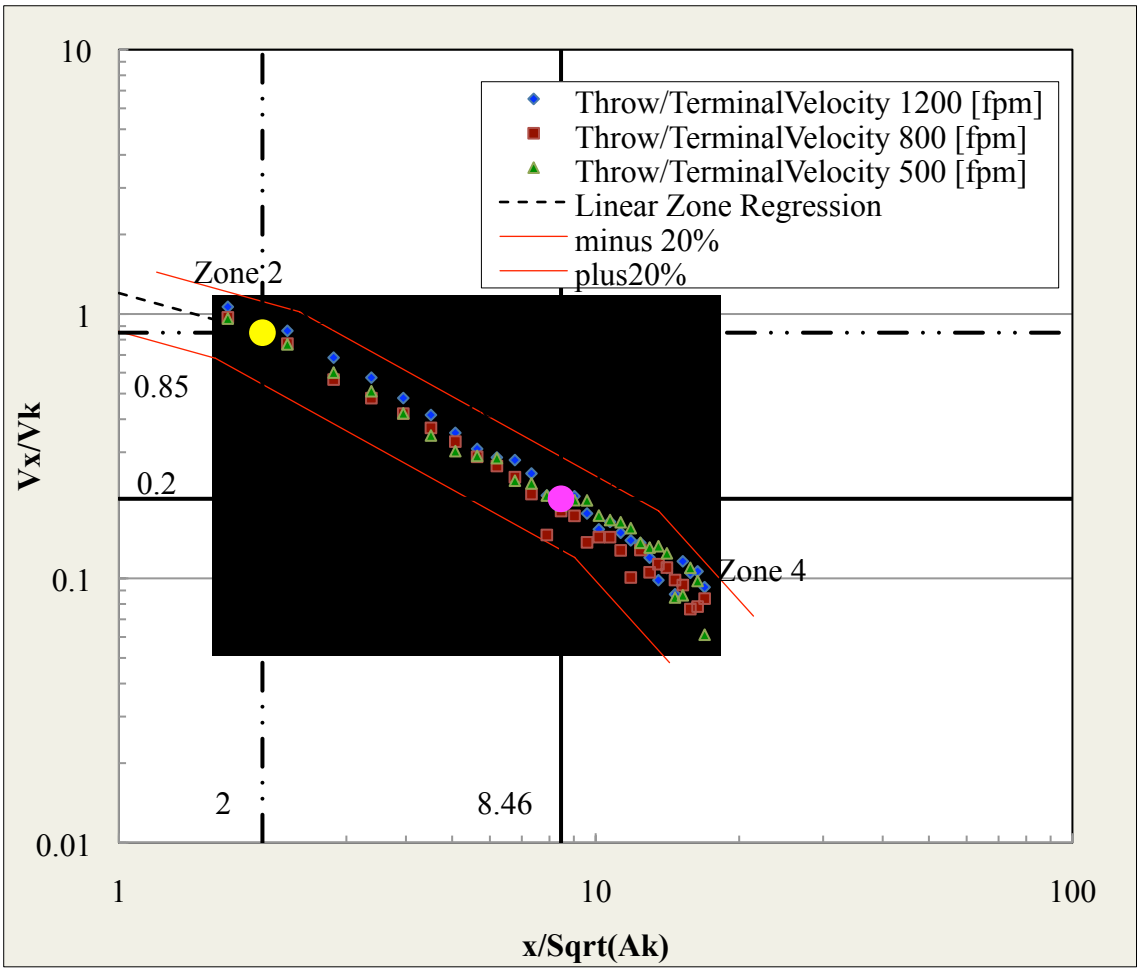


Figure 28. Standard 70 zone plot for 12" square diffuser, where (x1,y1) symbolizes start of zone 3 (yellow dot) and (pink dot) gives the x2 value when y2 is 0.2.

The change in NC level is a direct difference between the NC of the field-testing configurations and the NC of the Standard 70 tests. The often, low NC levels at 500 fpm were not always obtainable during the Standard 70 tests due to the background sound level of the throw room. Therefore, this data was not considered in the analysis. The total pressure ratio is determined by comparing the averaged total pressure of the field-testing configurations against the total pressure of the plenum in the Standard 70 tests.

For example, Figure 29 through Figure 32 show the throw velocities and corresponding zone plots for both forward and backward throw for run number 3 at 1200 fpm inlet duct velocity. Based on this data and the previously calculated Standard 70 data, the final results for throw asymmetry, sound and pressure ratio were determined.

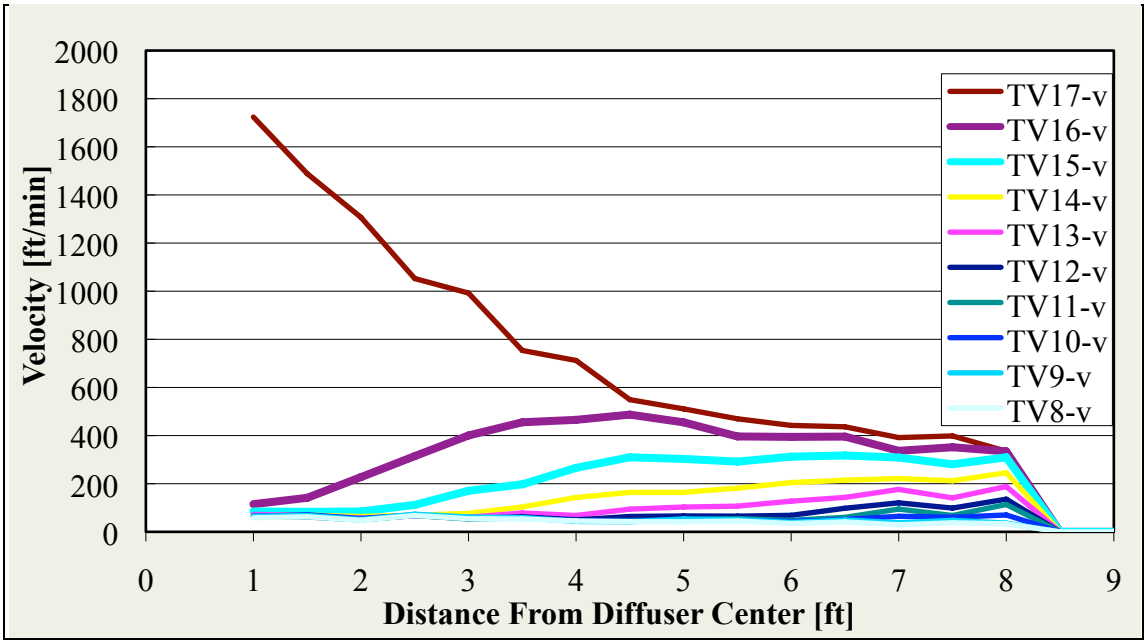


Figure 29. Field installation run #3 forward throw at 1200 fpm.

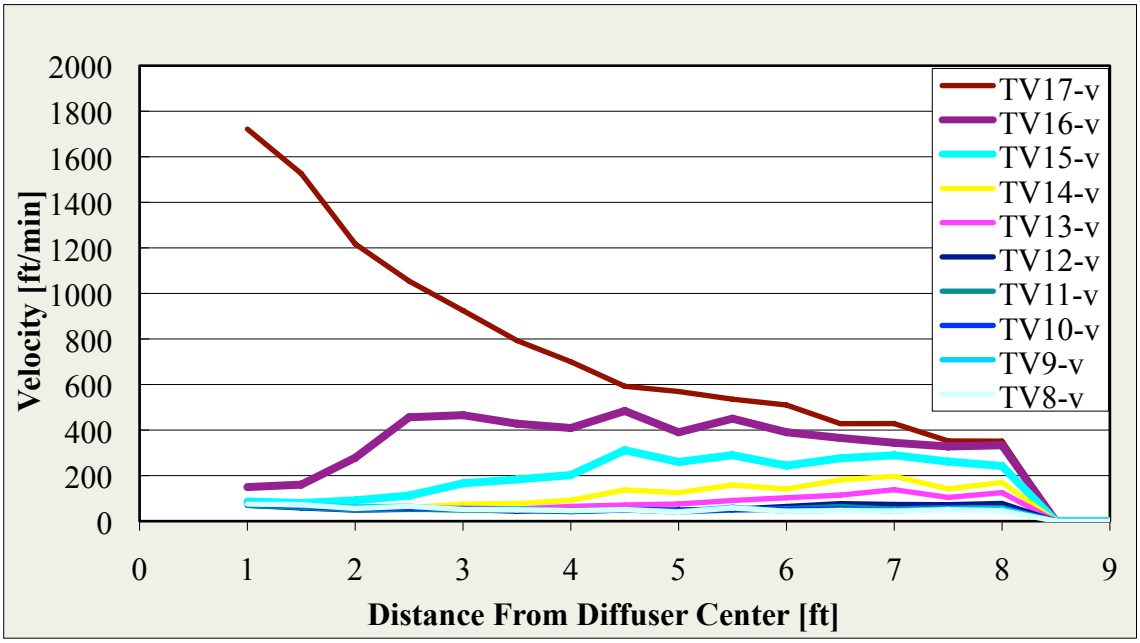


Figure 30. Field installation run #3 backward throw at 1200 fpm.

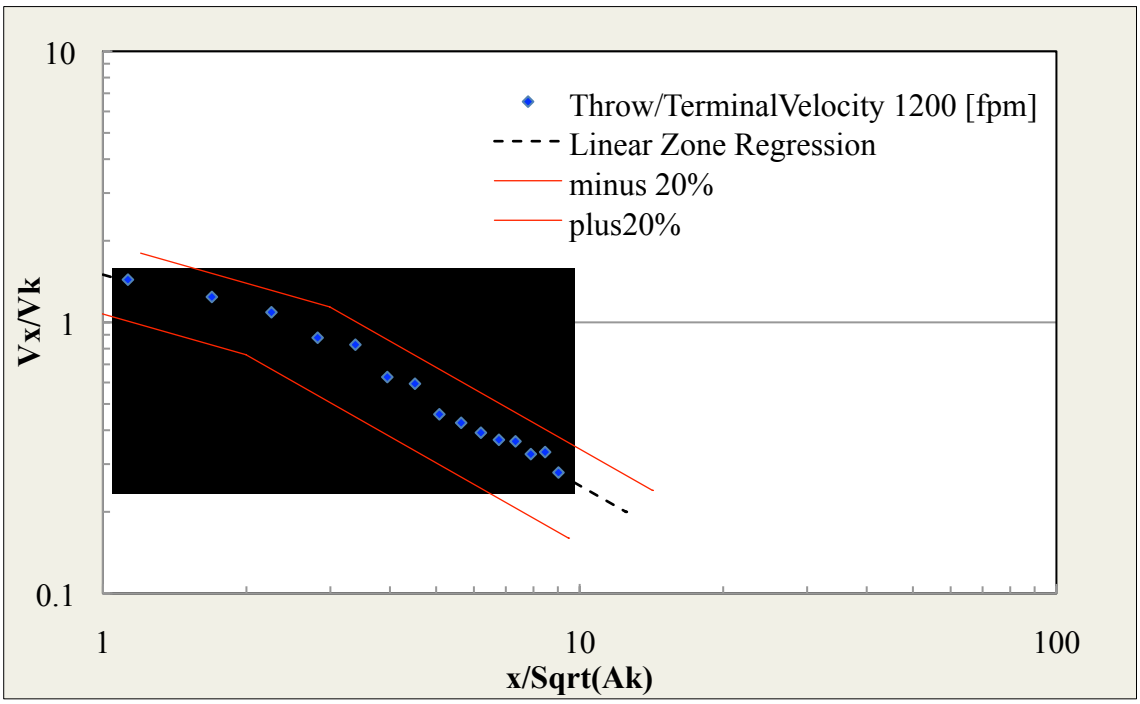


Figure 31. Zone plot of field install run #3 forward throw 1200 fpm.

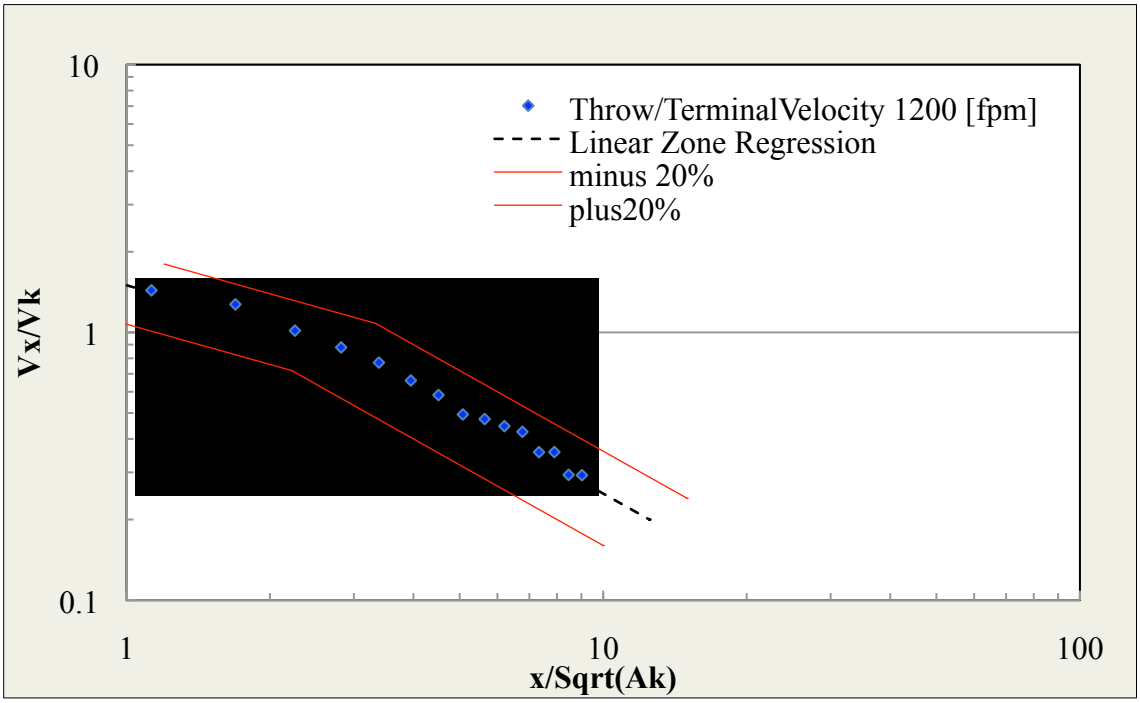


Figure 32. Zone plot of field install run #3 backward throw 1200 fpm.

Table 21 shows the recorded diffuser output throw ratios, noise criteria level changes and total pressure ratios for field installations compared to Standard 70 data for all test runs. A statistical analysis was conducted to help better develop diffuser throw, noise criteria and total pressure ratio prediction models for future field installations. In order to statistically analyze the output measures, they had to be quantifiable. The statistical tool used was Minitab. The main effects and interaction plots were determined based on the parameters listed in Table 18 independently for each output measure listed in Table 20.

Table 21. Diffuser output throw ratios, noise criteria level changes and total pressure ratios for field installations compared to Standard 70 data.

| Run # | Forward Throw Asymmetry, $T_f$ | | | Backward Throw Asymmetry, $T_b$ | | | Change in NC [dB] | | Total Pressure Ratio | | |
|---|---|---|---|---|---|---|---|---|---|---|---|
| | 500 fpm | 800 fpm | 1200 fpm | 500 fpm | 800 fpm | 1200 fpm | 800 fpm | 1200 fpm | 500 fpm | 800 fpm | 1200 fpm |
| 1 | 1.53 | 1.53 | 1.53 | 0.4 | 0.4 | 0.45 | 8.0 | 6.50 | 1.6 | 1.71 | 1.78 |
| 2 | 0.91 | 0.91 | 0.91 | 1.0 | 1.0 | 1.05 | 11. | 11.50 | 2.1 | 2.14 | 2.25 |
| 3 | 1.42 | 1.42 | 1.50 | 1.5 | 1.5 | 1.50 | 8.5 | 8.50 | 1.7 | 1.89 | 1.85 |
| 4 | 1.04 | 1.04 | 1.04 | 0.5 | 0.4 | 0.47 | 8.5 | 10.5 | 2.1 | 2.27 | 2.40 |
| 5 | 0.69 | 0.69 | 0.69 | 1.3 | 1.3 | 1.37 | 15. | 13.5 | 2.1 | 2.35 | 2.54 |
| 6 | 0.96 | 0.96 | 1.01 | 1.0 | 1.0 | 0.99 | 6.0 | 5.50 | 1.1 | 1.18 | 1.19 |
| 7 | 0.97 | 0.97 | 0.90 | 1.2 | 1.0 | 1.06 | 9.5 | 9.50 | 2.1 | 2.09 | 2.18 |
| 8 | 1.03 | 1.03 | 1.03 | 0.9 | 0.9 | 0.99 | 2.5 | 2.00 | 1.2 | 1.22 | 1.23 |
| 9 | 1.12 | 1.16 | 1.16 | 0.5 | 0.8 | 0.81 | 11. | 5.50 | 1.7 | 1.78 | 1.73 |
| 10 | 1.28 | 1.32 | 1.47 | 0.9 | 1.0 | 1.12 | 2.5 | 2.50 | 1.5 | 1.65 | 1.46 |
| 11 | 1.30 | 1.30 | 1.30 | 0.9 | 0.9 | 0.96 | 4.0 | 3.00 | 1.3 | 1.39 | 1.35 |
| 12 | 1.13 | 1.25 | 1.16 | 0.9 | 0.8 | 0.83 | 2.0 | 1.00 | 1.2 | 1.24 | 1.18 |
| 13 | 1.04 | 1.04 | 1.04 | 0.8 | 0.8 | 0.89 | 7.0 | 7.00 | 1.4 | 1.52 | 1.61 |
| 14 | 1.26 | 1.26 | 1.13 | 1.3 | 1.3 | 1.12 | 10. | 9.50 | 1.7 | 1.91 | 1.87 |
| 15 | 1.56 | 1.44 | 1.62 | 1.3 | 1.2 | 1.42 | 9.5 | 10.00 | 1.4 | 1.48 | 1.50 |
| 16 | 0.98 | 0.89 | 0.89 | 0.9 | 0.8 | 0.84 | 5.5 | 8.00 | 1.9 | 2.08 | 2.18 |
| 17 | 1.32 | 1.32 | 1.32 | 0.1 | 0.1 | 0.16 | 12. | 8.50 | 2.3 | 2.56 | 2.59 |
| 18 | 1.37 | 1.44 | 1.38 | 0.5 | 0.7 | 0.68 | 11. | 9.50 | 1.7 | 1.85 | 1.84 |

## 4.5 Analysis

The main effects show the average value of the measured output at the different levels of each of the input parameters. The example main effects plots used for data analysis of forward throw are shown in Figure 33. Forward throw is the output and each plot shows how the throw varied with each parameter at different levels. The horizontal line gives the overall averaged data means of the forward throw data and acts as the reference value to compare the effect of each parameter. Diffuser type and inlet diameter are parameters that were used during the Standard 70 testing. Duct height, duct type, damper and approach angle are significant to the field installation testing. In the statistical model, it is

assumed that each parameter is an additive parameter to the system mean. However based on the physics of the system, some of the parameters are known to affect the sensitivity of the system and become multipliers instead of additive values. In this experiment, diffuser type and inlet diameter are parameters that add sensitivity to the system. With different diffuser types, comes differing inlet to outlet ratios, meaning some diffusers have the same outlet size but changing inlet diameter, while others increase or decrease outlet size along with increased or decreased inlet diameter.

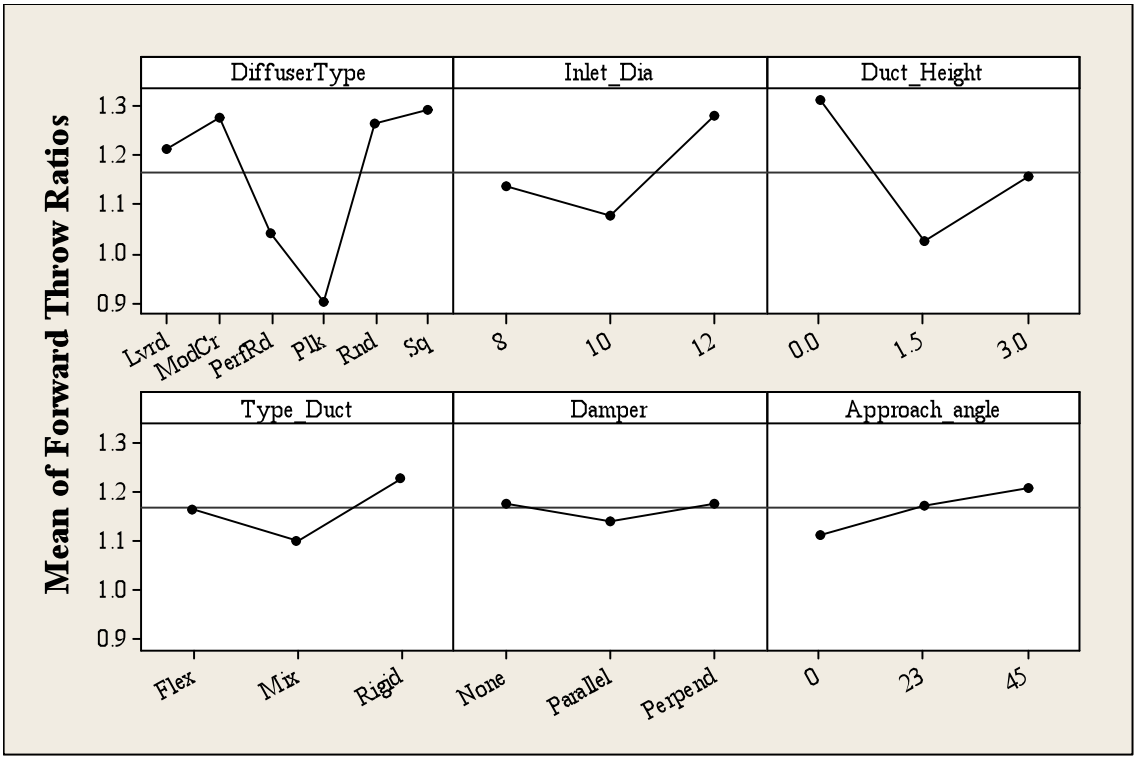


Figure 33. Main effects plot for field installations forward throw.

The example interaction plots for data analysis of the forward throw are shown in Figure 34. Each plot shows the average output level for the different combinations of two parameters. If the two variables have an interaction, which is shown when the lines cross

or are not parallel between points, then their effects on the output are not simply additive. Otherwise, if the lines between each point in Figure 34 are parallel, the output effects of the parameters are additive. For the interaction plots, when the lines between each point of each color on each graph are parallel, there is no interaction. When the lines cross or are not parallel, there is an interaction and the significance of the interaction is shown by the difference in the slope of each line. Like the main effects, depending on the determination of the importance of the interaction on the output, the combination of the two parameters may or may not be significant in determining the sensitivity to the system.

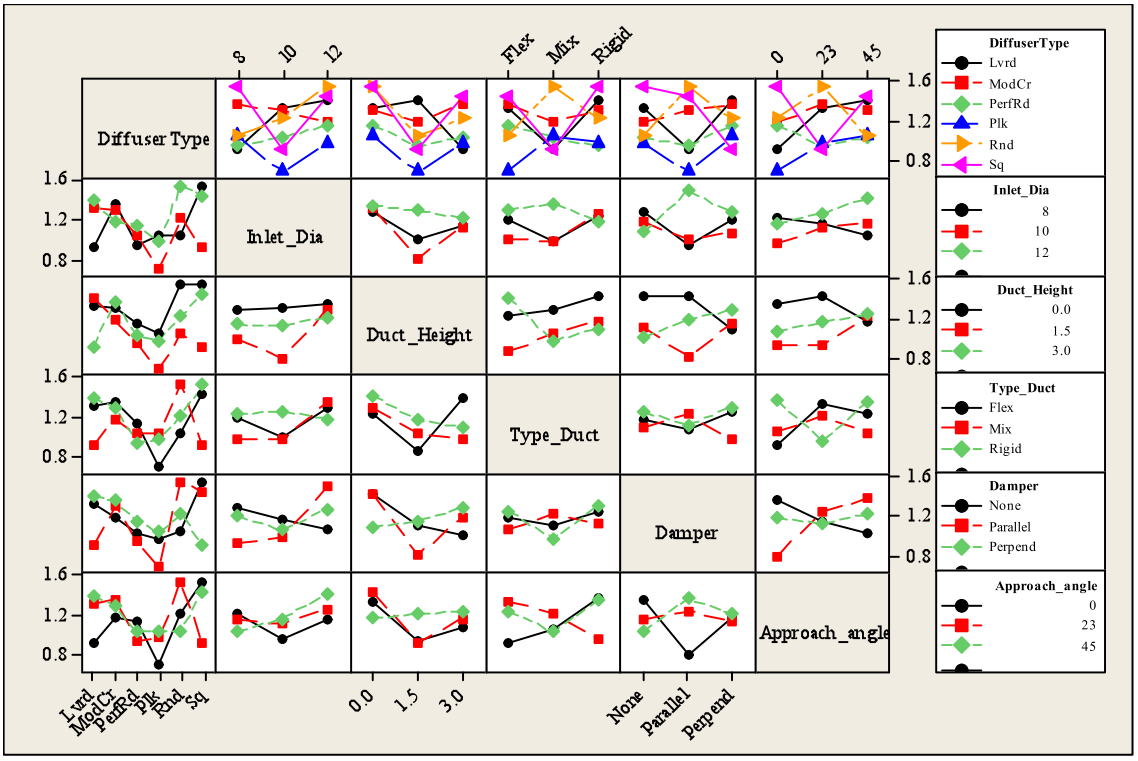


Figure 34. Interaction plots for field installations forward throw.

This evaluation was done for each diffuser output listed in Table 20, forward throw, backward throw, sound and pressure, for all configurations in the L18 fractional factorial test array. A predictive algorithm was developed using the main effects and interactions data for each of the four output measures. In some cases, main effect and interaction effect plots seem to indicate multiple effects occurring within the configurations, however, the physics of the system was also used as a basis behind all determinations of sensitivity. Thus if a reasonable physical explanation was not available for an effect, the effect was not included in the model. Also, it was found that when certain main effects and interactions were included in the predictive model, they did not improve the overall accuracy of the prediction and where thus removed from the prediction equation. Each output measure required an individual algorithm due to a different combination of significant parameter effects on sensitivity. Sections 4.5.1 through 4.5.4 cover the predictive equations for the four output measures.

4.5.1 Forward Throw Ratio ($T_f$)

Figure 33, Figure 34 and Table 22 were used to determine a predictive algorithm model for forward throw. From Figure 33, the diffuser type graph shows a significant sensitivity to the forward throw based on the type of diffuser used in the configuration. Inlet diameter also is considered to have a large sensitivity effect on the forward throw. These parameters are characteristics of the diffuser. Therefore these two values are multipliers in the prediction equation. The other four parameters in Figure 33 are field installation parameters. From the remaining four graphs of the main effects, duct height is the only one that results in significant output variation and will be used as an additive quantity to the multipliers. Duct type, damper, and approach angle have nominal effects

according to the graphs in Figure 33. Considering the interaction plots in Figure 34, it was determined that the interaction between duct height and damper resulted in a change from the sum effect of adding the individual main effects. Therefore, an interaction effect is included. This quantity was used as an additive quantity just as the main effect of duct height.

The predictive equation for the ratio of field installation forward throw to Standard 70 throw is:

$$FTR_{Prediction} = M_{DT} * M_{ID} * (A_{DCH} + A_{DCH*D}) + 1$$

The parameters in this equation were quantified as follows based on Figure 33, Figure 34 and any anomalies discovered during experimentation.

*Main Effect Parameters*

- For diffuser type;

Perforated Round: $M_{DT} = 0.8$

Round: $M_{DT} = 1.0$

Plaque: $M_{DT} = 0.6$

Square: $M_{DT} = 1.0$

Perforated Square: $M_{DT} = 1.0$

Louvered: $M_{DT} = 1.0$

❖ For inlet diameter;

12-inch inlet diameter: $M_{ID} = 1.2$

8 or 10-inch inlet diameter: $M_{ID} = 1.0$

❖ For duct height;

Duct height of 0: $A_{DCH} = 0.4$

Duct height of 1.5: $A_{DCH} = 0.1$

Duct height of 3: $A_{DCH} = 0$

*Interaction Parameters*

❖ For the interaction between duct height and damper;

Duct height of 0 and damper is perpendicular: $A_{DCH*D} = -0.2$

Duct height of 0 and damper is not perpendicular: $A_{DCH*D} = 0$

Duct height of 1.5 and damper is parallel: $A_{DCH*D} = -0.1$

Duct height of 1.5 and damper is not parallel: $A_{DCH*D} = 0$

Duct height of 3 and damper is 0 (no damper): $A_{DCH*D} = 0$

Duct height of 3 and damper is a damper and damper type is not round opposed blade: $A_{DCH*D} = 0.2$

Concerning the last interaction shown, it was discovered that when the duct height was 3 diameters, the round opposed blade damper, compared to other dampers, caused less of an increase in throw velocity in the forward direction. This equation gives a predicted

value that is compared to the actual value obtained for each configuration in Table 22 as it varies from a reference value of one. An error is established between the two values and then from this list of errors, a standard deviation is calculated to help determine if the algorithm is accurate for all the configurations. The standard deviations in Table 22 show that the current prediction algorithm is within 20 percent accuracy for the 18 test configurations used in the field-testing experiment. To verify the prediction model, Table 23 shows random configurations that were installed and tested.

Table 22. Predicted values and corresponding errors for forward throw.

| Run # | Predicted $T_f$ | Experiment $T_f$ | Error | Experiment $T_f$ | Error | Experiment $T_f$ | Error |
|---|---|---|---|---|---|---|---|
| | | 1200 fpm | | 800 fpm | | 500 fpm | |
| 1 | 1.40 | 1.53 | -0.13 | 1.53 | -0.13 | 1.53 | -0.13 |
| 2 | 1.10 | 0.91 | 0.19 | 0.91 | 0.19 | 0.91 | 0.19 |
| 3 | 1.24 | 1.50 | -0.26 | 1.42 | -0.18 | 1.42 | -0.18 |
| 4 | 1.12 | 1.04 | 0.08 | 1.04 | 0.08 | 1.04 | 0.08 |
| 5 | 1.00 | 0.69 | 0.31 | 0.69 | 0.31 | 0.69 | 0.31 |
| 6 | 1.00 | 1.01 | -0.01 | 0.96 | 0.04 | 0.96 | 0.04 |
| 7 | 1.00 | 0.90 | 0.10 | 0.97 | 0.03 | 0.97 | 0.03 |
| 8 | 1.00 | 1.03 | -0.03 | 1.03 | -0.03 | 1.03 | -0.03 |
| 9 | 1.19 | 1.16 | 0.03 | 1.16 | 0.03 | 1.12 | 0.07 |
| 10 | 1.20 | 1.47 | -0.27 | 1.32 | -0.12 | 1.28 | -0.08 |
| 11 | 1.40 | 1.30 | 0.10 | 1.30 | 0.10 | 1.30 | 0.10 |
| 12 | 1.12 | 1.16 | -0.04 | 1.25 | -0.13 | 1.13 | -0.01 |
| 13 | 1.10 | 1.04 | 0.06 | 1.04 | 0.06 | 1.04 | 0.06 |
| 14 | 1.20 | 1.13 | 0.07 | 1.26 | -0.06 | 1.26 | -0.06 |
| 15 | 1.48 | 1.62 | -0.14 | 1.44 | 0.04 | 1.56 | -0.08 |
| 16 | 1.20 | 0.89 | 0.31 | 0.89 | 0.31 | 0.98 | 0.22 |
| 17 | 1.40 | 1.32 | 0.08 | 1.32 | 0.08 | 1.32 | 0.08 |
| 18 | 1.12 | 1.38 | -0.26 | 1.44 | -0.32 | 1.37 | -0.25 |
| | | Average | 0.01 | Average | 0.02 | Average | 0.02 |
| | | Std Deviation | 0.17 | Std Deviation | 0.16 | Std Deviation | 0.14 |

Table 23. Verification testing configurations.

| Run # | Diffuser Type | Inlet | Duct Height | Type Duct | Damper | Damper Type | Approach Angle |
|---|---|---|---|---|---|---|---|
| 1 | Square | 10 | 1.5 | Rigid | 0 | RndSliding | 0 |
| 2 | Plaque | 10 | 1.5 | Rigid | 0 | RndOpBld | 0 |
| 3 | Plaque | 10 | 1.5 | Rigid | Parallel | RndSliding | 0 |
| 4 | Plaque | 10 | 1.5 | Rigid | Parallel | RndOpBld | 0 |
| 5 | Plaque | 10 | 3 | Rigid | Parallel | RndOpBld | 0 |
| 6 | Plaque | 10 | 3 | Rigid | Parallel | RndSliding | 0 |
| 7 | Plaque | 10 | 0 | Flex | Parallel | RndOpBld | 0 |
| 8 | Plaque | 10 | 0 | Flex | 0 | RndOpBld | 0 |

It was determined that approach angle has no affect on the configuration accept as to where the max throw exited the diffuser face and was left out of the verification testing. The parameters in Table 23 were used as such to develop comparisons based on a few important characteristics and to determine if the prediction model would hold true. The configurations were tested exactly as before, but only for the highest noise condition to test multiple configurations in less time. The results and prediction values are listed in Table 24 along with the errors and standard deviations.

Table 24. Results of verification testing configurations for forward throw.

| Run # | Predicted $T_f$ | Experiment $T_f$ | Error |
|---|---|---|---|
| | | 1200 fpm | |
| 1 | 1.10 | 1.03 | 0.07 |
| 2 | 1.06 | 1.02 | 0.04 |
| 3 | 1.00 | 1.19 | -0.19 |
| 4 | 1.00 | 0.90 | 0.10 |
| 5 | 1.00 | 0.88 | 0.12 |
| 6 | 1.12 | 1.15 | -0.03 |
| 7 | 1.24 | 0.96 | 0.28 |
| 8 | 1.24 | 1.29 | -0.05 |
| | | Average | 0.04 |
| | | Std Deviation | 0.14 |

Table 24 shows that the accuracy of the prediction model has a standard deviation well below 20 percent for the verification configurations. Therefore, the algorithm should be adequate in determining the performance of any ceiling diffuser installation forward throw asymmetry to within acceptable limitations.

The same process was repeated for the remaining three output measures of the ceiling diffuser installation configurations. The correction factors and prediction equations for the other three output measures are listed in the following sections using the same process used for the forward throw predictive algorithm.

4.5.2 Backward Throw Ratio ($T_b$)

The backward throw predictive algorithm was determined same as the forward throw. A main effect plots were derived along with interactions for the same parameters as forward throw. The main effects parameters, diffuser type and inlet diameter, have a large sensitivity on the backward throw and are characteristics of the diffuser, while duct height and damper have a smaller affect as they are field installation parameters. The parameters that are characteristics of the diffuser are multipliers and the parameters that are field installation related are additive quantities. The interactions between duct height and damper, duct height and duct type, and duct height and inlet diameter resulted in a change from the sum effect of adding the individual main effects leading to additive quantities in the predictive algorithm.

The predictive equation for the ratio of field installation backward throw to Standard 70 throw is:

$$BTR_{Prediction} = M_{DT} * M_{ID} * (A_{DCH} + A_D + A_{DCH*D} + A_{DCH*DCT} + A_{DCH*ID}) + 1$$

*Main Effect Parameters*

- For diffuser type;

Louvered: $M_{DT} = 1.2$

Not Louvered: $M_{DT} = 1.0$

- For inlet diameter;

12-inch inlet diameter: $M_{ID} = 1.1$

10-inch inlet diameter: $M_{ID} = 1.0$

8-inch inlet diameter: $M_{ID} = 0.9$

- For duct height;

Duct height of 0: $A_{DCH} = -0.4$

Duct height of 1.5: $A_{DCH} = -0.2$

Duct height of 3: $A_{DCH} = 0$

- For Damper;

Damper is parallel: $A_D = 0.3$

Damper is perpendicular: $A_D = 0.1$

Damper is 0 (no damper): $A_D = 0$

*Interaction Parameters*

❖ For the interaction between duct height and damper;

Duct height of 0 and damper is parallel: $A_{DCH*D} = 0.3$

Duct height of 0 and damper is perpendicular: $A_{DCH*D} = 0.1$

Duct height of 0 and damper is 0 (no damper): $A_{DCH*D} = 0$

Duct height of 1.5 and damper is parallel: $A_{DCH*D} = 0.1$

Duct height of 1.5 and damper is not parallel: $A_{DCH*D} = 0$

Duct height of 3: $A_{DCH*D} = 0$

❖ For the interaction between duct height and duct type;

Duct height of 0 and duct type is flex: $A_{DCH*DCT} = -0.1$

Duct height of 0 and duct type is not flex: $A_{DCH*DCT} = 0$

Duct height of 1.5: $A_{DCH*DCT} = 0$

Duct height of 3 and duct type is flex: $A_{DCH*DCT} = 0.1$

Duct height of 3 and duct type is not flex: $A_{DCH*DCT} = 0$

❖ For the interaction between duct height and inlet diameter;

Duct height of 0 and 12-inch inlet diameter: $A_{DCH*ID} = 0$

Duct height of 0 and 8 or 10-inch inlet diameter: $A_{DCH*ID} = -0.2$

Duct height of 1.5 or 3: $A_{DCH*ID} = 0$

From the given correction factors and the predictive equation, the following experimental backward throw values were compared to the predicted values in Table 25 and gave the standard deviation of 0.16 or 16 percent for each flow rate velocity. With a standard deviation below 20 percent, the accuracy of the predictive algorithm for backward throw was confirmed. Verification testing was not done for backward throw because it was found that forward throw, through verification, was accurate to within 20 percent and backward throw was given the same consideration.

Table 25. Predicted and corresponding values for backward throw.

| Run # | Predicted $T_b$ | Experiment $T_b$ | Error | Experiment $T_b$ | Error | Experiment $T_b$ | Error |
|---|---|---|---|---|---|---|---|
| | | 1200 fpm | | 800 fpm | | 500 fpm | |
| 1 | 0.46 | 0.45 | 0.01 | 0.49 | -0.03 | 0.49 | -0.03 |
| 2 | 0.90 | 1.05 | -0.15 | 1.05 | -0.15 | 1.05 | -0.15 |
| 3 | 1.44 | 1.50 | -0.06 | 1.50 | -0.06 | 1.50 | -0.06 |
| 4 | 0.64 | 0.47 | 0.17 | 0.47 | 0.17 | 0.50 | 0.14 |
| 5 | 1.20 | 1.37 | -0.17 | 1.37 | -0.17 | 1.37 | -0.17 |
| 6 | 1.00 | 0.99 | 0.01 | 1.01 | -0.01 | 1.01 | -0.01 |
| 7 | 1.18 | 1.06 | 0.12 | 1.06 | 0.12 | 1.21 | -0.03 |
| 8 | 1.00 | 0.99 | 0.01 | 0.99 | 0.01 | 0.99 | 0.01 |
| 9 | 0.67 | 0.81 | -0.14 | 0.81 | -0.14 | 0.59 | 0.08 |
| 10 | 1.18 | 1.12 | 0.06 | 1.07 | 0.11 | 0.99 | 0.19 |
| 11 | 1.00 | 0.96 | 0.04 | 0.96 | 0.04 | 0.96 | 0.04 |
| 12 | 0.78 | 0.83 | -0.05 | 0.88 | -0.10 | 0.93 | -0.15 |
| 13 | 0.82 | 0.89 | -0.07 | 0.89 | -0.07 | 0.89 | -0.07 |
| 14 | 1.10 | 1.12 | -0.02 | 1.30 | -0.20 | 1.30 | -0.20 |
| 15 | 1.22 | 1.42 | -0.20 | 1.29 | -0.07 | 1.32 | -0.10 |
| 16 | 1.32 | 0.84 | 0.48 | 0.84 | 0.48 | 0.94 | 0.38 |
| 17 | 0.16 | 0.16 | 0.00 | 0.14 | 0.02 | 0.13 | 0.03 |
| 18 | 0.87 | 0.68 | 0.19 | 0.70 | 0.17 | 0.56 | 0.31 |
| | | Average | 0.01 | Average | 0.01 | Average | 0.01 |
| | | Std Deviation | 0.16 | Std Deviation | 0.16 | Std Deviation | 0.16 |

### 4.5.3 Total Pressure Ratio ($P_{Total}$)

The total pressure ratio predictive algorithm was determined same as the forward throw. A main effect plots was derived along with interactions for the same parameters as forward throw. The main effects parameters diffuser type and inlet diameter have a large sensitivity on the total pressure ratio and are characteristics of the diffuser, while duct height, duct type, and damper have a smaller affect as they are field installation parameters. The parameters that are characteristics of the diffuser are multipliers and the parameters that are field installation related are additive quantities. The interaction between duct height and damper resulted in a change from the sum effect of adding the individual main effects leading to additive quantities in the predictive algorithm.

The predictive equation for the ratio of field installation pressure loss to Standard 70 pressure loss is:

$$TPR_{Prediction} = M_{DT} * M_{ID} * ( A_{DCH} + A_{DCT} + A_{D} + A_{DCH*D} ) + 1$$

*Main Effect Parameters*

- For diffuser type;

Louvered: $M_{DT} = 1.4$

Perforated Round: $M_{DT} = 1.0$

Round: $M_{DT} = 1.0$

Plaque: $M_{DT} = 1.2$

Square: $M_{DT} = 1.2$

Perforated Square: $M_{DT} = 0.6$

- For inlet diameter;

12-inch inlet diameter: $M_{ID} = 0.6$

8 or 10-inch inlet diameter: $M_{ID} = 1.0$

- For duct height;

Duct height of 0: $A_{DCH} = 0.6$

Duct height of 1.5: $A_{DCH} = 0.4$

Duct height of 3: $A_{DCH} = 0.2$

- For duct type;

Duct type is flex: $A_{DCT} = 0.3$

Duct type is mix: $A_{DCT} = 0.1$

Duct type is rigid: $A_{DCT} = 0$

- For Damper;

Damper is 0 (no damper): $A_D = 0$

Damper is not 0 and damper type is Round Sliding or Square Opposed Blade:

$$A_D = 0.5$$

Damper is not 0 and damper type is Round Opposed Blade:

$$A_D = 0.2$$

*Interaction Parameters*

- For the interaction between duct height and damper;

Duct height of 0 and damper is 0 (no damper): $A_{DCH*D} = 0$

Duct height of 0 and damper is not 0: $A_{DCH*D} = -0.1$

Duct height of 1.5 or 3: $A_{DCH*D} = 0$

The given predictive equation for pressure and the correction factors developed the predicted values given in Table 26 for each test configuration. Each was compared to the experimental values to obtain the given error values. From the error values, the standard deviations were determined and are less than 20 percent, giving an accurate predictive algorithm.

In Table 27, the diffuser inlet configurations used for verification were tested and gave the results listed in Table 28. With a standard deviation of 15 percent for all the verification tests performed, the accuracy of the predictive pressure algorithm was confirmed at 1200 fpm.

Table 26. Predicted and corresponding error values for pressure.

| Run # | Predicted $P_{Total}$ | Experiment $P_{Total}$ | Error | Experiment $P_{Total}$ | Error | Experiment $P_{Total}$ | Error |
|---|---|---|---|---|---|---|---|
| | | 1200 fpm | | 800 fpm | | 500 fpm | |
| 1 | 1.72 | 1.78 | -0.06 | 1.71 | 0.01 | 1.63 | 0.10 |
| 2 | 2.20 | 2.25 | -0.05 | 2.14 | 0.06 | 2.17 | 0.03 |
| 3 | 1.72 | 1.85 | -0.13 | 1.89 | -0.17 | 1.70 | 0.02 |
| 4 | 2.32 | 2.40 | -0.08 | 2.27 | 0.05 | 2.19 | 0.13 |
| 5 | 2.44 | 2.54 | -0.10 | 2.35 | 0.09 | 2.17 | 0.27 |
| 6 | 1.14 | 1.19 | -0.05 | 1.18 | -0.04 | 1.16 | -0.02 |
| 7 | 1.90 | 2.18 | -0.28 | 2.09 | -0.19 | 2.11 | -0.21 |
| 8 | 1.30 | 1.23 | 0.07 | 1.22 | 0.08 | 1.24 | 0.06 |
| 9 | 1.78 | 1.73 | 0.05 | 1.78 | 0.00 | 1.75 | 0.03 |
| 10 | 1.60 | 1.46 | 0.14 | 1.65 | -0.05 | 1.55 | 0.05 |
| 11 | 1.60 | 1.35 | 0.25 | 1.39 | 0.21 | 1.34 | 0.26 |
| 12 | 1.18 | 1.18 | 0.00 | 1.24 | -0.06 | 1.25 | -0.07 |
| 13 | 1.70 | 1.61 | 0.09 | 1.52 | 0.18 | 1.42 | 0.28 |
| 14 | 1.70 | 1.87 | -0.17 | 1.91 | -0.21 | 1.75 | -0.05 |
| 15 | 1.66 | 1.50 | 0.16 | 1.48 | 0.18 | 1.41 | 0.25 |
| 16 | 2.12 | 2.18 | -0.06 | 2.08 | 0.04 | 1.94 | 0.18 |
| 17 | 2.26 | 2.59 | -0.33 | 2.56 | -0.30 | 2.32 | -0.06 |
| 18 | 1.76 | 1.84 | -0.08 | 1.85 | -0.10 | 1.72 | 0.03 |
| | | Average | -0.03 | Average | -0.01 | Average | 0.07 |
| | | Std Deviation | 0.15 | Std Deviation | 0.14 | Std Deviation | 0.14 |

Table 27. Verification testing configurations.

| Run # | Diffuser Type | Inlet | Duct Height | Type Duct | Damper | Damper Type | Approach Angle |
|---|---|---|---|---|---|---|---|
| 1 | Square | 10 | 1.5 | Rigid | 0 | RndSliding | 0 |
| 2 | Plaque | 10 | 1.5 | Rigid | 0 | RndOpBld | 0 |
| 3 | Plaque | 10 | 1.5 | Rigid | Parallel | RndSliding | 0 |
| 4 | Plaque | 10 | 1.5 | Rigid | Parallel | RndOpBld | 0 |
| 5 | Plaque | 10 | 3 | Rigid | Parallel | RndOpBld | 0 |
| 6 | Plaque | 10 | 3 | Rigid | Parallel | RndSliding | 0 |
| 7 | Plaque | 10 | 0 | Flex | Parallel | RndOpBld | 0 |
| 8 | Plaque | 10 | 0 | Flex | 0 | RndOpBld | 0 |
| 9 | Plaque | 10 | 0 | Flex | Parallel | RndOpBld | 0 |
| 10 | Plaque | 10 | 0 | Flex | 0 | RndOpBld | 0 |

Table 28. Results of verification testing for pressure.

| Run # | Predicted $P_{Total}$ | Experiment $P_{Total}$ 1200 fpm | Error |
|---|---|---|---|
| 1 | 1.48 | 1.2 | 0.28 |
| 2 | 1.48 | 1.18 | 0.30 |
| 3 | 2.08 | 1.63 | 0.45 |
| 4 | 1.72 | 1.33 | 0.39 |
| 5 | 1.48 | 1.41 | 0.07 |
| 6 | 1.84 | 1.64 | 0.20 |
| 7 | 2.20 | 1.92 | 0.28 |
| 8 | 2.08 | 1.516 | 0.56 |
| 9 | 2.20 | 2.103 | 0.10 |
| 10 | 2.08 | 1.791 | 0.29 |
| | | Average | 0.29 |
| | | Std Deviation | 0.15 |

4.5.4 Sound Level (NC) in Decibels

The sound (NC) level predictive algorithm was determined same as the forward throw. A main effects plot was derived along with interactions for the same parameters as forward throw. The main effects parameter diffuser type had a large sensitivity on the sound level and was a characteristic of the diffuser, while duct height, duct type and damper have a smaller affect, as they are field installation parameters. The parameters that are characteristics of the diffuser are multipliers and the parameters that are field installation related are additive quantities. The interactions between duct height and damper resulted in a change from the sum effect of adding the individual main effects leading to additive quantity in the predictive algorithm.

The predictive equation for the increase in NC level to Standard 70 NC level is:

$$NC_{Prediction} = M_{DT} * ( A_{DCH} + A_{DCT} + A_{D} + A_{DCH*D} )$$

*Main Effect Parameters*

- For diffuser type;

Louvered: $M_{DT} = 1.1$

Perforated Round: $M_{DT} = 0.7$

Round: $M_{DT} = 1.3$

Plaque: $M_{DT} = 1.3$

Square: $M_{DT} = 1.1$

Perforated Square: $M_{DT} = 0.4$

- For duct height;

Duct height of 0: $A_{DCH} = 7$

Duct height of 1.5: $A_{DCH} = 3$

Duct height of 3: $A_{DCH} = 1$

- For duct type;

Duct type is flex: $A_{DCT} = 1$

Duct type is mix: $A_{DCT} = 1$

Duct type is rigid: $A_{DCT} = 0$

- For Damper;

Damper is 0 (no damper): $A_D = 0$

Damper is not 0 and damper type is round sliding: $A_D = 6.5$

Damper is not 0 and damper type is square opposed blade: $A_D = 5.5$

Damper is not 0 and damper type is round opposed blade: $A_D = 2$

*Interaction Parameters*

❖ For the interaction between duct height and damper;

Duct height of 0 and Damper is 0 (no damper): $A_{DCH*D} = 0$

Duct height of 0 and damper is not 0 and damper type is round sliding:

$A_{DCH*D} = -7$

Duct height of 0 and damper is not 0 and damper type is square opposed blade:

$A_{DCH*D} = -5$

Duct height of 0 and damper is not 0 and damper type is round opposed blade:

$A_{DCH*D} = -1$

Duct height of 1.5 or 3: $A_{DCH*D} = 0$

From the predictive equation for sound and the correction factors determined through testing, Table 29 shows the error calculated between the predicted and experimental sound data. The error and standard deviation for the sound level are not a percentage, but measured in decibels. This means that the standard deviation at 1200 fpm varies 1.34 dB for the initial test configurations. It was determined that a standard deviation of less than 3 dB would result in an accurate predictive algorithm. Again, due to the Standard 70 sound levels at 500 fpm for some diffusers being below the ambient of the UNLV throw room, no analysis is presented for this data.

Table 29. Predicted values and corresponding errors for sound level.

| Run # | Predicted NC | Experiment NC | Error | Experiment NC | Error |
|---|---|---|---|---|---|
| | | 1200 fpm | | 800 fpm | |
| 1 | 7.70 | 6.50 | 1.20 | 8.00 | -0.30 |
| 2 | 11.55 | 11.50 | 0.05 | 11.50 | 0.05 |
| 3 | 9.35 | 8.50 | 0.85 | 8.50 | 0.85 |
| 4 | 9.75 | 10.50 | -0.75 | 8.50 | 1.25 |
| 5 | 13.65 | 13.50 | 0.15 | 15.00 | -1.35 |
| 6 | 1.30 | 5.50 | -4.20 | 6.00 | -4.70 |
| 7 | 6.65 | 9.50 | -2.85 | 9.50 | -2.85 |
| 8 | 1.40 | 2.00 | -0.60 | 2.50 | -1.10 |
| 9 | 5.25 | 5.50 | -0.25 | 11.00 | -5.75 |
| 10 | 3.00 | 2.50 | 0.50 | 2.50 | 0.50 |
| 11 | 3.00 | 3.00 | 0.00 | 4.00 | -1.00 |
| 12 | 1.60 | 1.00 | 0.60 | 2.00 | -0.40 |
| 13 | 5.20 | 7.00 | -1.80 | 7.00 | -1.80 |
| 14 | 9.75 | 9.50 | 0.25 | 10.00 | -0.25 |
| 15 | 9.75 | 10.00 | -0.25 | 9.50 | 0.25 |
| 16 | 8.25 | 8.00 | 0.25 | 5.50 | 2.75 |
| 17 | 8.80 | 8.50 | 0.30 | 12.50 | -3.70 |
| 18 | 9.35 | 9.50 | -0.15 | 11.00 | -1.65 |
| | | Average | -0.37 | Average | -1.07 |
| | | Std Deviation | 1.34 | Std Deviation | 2.07 |

In Table 30, the verification configurations are listed and the resulting error calculations are given in Table 31. The standard deviation was found to be less than 3 dB and confirmed the accuracy of the predictive algorithm for sound at 1200 fpm.

Table 30. Verification testing configurations.

| Run # | Diffuser Type | Inlet | Duct Height | Type Duct | Damper | Damper Type | Approach Angle |
|---|---|---|---|---|---|---|---|
| 1 | Square | 10 | 1.5 | Rigid | 0 | RndSliding | 0 |
| 2 | Plaque | 10 | 1.5 | Rigid | 0 | RndOpBld | 0 |
| 3 | Plaque | 10 | 1.5 | Rigid | Parallel | RndSliding | 0 |
| 4 | Plaque | 10 | 1.5 | Rigid | Parallel | RndOpBld | 0 |
| 5 | Plaque | 10 | 3 | Rigid | 0 | RndOpBld | 0 |
| 6 | Plaque | 10 | 3 | Rigid | Parallel | RndOpBld | 0 |
| 7 | Plaque | 10 | 3 | Rigid | Parallel | RndSliding | 0 |
| 8 | Plaque | 10 | 0 | Flex | Parallel | RndOpBld | 0 |
| 9 | Plaque | 10 | 0 | Flex | 0 | RndOpBld | 0 |
| 10 | Plaque | 10 | 0 | Flex | Parallel | RndOpBld | 0 |
| 11 | Plaque | 10 | 0 | Flex | 0 | RndOpBld | 0 |

Table 31. Results of verification testing for sound level.

| Run # | Predicted $T_f$ | Experiment $T_f$ | Error |
|---|---|---|---|
| | | 1200 fpm | |
| 1 | 3.30 | 4.80 | -1.50 |
| 2 | 3.90 | 2.00 | 1.90 |
| 3 | 12.35 | 6.00 | 6.35 |
| 4 | 6.50 | 2.60 | 3.90 |
| 5 | 1.30 | 1.00 | 0.30 |
| 6 | 3.90 | 2.50 | 1.40 |
| 7 | 9.75 | 5.50 | 4.25 |
| 8 | 11.70 | 7.50 | 4.20 |
| 9 | 10.40 | 5.00 | 5.40 |
| 10 | 9.90 | 11.00 | -1.10 |
| 11 | 8.80 | 7.50 | 1.30 |
| | | Average | 2.40 |
| | | Std Deviation | 2.60 |

4.5.5 Summary of Field Condition Testing Analysis

A summary of the standard deviations for the results and verifications of the field-testing analysis are listed in Table 32. Note that verification testing was not done for backward throw since the results for forward throw suggested good compliance with the

prediction equation. All verification tests were performed at the inlet velocity with the highest noise level, 1200 fpm. The sound data has a standard deviation of decibels, not a percentage like the other three outputs. Due to background sound levels, the diffuser sound generation was not measurable for all field tests at the lowest inlet velocity condition.

Table 32. Summary of standard deviations for field-testing analysis.

| | Noise Condition | | | Verification |
|---|---|---|---|---|
| | 1200 fpm | 800 fpm | 500 fpm | 1200 fpm |
| Forward Throw, $T_f$ | 0.17 | 0.16 | 0.14 | 0.14 |
| Backward Throw, $T_b$ | 0.16 | 0.16 | 0.16 | -- |
| Sound, NC [dB] | 1.34 | 2.07 | -- | 2.60 |
| Pressure Ratio, $P_{Total}$ | 0.15 | 0.14 | 0.14 | 0.15 |

# CHAPTER 5

## CLOSE COUPLING AIR OUTLET PERFORMANCE

Diffuser performance measurements, where the installation used a short perpendicular branch duct to the diffuser taken off a main duct, were conducted and compared to the same diffuser performance from the Standard 70 characterization. That installation is referred to as close coupling. The setup included an 11-inch by 18-inch rectangular main duct that ran horizontally, approximately 16 feet in length and 1 foot above the ceiling. A vertical duct section of varying heights and diameter, with a diffuser at one end was then attached just beyond the midpoint of the rectangular main duct. The portion of the ceiling that the main duct overshadowed was left open to allow for discharge air velocity measurement of configurations where the shorter vertical duct heights put the diffuser above the suspended ceiling. Due to the varying heights of the vertical branch and the fixed position of the main duct in the ceiling, the ceiling height itself was varied to always have the diffuser at the same height and to align the diffuser face with the array of draft meters. The top six draft meters were the same height from the ceiling as that used in the Standard 70 tests, but the total height of the array was reduced to 7 feet to accommodate for the lower diffuser height. The variations included three vertical duct heights going into the diffuser intake, three types of diffusers and use of a damper in the intake. Discharge symmetry, pressure loss and noise generation were both affected by the variations in installation. Invariably, the Standard 70 characterizations had the least discharge asymmetry, lowest pressure loss and lowest noise generation. Increases in these output measures were quantified by comparison to the output levels measured in a

Standard 70 installation. Installers and designers can use the quantitative results in this report to predict the actual performance of a variety of close coupling installations.

## 5.1 Background

As the previous chapter showed, under typical field conditions, diffusers and outlets can have throw, pressure loss and noise performance that is significantly different from published performance obtained from ASHRAE Standard 70 testing. Particularly applicable to this experiment are field installations, where a perpendicular branch duct is tapped directly into a main duct with short or nearly no branch duct length. The magnitude of the changes in the diffuser performance effects associated with these installations can also depend on variations out of the control of the installer such as variations in the main duct air velocity and duct static pressure.

## 5.2 Objective

The objective of this testing is to develop guidelines that will relate manufactures air outlet cataloged data that have been obtained using ASHRAE Standard 70 to close coupling installation applications. The testing collected data of diffusers obtained under a collection of vertical branch inlet conditions and compared that data to base performance data obtained from testing using ASHRAE Standard 70. From that comparison, correction factors for diffuser throw and sound data were determined.

## 5.3 Methodology

Output measures and derived output measures included:

1. Sound Power Level and Resulting Room NC.
2. Diffuser throw distance ratio of total throw in close coupling installation to throw in a Standard 70 test taken in opposite directions enabling calculation of a throw asymmetry ratio.
3. Ratio of main duct static pressure in field installation to total pressure in a Standard 70 test.

5.3.1 Laboratory Instrumentation

All tests for this project were run under steady-state conditions similar to the Standard 70 tests. Volume airflow corresponding to the required inlet velocity was set and allowed to stabilize. The throw room measurement instrument configuration was the same as in the Standard 70 testing except that the draft meter array was reduced to a vertical height of 7 feet. The ceiling height was adjusted so that the diffuser discharge plane was 0.75 inches above the highest draft meter. Also, the same LabView virtual instrument was used to monitor and record airflow, supply air temperature, room temperature, main duct static pressure, draft meter array position and draft meter readings. Sound level measurements were made with all systems off except for the air supply, boom microphone and the monitoring and recording computer. Sound measurements were taken with the air supply on and off to record the diffuser generated sound with airflow and a background noise level without airflow.

5.3.2 Experimental Design

The ideal energy transformation is for air to flow into the diffuser inlet and exit at the diffuser discharge with, no pressure loss other than velocity pressure, no sound generation and a discharge velocity pattern as intended by the diffuser design. Thus, any

variations from ideal would be variations in pressure measured in the duct upstream and downstream of the diffuser inlet, increases in sound level measured in the discharge room and unintended asymmetry in diffuser throw measured in the discharge room. Standard 70 measurements show variations from ideal due to flow restrictions in the diffuser, turbulence induced in the flow due to diffuser structure and anomalies in discharge throw due to the geometry of the diffuser design. The Standard 70 measurements obtained are considered to be the closest to ideal with the diffusers tested. In this experiment, the Standard 70 results are used as a standard while the test results are compared to that standard. The experimental setup is diagrammed in Figure 35.

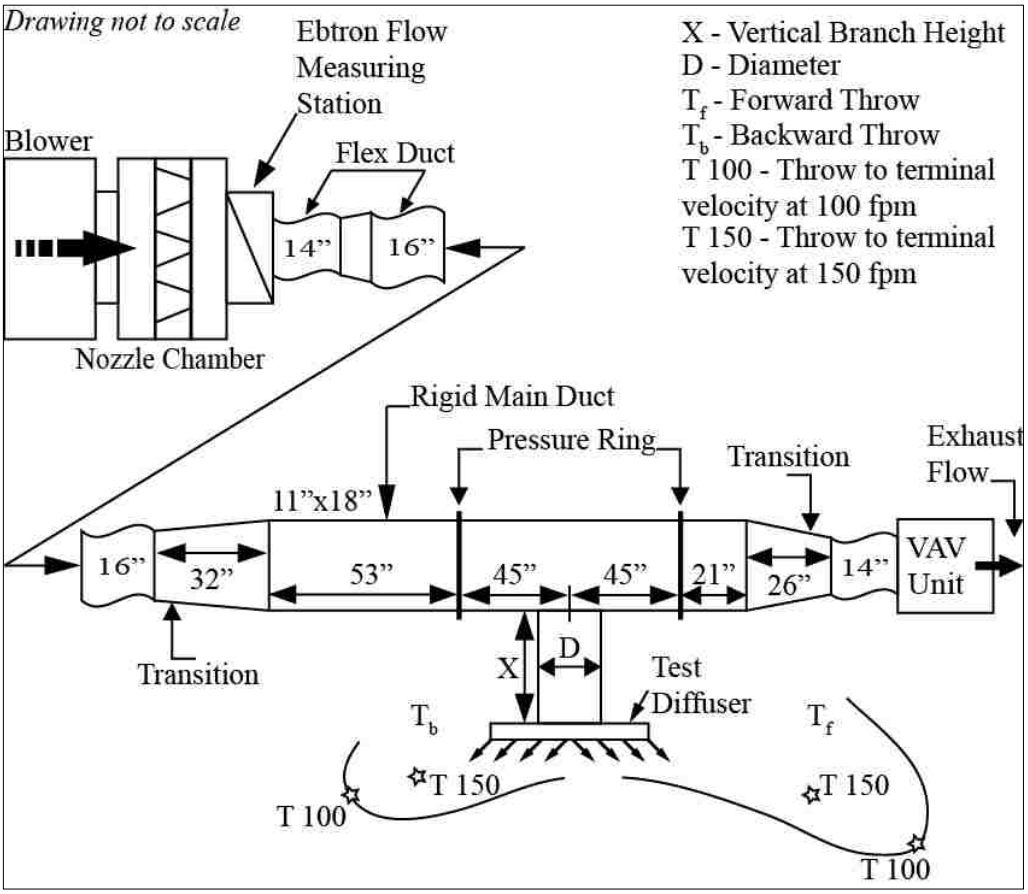


Figure 35. Experimental setup for close coupling laboratory testing.

Experimental output measures were obtained using the same or comparable methods used for standard 70 testing and thus can be compared to Standard 70 measurements. The pressure ring in the VAV unit at the end of the setup was used to determine the main duct flow that bypassed the branch. Using the velocity pressure, the temperature of the air traveling through the VAV, a correction value and a multiplier determined through regression analysis of dynamic pressure, $P_{dyn} = (1/2)\rho v^2$, an equation was formulated to calibrate the volume flow rate of air leaving the VAV unit, $VAV_{Flow}$, and can be found in Appendix A, section A.2.2. Airflow that went through the branch was calculated to be total airflow minus the branch bypass airflow. These calculations were crosschecked using a portable flow hood.

Sound measurements were recorded using the same method as the field installation tests, using a rotating boom microphone pictured in Figure 11 in Chapter 3, where 1/3 octave band sound levels were recorded. Diffuser discharge velocities at incremental distances from the diffuser were measured using the same array of draft meters at varying heights in the room as used in the Standard 70 measurements. The array of draft meters was scanned along the open ceiling perpendicular to the diffuser face pictured from the top view in Figure 36. Due to the fixed position of the main duct and height variation of the draft meters, the ceiling was varied in height to align the diffuser face with the top draft meter.

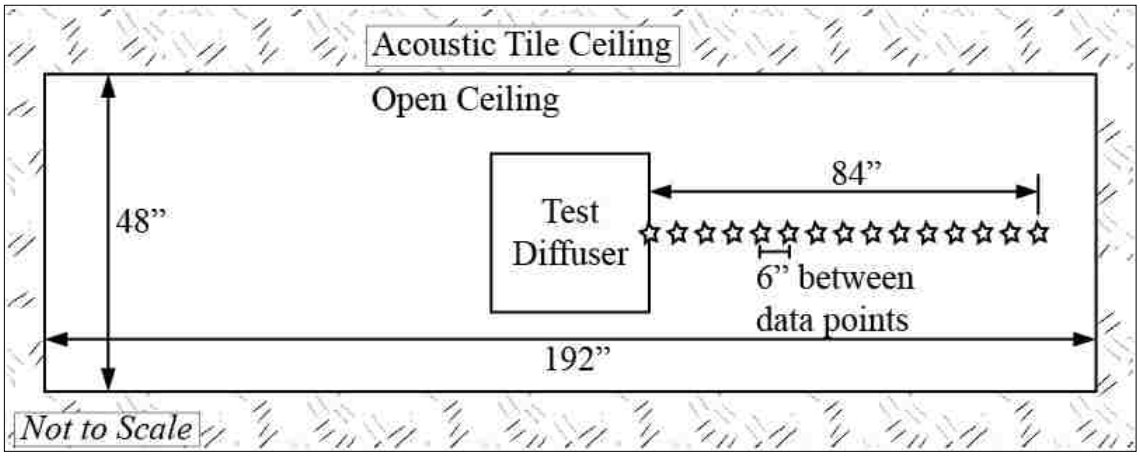


Figure 36. Top view of close coupling scan pattern.

For this experiment, inlet main duct velocity was the noise condition. Noise conditions, in product optimization, are conditions that are not controlled by the designer but are set by the product user or result from external factors not controlled by either the designer or the user. Airflow velocities used were 1150, 600, and 300 fpm in the rectangular main duct. These velocities cover a large span of typical main duct flow conditions including what is typically seen in actual installations.

Four parameters were used in the performance characterization experiment. They were diffuser type, diffuser inlet diameter, vertical duct height directly above the diffuser inlet and damper configuration in the diffuser inlet. The parameter and noise configurations with levels are shown in Table 33. Three diffuser types were used in the experiment. All these diffusers had fixed outlet sizes and differing inlet neck sizes. Thus the three diffuser types had different free face area to duct area ratio as the inlet size changed.

Table 33. Test parameters and noise conditions with different states.

| Parameter | State 1 | State 2 | State 3 |
|---|---|---|---|
| 1. Diffuser Type | Square | Plaque | Perforated Round Neck |
| 2.Inlet Diameter | 8 inches | 10 inches | 12 inches |
| 3. Vertical Duct Height | 0 Duct Diameters | 1.5 Duct Diameters | 3 Duct Diameters |
| 4. Damper | No Damper | Cross Damper | X Damper |
| Noise Condition | Low State | Medium State | High State |
| 1. Main Duct Velocity | 300 fpm | 600 fpm | 1150 fpm |

The most economical (least run) fractional factorial array was used to set up the experiment that could be used to extract the main effects of the test parameters and the variation of those main effects due to the noise conditions. An L9 array was used. The test array has 9 runs with four parameters at three levels. The L9 array has 8 degrees of freedom (DOF), which is the total number of tests minus one. The total DOF needed for the main effects are 8. The DOF needed for the main effects was determined by taking the total number of levels of each parameter minus one and summing the result for all the parameters (2 x 4). The array is shown in Table 34. Note that the branch duct connecting the diffuser to the rectangular main duct was rigid for all installations. The damper used was a round opposed blade damper and was always fully open. An example of a close coupling configuration installation is shown in Figure 37. There were three sets of output measures, one for each noise condition. The output array for one noise condition is shown in Table 35.

Table 34. Test array for close coupling experiment.

| Run Order | Run # | Diffuser Type | Inlet | Duct Height | Damper |
|---|---|---|---|---|---|
| 2 | 1 | Square | 8 | 0 | None |
| 7 | 2 | Square | 10 | 1.5 | X |
| 6 | 3 | Square | 12 | 3 | Cross |
| 4 | 4 | Plaque | 8 | 1.5 | Cross |
| 5 | 5 | Plaque | 10 | 3 | None |
| 1 | 6 | Plaque | 12 | 0 | X |
| 8 | 7 | Perf Rnd | 8 | 3 | X |
| 9 | 8 | Perf Rnd | 10 | 0 | Cross |
| 3 | 9 | Perf Rnd | 12 | 1.5 | None |

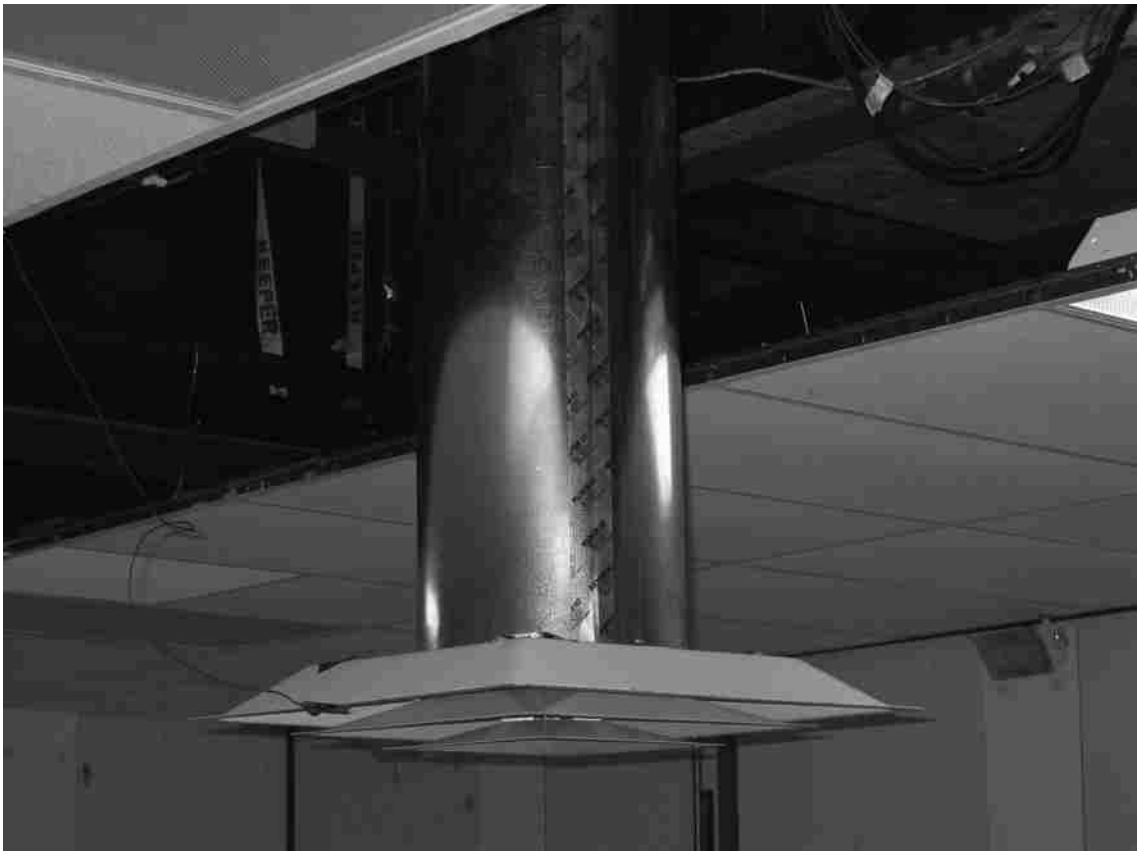

Figure 37. Example close coupling configuration.

Table 35. Output array for the close coupling experiment.

| Run # | Forward Throw Asymmetry, $T_f$ | Backward Throw Asymmetry, $T_b$ | Change in NC | Pressure Ratio |
|---|---|---|---|---|
| | Noise Level | Noise Level | Noise Level | Noise Level |
| 1 | | | | |
| 2 | | | | |
| … | | | | |
| 8 | | | | |
| 9 | | | | |

## 5.4 Results

Each diffuser output measure is a comparison of the close coupling configurations against the corresponding data from the base Standard 70 tests. For example, the Standard 70 velocity profile data in Figure 38 was used for comparison against the data from the same diffuser type used in the close coupling tests in Figure 39 and Figure 40. The asymmetry was determined by comparing the throw distance in zone 3 or zone 4 of the zone plots from the close coupling configurations and the Standard 70 tests based on the zone plot procedure described in Chapters 3 and 4.

To determine the zone throw distance at each recorded data point, the same approach that was used for Standard 70 and field installation tests was done for the close coupling installations. If the y2 value, reference Figure 28 from Chapter 4, of 0.2 was in zone 4, the same procedure was followed from the field installation chapter using the beginning of the zone 4 slope for x1 and y1, but the square root of the x2 value, calculated from the comparison between close coupled and Standard 70 data, was taken to compensate for the effect of the open ceiling.

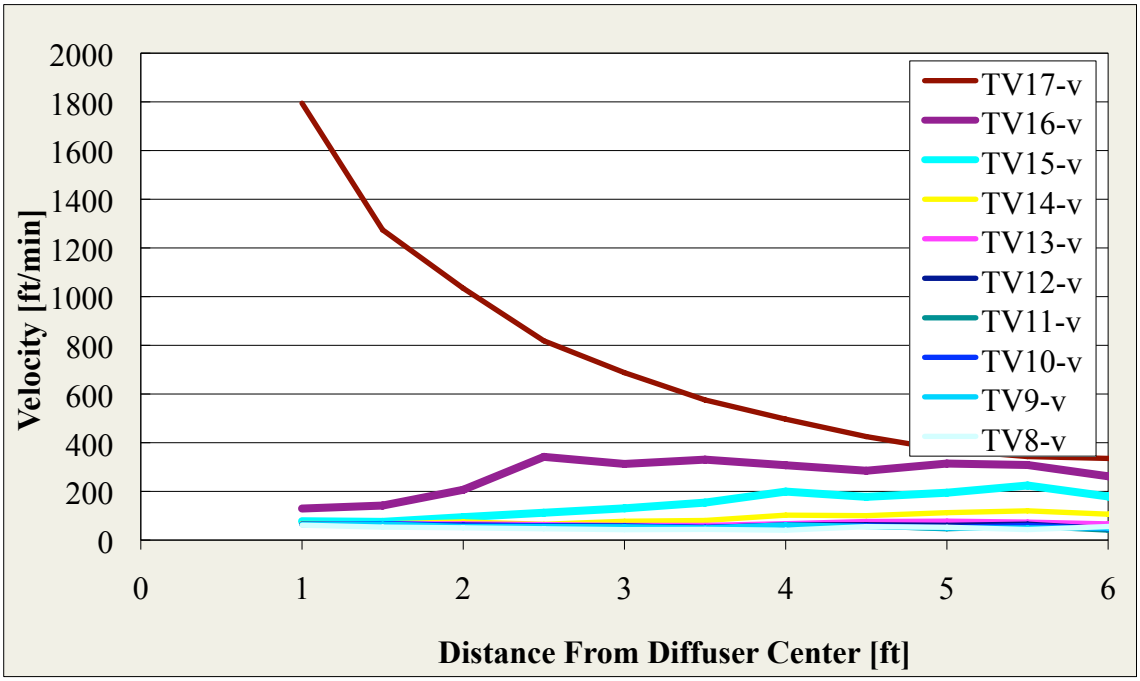


Figure 38. Standard 70 throw data at 1200 fpm for 12" square diffuser.

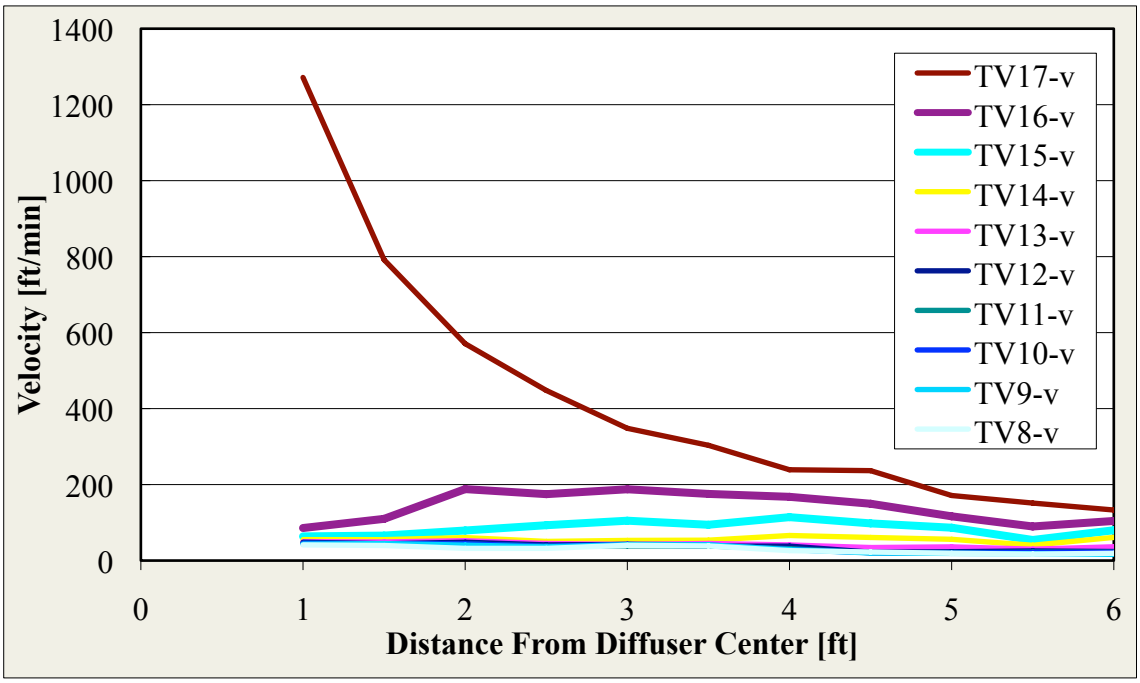


Figure 39. Close coupling forward throw data at 1150 fpm (in main duct) for Run #3.

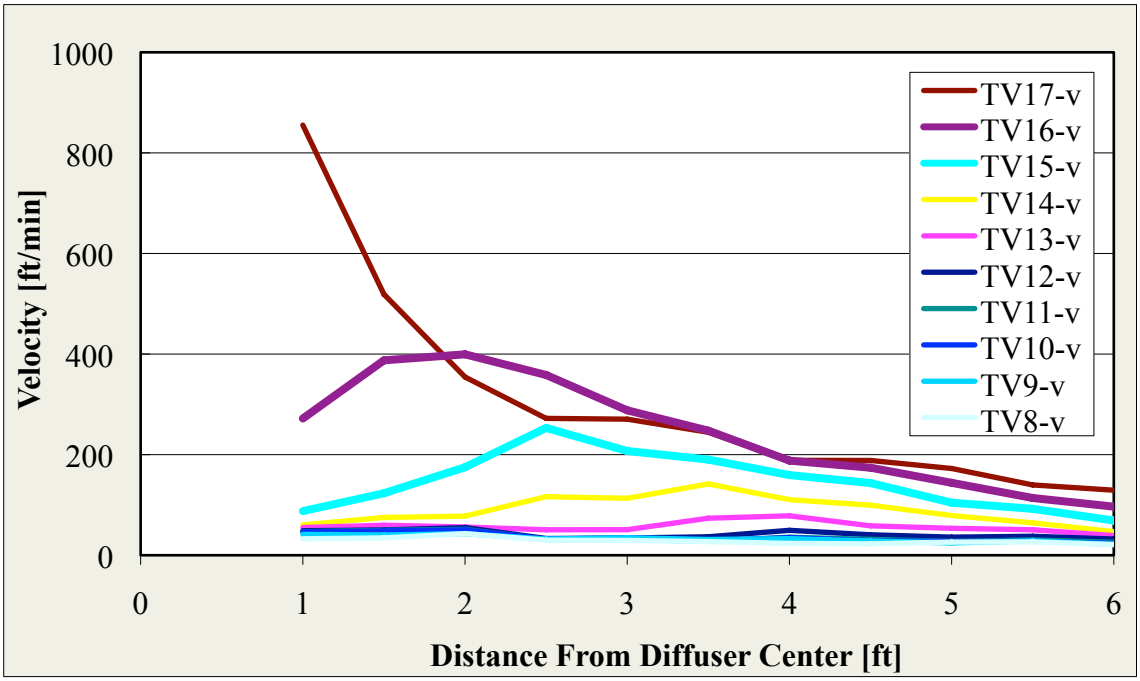


Figure 40. Close coupling backward throw data at 1150 fpm (in main duct) for Run #3.

For example, Figure 41 and Figure 42 have an x2 value that occurs in zone 4 as the y2 value of 0.2 was traced across through zone 4. This produced the throw ratio between the close coupling data and the Standard 70 data. The change in NC level is a direct difference between the NC of the close coupling configurations and the NC of the new estimated Standard 70 data.

Using the volumetric flow rate values obtained from the $VAV_{Flow}$ equation and comparison recordings using an Alnor ABT Balometer Capture Hood, approximated volumetric flow rates were determined for each noise condition. To determine the new Standard 70 data for 300, 600 and 1150 fpm, inlet neck area of the diffuser was used to calculate the corresponding neck velocity at each flow rate. Using the original Standard 70 and published manufacturer data, estimations were made that represented new Standard 70 data to compare to the close coupling output measure values. In some cases,

the NC levels at 300 fpm were below the room ambient sound level and have been left out of the analysis. Table 36 shows the forward and backward throw ratios between the close coupled and Standard 70 data at corresponding throw velocities. It also provides the sound level differences between the close coupling configurations and Standard 70 as well as the pressure ratio between the close coupling main duct static pressure and the Standard 70 supply plenum total pressure. It was determined that for calculating diffuser pressure loss within the vertical branch in this experiment, the static pressure in the rectangular main duct was equivalent to the static pressure in the plenum used for Standard 70 testing. The upstream pressure ring from the vertical branch measured static pressure, but a small velocity pressure also existed within the duct. As the air moved passed the opening for the vertical branch, velocity pressure was lost. At the second pressure ring downstream from the vertical branch, static pressure increased to account for the velocity pressure lose and any energy losses experienced between the two pressure rings.

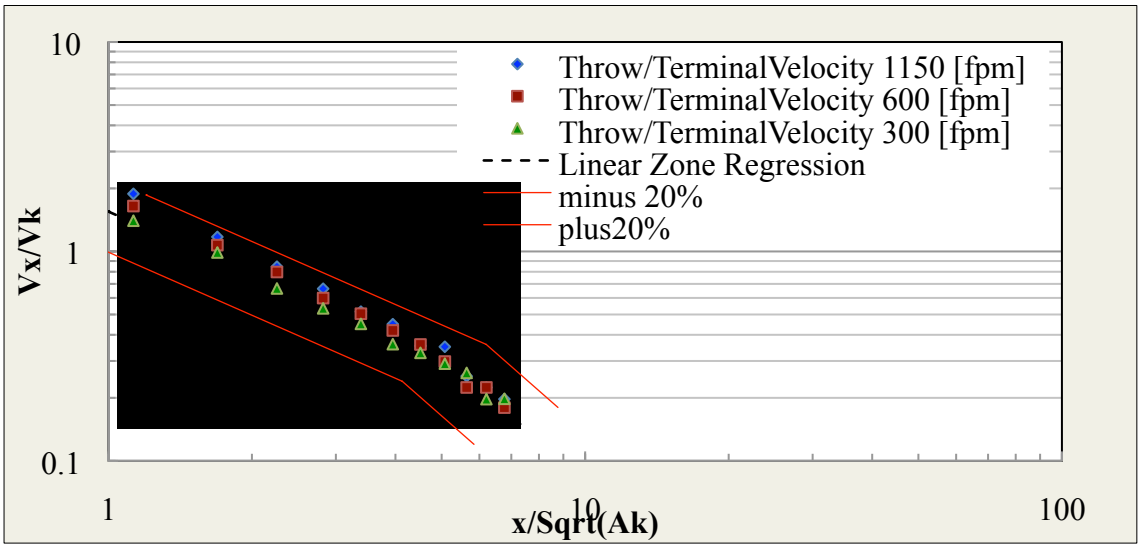


Figure 41. Run #3 forward throw zone plot data.

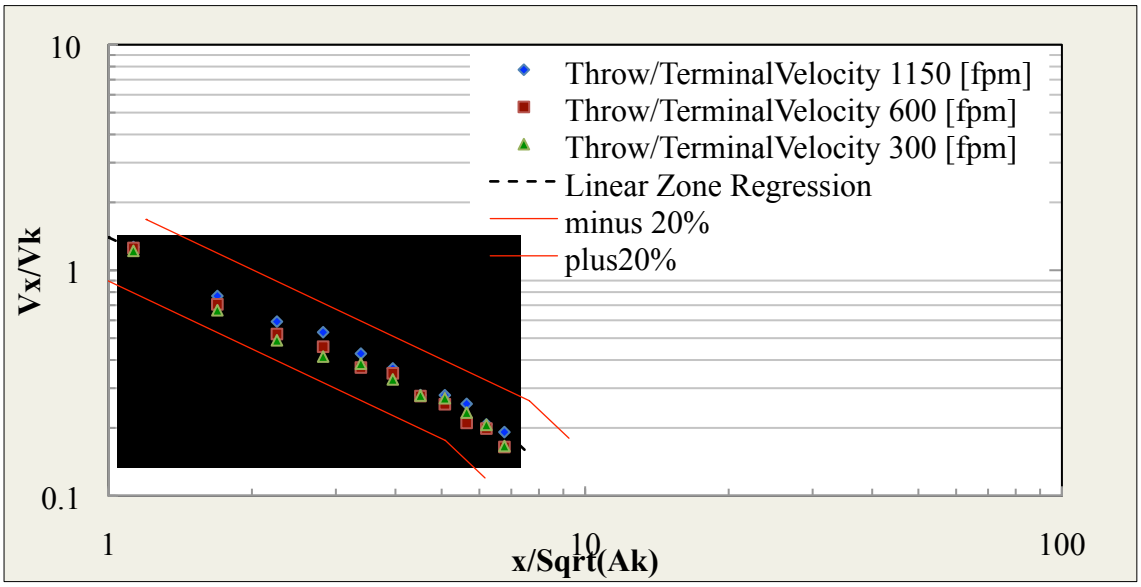


Figure 42. Run #3 backward throw zone plot data.

Table 36. Diffuser output throw ratios and noise criteria level changes for close coupling compared to Standard 70 data.

| Run # | Forward Throw Asymmetry, $T_f$ | | | Backward Throw Asymmetry, $T_b$ | | | Change in Sound (NC) Level [dB] | | | Total Pressure Ratio, $P_{Total}$ | | |
|---|---|---|---|---|---|---|---|---|---|---|---|---|
| | 300 fpm | 600 fpm | 1150 fpm | 300 fpm | 600 fpm | 1150 fpm | 300 fpm | 600 fpm | 1150 fpm | 300 fpm | 600 fpm | 1150 fpm |
| 1 | 0.9 | 1.0 | 1.16 | 0.8 | 0.8 | 0.82 | 5 | 6 | 13 | 1.4 | 1.5 | 1.86 |
| 2 | 1.1 | 1.1 | 1.10 | 0.6 | 0.9 | 0.91 | 9.5 | 11.5 | 17 | 1.6 | 1.8 | 1.89 |
| 3 | 1.0 | 1.1 | 1.10 | 0.9 | 0.9 | 0.97 | -- | 11 | 19.5 | 1.2 | 1.3 | 1.43 |
| 4 | 0.9 | 1.0 | 1.09 | 1.0 | 1.0 | 1.19 | 8.5 | 10 | 17 | 1.4 | 2.4 | 3.22 |
| 5 | 0.9 | 0.9 | 1.09 | 0.8 | 0.8 | 1.08 | -- | 7 | 19.5 | 1.7 | 1.8 | 2.57 |
| 6 | 0.9 | 1.0 | 1.17 | 0.9 | 1.1 | 0.99 | 6.5 | 8.5 | 20.5 | 2.2 | 2.3 | 2.44 |
| 7 | 0.7 | 0.7 | 0.74 | 0.7 | 0.7 | 0.79 | 6.5 | 11 | 13 | 1.7 | 1.9 | 1.67 |
| 8 | 0.9 | 1.0 | 1.12 | 0.8 | 0.8 | 0.86 | 4 | 8.5 | 14.5 | 1.2 | 1.5 | 1.57 |
| 9 | 1.1 | 1.3 | 1.57 | 0.8 | 0.9 | 0.98 | 4 | 7 | 14 | 1.0 | 1.2 | 1.12 |

5.4.1 Square Diffuser Performance Variation Effects when not Flush with the Ceiling

An important phenomenon was discovered during Run #1 when using the 8” square diffuser without having a ceiling in line with the diffuser face. The testing of this diffuser

generated a zone plot that skipped past zones 2 and 3, directly into zone 4 as shown in Figure 43.

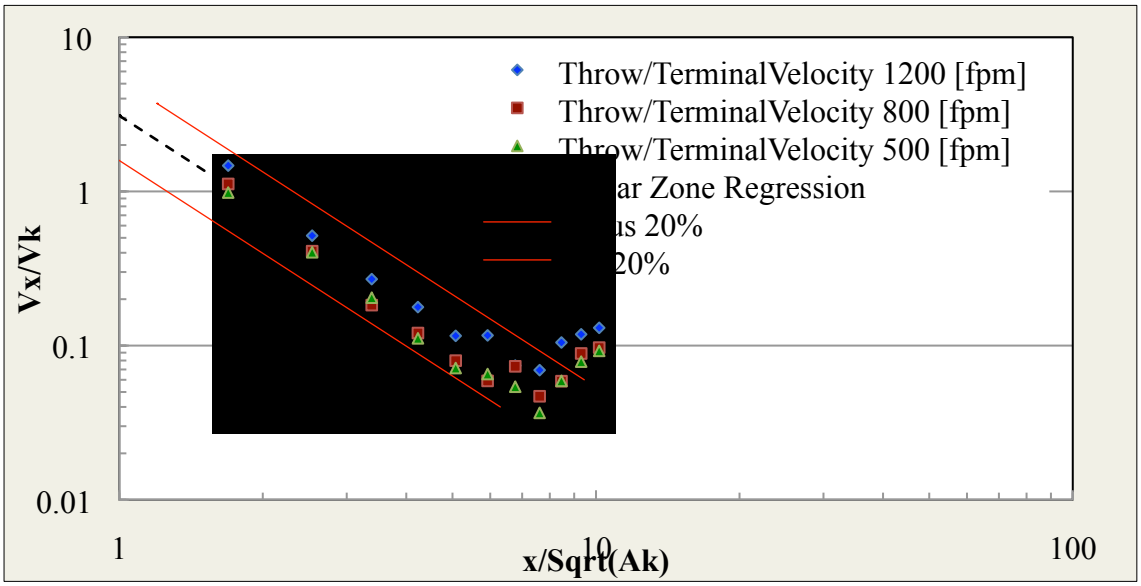


Figure 43. Zone plot for forward throw of Run #1 without ceiling.

The direct convergence into zone four means that the air being thrown perpendicular to the diffuser side was nearly vertical directly after leaving the outlet diffuser face. This behavior of the diffuser is uncommon and the test was repeated to ensure accuracy. To determine if free air discharge was the issue, a ceiling flush with the diffuser over the plane of measurement was installed as shown in Figure 44 and the test was repeated. Figure 45 shows that with a ceiling, the diffuser performs more like a typical diffuser than without a ceiling by spreading the flow along the ceiling and falling into zone 4 at a much farther distance from the diffuser center.

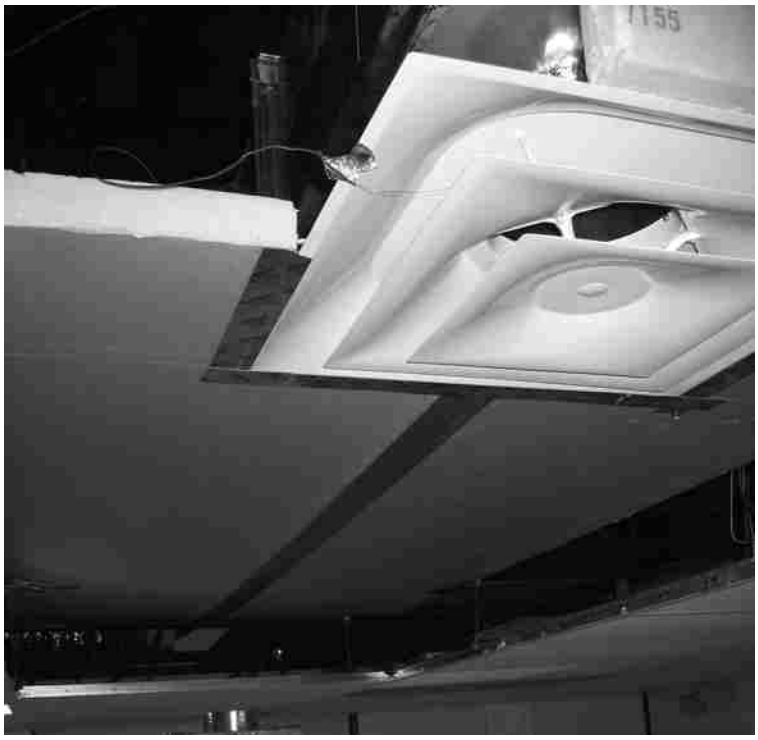

Figure 44. Styrofoam ceiling for Run #1 redo.

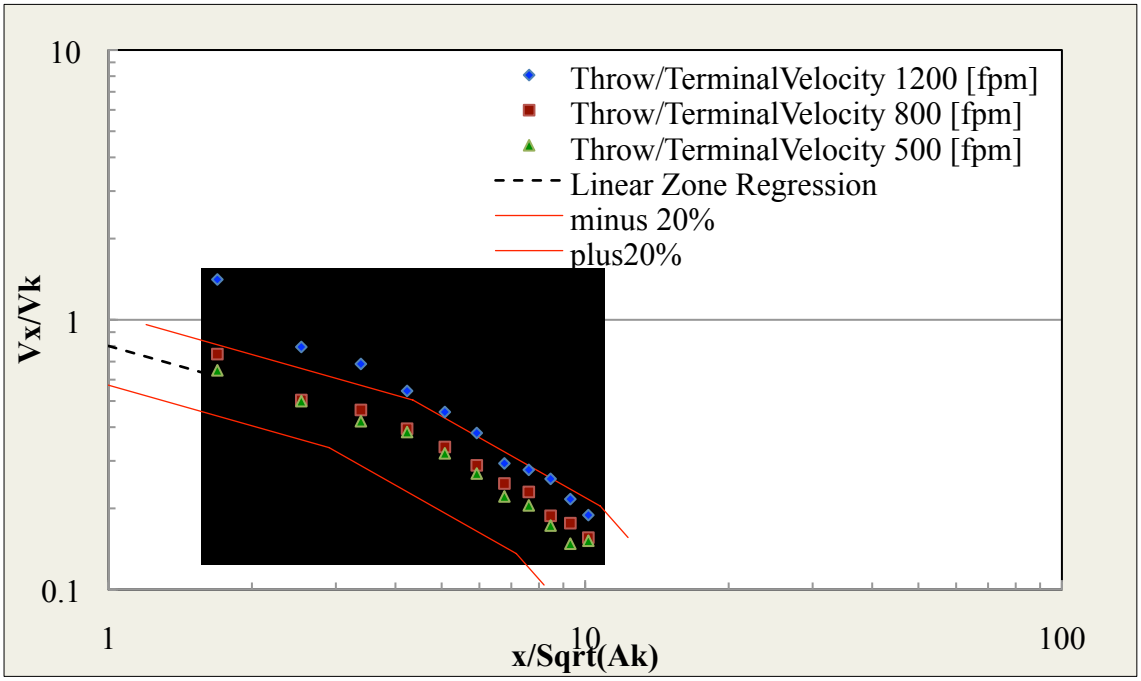


Figure 45. Zone plot for forward throw of Run #1 with ceiling.

## 5.5 Analysis

A statistical analysis was conducted to help better develop diffuser throw, pressure loss and noise criteria prediction models for close coupling installations. The main effects and interaction plots were determined based on the parameters listed in Table 33 individually for each output measure listed in Table 35.

To develop accurate and reliable prediction algorithms, as was done in Chapter 4 for the field-testing analysis, the same algorithms were used for close coupling data that were used for the field-testing data. Through acknowledgement of physics, certain parameters were removed, while the parameters that were known to have an affect on the diffuser performance, were kept in the predictive algorithm. The predictive algorithms for the close coupling data most often turned out to have a worse standard deviation than the field-testing configurations. One reason is likely the smaller testing array and fewer inlet test parameters, thus fewer tests at each level of the test parameters. The predictive algorithms are tabulated in sections 5.5.1 through 5.5.4.

### 5.5.1 Forward Throw Ratio ($T_f$)

An analysis of variance (ANOVA) was performed for the values of the forward throw ratio against the four inlet parameters and was determined that three of the four parameters had a significant affect on the diffuser performance. Relying on physics and the predictive algorithm determined for the field-testing analysis, the following equation to predict the forward throw ratio in a close coupling system was developed:

$$FTR_{Prediction} = M_{DT} * M_{ID} * A_{DCH} + 1$$

The parameters in this equation were quantified as follows based on the main effects, interaction plots and any anomalies discovered during experimentation.

*Main Effect Parameters*

- For diffuser type;

Perforated Round: $M_{DT} = 0.8$

Plaque: $M_{DT} = 0.6$

Square: $M_{DT} = 1.0$

- For inlet diameter;

12-inch inlet diameter: $M_{ID} = 1.2$

8 or 10-inch inlet diameter: $M_{ID} = 1.0$

- For duct height;

Duct height of 0: $A_{DCH} = 0.4$

Duct height of 1.5: $A_{DCH} = 0.1$

Duct height of 3: $A_{DCH} = 0$

From the predictive algorithm for forward throw ratio, the predicted values for each configuration tested were calculated in Table 37. The actual test results are listed in the table as well in the experiment columns and the corresponding errors represent the difference between the predicted and the experimental data. The standard deviations in

the table gave values that were slightly higher than the field-testing configurations and the high state happens to be above the threshold of accuracy held at 20 percent.

Table 37. Predicted values and corresponding error for forward throw.

| Run # | Predicted $T_f$ | Experiment $T_f$ | Error | Experiment $T_f$ | Error | Experiment $T_f$ | Error |
|---|---|---|---|---|---|---|---|
| | | 1150 fpm | | 600 fpm | | 300 fpm | |
| 1 | 1.40 | 1.17 | 0.23 | 1.03 | 0.37 | 0.96 | 0.44 |
| 2 | 1.10 | 1.11 | -0.01 | 1.11 | -0.01 | 1.11 | -0.01 |
| 3 | 1.00 | 1.11 | -0.11 | 1.11 | -0.11 | 1.03 | -0.03 |
| 4 | 1.06 | 1.10 | -0.04 | 1.01 | 0.05 | 0.96 | 0.10 |
| 5 | 1.00 | 1.10 | -0.10 | 1.00 | 0.00 | 1.00 | 0.00 |
| 6 | 1.29 | 1.17 | 0.12 | 1.07 | 0.22 | 0.97 | 0.32 |
| 7 | 1.00 | 0.74 | 0.26 | 0.74 | 0.26 | 0.74 | 0.26 |
| 8 | 1.32 | 1.13 | 0.19 | 1.05 | 0.27 | 0.95 | 0.37 |
| 9 | 1.10 | 1.57 | -0.48 | 1.34 | -0.25 | 1.13 | -0.03 |
| | | Average | 0.01 | Average | 0.09 | Average | 0.16 |
| | | Std Deviation | 0.23 | Std Deviation | 0.20 | Std Deviation | 0.19 |

5.5.2 Backward Throw Ratio ($T_b$)

An ANOVA was performed for the values of the backward throw ratio against the four inlet parameters and it was determined that two of the four parameters had a significant affect on the diffuser performance. Relying on physics and the predictive algorithm determined for the field-testing analysis, the following equation to predict the backward throw ratio in a close coupling system was developed:

$$BTR_{Prediction} = M_{DT} * M_{ID} * A_{DCH} + 1$$

*Main Effect Parameters*

- For diffuser type;

Perforated Round: $M_{DT} = 0.8$

Plaque: $M_{DT} = 0.6$

Square: $M_{DT} = 1.0$

- For inlet diameter;

12-inch inlet diameter: $M_{ID} = 1.1$

10-inch inlet diameter: $M_{ID} = 1.0$

8-inch inlet diameter: $M_{ID} = 0.9$

- For duct height;

Duct height of 0: $A_{DCH} = -0.4$

Duct height of 1.5: $A_{DCH} = -0.2$

Duct height of 3: $A_{DCH} = 0$

The predictive algorithm for backward throw ratio shows the calculated predicted values for each configuration tested in Table 38. The standard deviations in the table gave values that were slightly higher than the field-testing configurations but the threshold of accuracy held at less-than-or-equal-to 20 percent was met.

Table 38. Predicted values and corresponding errors for backward throw.

| Run # | Predicted $T_b$ | Experiment $T_b$ | Error | Experiment $T_b$ | Error | Experiment $T_b$ | Error |
|---|---|---|---|---|---|---|---|
| | | 1150 fpm | | 600 fpm | | 300 fpm | |
| 1 | 0.64 | 0.8246 | -0.18 | 0.8246 | -0.18 | 0.8246 | -0.18 |
| 2 | 0.80 | 0.9141 | -0.11 | 0.9141 | -0.11 | 0.6884 | 0.11 |
| 3 | 1.00 | 0.9756 | 0.02 | 0.9401 | 0.06 | 0.9401 | 0.06 |
| 4 | 0.89 | 1.1917 | -0.30 | 1.032 | -0.14 | 1.032 | -0.14 |
| 5 | 1.00 | 1.0879 | -0.09 | 0.8592 | 0.14 | 0.8592 | 0.14 |
| 6 | 0.74 | 0.9941 | -0.26 | 1.1716 | -0.44 | 0.9941 | -0.26 |
| 7 | 1.00 | 0.7958 | 0.20 | 0.7958 | 0.20 | 0.7958 | 0.20 |
| 8 | 0.68 | 0.8672 | -0.19 | 0.8672 | -0.19 | 0.8672 | -0.19 |
| 9 | 0.82 | 0.9868 | -0.16 | 0.9868 | -0.16 | 0.8808 | -0.06 |
| | | Average | -0.12 | Average | -0.09 | Average | -0.03 |
| | | Std Deviation | 0.15 | Std Deviation | 0.20 | Std Deviation | 0.17 |

5.5.3 Total Pressure Ratio ($P_{Total}$)

An ANOVA was performed for the values of the total pressure ratio against the four inlet parameters and it was determined that one of the four parameters had a significant affect on the diffuser performance. Relying on physics and the predictive algorithm determined for the field-testing analysis, the following equation to predict the total pressure ratio in a close coupling system was developed:

$$TPR_{Prediction} = M_{DT} * M_{ID} * ( A_{DCH} + A_D ) + 1$$

*Main Effect Parameters*

- For diffuser type;

Perforated Round: $M_{DT} = 1.0$

Plaque: $M_{DT} = 1.2$

Square: $M_{DT} = 1.2$

- For inlet diameter;

12-inch inlet diameter: $M_{ID} = 0.6$

8 or 10-inch inlet diameter: $M_{ID} = 1.0$

- For duct height;

Duct height of 0: $A_{DCH} = 0.6$

Duct height of 1.5: $A_{DCH} = 0.4$

Duct height of 3: $A_{DCH} = 0.2$

- For Damper;

Damper is 0 (no damper): $A_D = 0$

Damper is not 0: $A_D = 0.2$

The predictive algorithm for total pressure ratio, main duct upstream static pressure versus Standard 70 supply plenum total pressure, shows the calculated predicted values for each configuration tested in Table 39. The standard deviations in the table gave values that were much higher than the field-testing configurations and the threshold of accuracy held at less-than-or-equal-to 20 percent was not met.

Table 39. Predicted values and corresponding errors for total pressure ratio.

| Run # | Predicted $P_{Total}$ | Experiment $P_{Total}$ | Error | Experiment $P_{Total}$ | Error | Experiment $P_{Total}$ | Error |
|---|---|---|---|---|---|---|---|
| | | 1150 fpm | | 600 fpm | | 300 fpm | |
| 1 | 1.72 | 1.869 | -0.15 | 1.561 | 0.16 | 1.442 | 0.28 |
| 2 | 1.72 | 1.898 | -0.18 | 1.874 | -0.15 | 1.649 | 0.07 |
| 3 | 1.29 | 1.439 | -0.15 | 1.396 | -0.11 | 1.210 | 0.08 |
| 4 | 1.72 | 3.226 | -1.51 | 2.412 | -0.69 | 1.460 | 0.26 |
| 5 | 1.24 | 2.576 | -1.34 | 1.891 | -0.65 | 1.791 | -0.55 |
| 6 | 1.58 | 2.441 | -0.86 | 2.332 | -0.76 | 2.284 | -0.71 |
| 7 | 1.40 | 1.677 | -0.28 | 1.911 | -0.51 | 1.775 | -0.37 |
| 8 | 1.80 | 1.576 | 0.22 | 1.596 | 0.20 | 1.253 | 0.55 |
| 9 | 1.24 | 1.129 | 0.11 | 1.210 | 0.03 | 1.090 | 0.15 |
| | | Average | -0.46 | Average | -0.28 | Average | -0.03 |
| | | Std Deviation | 0.62 | Std Deviation | 0.38 | Std Deviation | 0.42 |

5.5.4 Sound Level (NC) in Decibels

The close coupling test system was a substantially new room configuration and ran the airflow at higher levels than the field-testing configuration. Therefore the close coupling test room configuration was evaluated for background noise levels at all test conditions. It was determined that at a main duct airflow rate of 1150 fpm, the supply flex duct at 14 inches in diameter, generated breakout sound levels significantly above the throw room ambient and near the test run recorded sound level data. Therefore, the test run sound data for the 1150 fpm runs was not used in the analysis.

Initial analysis of the sound data showed that a test condition other than the four test parameters was affecting the recorded sound levels. Figure 46 shows the correlation between main duct velocity and change in NC levels. The points on the graph show a large variance at each main duct velocity due to different levels of the four test parameters, but the average NC level shows a significant increase with an increase in the

main duct velocity. The linear regression does not cross through the origin because the damper has a minimum of approximately 3 dB affect on the output, which if the regression line was extended towards the origin, it crosses at a delta NC value of about 3 dB.

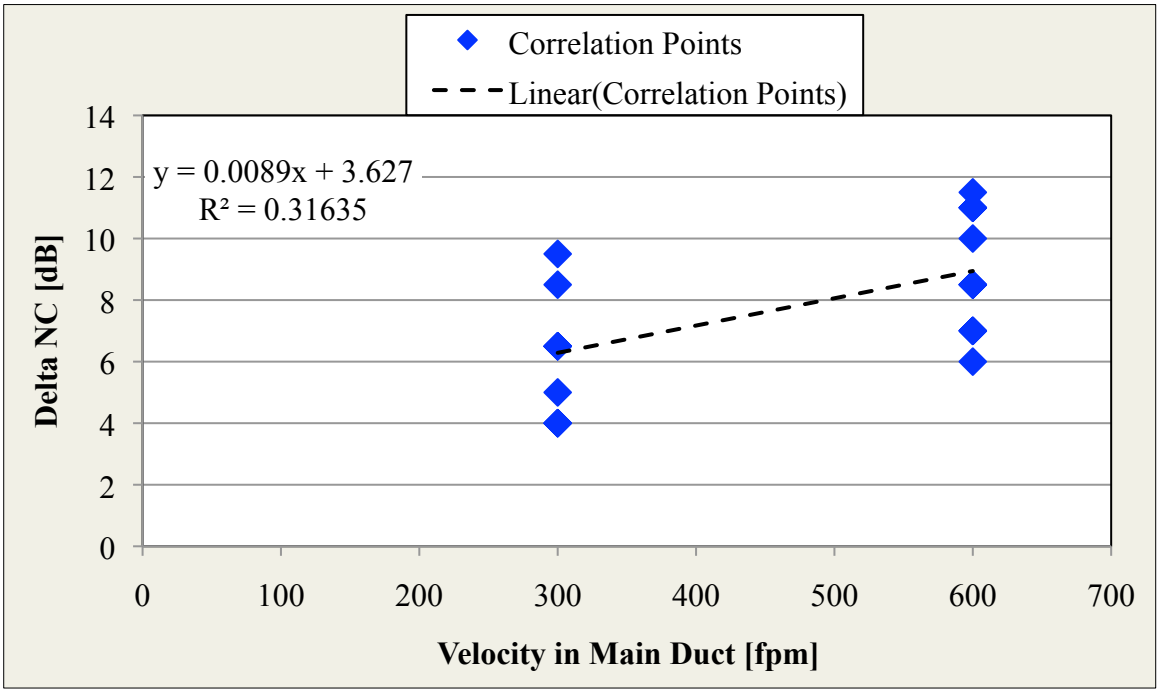


Figure 46. Comparison between change in sound [dB] and main duct velocity.

The following regression equation was developed to calculate an estimated increase in NC level based on the main duct velocity with 31.6 percent of the variance accounted for from the coefficient of determination.

$$\Delta NC\ [dB] = 0.009 * ( Velocity_{MD} ) + 3.63$$

Using the statistical software Minitab, a Pearson Product Moment Correlation was used to prove that the correlation between the main duct velocity and the difference in sound level was indeed accurate. The Pearson Correlation converts the ratio data into z-scores so that each set of data are on the same scale. It is a linear dependant function that compares two variables, X and Y, and uses hypothesis testing to determine the probability that X and Y result in Pearson Correlation of zero. The closer the P-value is to zero, the stronger the rejection is of the null hypothesis, $\rho = 0$. [13,14]

$$\rho = \frac{\sum_{i=1}^{n}\left(x_i - \bar{x}\right)\left(y_i - \bar{y}\right)}{\left(n-1\right)s_x s_y}$$

where: $\bar{x}$ = sample mean for first variable

$s_x$ = standard deviation for first variable

$\bar{y}$ = sample mean for the second variable

$s_y$ = standard deviation for the second variable

$n$ = column length

Note that the data columns must be the same length.

The closer the Pearson Correlation coefficient to one or negative one, the more the variables are correlated and since the values in comparison are both increasing, the correlation approaches one. Also, if the probability value (P-value) is less than the significance level of 0.05, the significance of the correlation is proven strong on the 95 percent confidence interval. If the P-value were greater than the significance level of

0.05, the two variables would have an unlikely correlation. [13,14] With the sound data adjusted based on the damper configuration, the Pearson Correlation was determined to be 0.562 with a Probability value (P-value) of 0.023. Therefore, the correlation is significant and the two sets of data are not random.

Based on the velocity having a significant affect on the diffuser performance, the velocity in the main duct was accounted for by taking the velocity times the slope of the regression line ($0.009*Velocity_{MD}$) described previously and subtracting that value from the NC levels in Table 36. This resulted in NC levels listed in Table 40.

Table 40. Adjusted NC levels that account for damper and not main duct velocity.

| Run # | Change in Sound (NC) Level [dB] | |
|---|---|---|
| | 300 fpm | 600 fpm |
| 1 | 2.30 | 0.60 |
| 2 | 6.80 | 6.10 |
| 3 | -- | 5.60 |
| 4 | 5.80 | 4.60 |
| 5 | -- | 1.60 |
| 6 | 3.80 | 3.10 |
| 7 | 3.80 | 5.60 |
| 8 | 1.30 | 3.10 |
| 9 | 1.30 | 1.60 |

Performing an ANOVA on the adjusted NC levels against all four of the inlet parameters, the one parameter that showed significance with a P-value below 0.05 was the damper at 0.002. The damper was determined independent of the other three parameters. With this in mind, the main effects plot suggested a 3 dB increase when a damper was present in the installation between 300 fpm and 600 fpm. The following

predictive algorithm for NC calculation in a close coupling system was developed to reflect the affects of both main duct velocity and damper installation.

$$NC_{Prediction} = A_D + A_{MD} * V_{MD}$$

*Main Effect Parameters*

- For damper;

Damper is 0 (no damper): $A_D = 0$

Damper is not 0: $A_D = 3$

- For main duct velocity;

Additive correction coefficient for main duct velocity in ΔNC/fpm:

$$A_{MD} = 0.009$$

Main duct velocity in fpm: $V_{MD}$

The predictive algorithm for sound (NC) level, the difference between the experimental and the Standard 70 data in decibels, shows the calculated predicted values for each configuration tested in Table 41. The standard deviations in the table gave values that were slightly lower than the field-testing configurations and the threshold of accuracy held at less than 3 dB was satisfied. Also note that the Standard 70 data for the high state of 1150 fpm was unreliable, as stated previously, because it experienced added sound penetration from the supply duct to the background NC level and was omitted.

Table 41. Predicted values in dB and corresponding errors for sound (NC) level.

| Predicted NC [dB] | Experiment NC [dB] | Error [dB] | Predicted NC [dB] | Experiment NC [dB] | Error [dB] |
|---|---|---|---|---|---|
| 300 fpm | | | 600 fpm | | |
| 2.70 | 5.0 | -2.3 | 5.40 | 6 | -0.6 |
| 5.70 | 9.5 | -3.8 | 8.40 | 11.5 | -3.1 |
| 5.70 | -- | -- | 8.40 | 11 | -2.6 |
| 5.70 | 8.5 | -2.8 | 8.40 | 10 | -1.6 |
| 2.70 | -- | -- | 5.40 | 7 | -1.6 |
| 5.70 | 6.5 | -0.8 | 8.40 | 8.5 | -0.1 |
| 5.70 | 6.5 | -0.8 | 8.40 | 11 | -2.6 |
| 5.70 | 4.0 | 1.7 | 8.40 | 8.5 | -0.1 |
| 2.70 | 4.0 | -1.3 | 5.40 | 7 | -1.6 |
| | Average | -1.44 | | Average | -1.54 |
| | Std Deviation | 1.77 | | Std Deviation | 1.10 |

5.5.5 Summary of Results for Close Coupling Testing

A summary of the results for the close coupling testing configurations is shown Table 42. Even though prediction equations have been established, it may be conducive to conduct further experimentation, including more testing configurations, to achieve a better determination of which inlet parameters have even more of a significant affect on diffuser performance.

Table 42. Summary of standard deviations for close coupling testing.

| | Noise Condition | | |
|---|---|---|---|
| | 1150 fpm | 600 fpm | 300 fpm |
| Forward Throw, $T_f$ | 0.23 | 0.20 | 0.19 |
| Backward Throw, $T_b$ | 0.15 | 0.20 | 0.17 |
| Sound, NC [dB] | -- | 1.10 | 1.77 |
| Pressure Ratio, $P_{Total}$ | 0.62 | 0.38 | 0.42 |

# CHAPTER 6

# CONCLUSIONS AND RECOMMENDATIONS

This investigation obtained quantitative diffuser throw, back-pressure and noise generation data on the effects of field installation variations compared to published Standard 70 data. The data, when presented in an easily usable form, can aid designers and installers in their efforts to produce energy efficient, comfortable, quiet and effective air distribution systems. All four phases of the investigation, plenum design, baseline testing, field installation testing and close coupling testing produced such quantitative data.

## 6.1 Diffuser Supply Plenum Design

The test results analysis from the plenum optimization experiment identified a method of introducing air into the plenum and a design and position of the flow equalization device that produced diffuser inlet velocity conditions that had variation well below the requirement for Standard 70 testing. Perhaps more importantly, this investigation resulted in guidance on plenum design that can be used for future plenum builds to optimize the airflow into the diffuser inlet using robust design. The robust design method was a good tool for economically deriving main effects of the system parameters and showed the necessity to consider the physics and interactions in order to perform verification tests and identify accuracy. Through verification testing, it was determined that the ducted method and plenum method of testing suggested by Standard 70, gave similar results for throw, sound and pressure data when performed in the UNLV throw room. The final results show that variation significantly lower than the Standard 70

specification can be achieved with proper plenum design. The results also indicate that a minimum straight inlet duct of 7-10 inches be specified in the design regardless of low airflow variation without the added duct length.

This plenum design experiment helped to develop testing methods that were later used in the Standard 70 and field condition testing. The use of orthogonal test arrays for determining the experiment test run conditions proved to be efficient and effective for output analysis. Similar arrays used in the field condition testing analysis will allow practical testing with multiple parameters.

## 6.2 Standard 70 Characterization

Following the guidelines in Standard 70, a baseline data set for comparison to real field installations was developed. The data conforms to the linear regression described by the zone plot formulation. The zone plot method produced characterizations of different diffusers with differing inlet neck sizes and flow rates. The method also showed that while similar diffusers from different manufacturers often perform nearly identical, that is not always the case. Sufficient data was obtained to perform comparisons between baseline and field installation performance. From this comparison, a set of calculated algorithms were developed to determine the effect each physical parameter has on the field installations. The Standard 70 plenum method was shown to be an accurate and economical method to test for ideal diffuser performance.

## 6.3 Field Installations

Prediction algorithms for the performance difference ratio between field installations and Standard 70 data were obtained. These algorithms are adequate for determining how a ceiling diffuser installation is going to perform based on inlet configuration characteristics. The quantitative data reflects averaged results across different manufacturers and different airflows while taking into account inlet condition parameters such as duct type, approach angle, damper type, damper orientation and vertical duct height attached to the diffuser inlet. Several design conditions cause variation in throw asymmetry, pressure and sound generation of the test diffuser. Also, the different types of diffusers and different inlet to outlet area ratios affected the performance sensitivity of the installation to variations in installation.

For throw asymmetry, duct height was the most important installation parameter. No vertical duct leading into the diffuser resulted in significant asymmetry. A damper in the inlet, depending on damper blade orientation, could reduce that asymmetry. The larger inlet diameter (higher inlet to outlet area ratio) was more sensitive to installation, causing more throw asymmetry than smaller diameters.

Both a damper in the diffuser inlet and the duct configuration that led into the diffuser inlet affected pressure drop of the system. A damper at the diffuser inlet increased pressure drop. Flex duct caused a higher pressure drop than rigid duct. When the duct was connected directly to the diffuser inlet with no vertical duct height, pressure drop was increased. The louvered diffuser was most sensitive to installation variation while the modular core perforated square diffuser was the least sensitive. A larger inlet diameter

(higher inlet to outlet area ratio) reduced sensitivity to installation, causeing performance variation.

Diffuser generated sound (NC level) was most affected by vertical duct height above the inlet with no vertical duct resulting in a 7 dB increase in NC level. Damper installation caused a minimum 2 dB increase and up to a 7 dB increase. Duct height and damper effects are not always additive, such that the combination of no vertical duct and a damper generate less noise than the sum of both effects. Plaque and round diffusers had the highest sound performance sensitivity to installation variation while the modular core perforated square had the least.

## 6.4 Close Coupling

In a close coupling installation with all rigid duct, the effect of diffuser type, branch length and damper were not predictable using the exact same field installation formulas. For close coupling, the main duct velocity and damper installation were the significant factors in the determination of sound generation in a close coupling field installation. As the velocity increases, the ratio of sound generation to the Standard 70 sound levels increases. At slower main duct velocities, it was determined that for every 100 fpm, add one decibel to the sound level prediction. Because the main duct velocity had such an effect, a calculation was made to remove this affect from the sound data, so that only the installation of a damper, which was independent of the other three parameters, had an effect on the diffuser performance. The resulting data was used to develop the predictive algorithm. Quantitative data for predicting the noise generation were determined. It was

also found that to achieve the proper flow velocity profile for any diffuser in the close coupling position, a ceiling should be flush with the diffuser outlet face.

## 6.5 Recommendations for Designers and Installers

The algorithms developed in this investigation should be used to develop more efficient, effective, comfortable and quiet air distribution systems. The formulas can also be simplified into an easy to use table of corrections for most of the common installation variations. Anyone building a laboratory test system using a plenum air supply will find the plenum design results to be useful. Consideration should be given to have Standard 70 diffuser inlet airspeed variation specification given in terms of a standard deviation from the mean, which more accurately reflects the quality of the inlet flow. Also Standard 70 should specify a minimum vertical duct height from the diffuser inlet to the inlet cone regardless of flow uniformity.

# APPENDIX A

# TEST FACILITY

The following information describes the laboratory instrumentation, equipment and the software used to manipulate each. Certain instruments were project specific and thus were labeled as such. Most instruments and equipment pieces are physically apart of the laboratory and are usable for much more than what was needed for this project.

## A.1 Throw Room Description

The Center of Mechanical & Environmental Technology (CMEST) throw room is a unique, state-of-the-art, automated testing facility. It can be used to measure the quality, efficiency, and effectiveness of different heating, ventilating, and air conditioning (HVAC) system components and configurations, and their related effects on building occupants. The throw room is 30 ft (9.1 m) long by 20 ft (6.1 m) wide. The height of the room ceiling, measured from the floor, can be varied from 7 ft (2.1 m) to 11 ft (3.3 m). The throw room is equipped with both a traditional air distribution (CAD) system and UFAD system. It can be rapidly reconfigured from CAD to UFAD systems with different diffuser, grill, and load configurations. It can be easily set up as an office space with partitions, a moderate size meeting room, a classroom, or a hotel suite. The system can also be easily modified to add a displacement ventilation system by putting a displacement terminal unit against the north wall where the vertical shaft for UFAD systems is located. The side view of the throw room is shown in Figure 47. The figure shows the supply air fan chamber and ASME nozzle chamber used to measure and monitor the supply airflow rate to the throw room, the UFAD plenum, the interior room

space, the adjustable height room ceiling, the ceiling plenum, CAD and UFAD system duct and the vertical shaft for UFAD system. The throw room has precision measurement capabilities including [15]:

1. Airflow and room air distribution characteristics of grills, registers, diffusers, and other types of room ventilation devices.
2. Airspeed, temperature, humidity and contaminant concentrations at precise points throughout the entire room.
3. Temperatures at multiple wall, floor, ceiling, under-floor, and above ceiling airspace locations.
4. Airflow, temperature, humidity, contaminant concentrations and pressure at various locations in the supply and return ductwork and plenums.
5. Energy inputs from interior room, room lighting, and simulated exterior solar loads and energy consumption of the HVAC system.

Its precision control capabilities include [15]:

1. Perimeter heating and cooling loads through the control of all room surface temperatures by zone. Each room surface (includes walls, floor below the raised floor, and ceiling above the dropped ceiling) is divided into one to three zones. The surface temperature of each zone can be independently controlled. Each zone can be heated or cooled independently as required to maintain the desired wall temperature.
2. Interior room heating and cooling loads. Load simulators for humans and machines can be placed throughout the room. Their individual and total energy

consumption can be monitored and controlled.

3. Supply airflow at 2,000 CFM BI centrifugal fan supplies air to the room, in a closed loop or ventilated mode.
4. Supply air temperature is digitally controlled heat pump supplies air at preset supply air temperatures to the room, in a closed loop or ventilated mode.
5. Precision automated instrument positioning from a computer-controlled, two-axis (two translational axes) traversing system can hold multiple instruments for measuring airspeed, temperature, sound, contaminant concentration and humidity at any point in the room. The control system automatically moves the instruments to the test positions while capturing and recording the measurements at those positions. The sensors on the traversing mechanism are fixed.
6. Automatic monitoring of test conditions, both prior to start and during testing. Operator warnings are sent if test and measurement conditions drift out of predefined limits. Tests can be paused, resumed, or halted at any time.

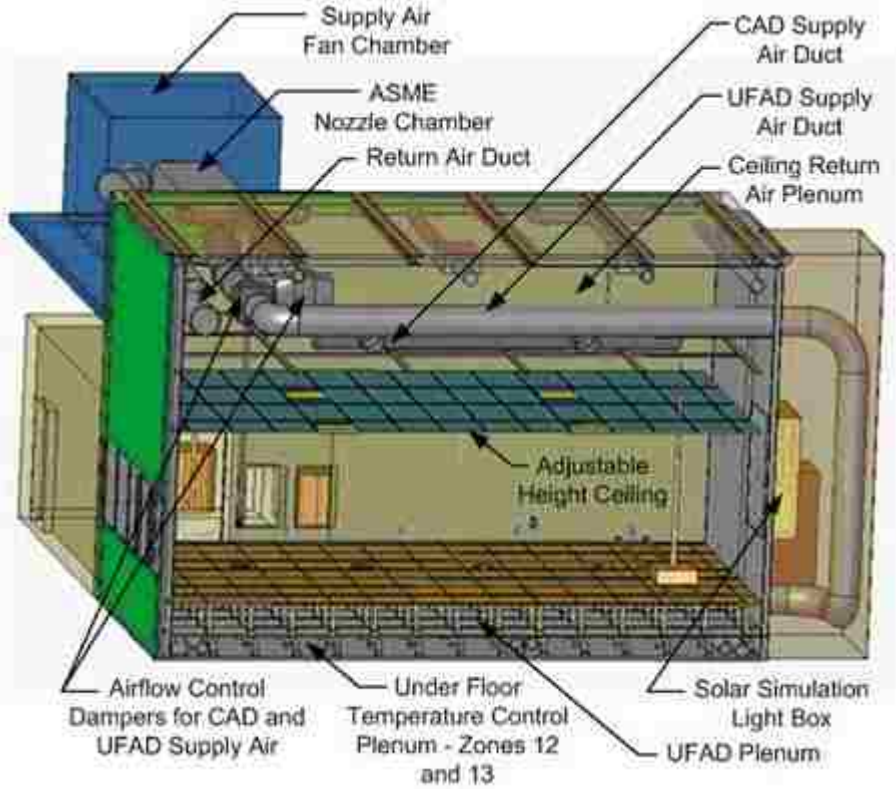


Figure 47. Side view of the UNLV throw room [15].

## A.2 Throw Room Data Acquisition Instrumentation

The following information describes the instrumentation used to control and verify the thermal conditions in the UNLV throw room. A central computer is used to control the instrumentation, data acquisition and motion control systems using a custom written LabView program. This software will simultaneously monitor the room conditions and instrument performance. A test could be stopped, continued or restarted at any point in time with this software. Figure 48 and Figure 49 show the interfaces used by LabView for monitoring the sensors and supply duct parameters in the UNLV throw room. Table 43 shows the instrumentation used by the National Instruments LabView program to record supplemental data at a user set time interval of 4 seconds per sample. Table 44

shows the equipment used to control the supply duct air flow characteristics and measure supplemental data with and without LabView. A separate interface was used to control the motion of the throw room traversing mechanism that had the throw velocity sensors attached given in Figure 50. To set up the path that the sensors followed, another interface was called upon through the motion control interface in Figure 51, where the red box signified the diffuser dimensions. This interface could produce alternate path types other than linear, such as, angled, raster and three sided to accommodate any situation. All the instrumentation and equipment worked together to produce isothermal conditions within the throw room during periods of testing.

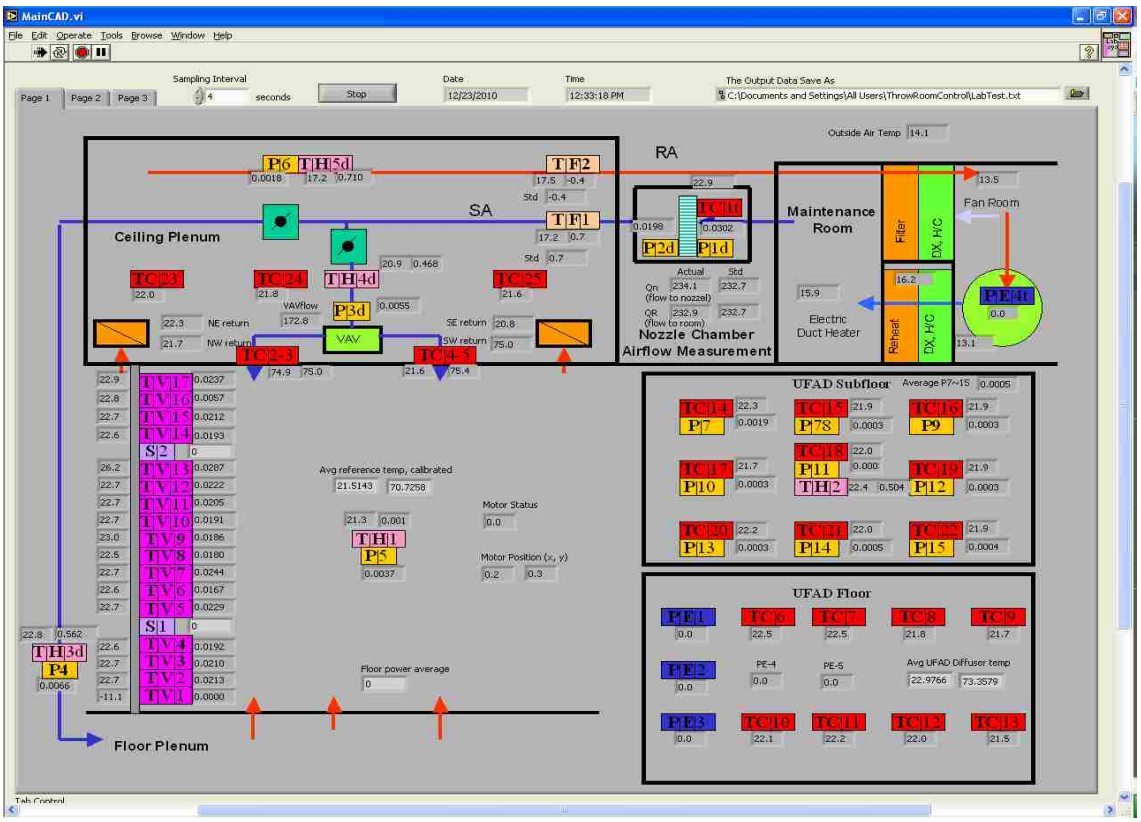


Figure 48. Labview main interface for monitoring system conditions.

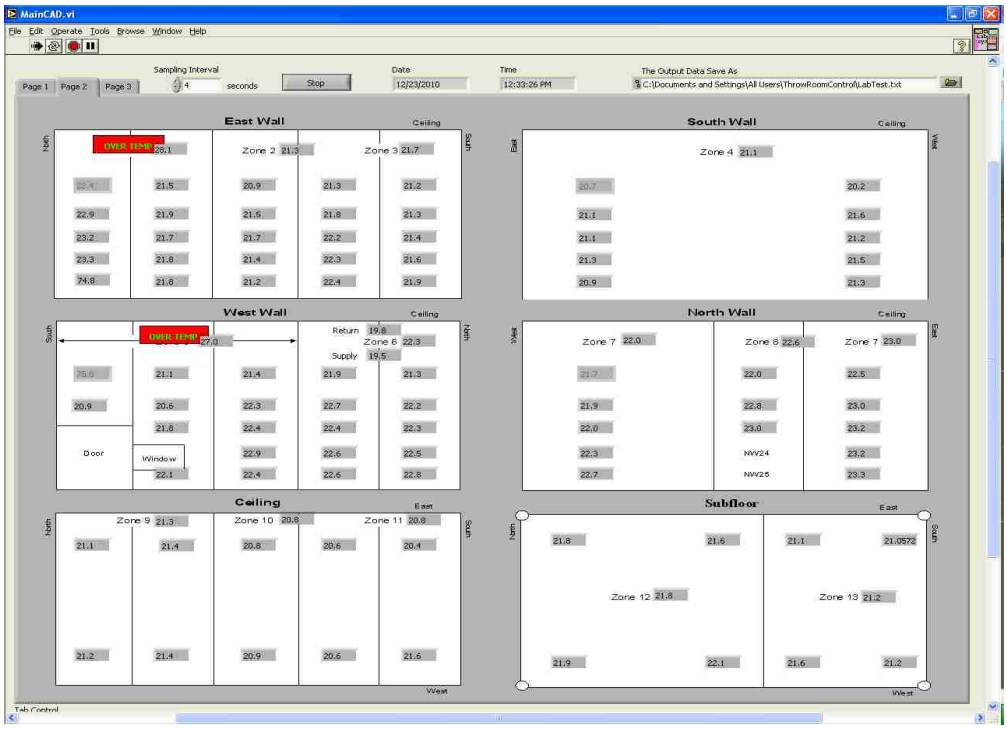


Figure 49. Interface for monitoring throw room surface temperatures.

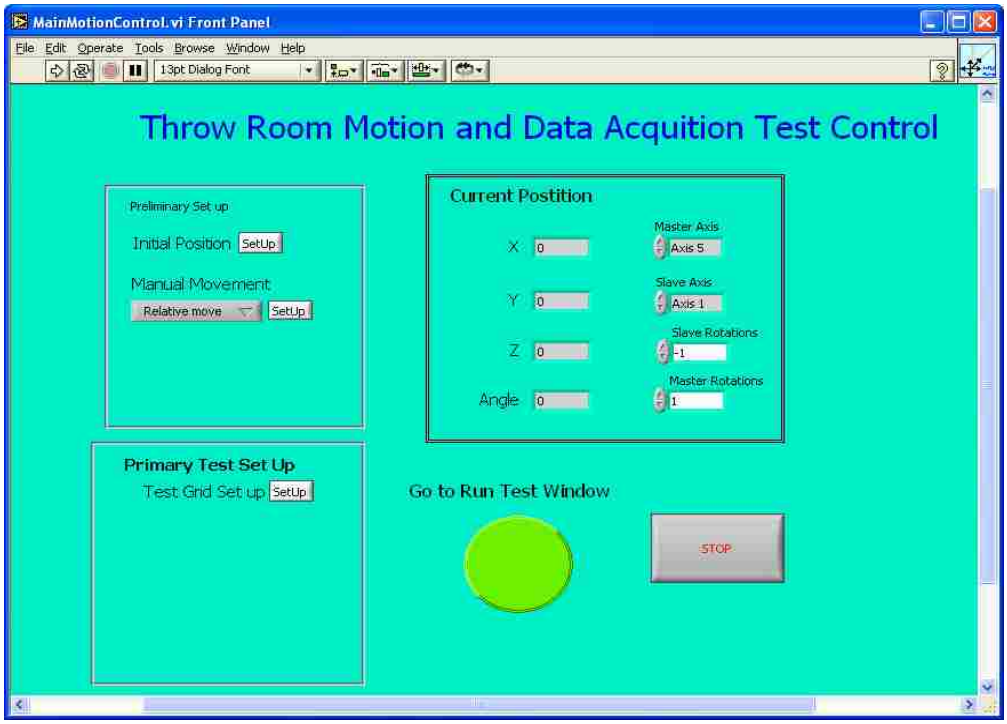


Figure 50. Throw room LabView motion controller interface.

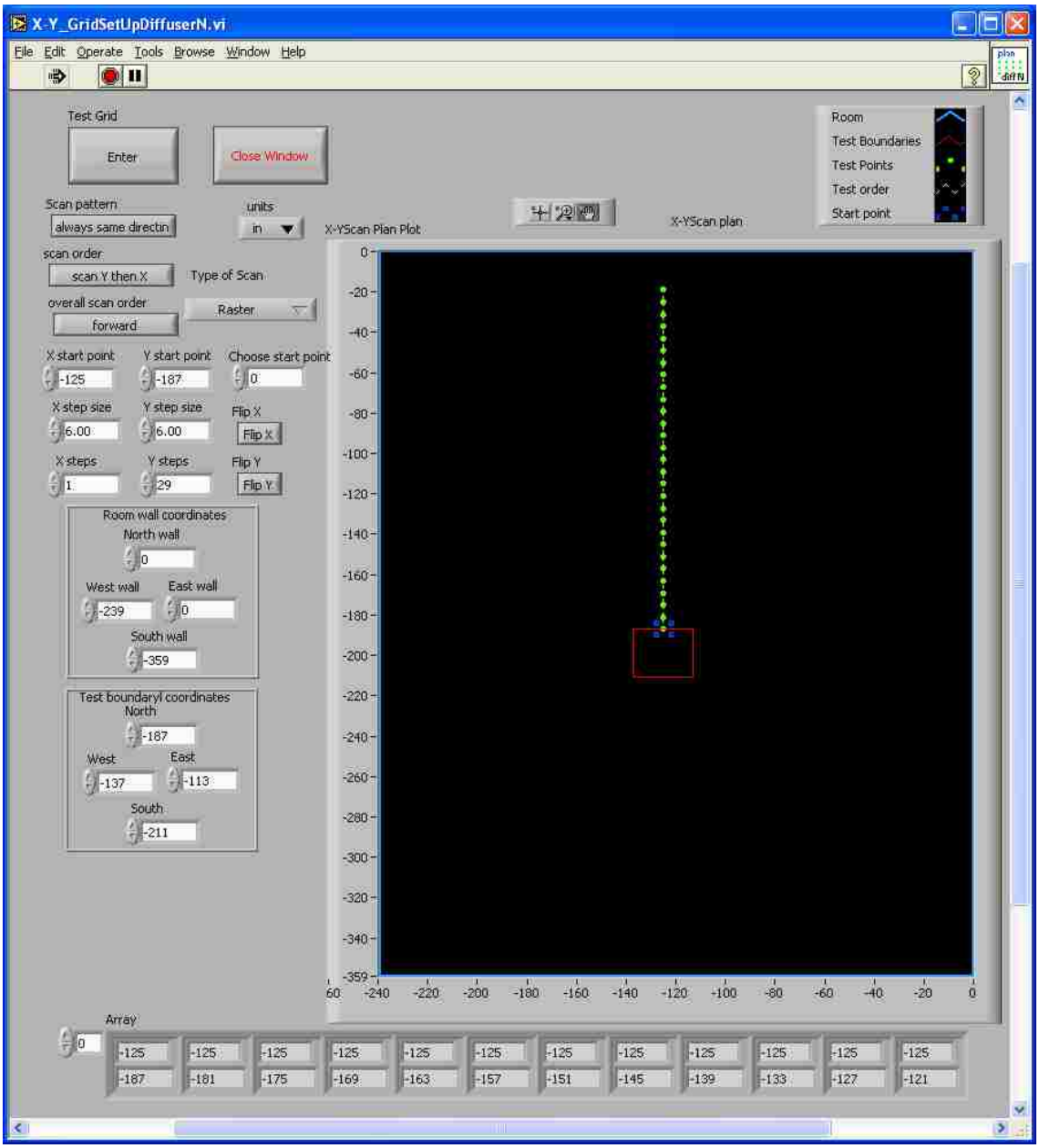


Figure 51. Throw velocity sensor path setup interface.

Table 43. Throw room instrumentation used along with NI LabView.

| Symbol | No. | Suffix | Measured Parameter | Instrument Name and Model | Quantity | Location | Sampling, Storage and Display Rate, [Hz] | Accuracy |
|---|---|---|---|---|---|---|---|---|
| TV | 1 - 17 | t,v | Air Temperature ($^{o}$C) and Velocity (m/s) | Sensor Technology HT-400 | 17 | Traversing Mechanism pole | 0.5 | Temperature: ±2 $^{o}$C Velocity: 0.05 to 1m/s, ±1% of reading; 1 to 5m/s, ±3% of reading |
| TH | 1 - 2 | | Air Temperature ($^{o}$C) and Humidity (%) | Omega HX93 AV | 2 | Room (TH1) and Ceiling Plenum (TH2) | 0.5 | Temperature: ±0.5 $^{o}$C Relative Humidity: ±2.5% |
| TH | 3 - 5 | d | Air Temperature ($^{o}$C) and Humidity (%) | Omega HX93 AV-D, Duct Mounted | 3 | Supply (TH3d-4d) and Return Ducts | 0.5 | Temperature: ±0.5 $^{o}$C Relative Humidity: ±2.5% |
| TC | 1 | t | Air Temperature ($^{o}$C) | Omega Thermal Couples, T type with 24 in. probe | 1 | Nozzle Chamber | 0.5 | Temperature: ±0.5 $^{o}$C |
| TC | 2 - 25 | | Air Temperature ($^{o}$C) | Omega Thermal Couples, K type with 12 in. probe | 24 | Ceiling Supply Diffusers (TC2-5), Floor Supply Diffusers (TC6-13), Floor Plenum (TC14-22), Ceiling Plenum (TC23-25) | 0.5 | Temperature: ±1.1 $^{o}$C |
| T4 | 1 - 97 | | Wall Temperature ($^{o}$C) | Omega Thermal Couples, SA1K | 97 | Walls, Ceiling, Floor | 0.5 | Temperature: ±1.1 $^{o}$C |
| P | 1 - 3 | d | Static or Differential Pressure (in. $H_2O$) | Omega PX277-05D5V | 3 | Nozzle Chamber (P1d-2d), Supply Plenum (P3d) | 0.5 | Pressure: ±1% of full scale |
| P | 4 - 15 | | Static Pressure (in. $H_2O$) | Omega PX277-01D5V | 12 | Close Coupled Main/Supply Duct (P4,P6), | 0.5 | Pressure: ±1% of full scale |

| | | | | | | | | |
|---|---|---|---|---|---|---|---|---|
| | | | | | | Return Duct and Floor Plenum (P5,P7-P15) | | |
| TF | 1 - 2 | | Air Temperature ($^{o}$C) and Flow Rate (cfm) | EBTRON GTx116-Pc | 2 | Supply (TF1) and Return (TF2) Ducts | 0.5 | Temperature: ±0.075 $^{o}$C Airflow Rate: ±2% to 3% of reading |

Table 44. Testing equipment used in part with throw room.

| Instrument Name and Model | Measured Parameter | Location | Accuracy | Note |
|---|---|---|---|---|
| TSI VelociCalc Plus Meter 8386A | Velocity (m/s), Temperature ($^{o}$C), and Relative Humidity (%) | Handheld Device | Velocity: ±3% of reading Temperature: ±0.25$^{o}$C Relative Humidity: ±3% | Used for verification and plenum optimization data |
| TSI Alnor LOFLO Balometer 6200 | Airflow Rate (cfm) | Handheld Device | Flow Rate: ±(3%+5cfm) | Range: 10 to 500 cfm |
| TSI AccuBalance Airflow Capture Hood 8371 | Airflow Rate (cfm) | Handheld Device | Flow Rate: ±(5%+5cfm) | Range: 30 to 2000 cfm |
| Bruel & Kjaer Type 4942 | Sound (dBA) | Boom Microphone | NC: 0.2 dB at 95% CI | Capture Sound Data in Throw Room |

Table 45. Systems used in part with the throw room.

| System Name and Model | Measured Parameter | Location | Accuracy | Note |
|---|---|---|---|---|
| Greenheck Centrifugal Fan 15-BISW-I | Airflow Rate (cfm) | Blower Room | | Produces Airflow for Throw Room Max 2674 rpm |
| 3-Phase Lincoln Motor (Leeson) SSF4P5T61 | Frequency (Hz) | Blower Room | | Fan Motor, 5 HP, 60 Hz, 1745 rpm |
| PDL Electronics LTD XTRAVERT X712 | Fan Frequency (Hz) | Lab Room | 97% Electrical Efficiency | Controls Motor That Controls Fan |
| White Rodgers IF93-380 | Temperature ($^{o}$C) | Lab Room | | Thermostat w/ Setpoint Range (7-37$^{o}$C) |
| Daikin Unit VRV II REYQ96MTJU | Temperature ($^{o}$C) | Outside | | Cool/Heat Walls of Throw Room |
| Bryant Heat pump 213RNA036-D | Temperature ($^{o}$C) | Outside | | Cool/Heat Supply Air 1.5-5 Tons |
| Titus VAV box | Pressure (in. $H_2O$), Temperature ($^{o}$C) | Throw Room | | Variable Air Volume |

A.2.1 Calibration of the Ebtron flow measurement unit

Also note that the ASME approved nozzle chamber used complicated calculations with the LabView interface to provide accurate throw into the system that was measured

by the Ebtron unit installed at the supply duct. A test was run to check the calibration of the calculations, see Figure 52, and it was found that the setup was accurate up to a flow rate of 1,000 cubic feet per minute, where soon thereafter, the data showed increasing degradation in accuracy of the nozzle calculations with increasing flow rate. The configuration of the nozzle chamber was changed for each range of flow according to it's manufacturer calibration. The points that represent F1 are the points that were set by the tester. The points that represent Q_R are the calibrated values measured by the Ebtron unit after the air is pumped through the nozzle chamber.

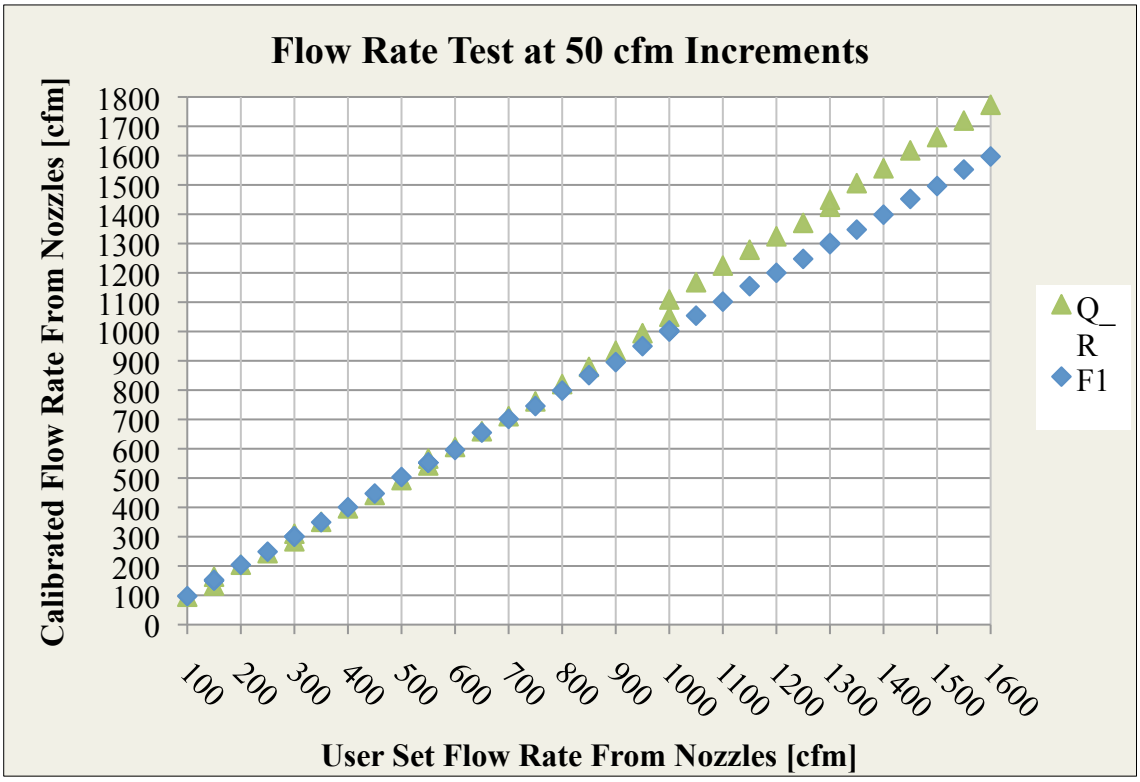


Figure 52. Calibrated nozzle chamber versus Ebtron unit.

A.2.2 Calibration of the VAV unit

The variable air volume (VAV) unit was calibrated as well before conduction the close coupled tests to better determine the amount of air leaving the vertical branch. Like the Ebtron unit, the VAV had a pressure ring that was used to determine the flow of air at a given point in time. The damper built into the VAV was fully open and the supply air, determined by the Ebtron, was increased at increments to determine the pressure increase read by the pressure ring inside the VAV. The value for the flow rate of F1 shown in Figure 53 was squared to linearize the correlation with pressure of P3d. At more than 99.5 percent of the variance accounted for, the two parameters are highly correlated.

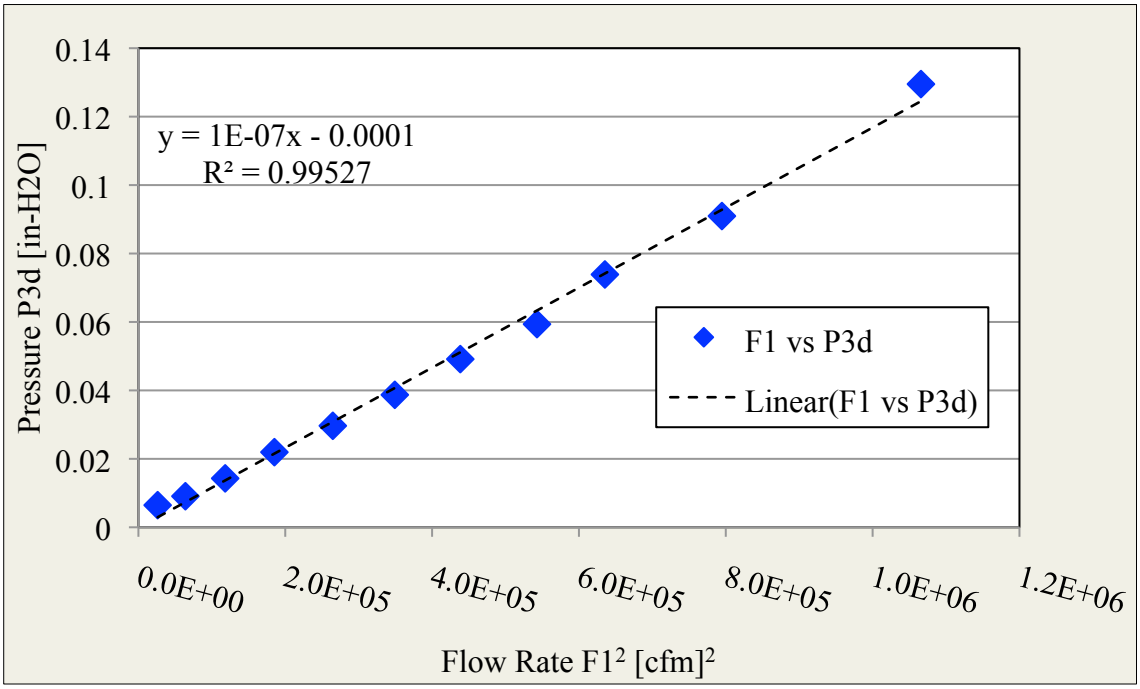


Figure 53. VAV unit calibration.

Taking the total pressure of the duct system and subtracting the static pressure measured at the VAV, the velocity pressure was determined. Velocity pressure is

calculated from measurement of the total airflow and knowledge of the main duct cross-sectional area. Using the velocity pressure, the temperature of the air traveling through the VAV, a correction value and a multiplier determined through regression analysis of dynamic pressure, the following equation was used to determine the volume flow rate of air leaving the VAV unit, where $T_{VAV}$ is the temperature of air inside the VAV unit and $P_{VAV}$ is the pressure inside the VAV unit.

$$VAV_{Flow} = 2740 * \{[( T_{VAV} + 273 ) / 297 ]^{(1/2)} \} * ( P_{VAV} )^{(1/2)} - 29$$

Using the above equation and the known value of the incoming flow from the Ebtron flow measuring unit, the difference between the two yields the flow exiting the diffuser attached to the branch on the rectangular main duct in the close coupling design shown in Figure 35.

## A.3 Project Specific Data Acquisition Instrumentation

The following instrumentation is specific to the experimentation done for this research. The plenum was built in-house per ASHRAE Standard 70-2006 and meets the minimum requirements from this standard. The boom microphone was used to calculate the room NC levels during testing.

### A.3.1 Optimized supply plenum leak test

The data points shown in Figure 54 represent a leak test that was conducted after the finalized construction of the optimized plenum before any Standard 70 baseline tests were performed. The supply air inlet conditions were kept at the optimal settings and the

opening for the diffuser installation was sealed. Increasing the airflow into the plenum caused the pressure to increase within the plenum. These two parameters, flow and pressure, were correlated with one another to determine the leakage from the plenum. At nearly 99 percent of the variance accounted for in the correlation, the leakage from the supply plenum is very small.

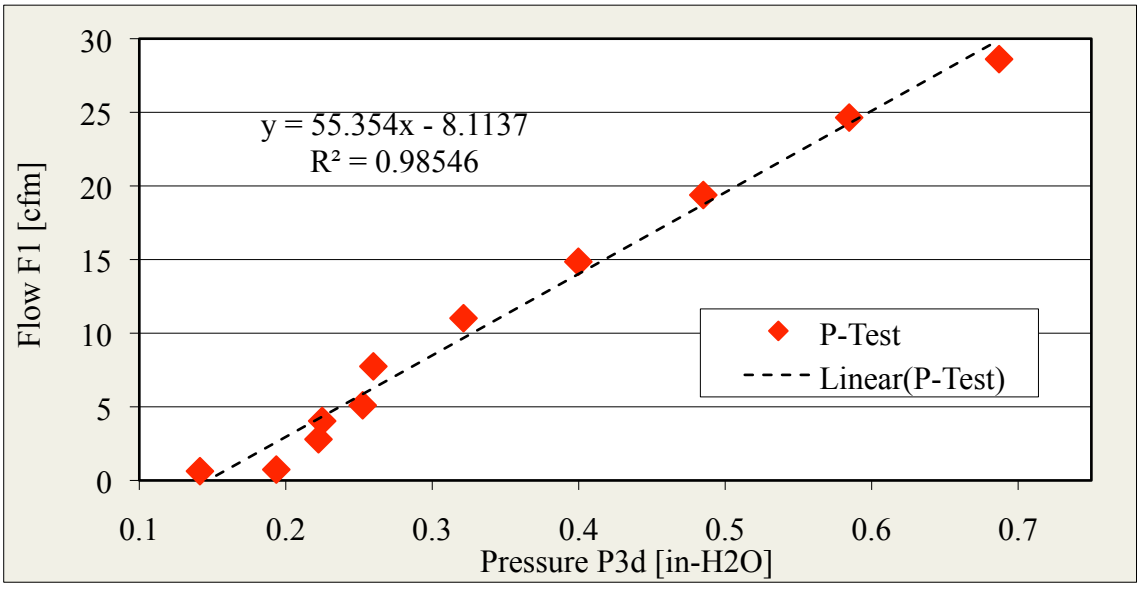


Figure 54. Plenum pressure test.

A.3.2 Boom microphone throw room calibration

The boom microphone was setup to capture an averaged sound level within the throw room by recording points at different locations in the reverberant field. The boom microphone, pictured in Figure 11, rotated 180 degrees and recordings were made every five seconds as the boom traversed along it's path. All recorded points were averaged over a minimum of 60 seconds. NC contour curves, shown in Figure 55, were used to determine the point of tangency with the highest-ranking NC curve. [6,8]

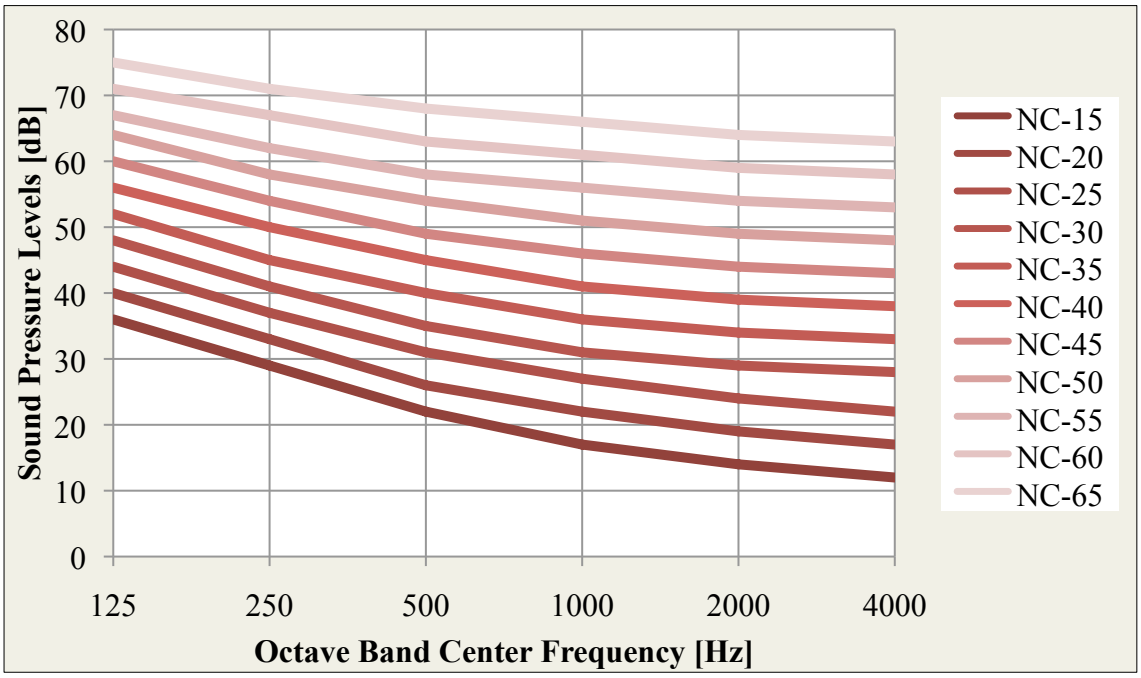


Figure 55. Published NC contour curves.

This set the NC rating for the current configuration of the UNLV throw room and for each 1/1 octave band center frequencies, given below, an equation was formulated specific to the UNLV throw room. Another LabView interface was used to accomplish this and is shown in Figure 56.

Boom microphone NC calculations:

$$125\ \text{Hz [dB]} = X1 - X2 - 10 - 64 \cdot 108 + 50$$

$$250\ \text{Hz [dB]} = X1 - X2 - 10 - 58 \cdot 108 + 50$$

$$500\ \text{Hz [dB]} = X1 - X2 - 10 - 54 \cdot 109 + 50$$

$$1000\ \text{Hz [dB]} = X1 - X2 - 10 - 51 + 50$$

$$2000\ \text{Hz [dB]} = X1 - X2 - 10 - 49 + 50$$

$$4000\ \text{Hz [dB]} = X1 - X2 - 10 - 48 + 50$$

where, X1 = 1/1 octave band sound pressure level in dB,

X2 = R-values for the throw room using a noise maker and 60 second decay method,

Minus 10 is for the Standard 70 room correction due to attenuation.

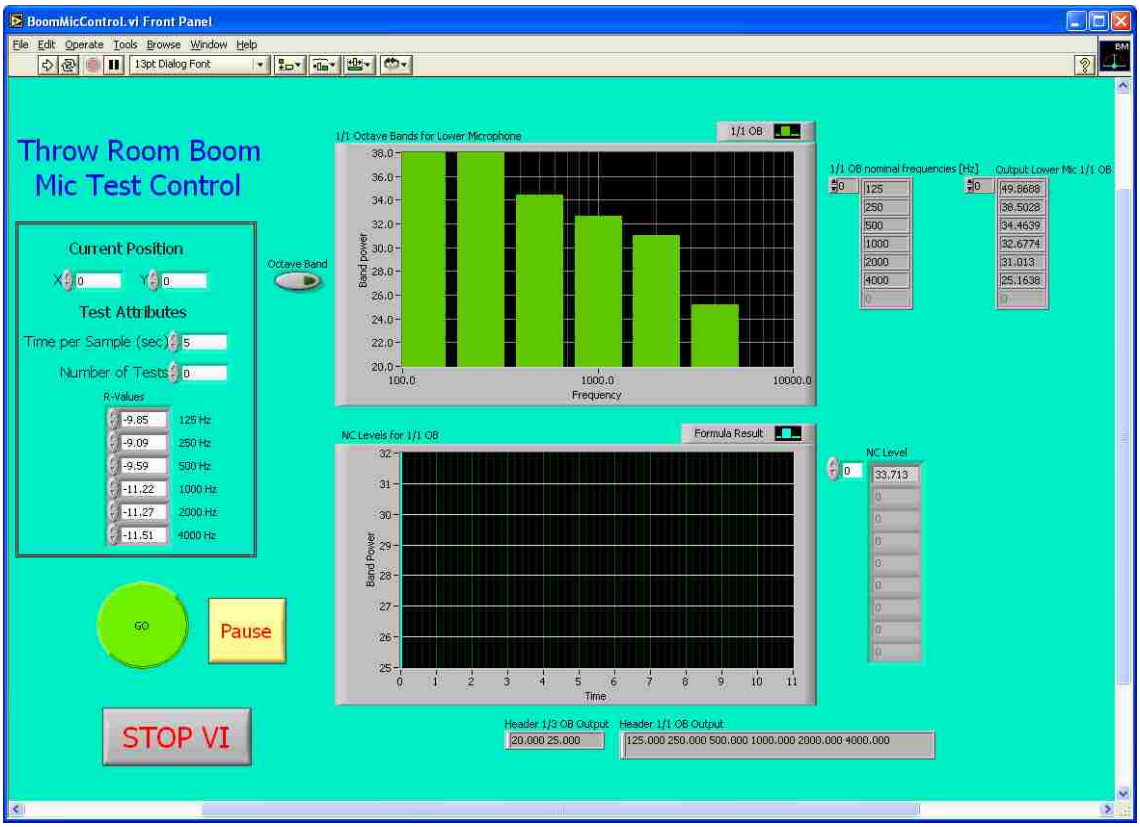


Figure 56. Sound capture interface using the boom microphone.

Combined with these calculations was an ambient background sound level, of the current throw room configuration, to determine the overall NC during each test performed in the throw room.

# APPENDIX B

# FIELD INSTALLATION TEST RESULTS DIFFUSER DISCHARGE AIRFLOW ZONE PLOTS

The following figures represent the zone profile for each configuration tested in the field installations Taguchi mixed array in Chapter 4. The majority of the data resided in zone three and four as the jet of airflow from the diffuser face spread downward and away from the diffuser along the ceiling, but the zone two profile existed a short distance from the diffuser face where throw velocity was the highest. The process used to create these plots was given in ASHRAE Standard 70-2006. For each field installation configuration the velocity profiles for each terminal velocity air speed from the array of draft meters was used to determine throw distance, x, and the corresponding velocity, $V_x$. Then calculating the inlet neck area, $A_k$, and the neck velocity, $V_k$, the dimensionless comparison was made below in each figure. These data points were compared to the similarly plotted zone data points for the Standard 70 baseline data. This comparison led to the throw ratio values between the field install and the Standard 70 configurations used in the field installation statistical analysis. Refer to Table 46 for a list of the run numbers and their corresponding inlet conditions.

Table 46. Inlet conditions for field testing runs.

| Run # | Diffuser Type | Inlet | Duct Height | Type Duct | Damper | Damper Type | Approach Angle |
|---|---|---|---|---|---|---|---|
| 1 | Square | 8 | 0 | Rigid | None | RndSliding | 0 |
| 2 | Square | 10 | 1.5 | Mix | Perpendicular | RndSliding | 23 |
| 3 | Square | 12 | 3 | Flex | Parallel | RndSliding | 45 |
| 4 | Plaque | 8 | 0 | Mix | Perpendicular | RndSliding | 45 |
| 5 | Plaque | 10 | 1.5 | Flex | Parallel | RndSliding | 0 |
| 6 | Plaque | 12 | 3 | Rigid | None | RndSliding | 23 |
| 7 | Perf Rnd | 8 | 1.5 | Rigid | Parallel | RndSliding | 23 |
| 8 | Perf Rnd | 10 | 3 | Mix | None | RndSliding | 45 |
| 9 | Perf Rnd | 12 | 0 | Flex | Perpendicular | RndSliding | 0 |
| 10 | Mod Core | 8 | 3 | Flex | Perpendicular | SqOpBld | 23 |
| 11 | Mod Core | 10 | 0 | Rigid | Parallel | SqOpBld | 45 |
| 12 | Mod Core | 12 | 1.5 | Mix | None | SqOpBld | 0 |
| 13 | Round | 8 | 1.5 | Flex | None | RndSliding | 45 |
| 14 | Round | 10 | 3 | Rigid | Perpendicular | RndSliding | 0 |
| 15 | Round | 12 | 0 | Mix | Parallel | RndSliding | 23 |
| 16 | Louvered | 8 | 3 | Mix | Parallel | SqOpBld | 0 |
| 17 | Louvered | 10 | 0 | Flex | None | SqOpBld | 23 |
| 18 | Louvered | 12 | 1.5 | Rigid | Perpendicular | SqOpBld | 45 |

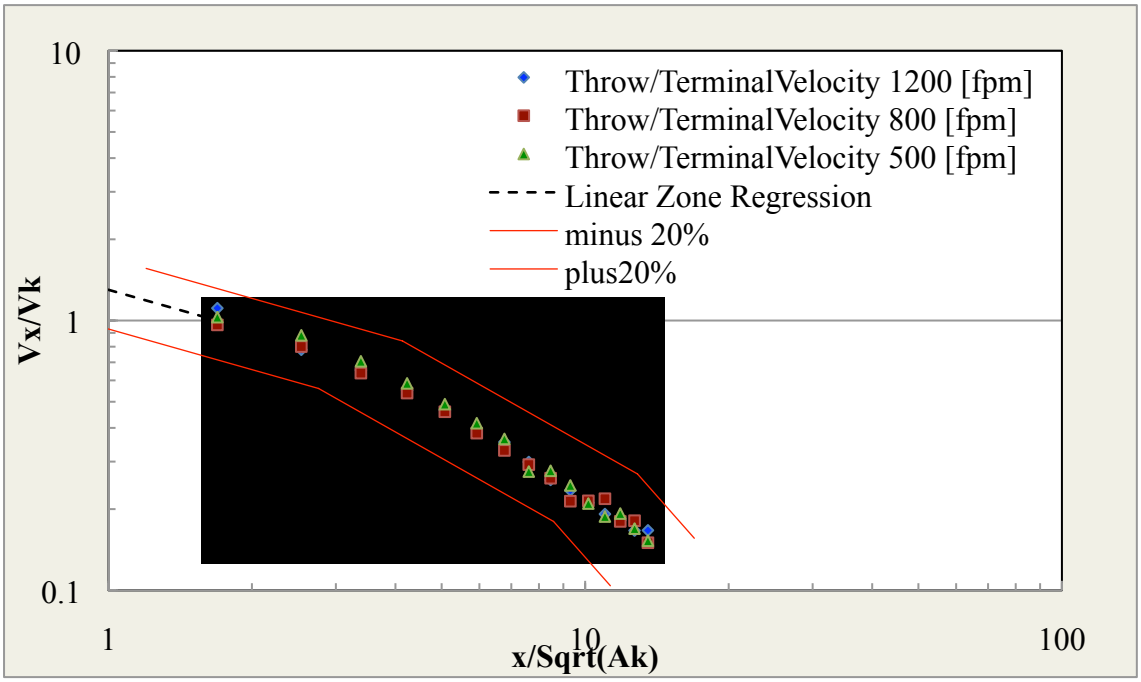


Figure 57. Forward throw for Run #1.

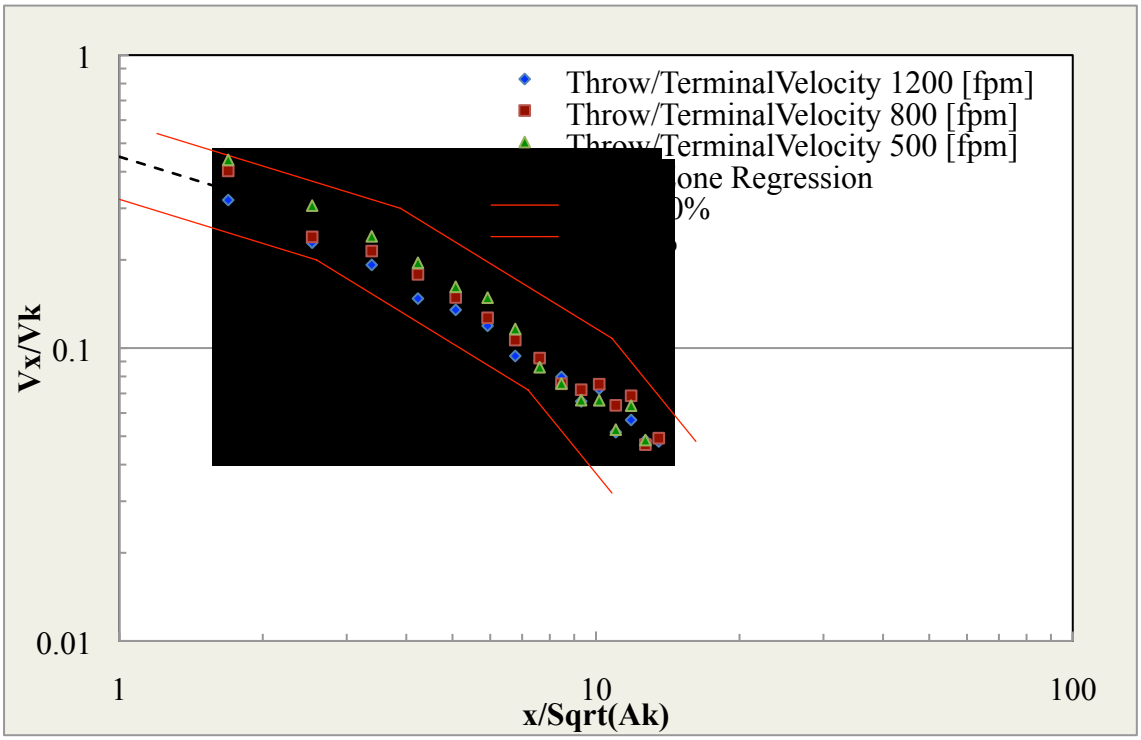


Figure 58. Backward throw for Run #1.

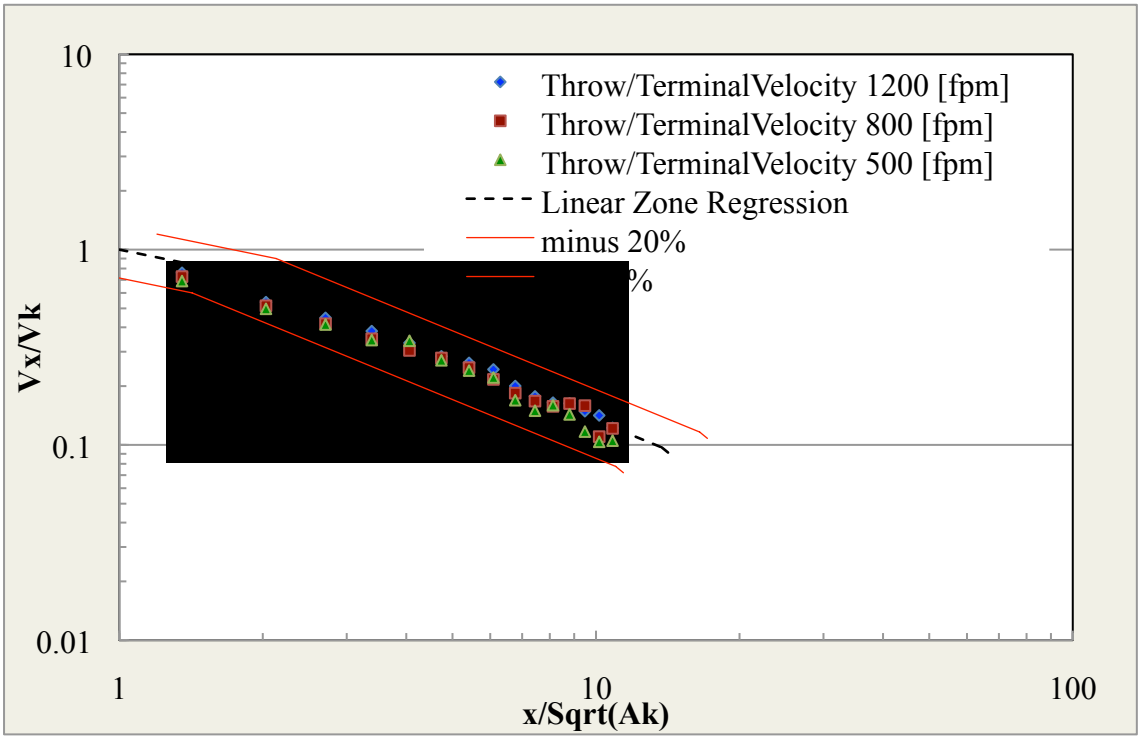


Figure 59. Forward throw for Run #2.

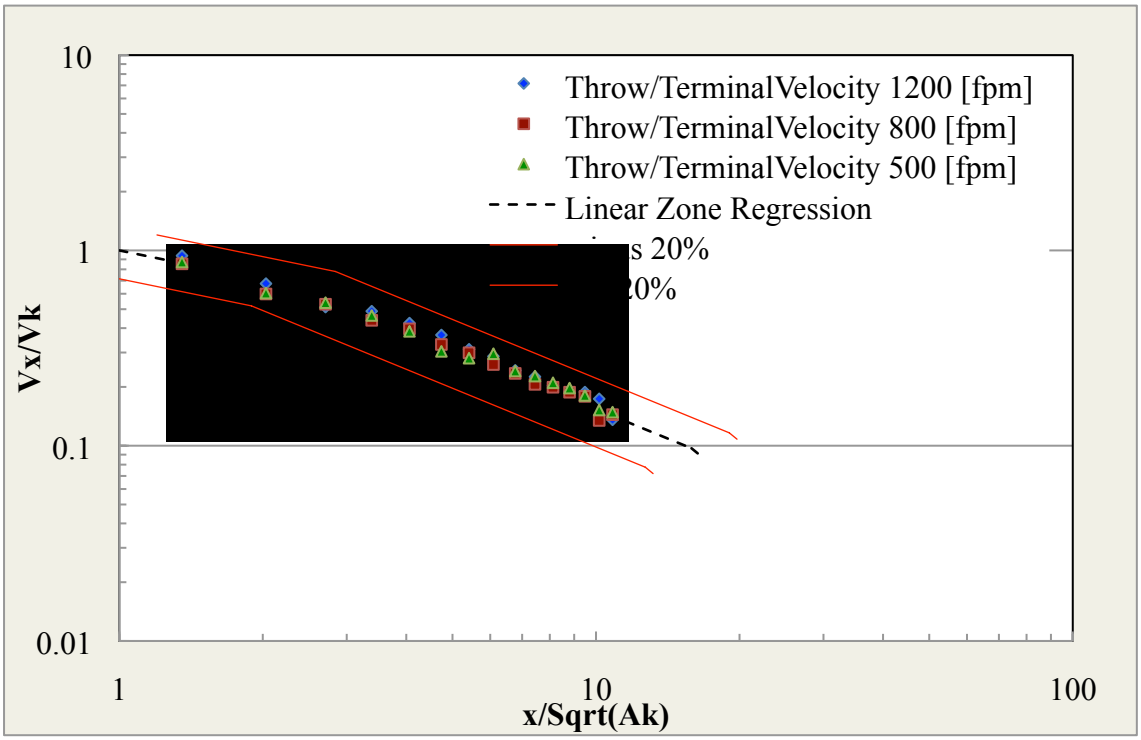


Figure 60. Backward throw for Run #2.

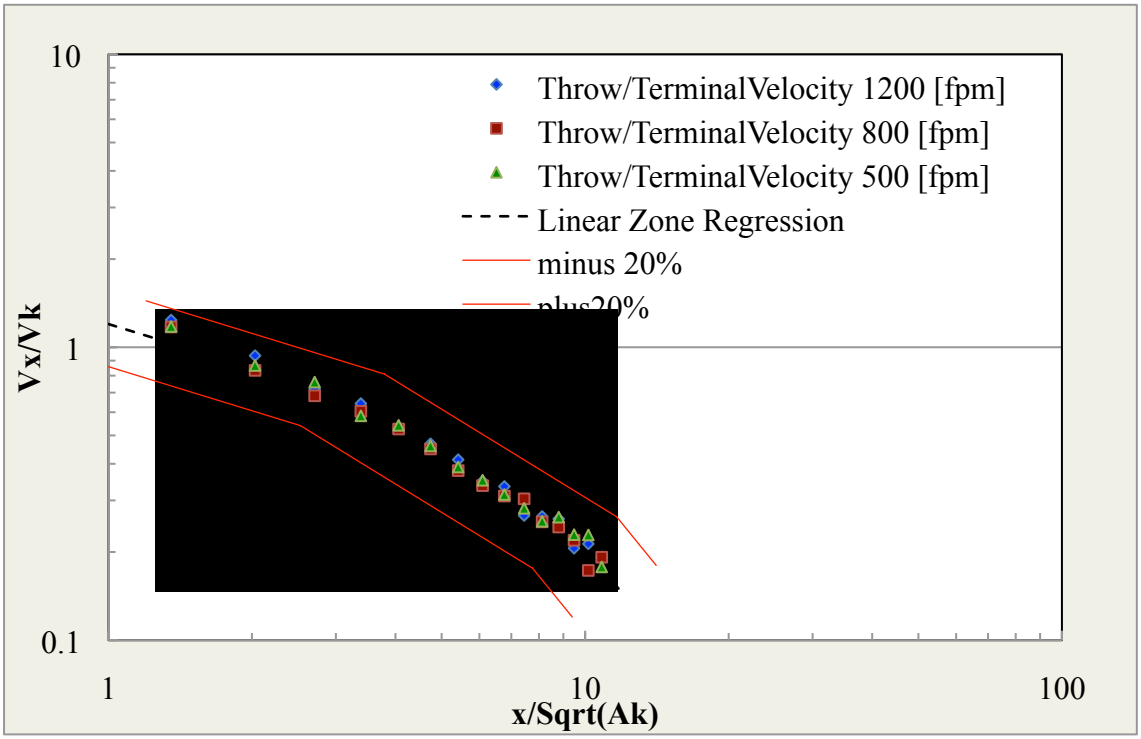


Figure 61. Right side throw for Run #2.

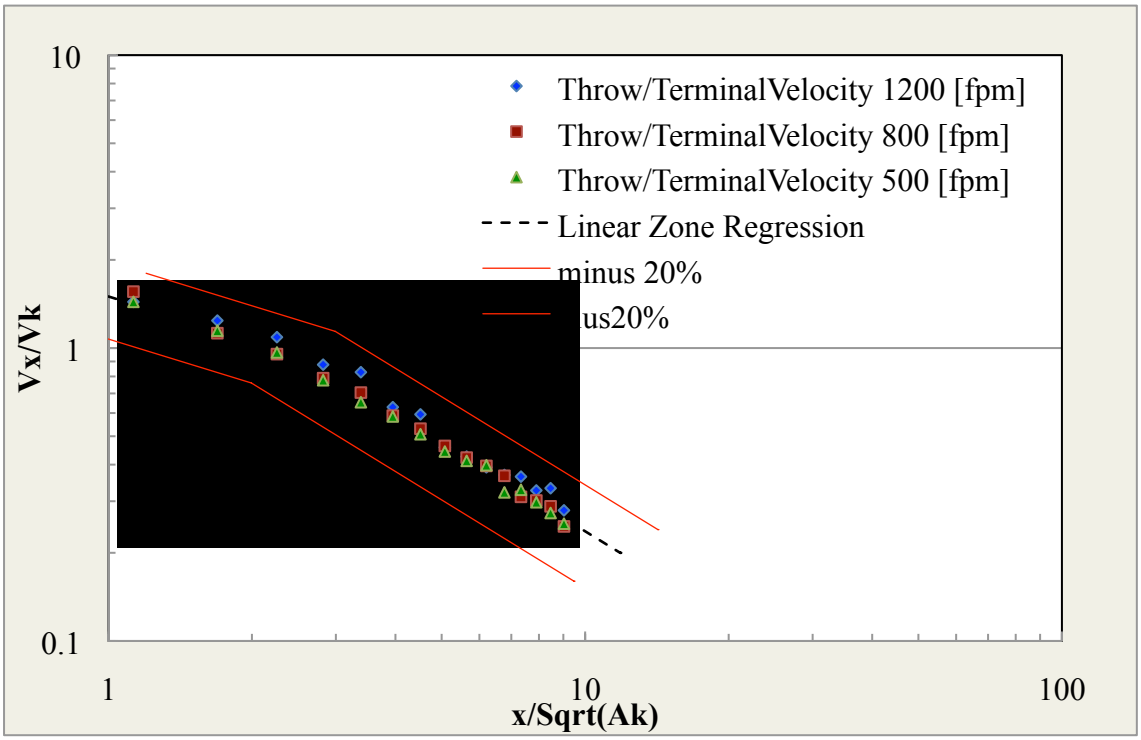


Figure 62. Forward throw for Run #3.

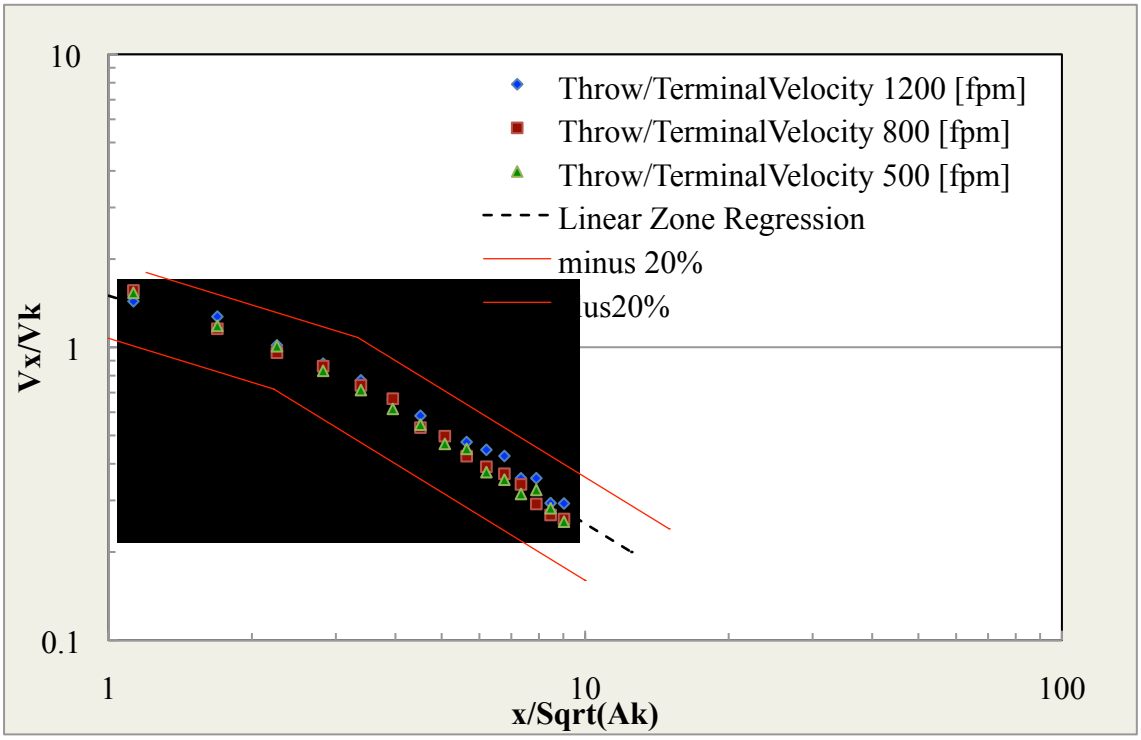


Figure 63. Backward throw for Run #3.

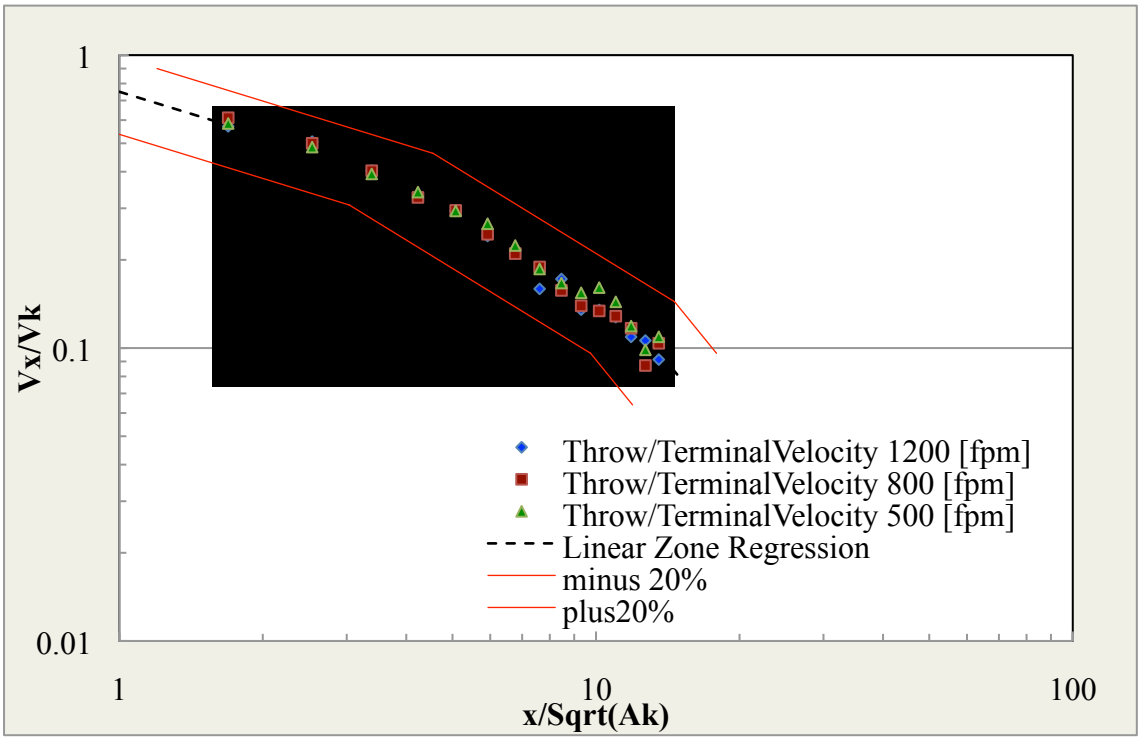


Figure 64. Forward throw for Run #4.

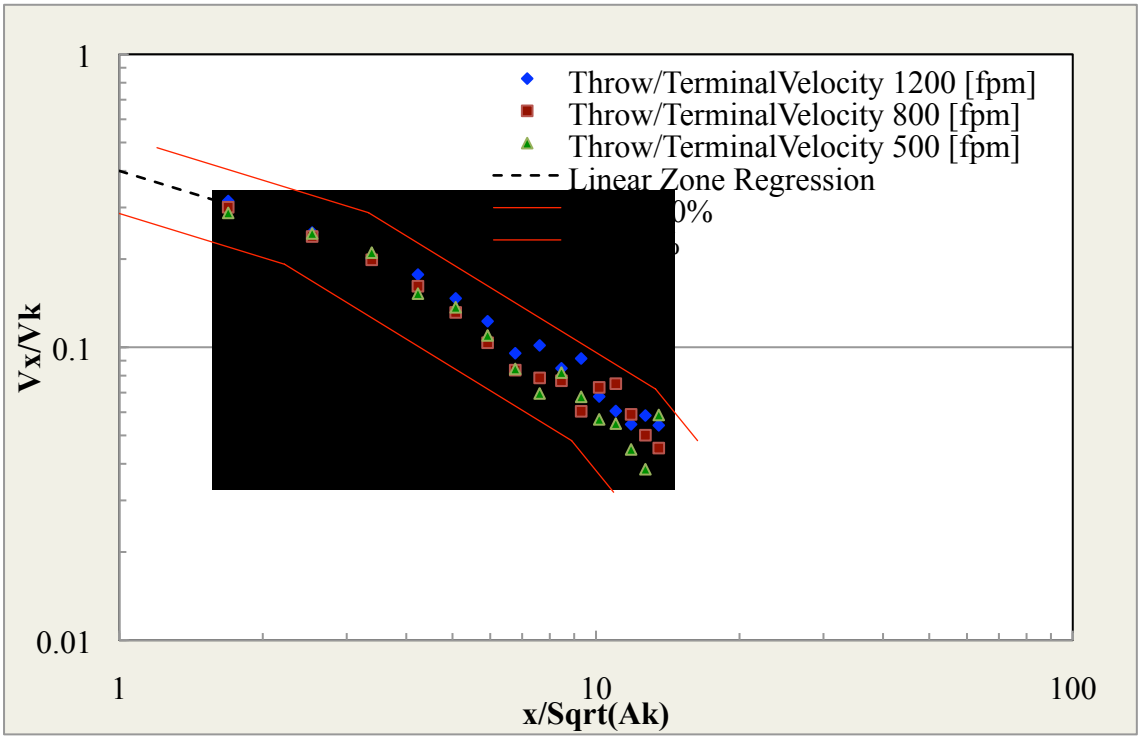


Figure 65. Backward throw for Run #4.

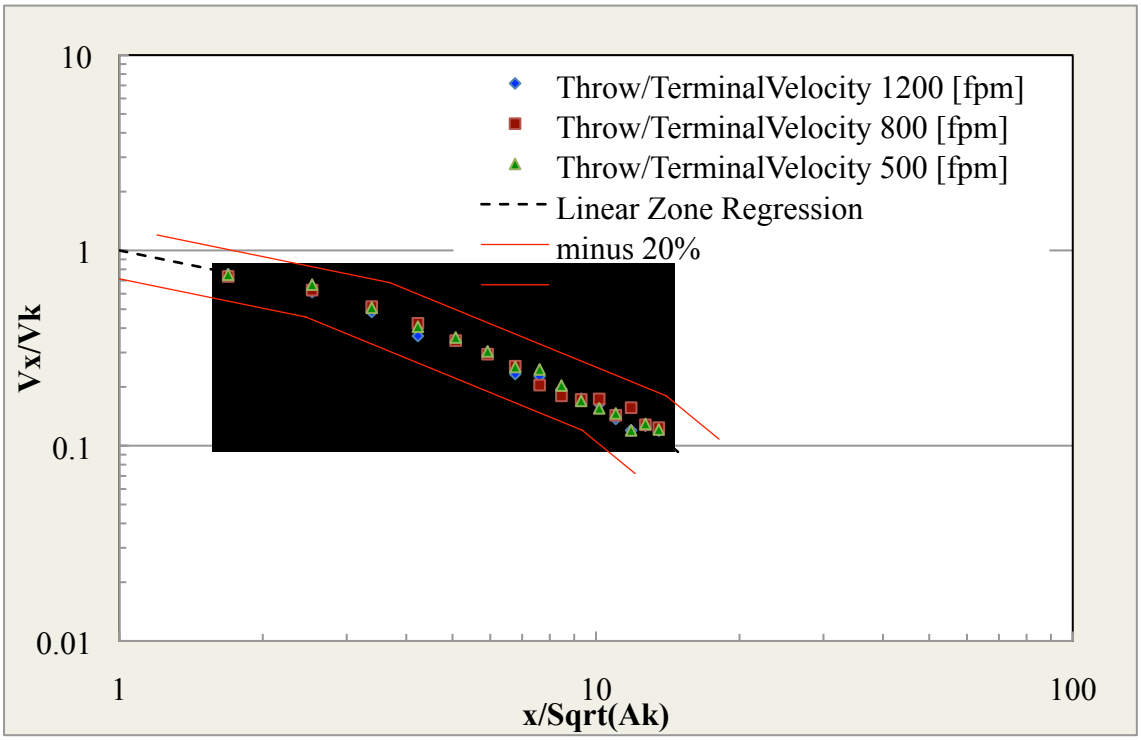


Figure 66. Right side throw for Run #4.

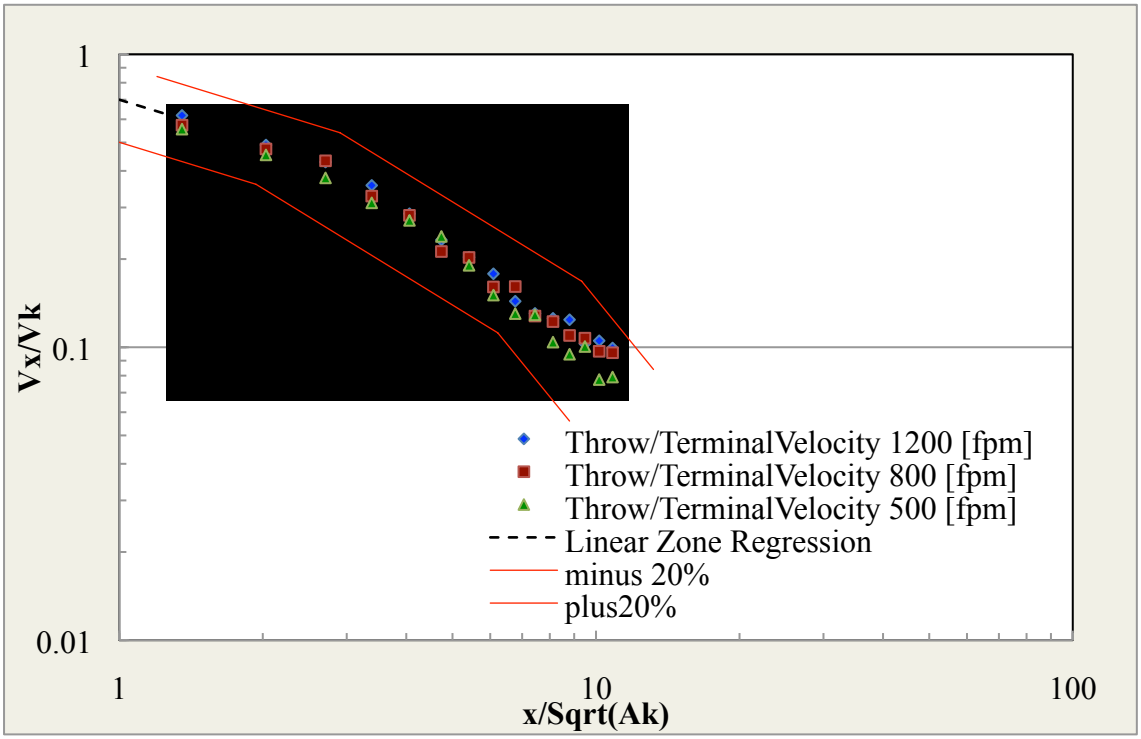


Figure 67. Forward throw for Run #5.

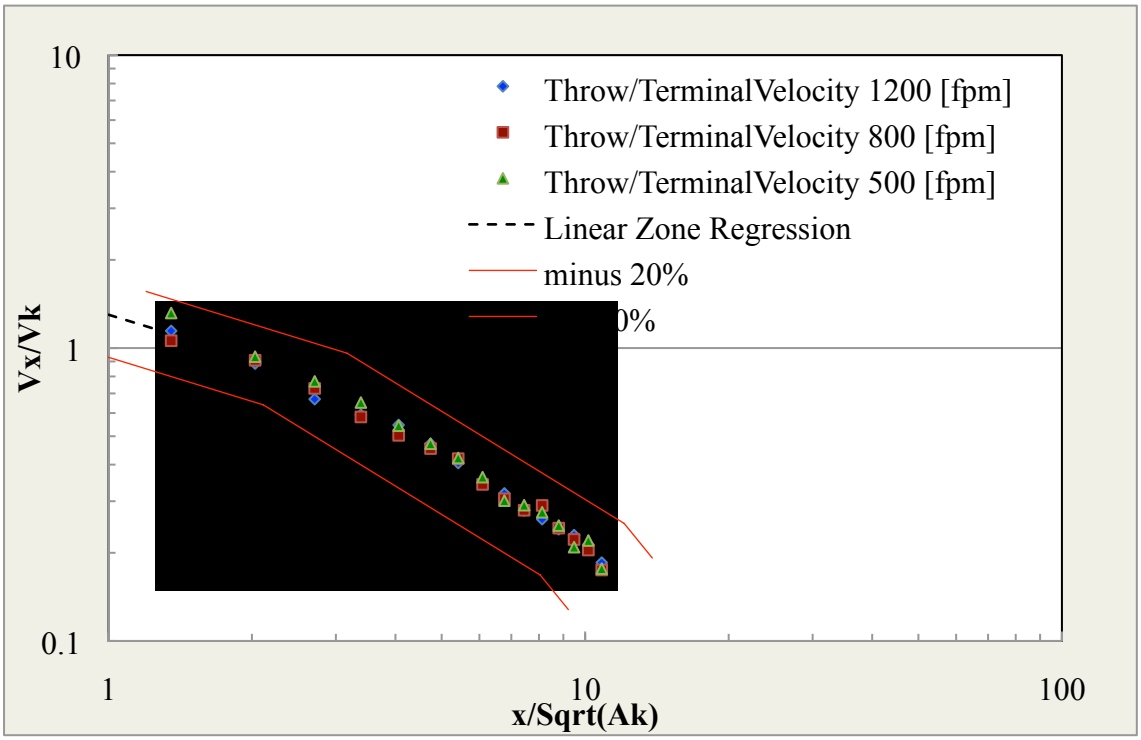


Figure 68. Backward throw for Run #5.

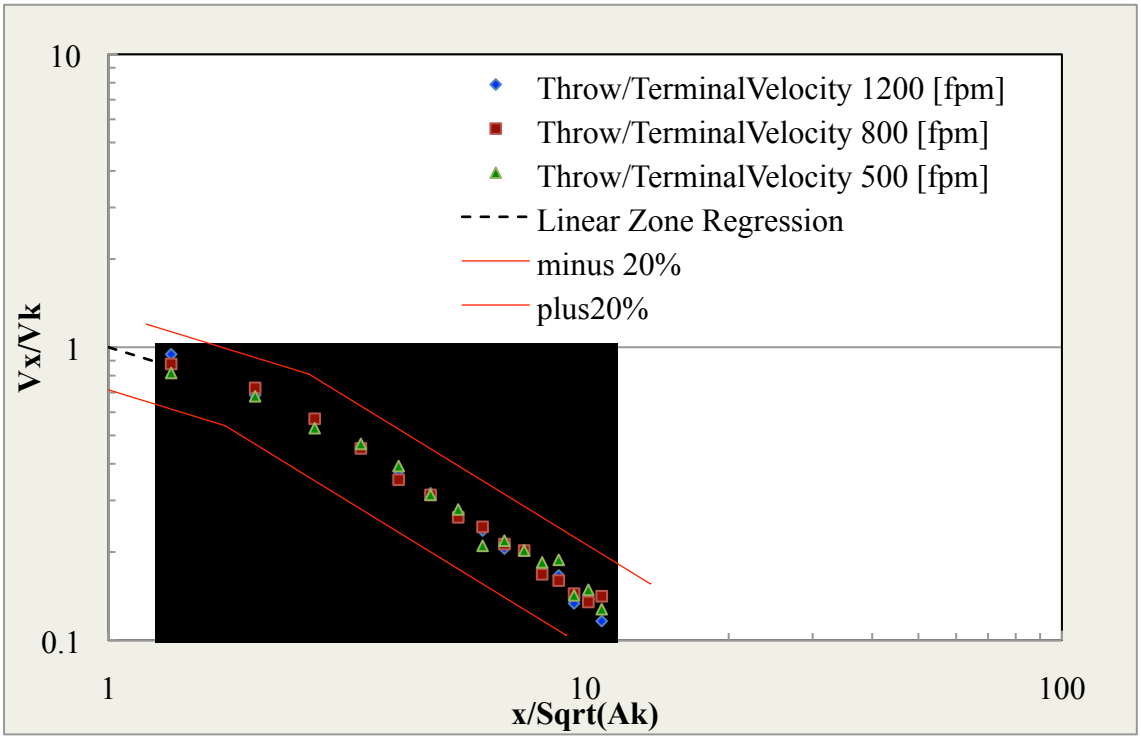


Figure 69. Left side throw for Run #5.

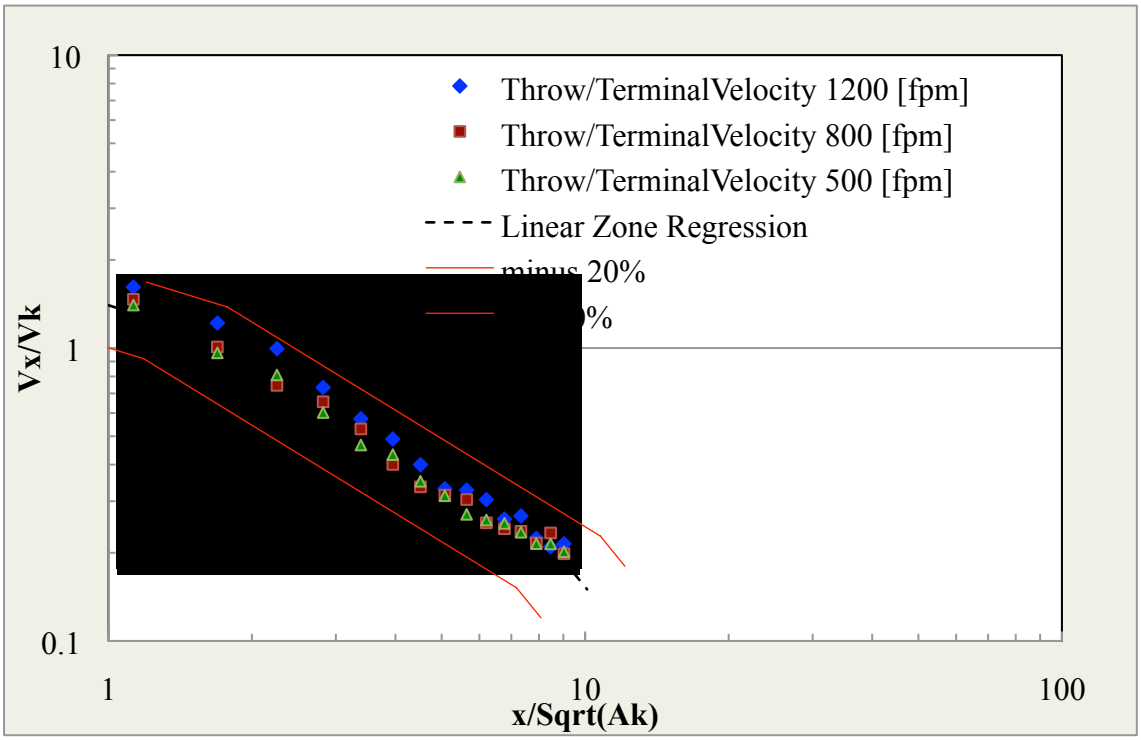


Figure 70. Forward throw for Run #6.

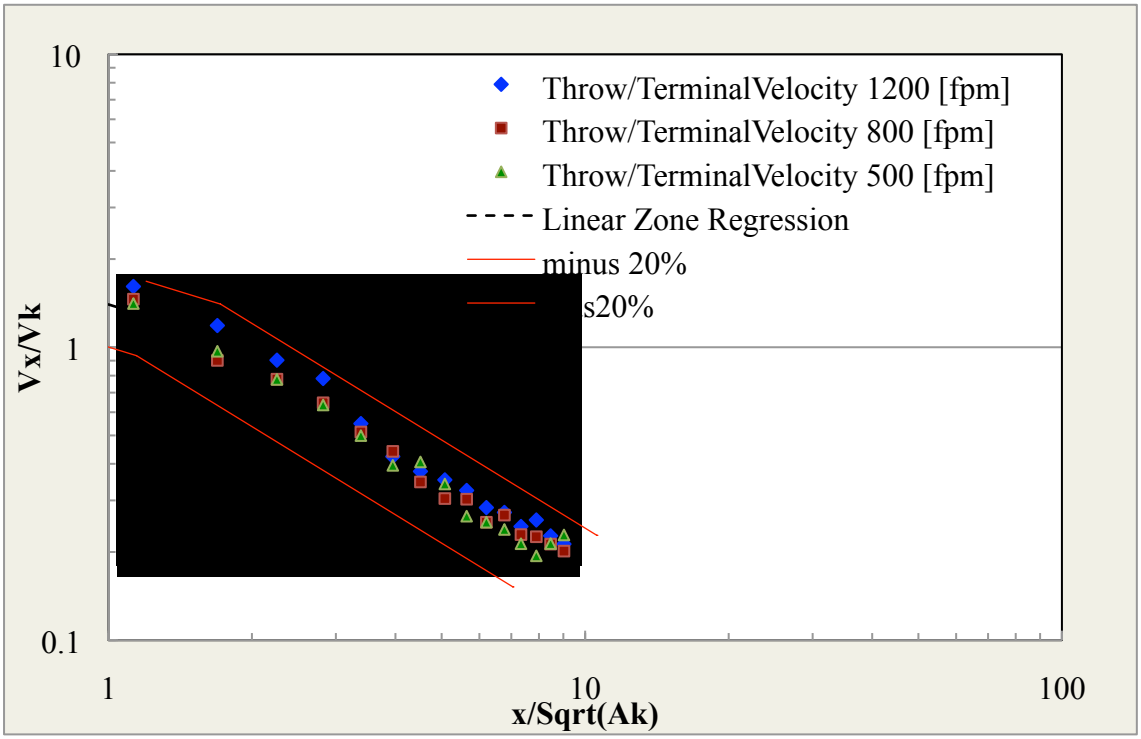


Figure 71. Backward throw for Run #6.

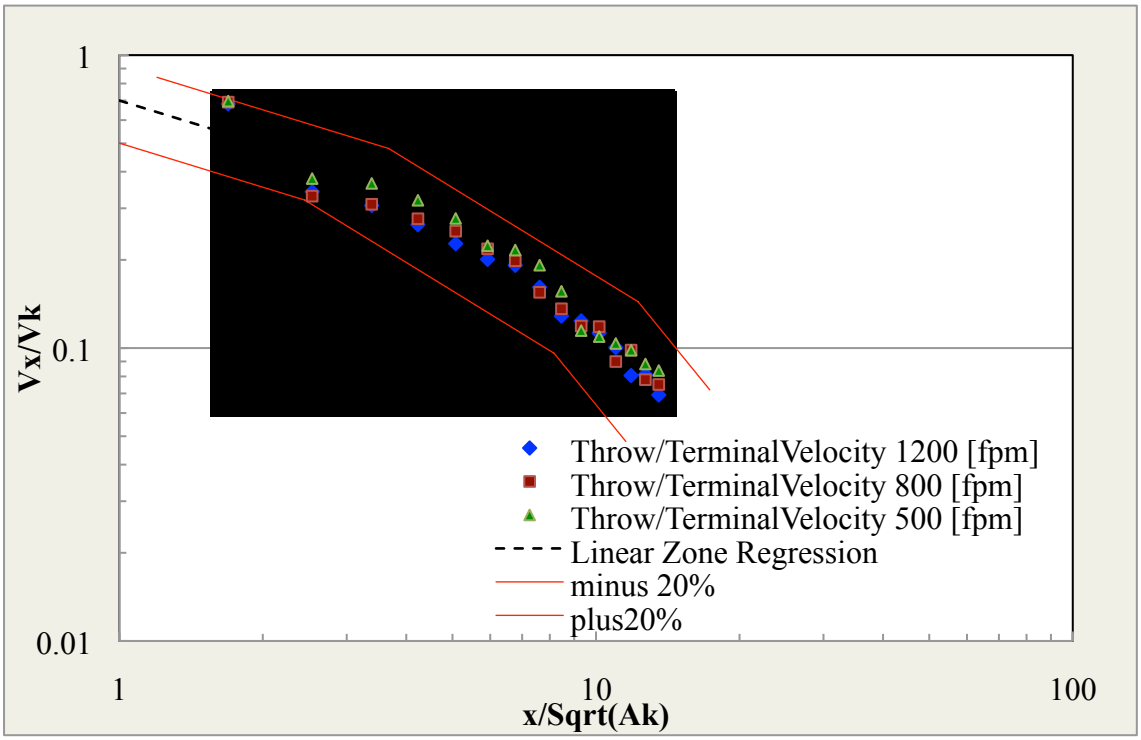


Figure 72. Forward throw for Run #7.

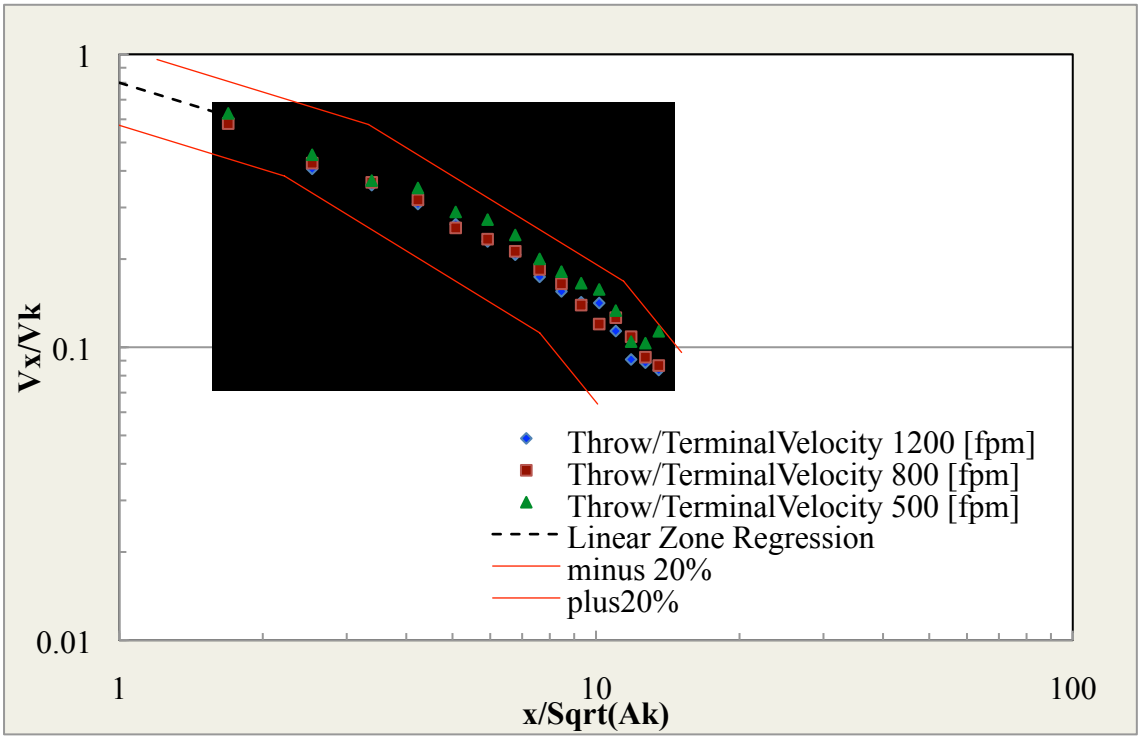


Figure 73. Backward throw for Run #7.

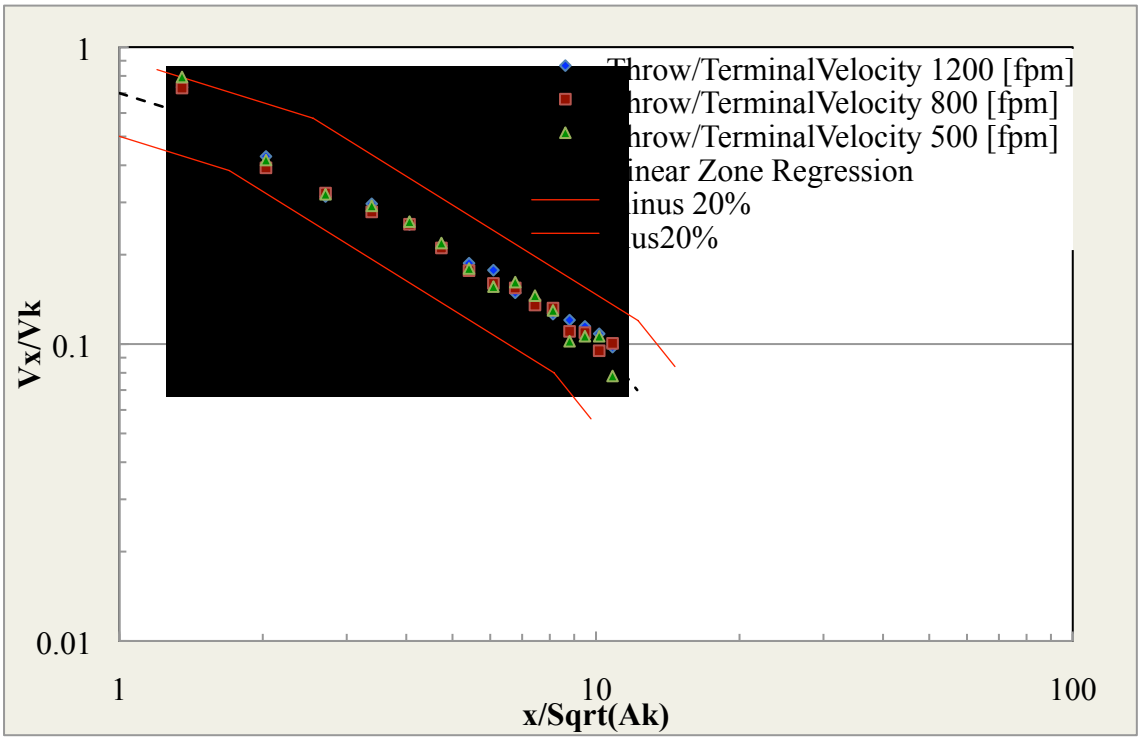


Figure 74. Forward throw for Run #8.

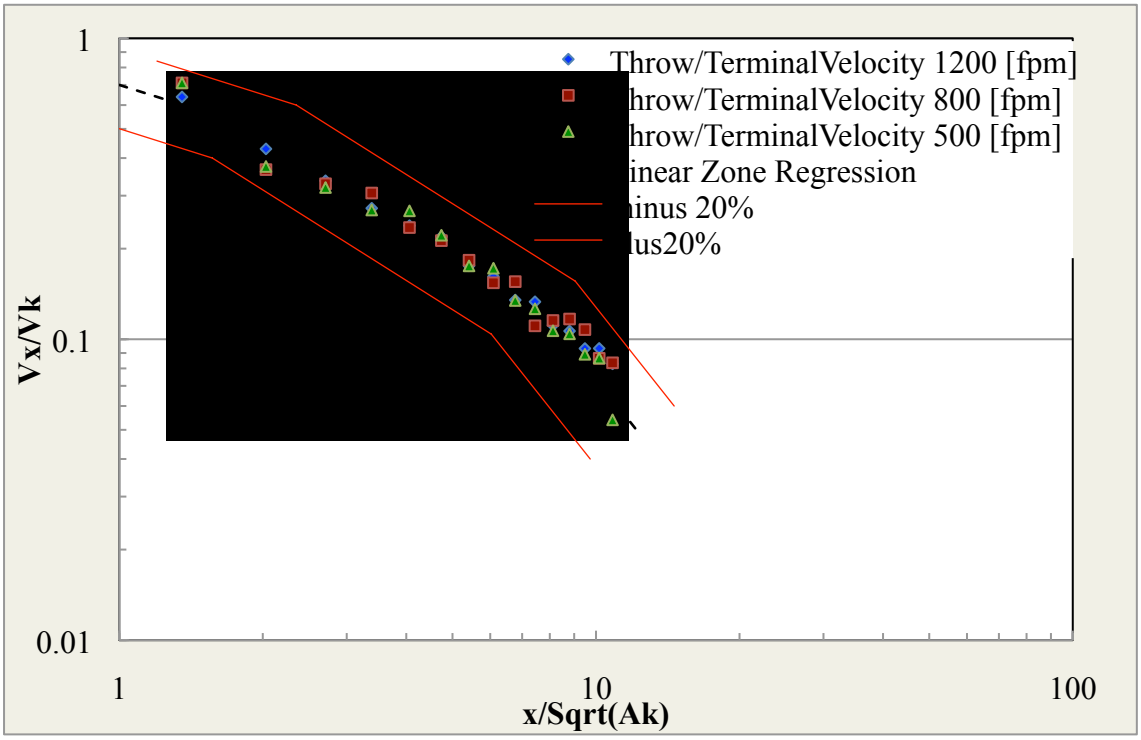


Figure 75. Backward throw for Run #8.

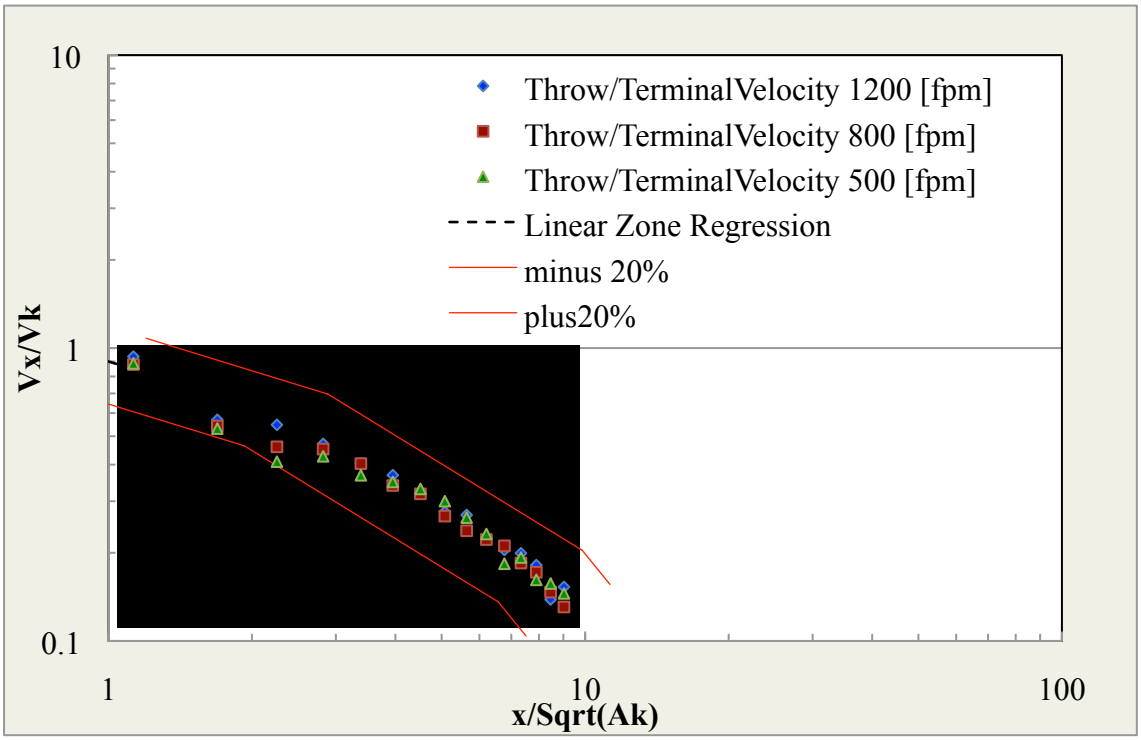


Figure 76. Forward throw for Run #9.

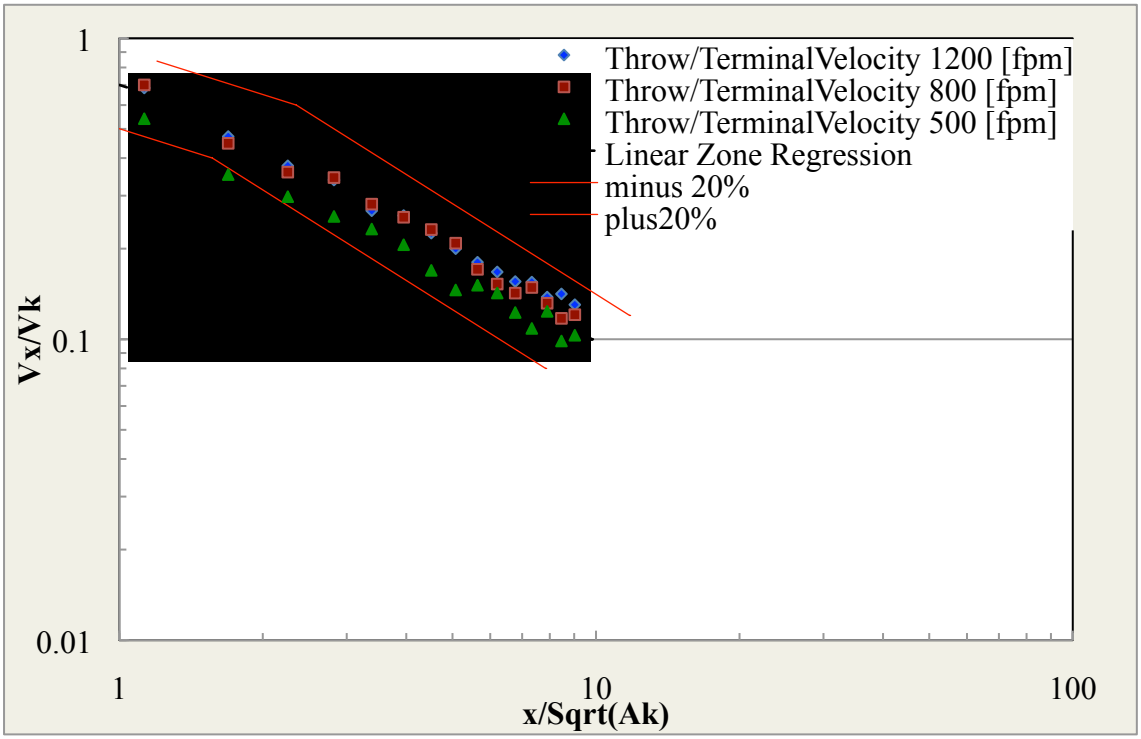


Figure 77. Backward throw for Run #9.

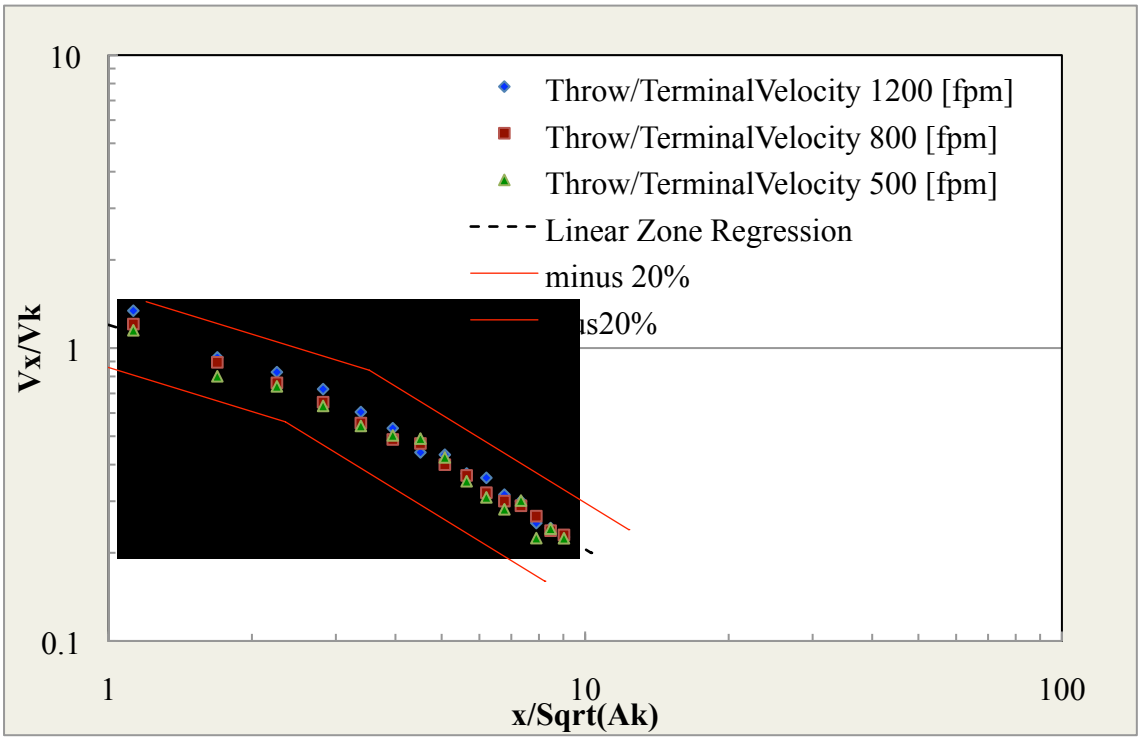


Figure 78. Right side throw for Run #9.

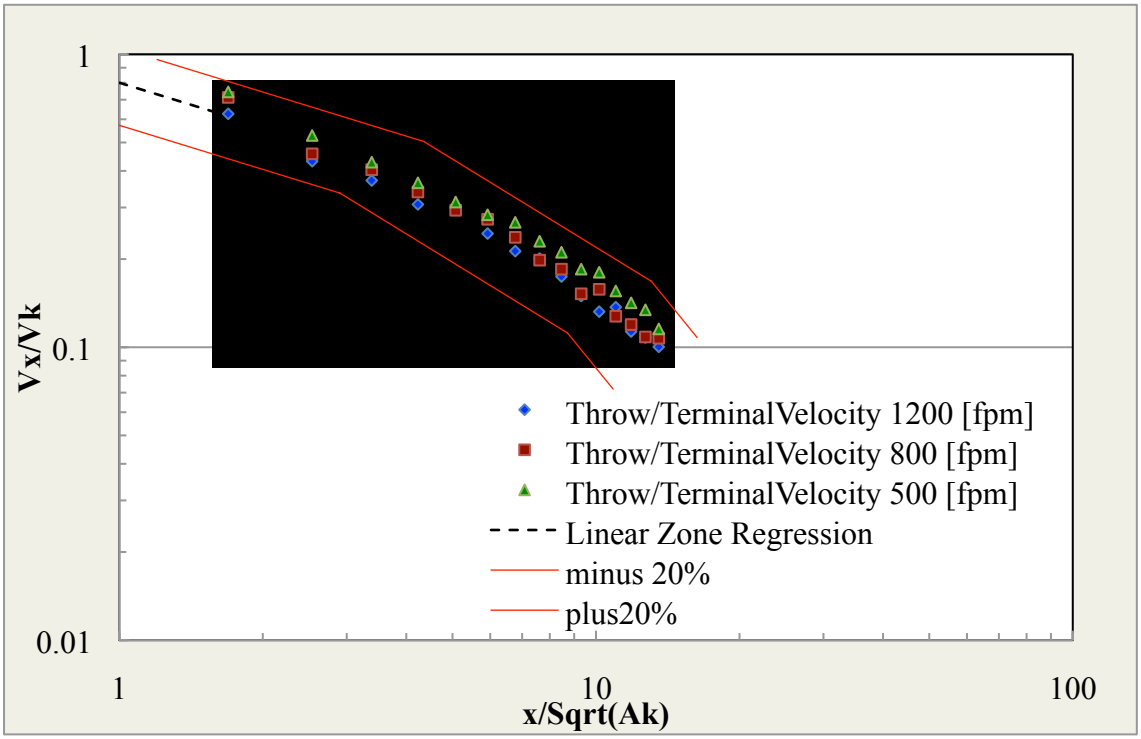


Figure 79. Forward throw for Run #10.

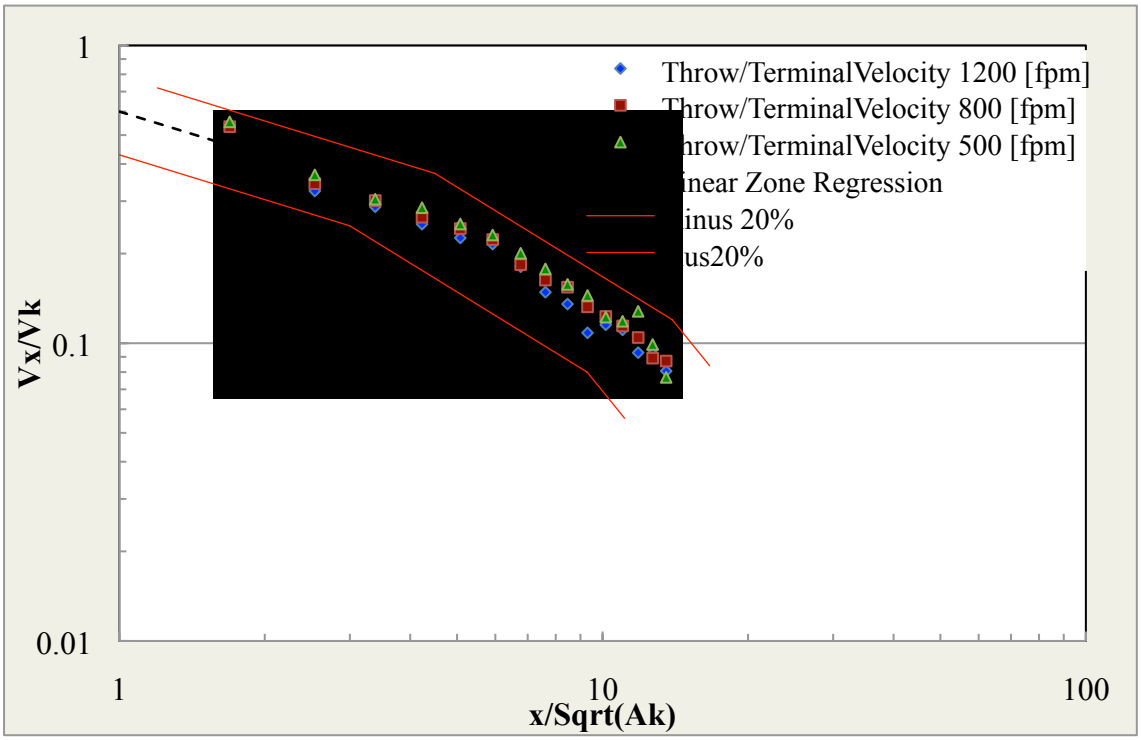


Figure 80. Backward throw for Run #10.

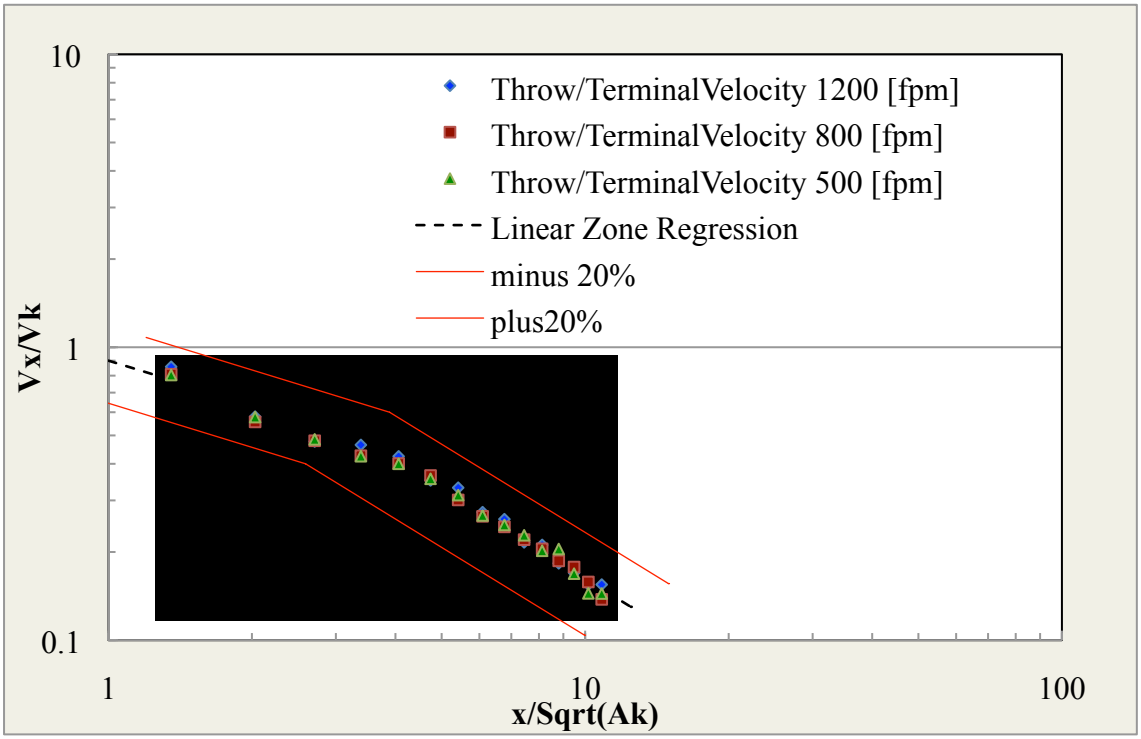


Figure 81. Forward throw for Run #11.

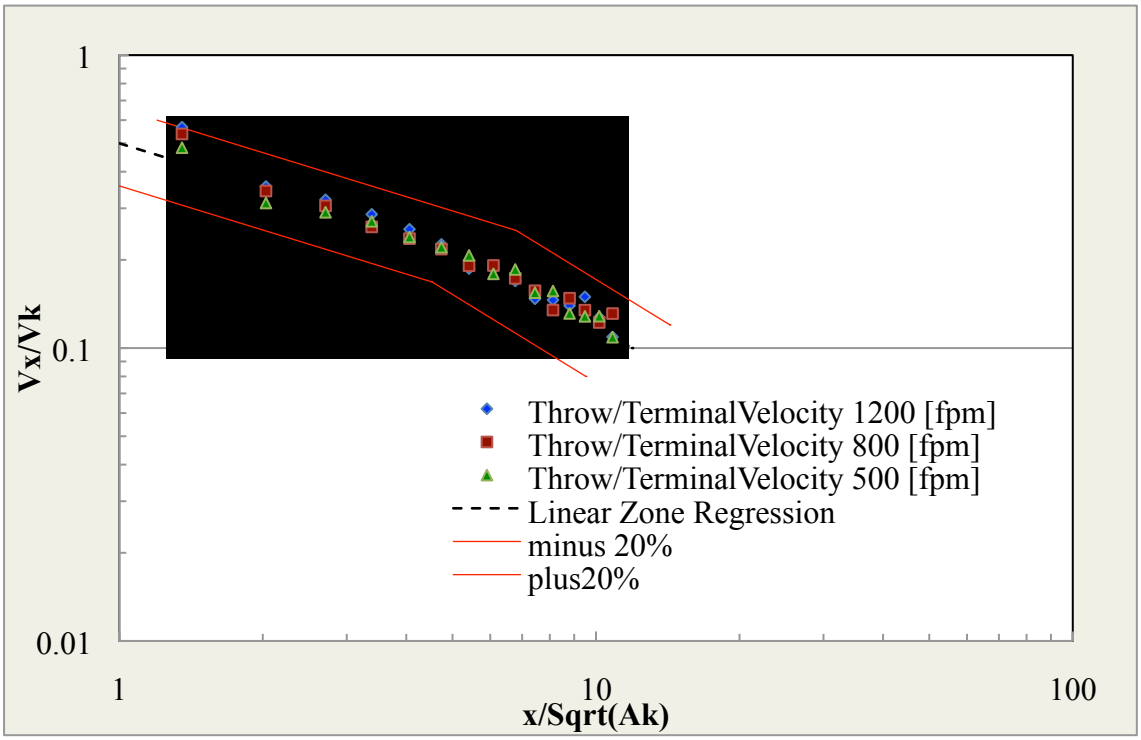


Figure 82. Backward throw for Run #11.

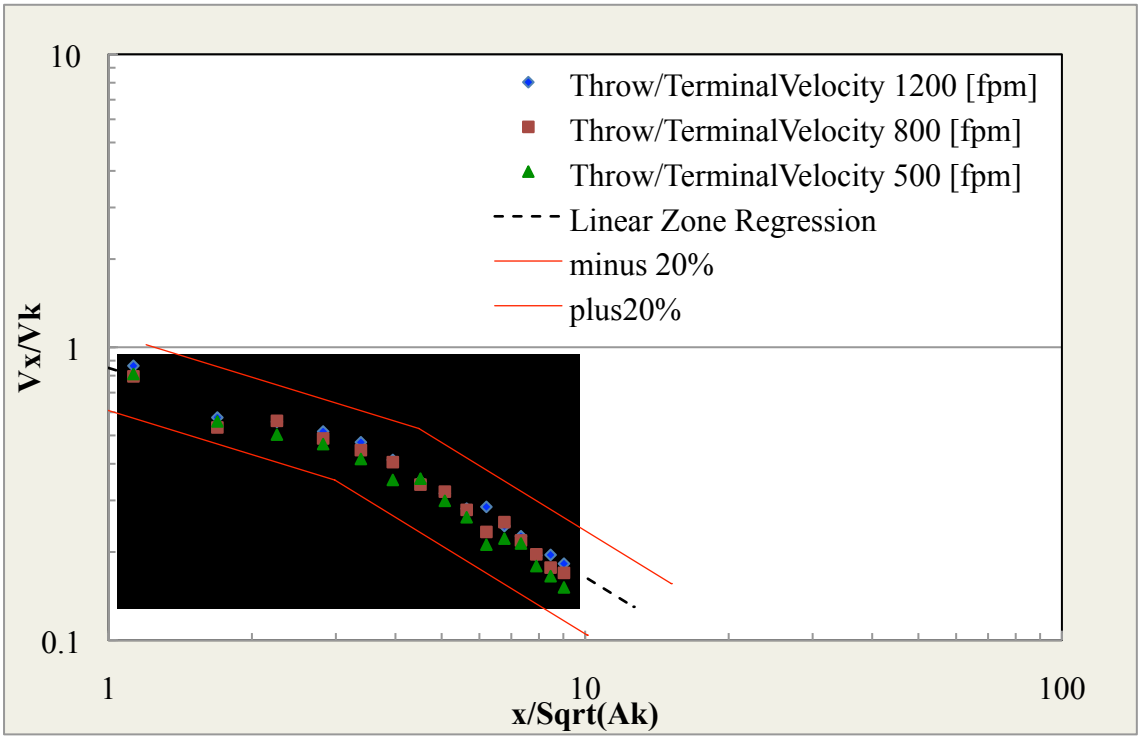


Figure 83. Forward throw for Run #12.

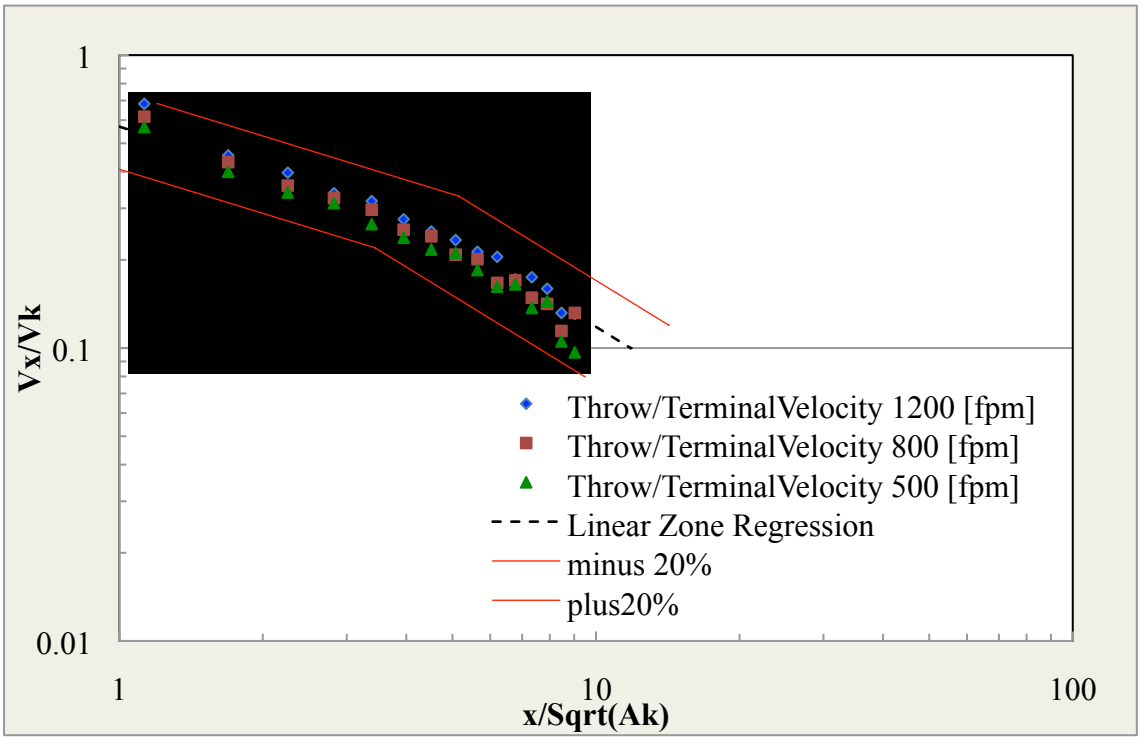


Figure 84. Backward throw for Run #12.

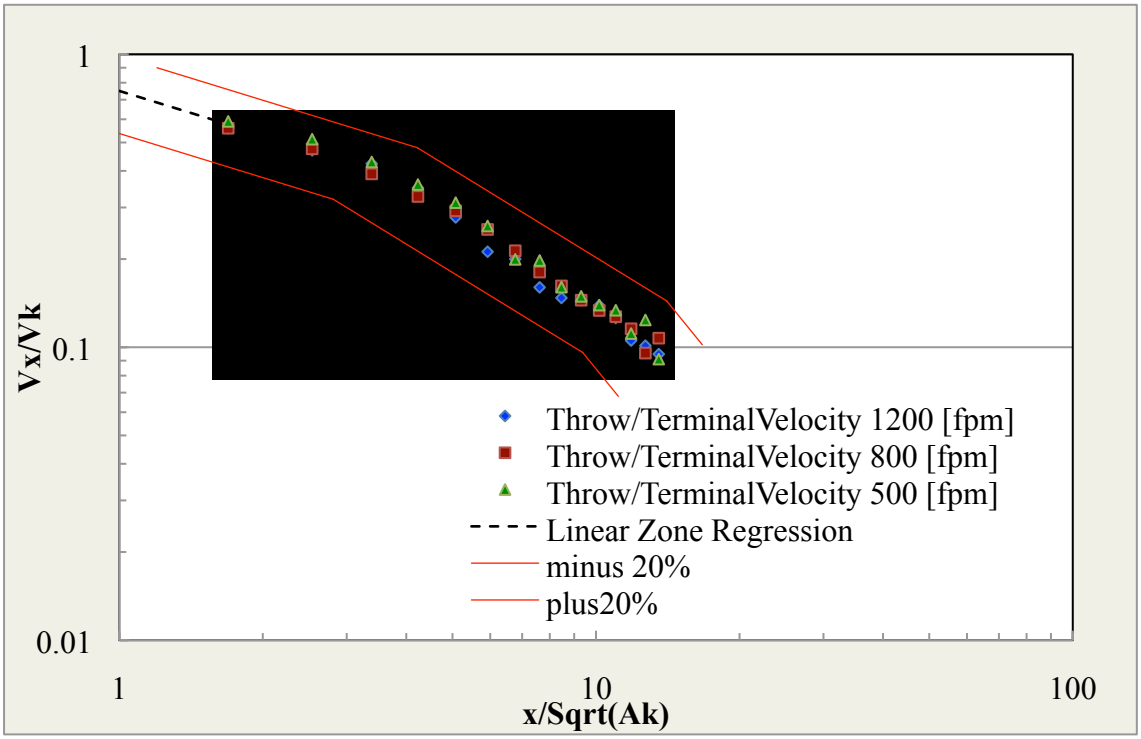


Figure 85. Forward throw for Run #13.

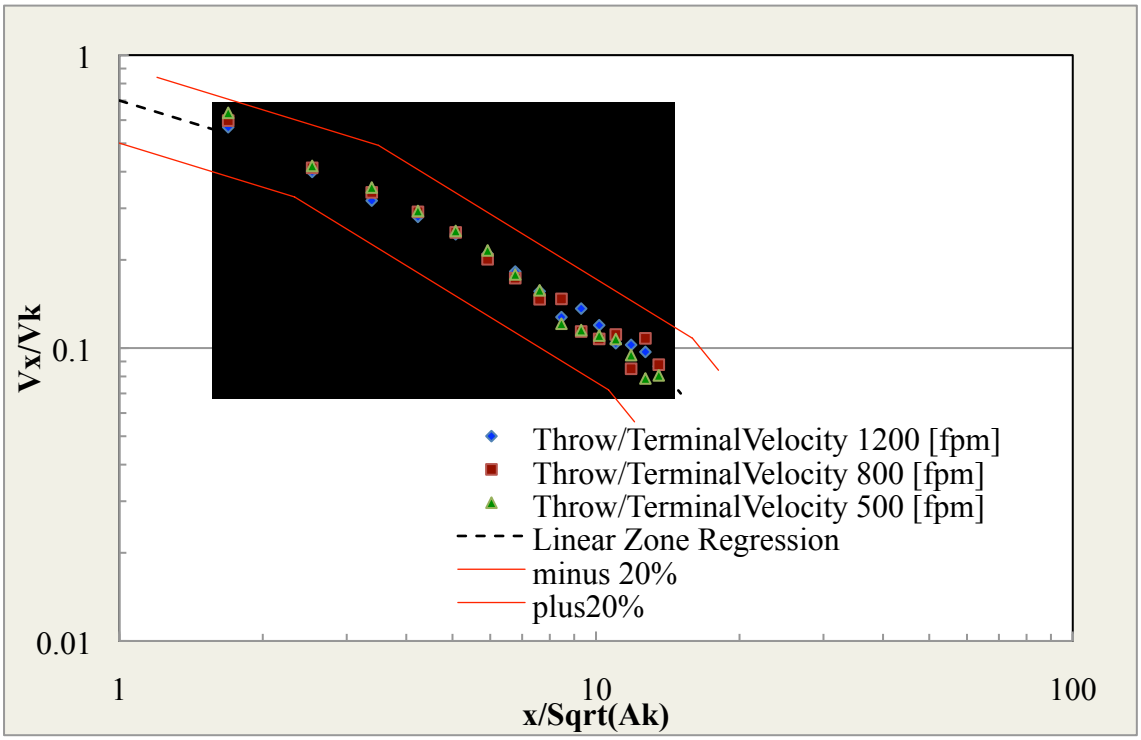


Figure 86. Backward throw for Run #13.

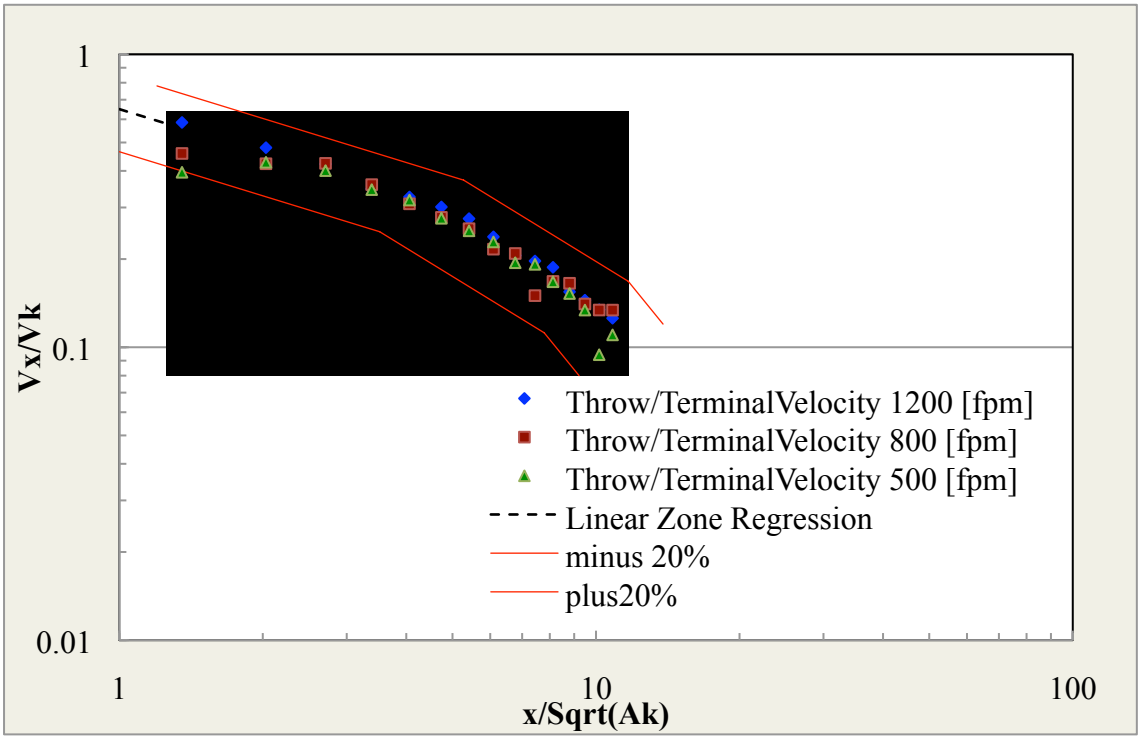


Figure 87. Forward throw for Run #14.

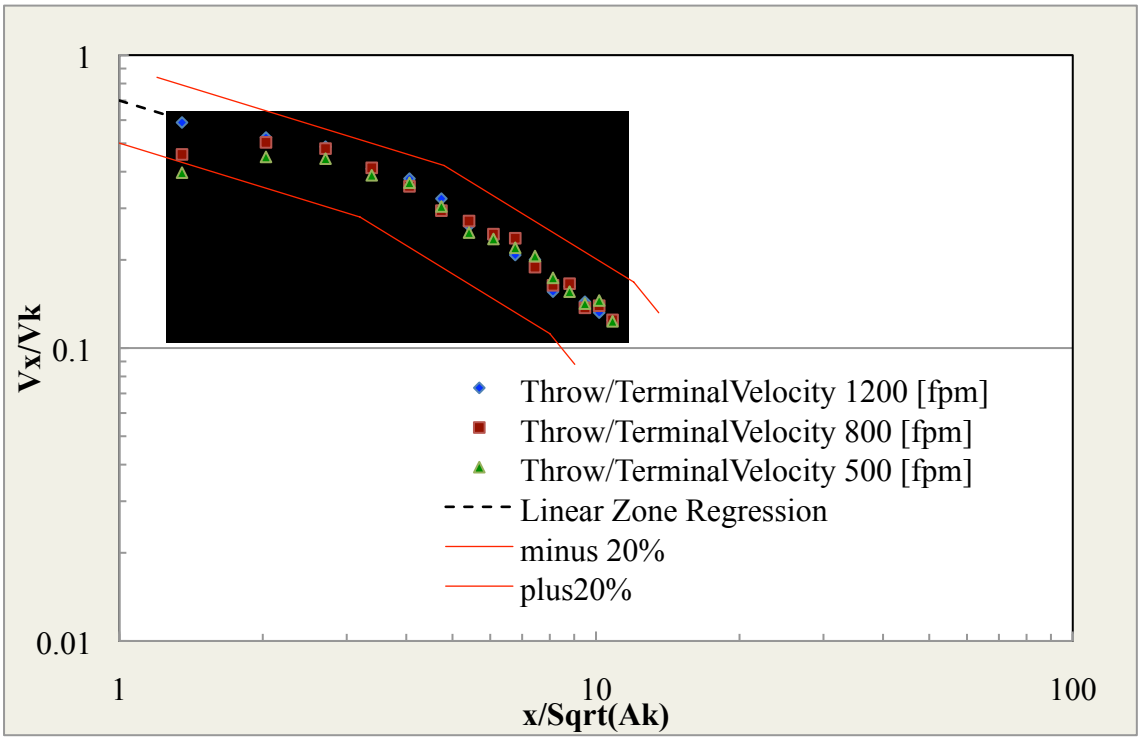


Figure 88. Backward throw for Run #14.

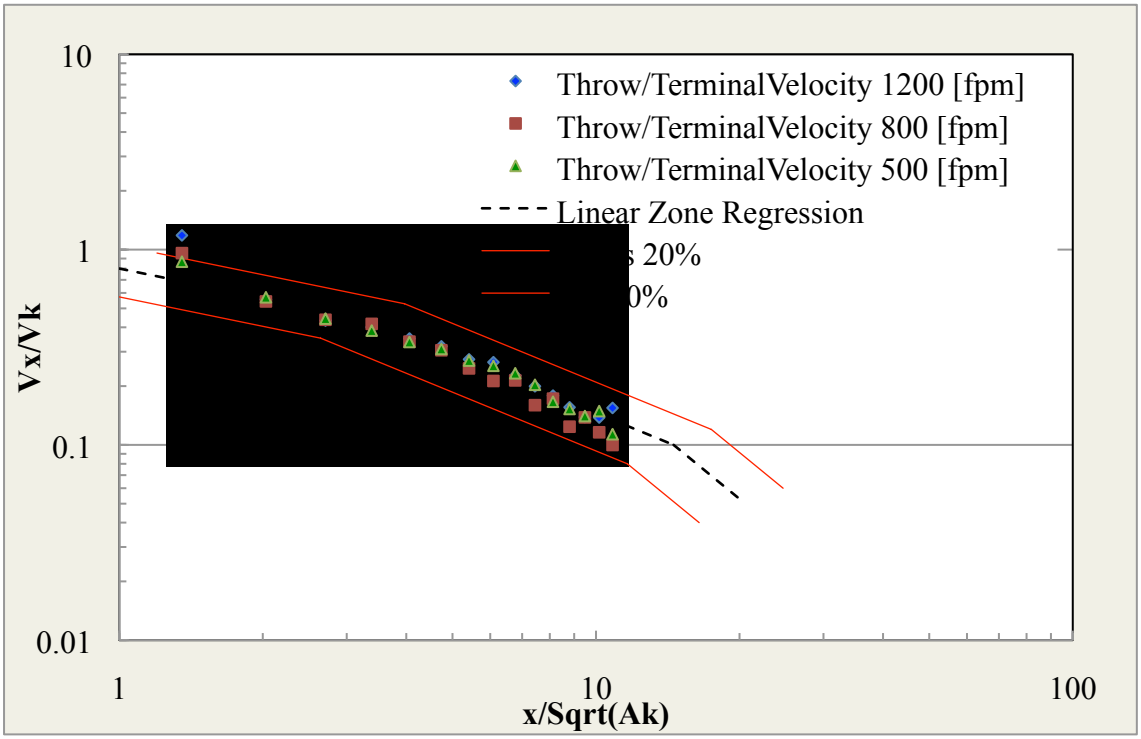


Figure 89. Right side throw for Run #14.

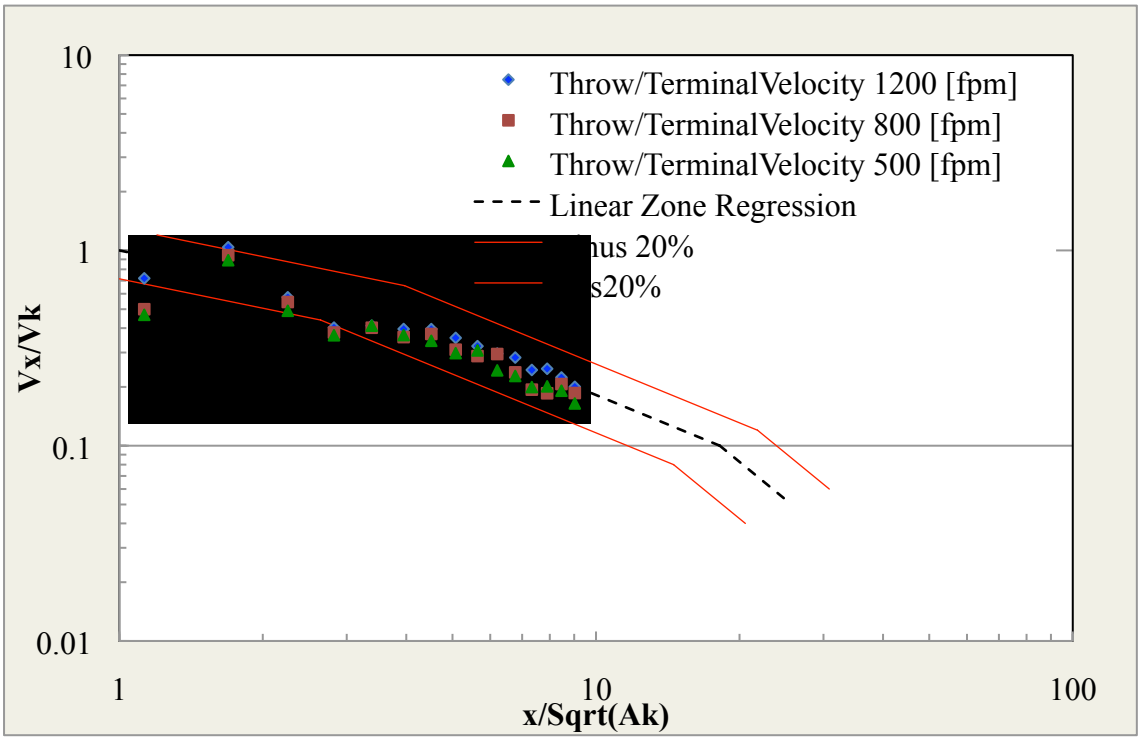


Figure 90. Forward throw for Run #15.

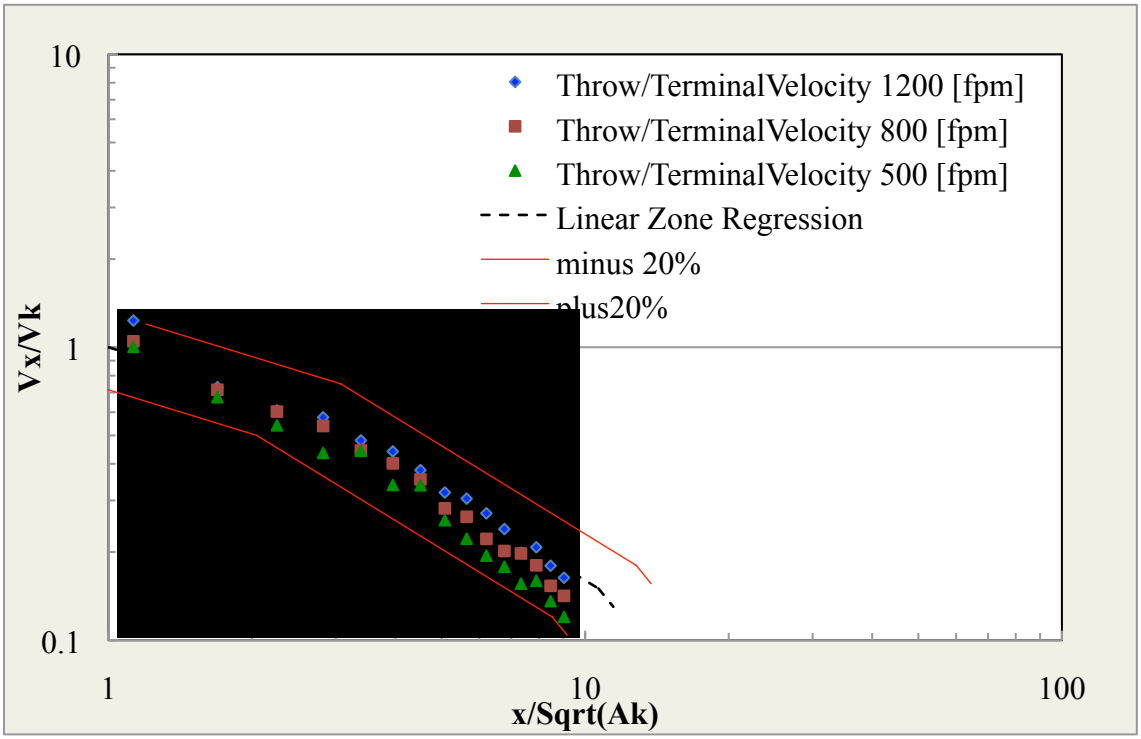


Figure 91. Backward throw for Run #15.

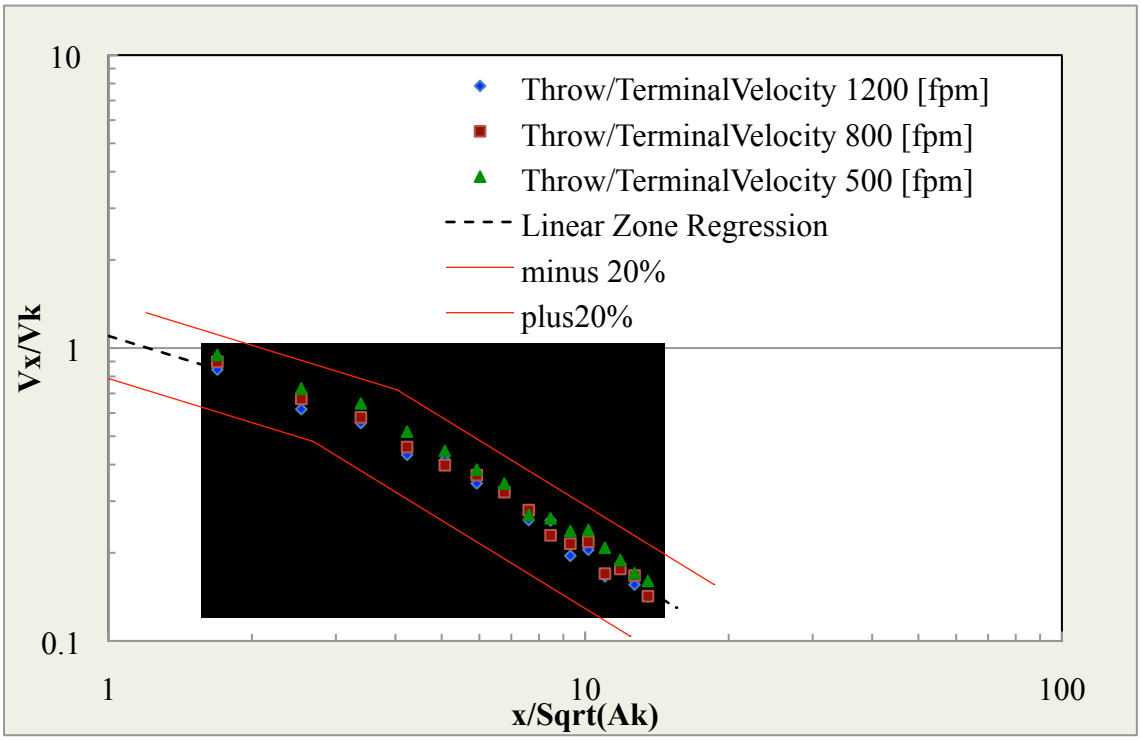


Figure 92. Forward throw for Run #16.

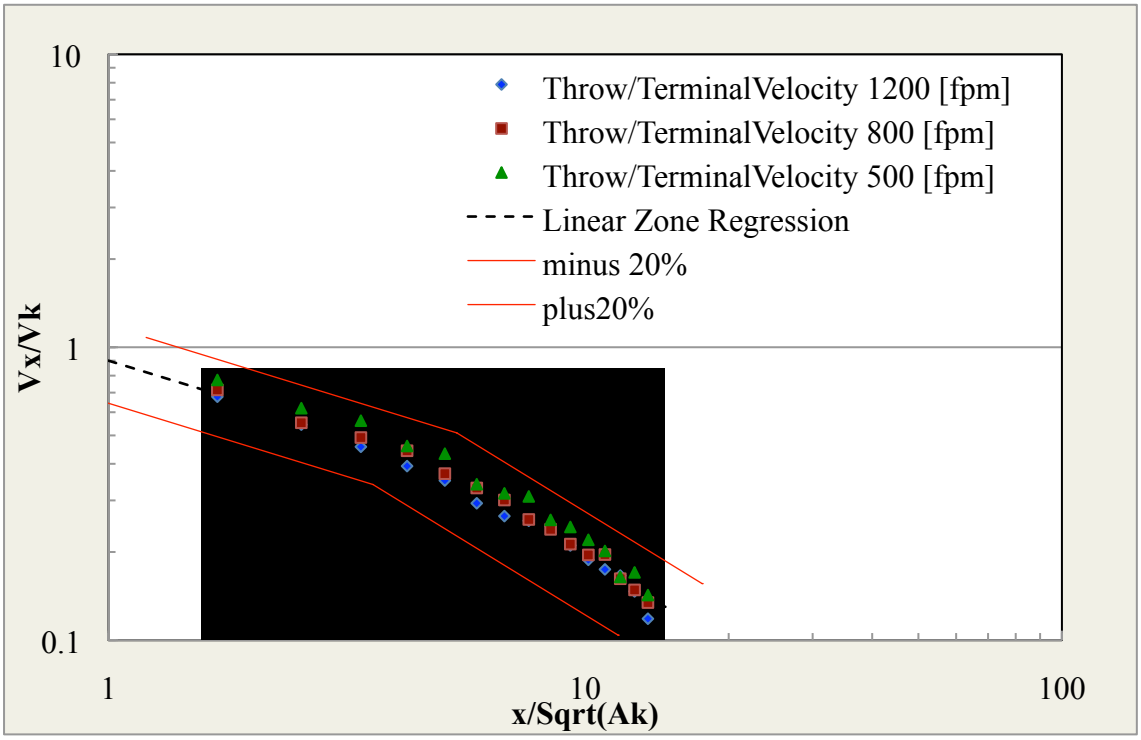


Figure 93. Backward throw for Run #16.

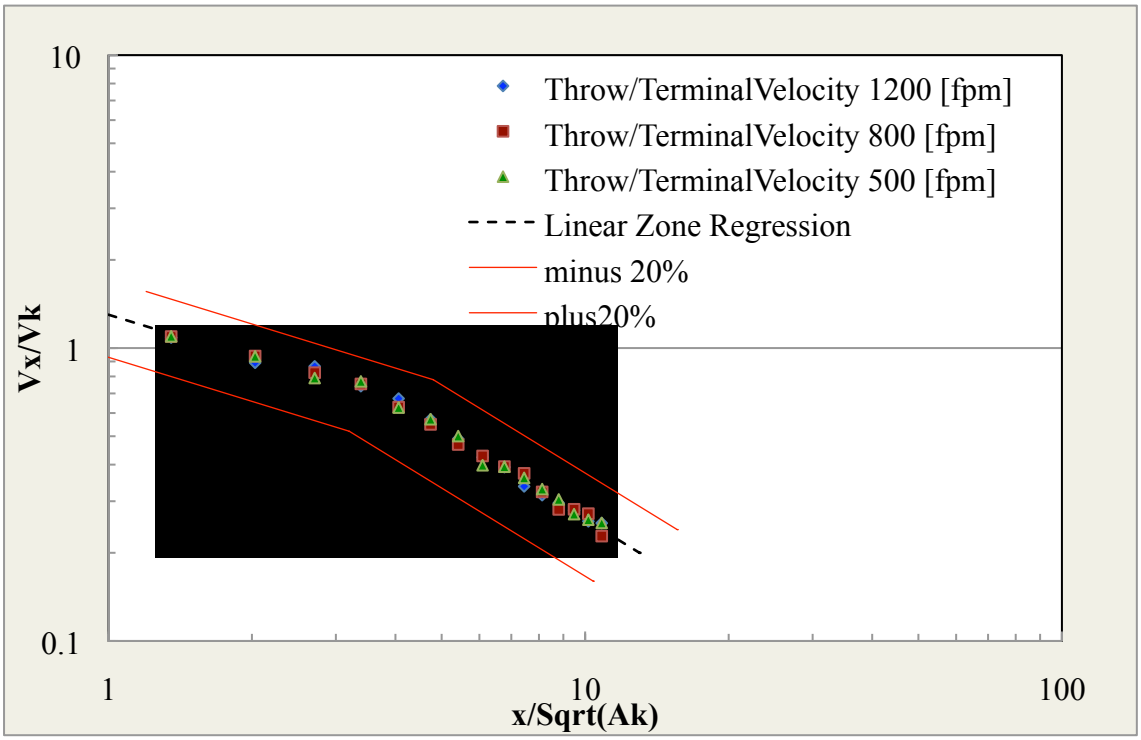


Figure 94. Forward throw for Run #17.

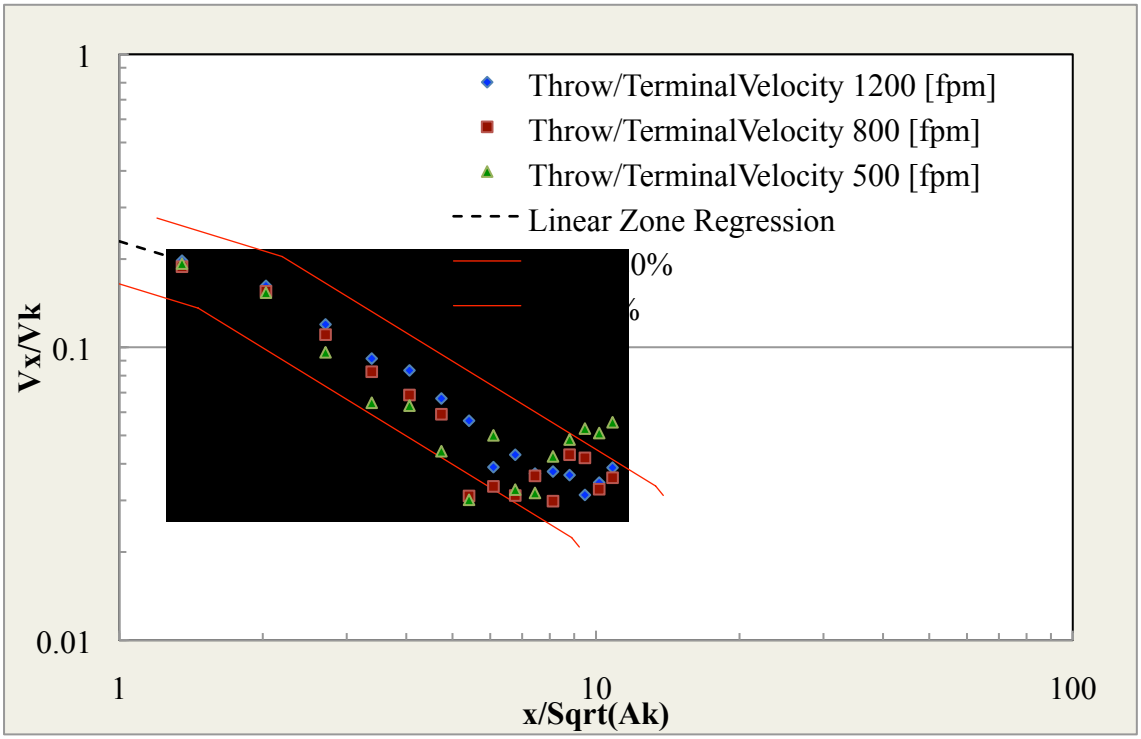


Figure 95. Backward throw for Run #17.

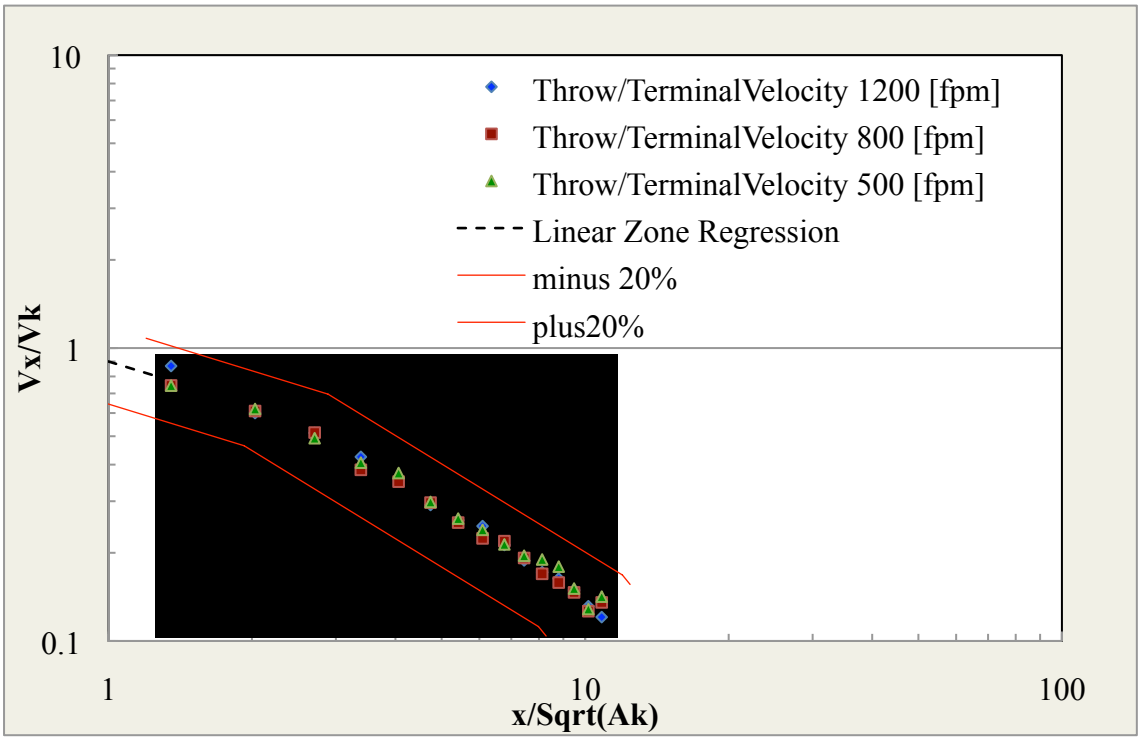


Figure 96. Right side throw of Run #17.

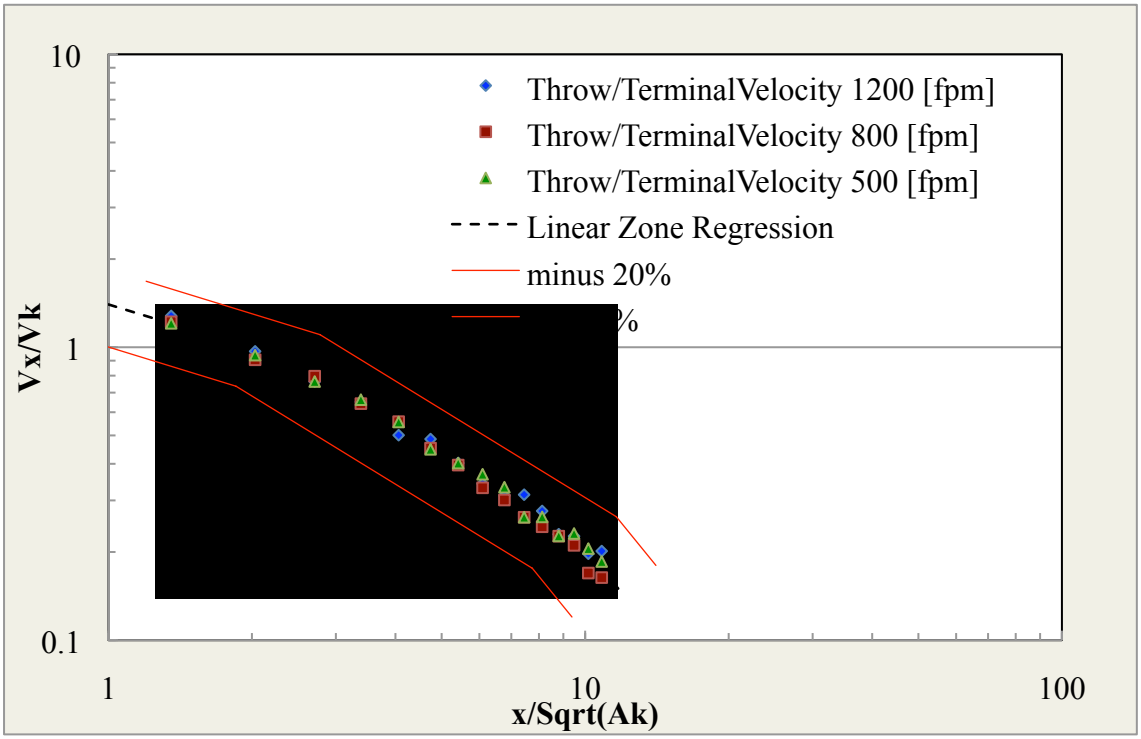


Figure 97. Left side flow for Run #17.

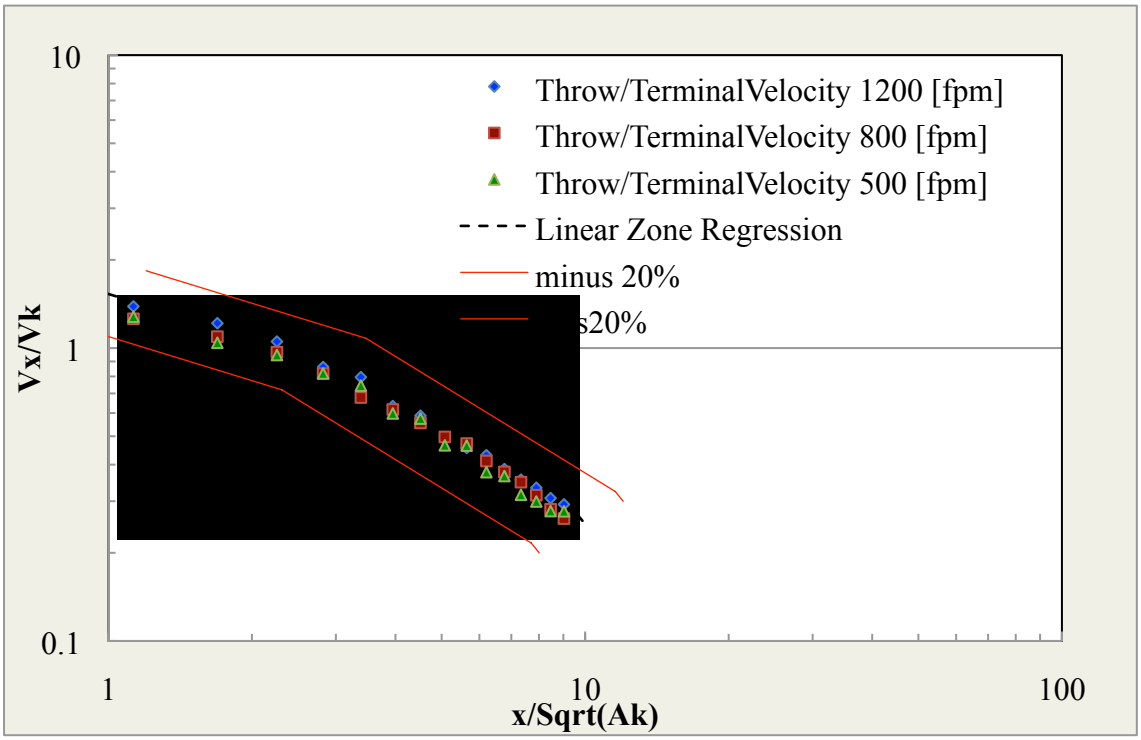


Figure 98. Forward throw for Run #18.

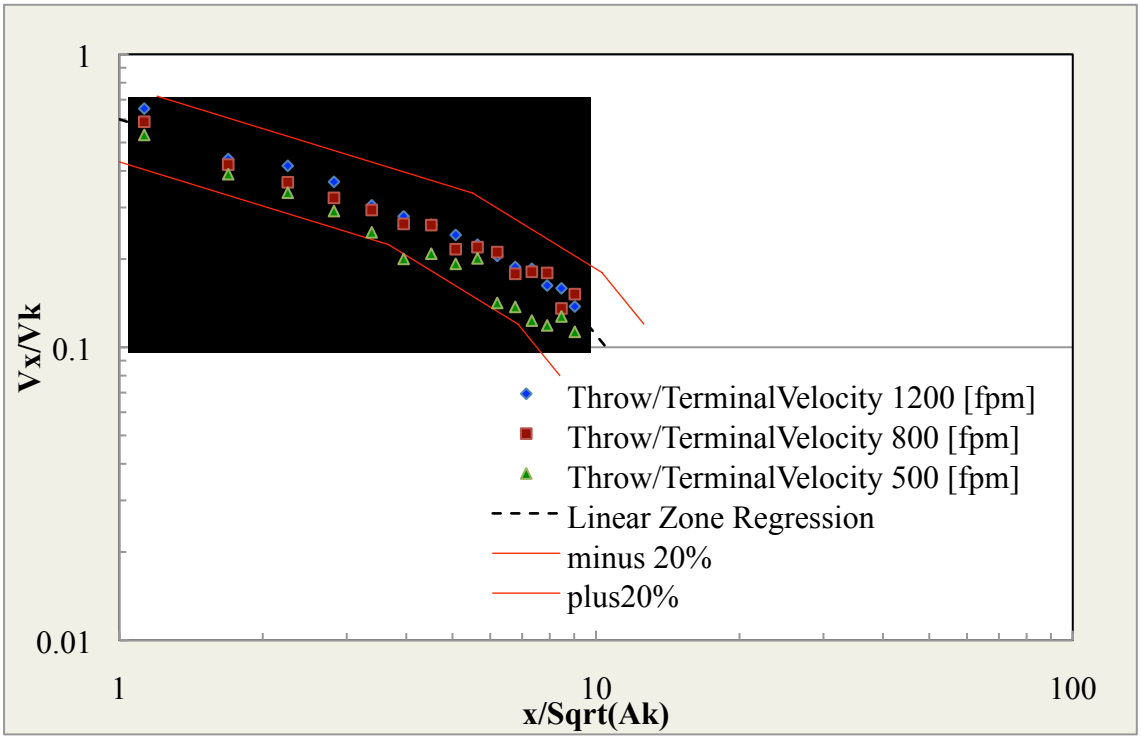


Figure 99. Backward throw for Run #18.

# APPENDIX C

## CLOSE COUPLING TEST RESULTS DIFFUSER DISCHARGE AIRFLOW ZONE PLOTS

The following figures are the zone plots for each of the nine configurations in the L9 mixed array used in the Taguchi analysis of the close coupling setup. The majority of the data was found to be in zone three and four as the jet of airflow from the diffuser face was directed in a more vertical pattern without a ceiling present, but occasionally a zone two profile existed a short distance from the diffuser face where throw velocity was highest, even without a ceiling installed. The process used to create these plots was given in ASHRAE Standard 70-2006. For each close coupling installation configuration the velocity profiles for each terminal velocity air speed from the array of draft meters was used to determine throw distance, x, and the corresponding velocity, $V_x$. Then calculating the inlet neck area, $A_k$, and the neck velocity, $V_k$, the dimensionless comparison was made below in each figure. These data points were compared to the similarly plotted zone data points for the Standard 70 baseline data. This comparison led to the throw ratio values between the close coupling and the Standard 70 configurations used in the close coupling installation statistical analysis. Refer to Table 47 for the run numbers and their corresponding inlet conditions.

Table 47. Inlet conditions for close coupling runs.

| Run # | Diffuser Type | Inlet | Duct Height | Damper |
|---|---|---|---|---|
| 1 | Square | 8 | 0 | None |
| 2 | Square | 10 | 1.5 | X |
| 3 | Square | 12 | 3 | Cross |
| 4 | Plaque | 8 | 1.5 | Cross |
| 5 | Plaque | 10 | 3 | None |
| 6 | Plaque | 12 | 0 | X |
| 7 | Perf Rnd | 8 | 3 | X |
| 8 | Perf Rnd | 10 | 0 | Cross |
| 9 | Perf Rnd | 12 | 1.5 | None |

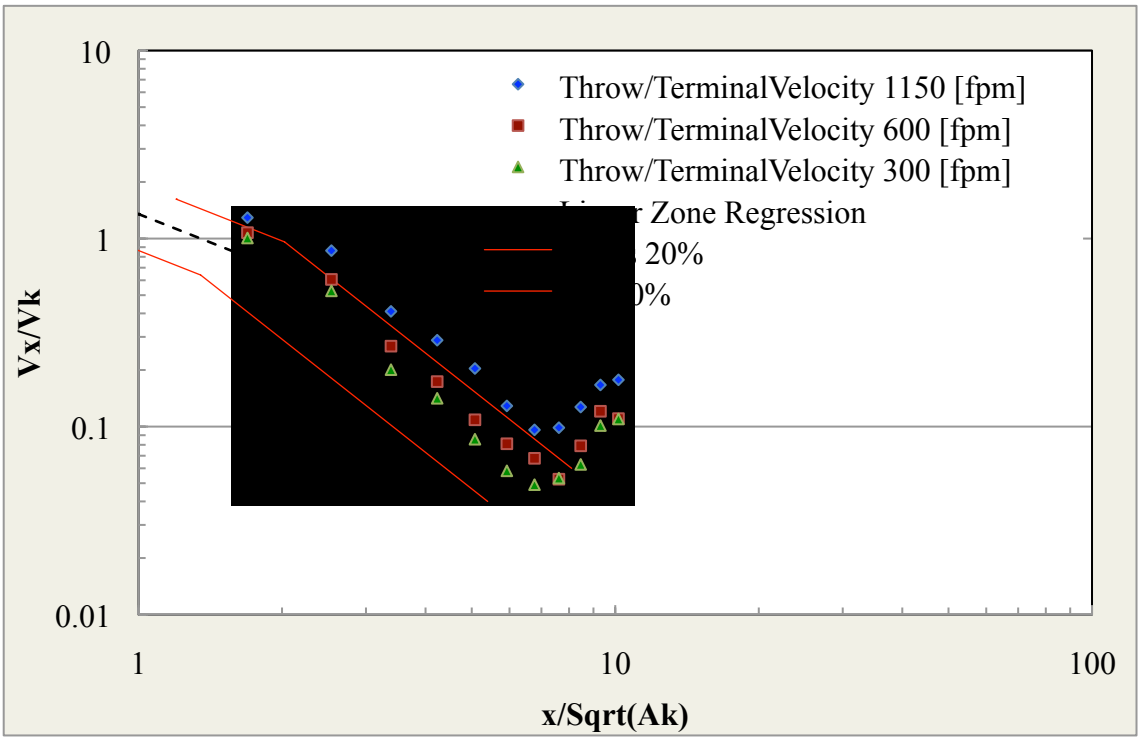


Figure 100. Forward throw for Run #1 with no ceiling.

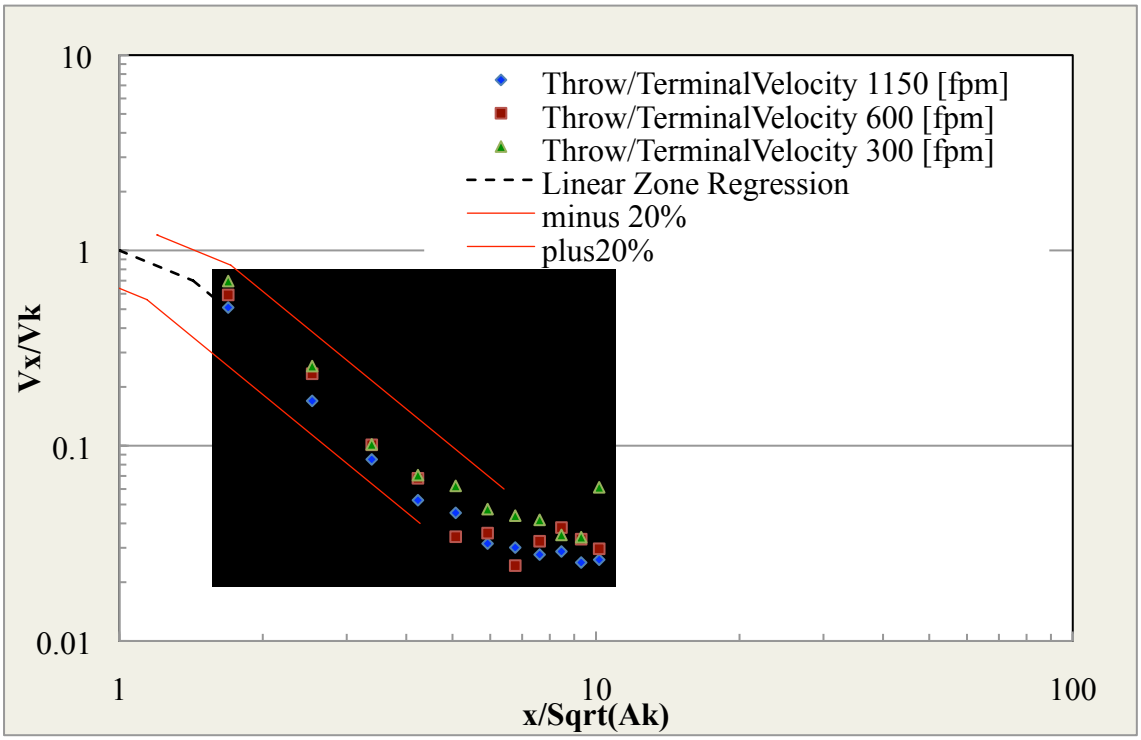


Figure 101. Backward throw for Run #1 with no ceiling.

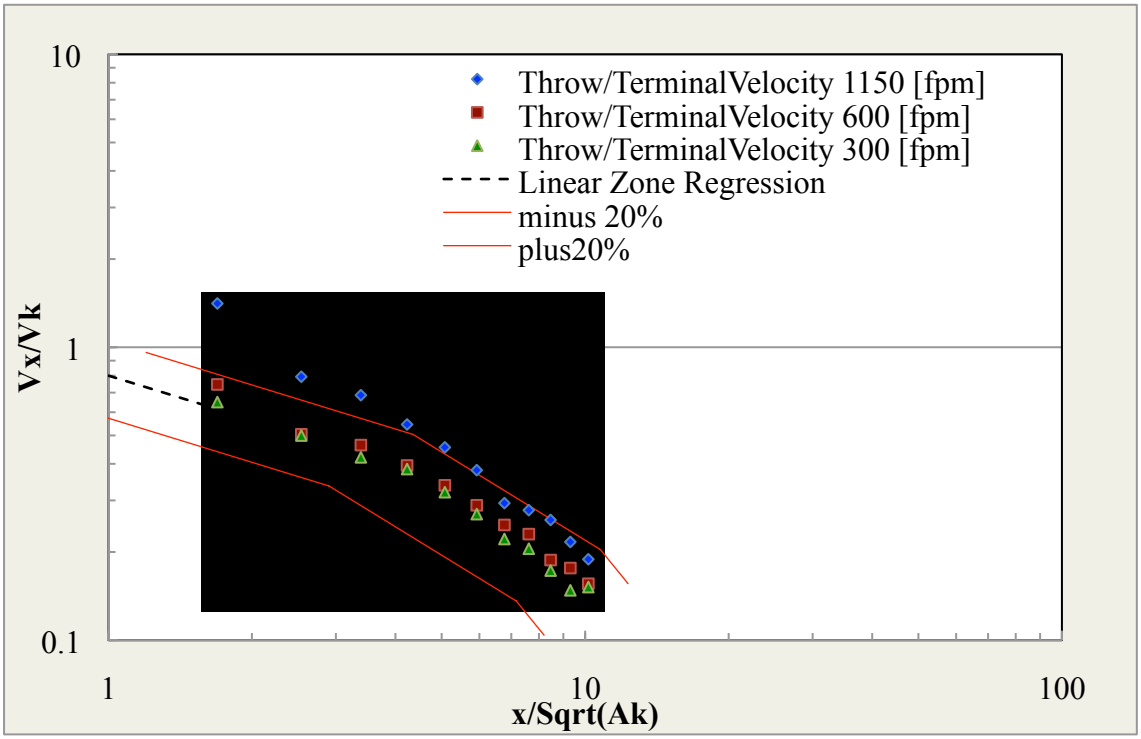


Figure 102. Forward throw for Run #1 with ceiling.

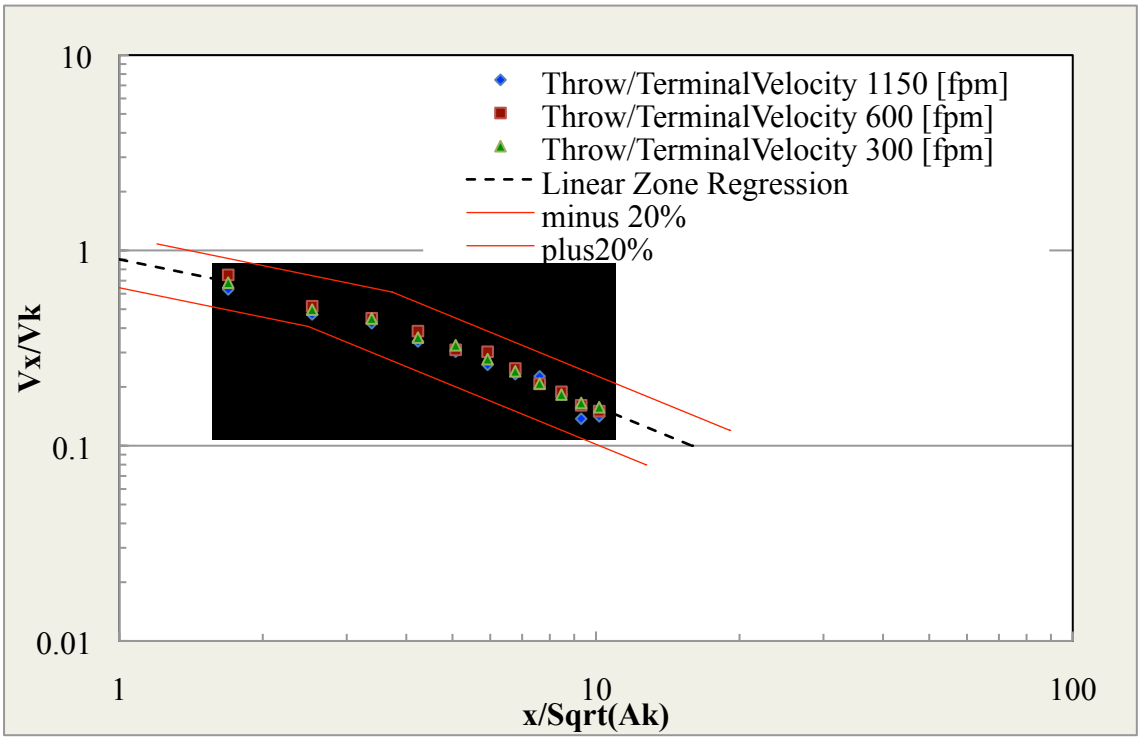


Figure 103. Backward throw for Run #1 with ceiling.

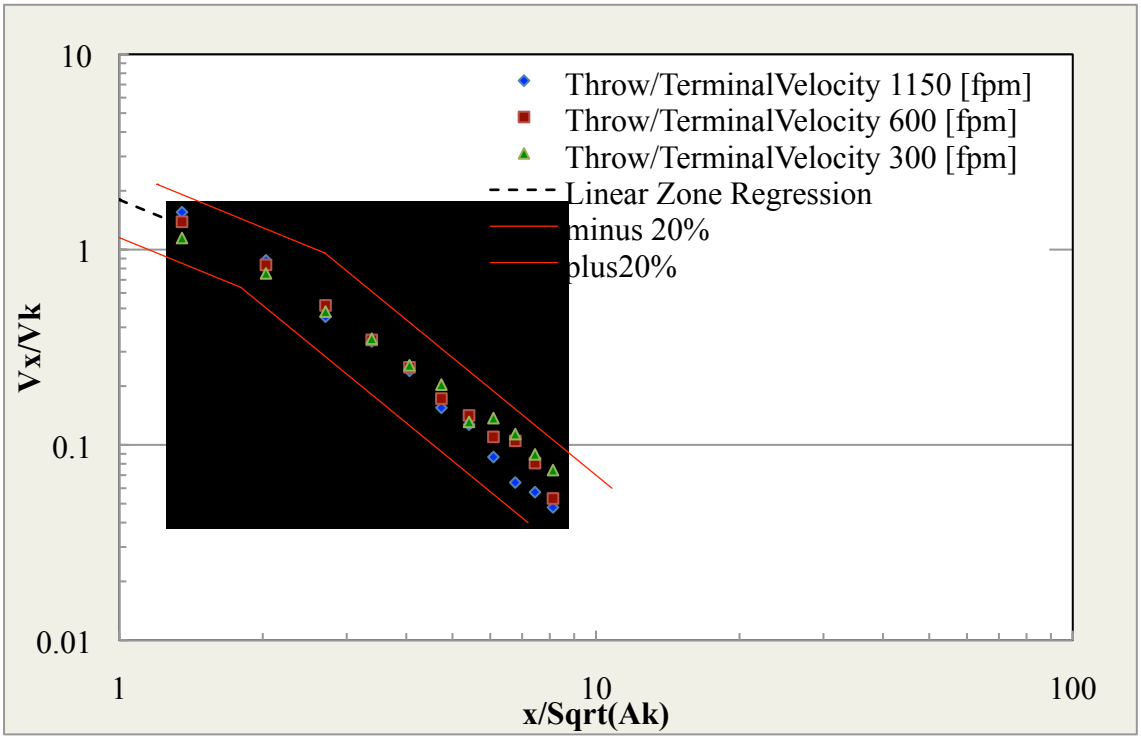


Figure 104. Forward throw for Run #2.

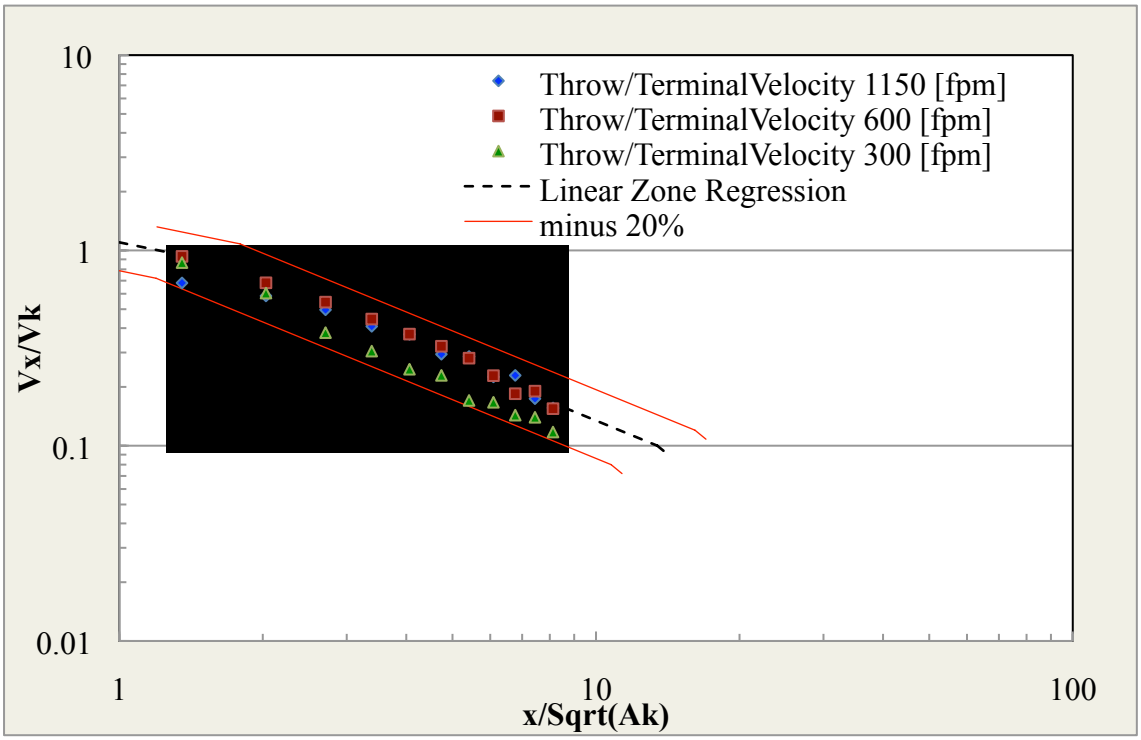


Figure 105. Backward throw for Run #2.

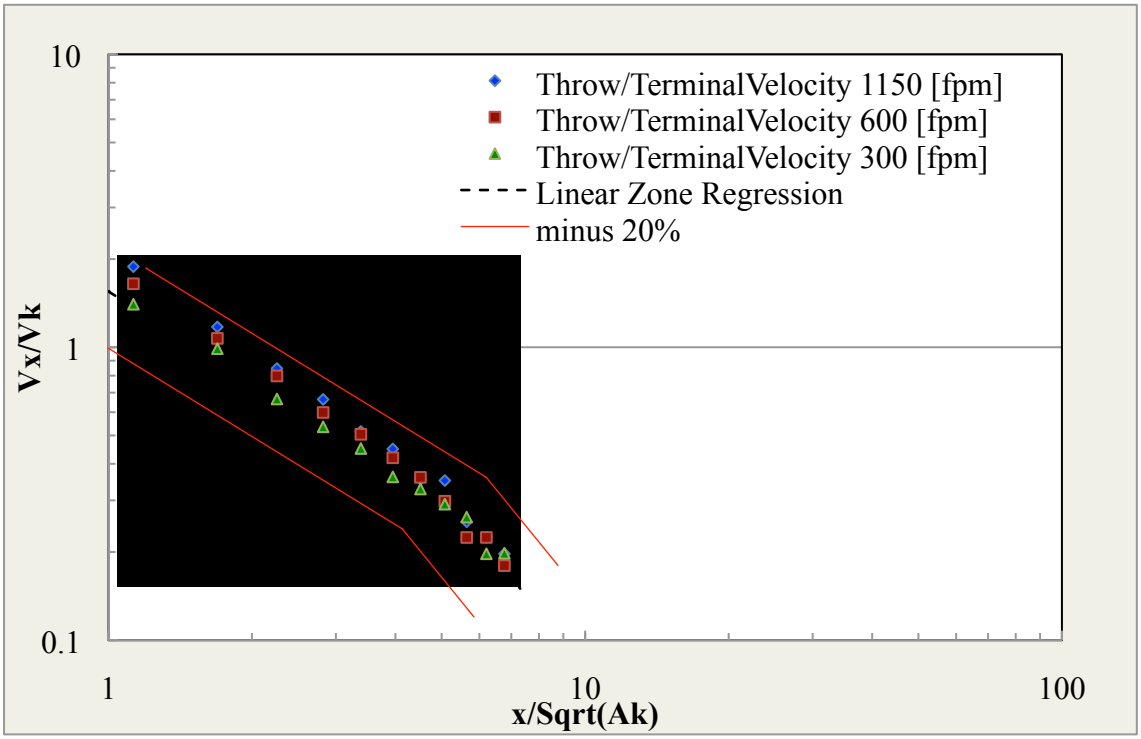


Figure 106. Forward throw for Run #3.

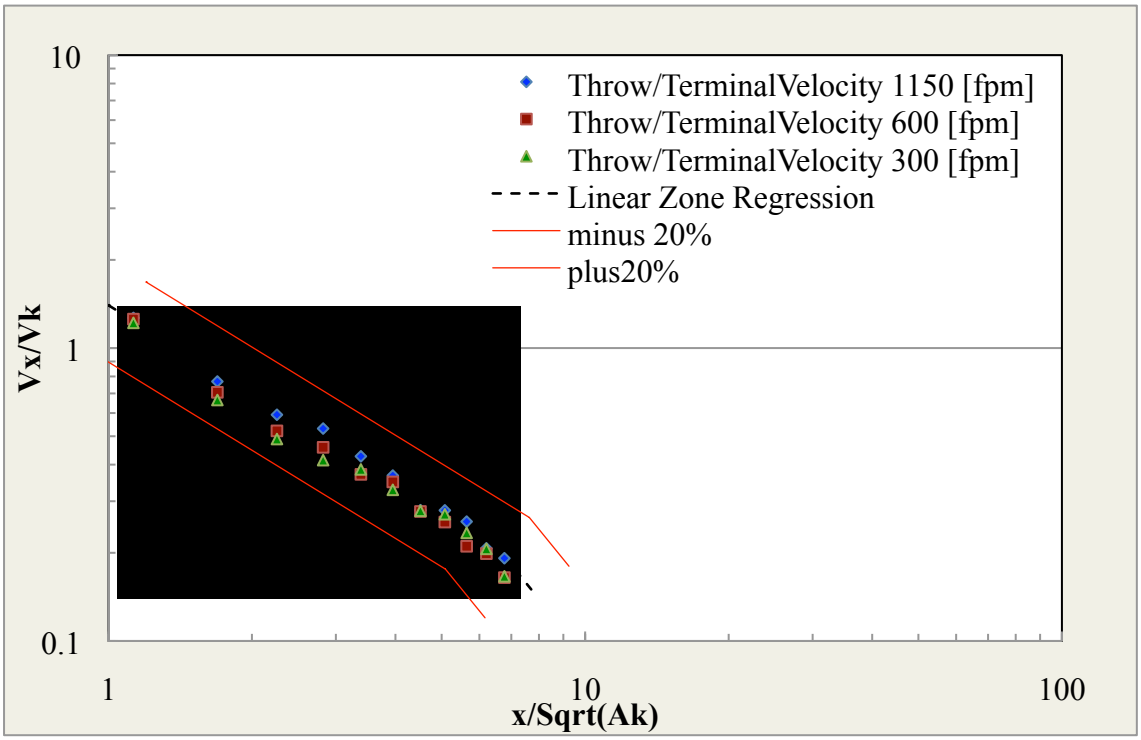


Figure 107. Backward throw for Run #3.

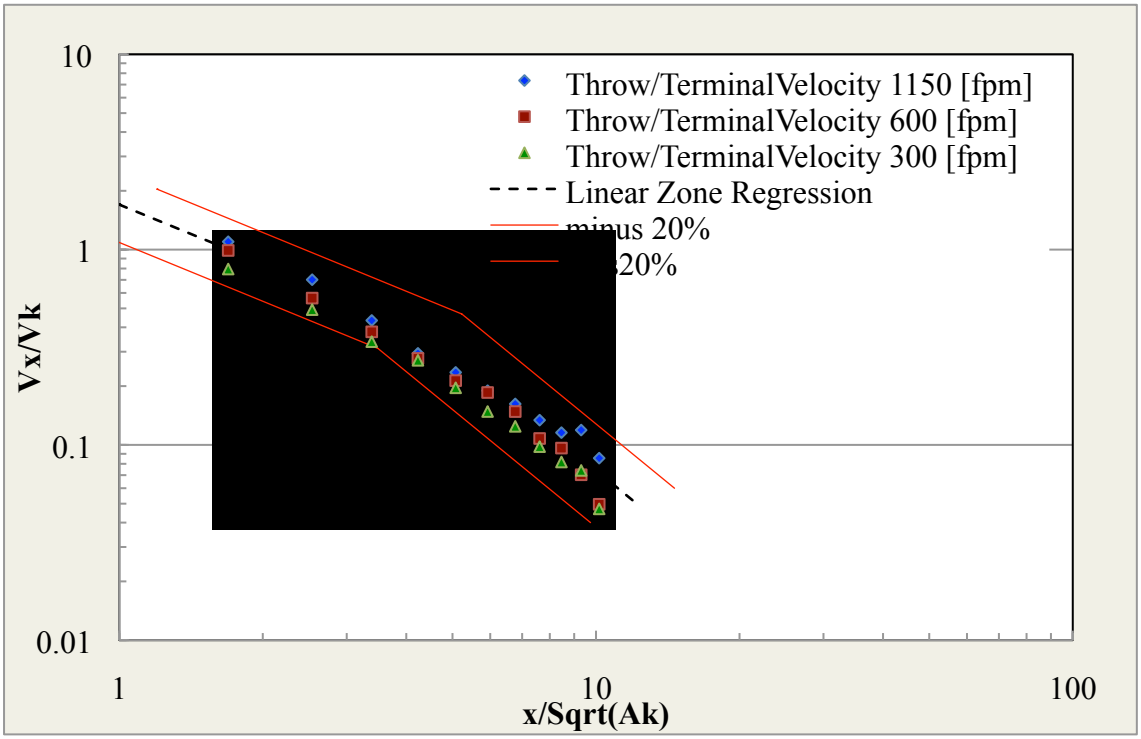


Figure 108. Forward throw for Run #4.

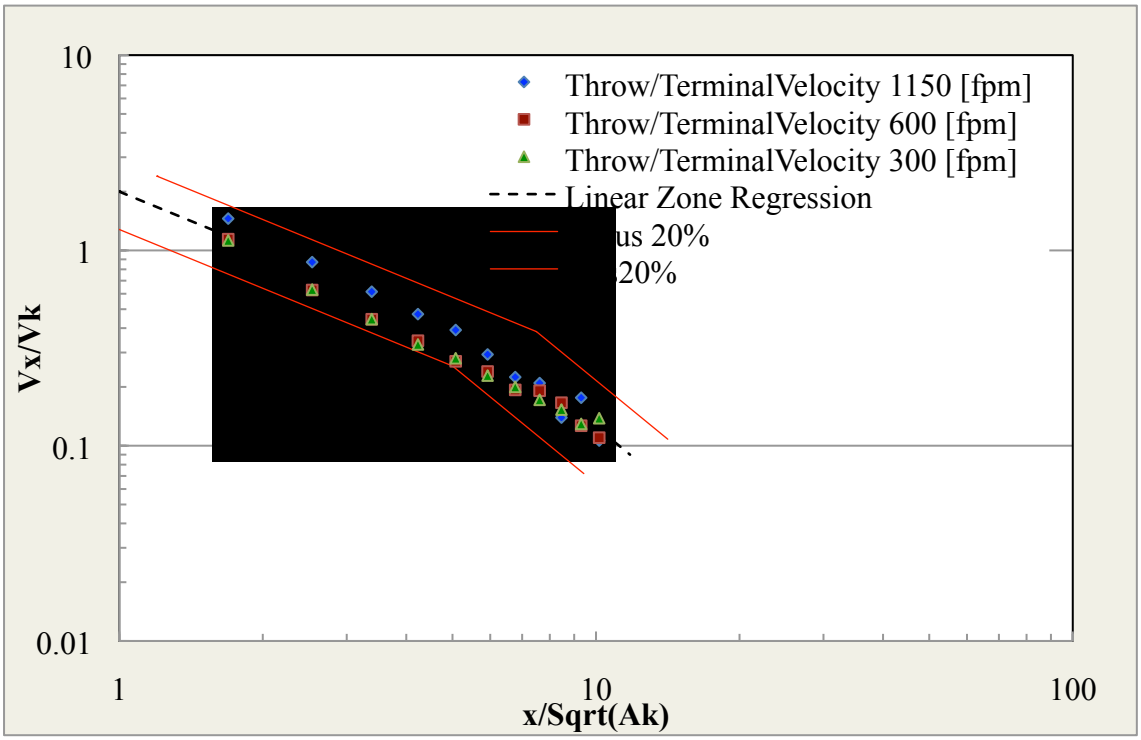


Figure 109. Backward throw for Run #4.

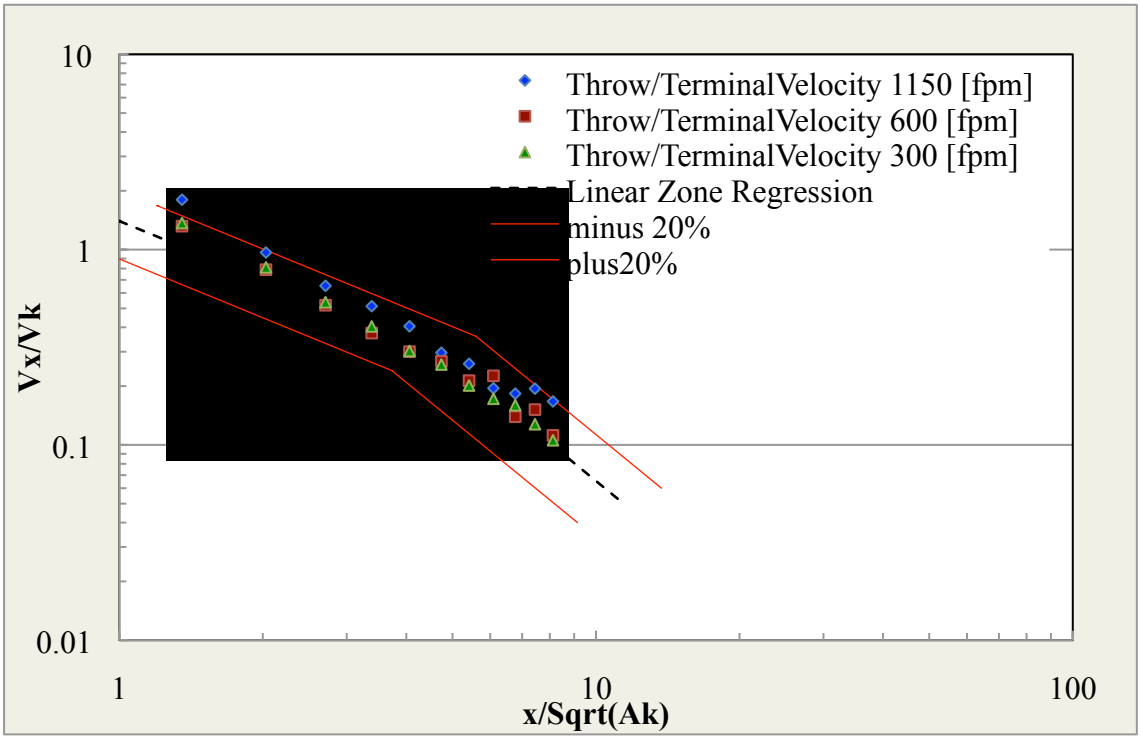


Figure 110. Forward throw for Run #5.

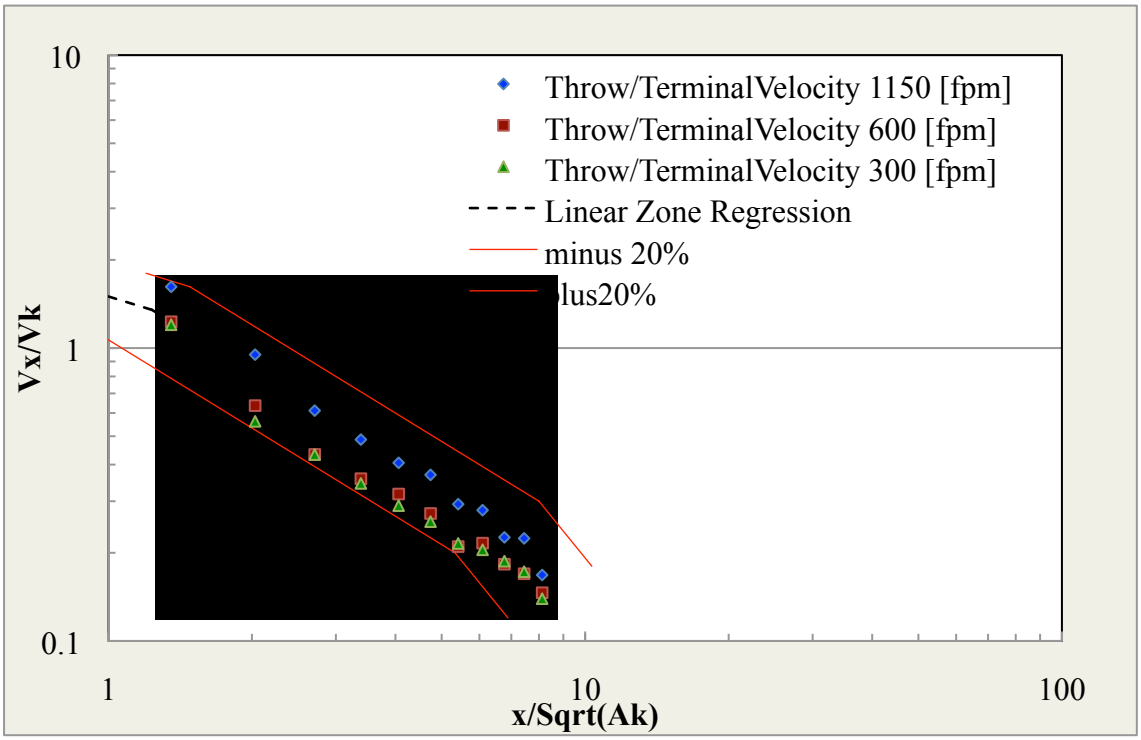


Figure 111. Backward throw for Run #5.

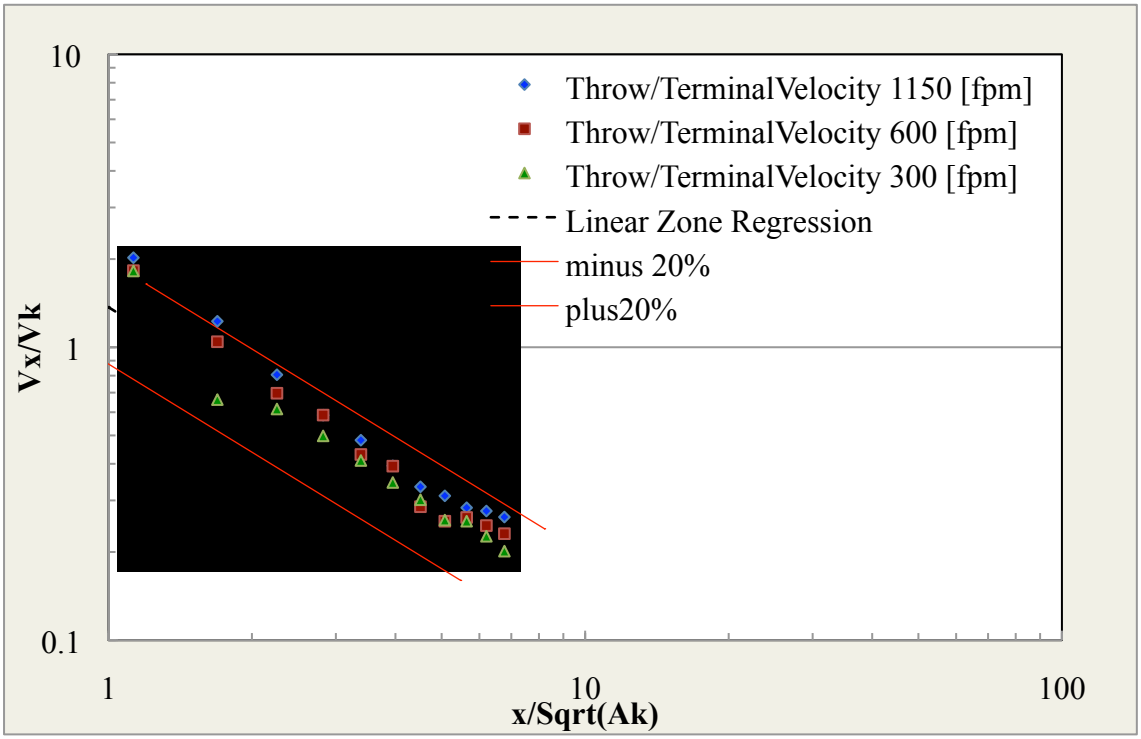


Figure 112. Forward throw for Run #6.

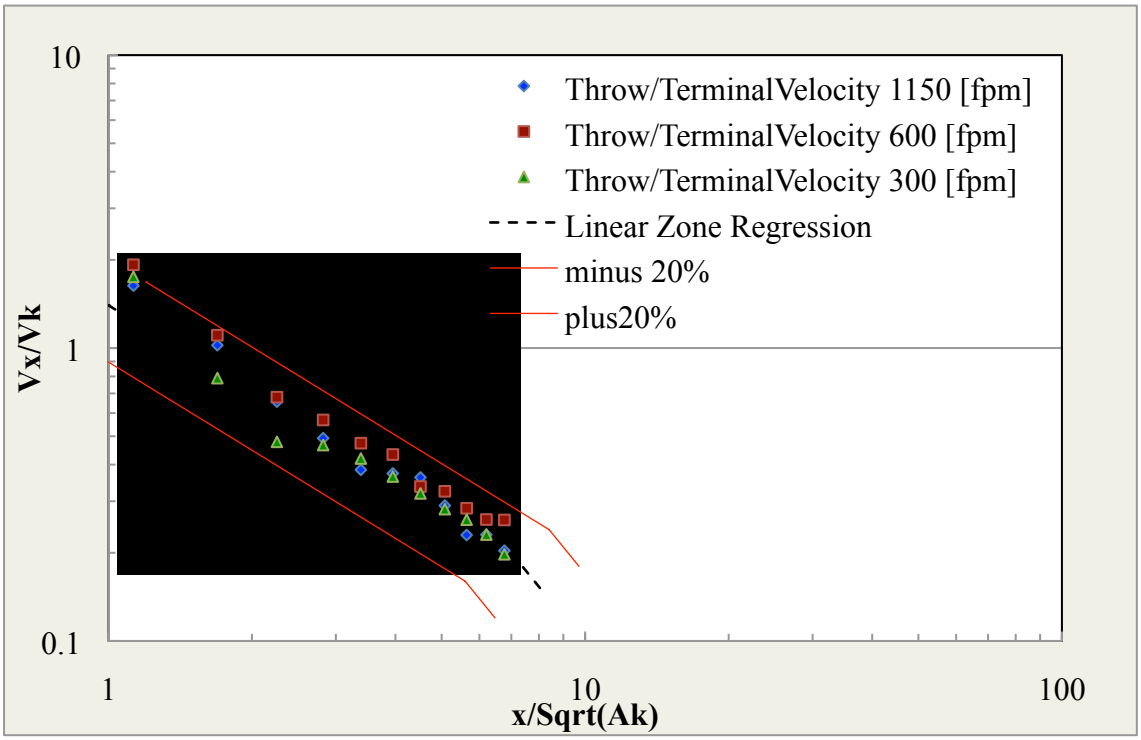


Figure 113. Backward throw for Run #6.

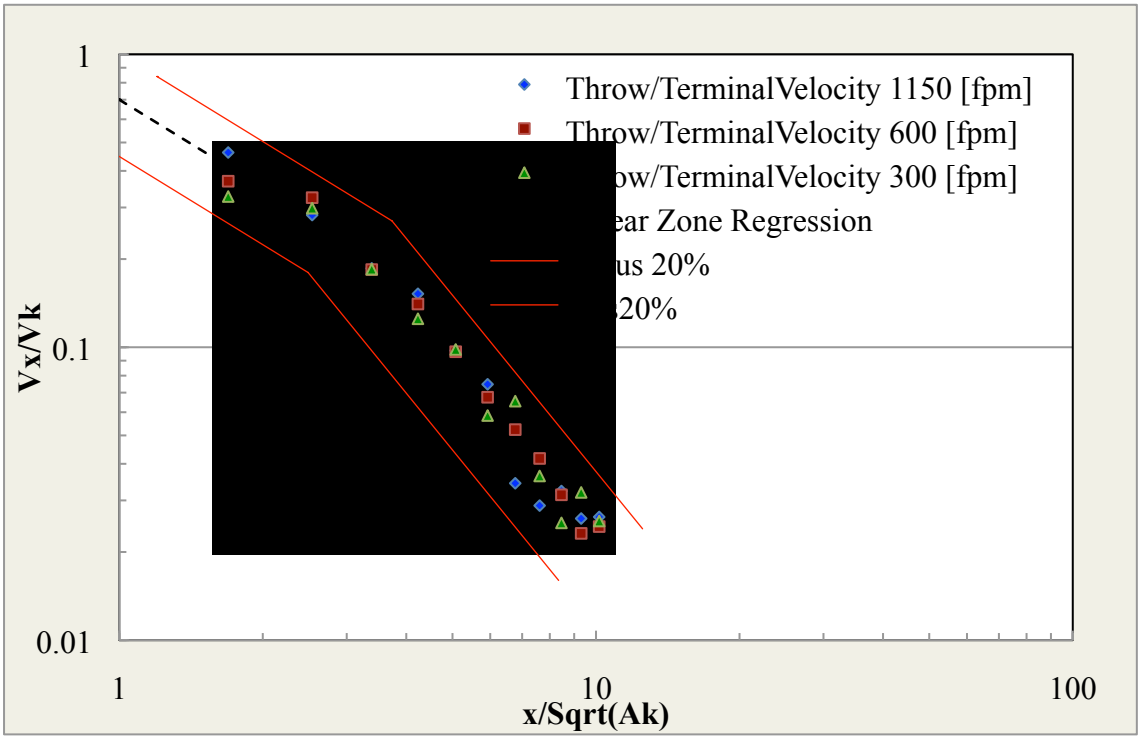


Figure 114. Forward throw for Run #7.

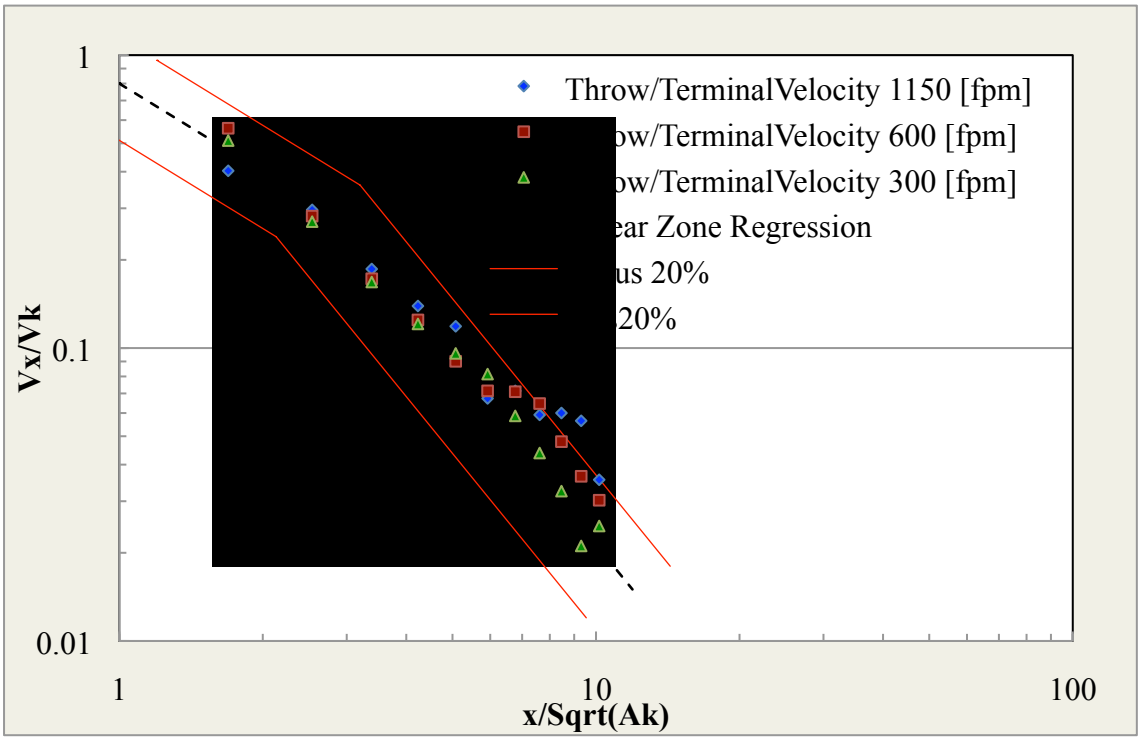


Figure 115. Backward throw for Run #7.

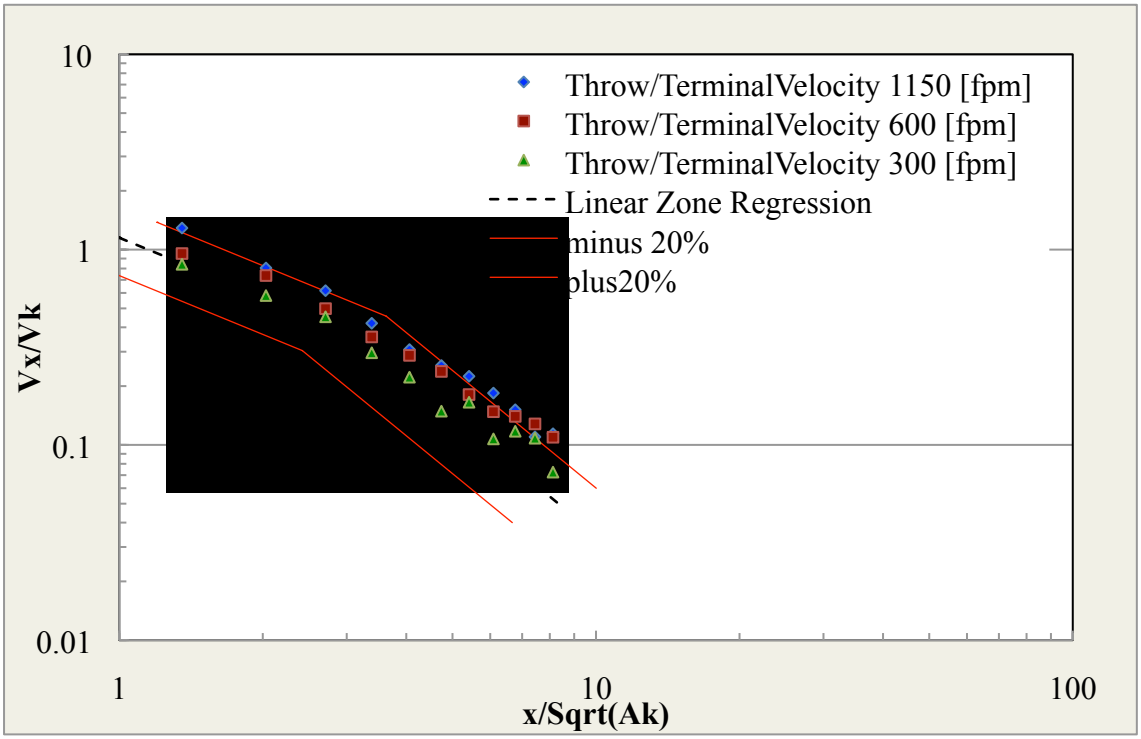


Figure 116. Forward throw for Run #8.

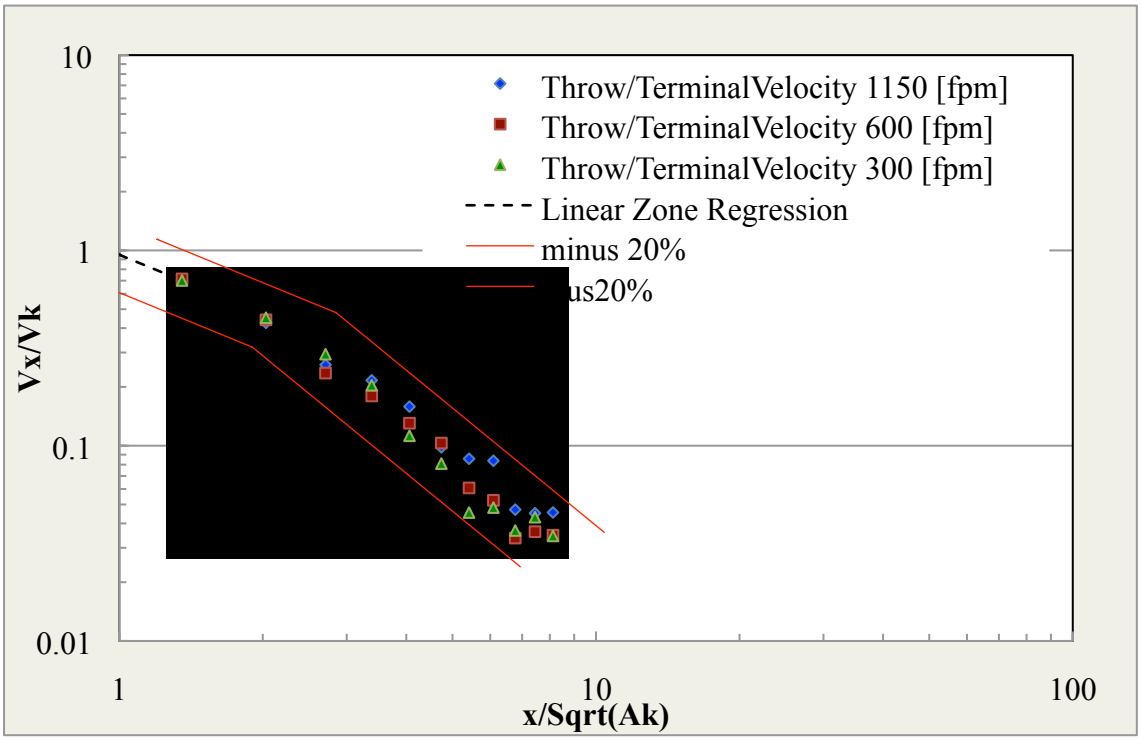


Figure 117. Backward throw for Run #8.

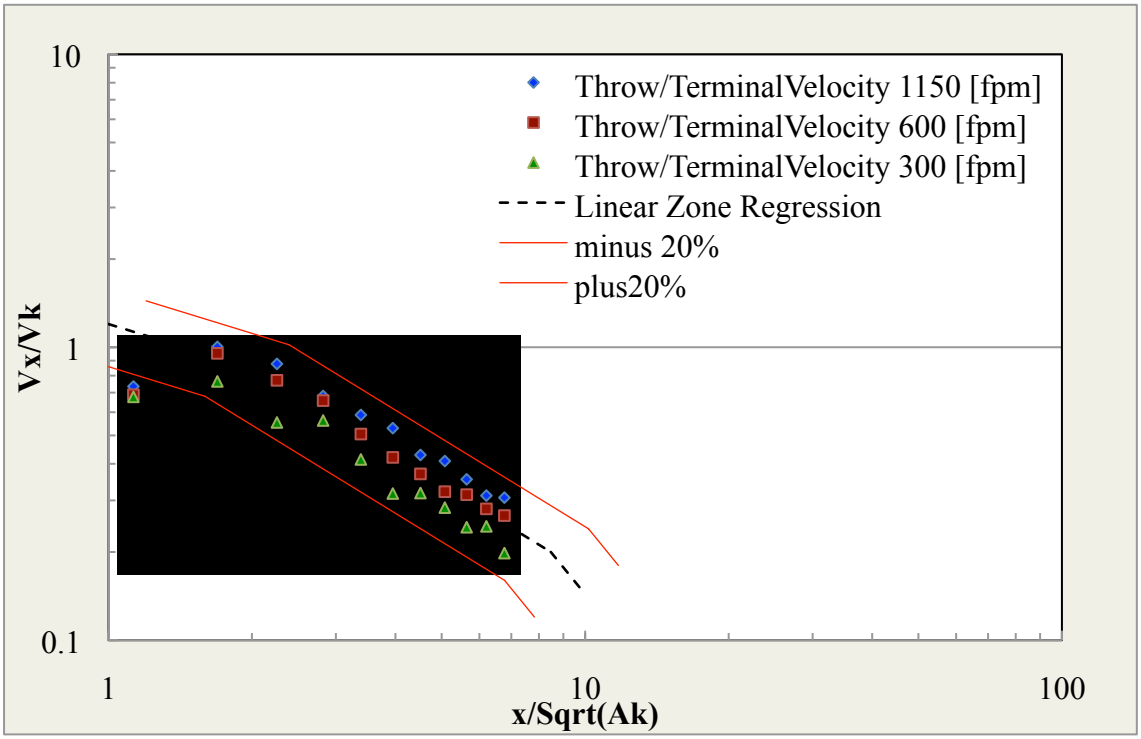


Figure 118. Forward throw for Run #9.

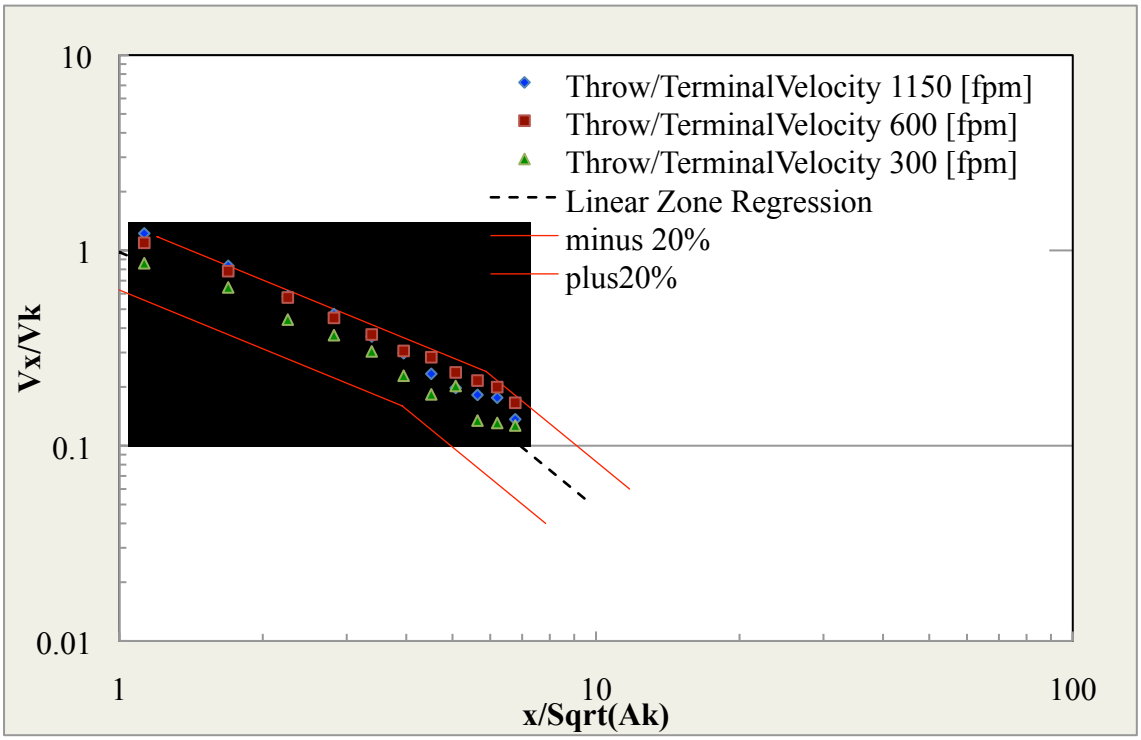


Figure 119. Backward throw for Run #9.

# BIBLIOGRAPHY


[1] ASHRAE *Handbook of HVAC Applications*. Chapter(s): 47.9, 56.1. Atlanta, GA: ASHRAE, 2007.

[2] Hydeman, M., S. Taylor, J. Stein, Taylor Engineering, E. Kolderup, T. Hong, and Eley Associates. *Advanced Variable Air Volume System Design Guide: Design Guidelines*. C.E. Commission, Editor. 2003.

[3] ASHRAE *Handbook of Fundamentals*. Chapter(s): 32.14, 34.1. Atlanta, GA: ASHRAE, 2009.

[4] Landsberger, B., L. Tan, X. Hu. *Energy and Acoustic Performance Effects Due to VAV Duct Design and Installation Practice Variation.* Las Vegas, NV: HVAC&R Research, 2008. 14(4).

[5] Koestel, A. and G.L. Tuve. *Performance and Evaluation of Room Air Distribution Systems*. ASHRAE Transactions 61:533, 1955.

[6] Rock, B.A. and D. Zhu. *Designer's Guide to Ceiling-Based Air Diffusion*. Atlanta, GA: ASHRAE, 2002.

[7] Spengler, J. D., Samet, J. M., and McCarthy, J. F. Indoor Air Quality Handbook. New York, NY: McGraw-Hill Companies, Inc., 2001.

[8] Schaffer, M. E. A Practical Guide to Noise and Vibration Control for HVAC Systems. 2nd Edition (pp. 198). Atlanta, GA: ASHRAE, Inc., 2005.

[9] ANSI/ASHRAE Standard 70-2006. *Method of Testing the Performance of Air Outlets and Air Inlets*. Atlanta, GA: ASHRAE, 2006.

[10] Fowlkes, W., and C. Creveling. Engineering Methods for Robust Product Design*: Using Taguchi Method in Technology and Product Development*. 1st Edition. Reading, MA: Prentice Hall, 1995.

[11] Reynolds, Douglas. Engineering Principles of Acoustics and Noise Control. Las Vegas, NV: DDR, Inc., 1997.

[12] Goodfellow, H. D., and Tähti, E. Industrial Ventilation Guide Book. San Diego, CA: Academic Press, 2001.

[13] Jackson, Sherri L. Research Methods and Statistics: A Critical Thinking Approach. 3rd Edition (pp. 151-155). Belmont, CA: Wadsworth, 2009.

[14] Minitab 16 Statistical Software (2010). [Computer software]. State College, PA: Minitab, Inc. (www.minitab.com)

[15] Landsberger, B., Tan, L., Novosel, D. *Underfloor Air Distribution (UFAD)*. Las Vegas, NV: U.S. Department of Energy, 2006.

# VITA

Graduate College
University of Nevada, Las Vegas

Zaccary A. Poots

Degree:
Bachelor of Science, Mechanical Engineering, 2009
University of Nevada, Las Vegas

Thesis Title: Effects of Inlet Conditions on Diffuser Outlet Performance

Thesis Examination Committee:
Chairperson, Douglas Reynolds, Ph. D.
Committee Member, Brian Landsberger, Ph. D.
Committee Member, Samir Moujaes, Ph. D.
Graduate Faculty Representative, Sandra Catlin, Ph. D.